

X-ray emission from clusters of galaxies

Craig L. Sarazin

Department of Astronomy, University of Virginia, Charlottesville, Virginia 22903
and Institute for Advanced Study, Princeton, New Jersey 08540*

Clusters of galaxies are gravitationally bound configurations containing typically hundreds of galaxies in a region about 10^{25} cm in size. They range from irregular clusters, with strong subclustering, no strong central concentration, and mainly spiral galaxies, to regular clusters, with smooth and centrally condensed galaxy distributions containing few spiral galaxies. Observations of these clusters of galaxies show that they are bright x-ray sources, with luminosities of 10^{43-45} ergs/sec. It is now established that the emission mechanism is thermal bremsstrahlung from hot ($\sim 10^8$ K), low-density ($\sim 10^{-3}$ atoms/cm $^{-3}$) gas. This intracluster gas has a distribution similar to that of the galaxies in the cluster and fills the space between the galaxies. Remarkably, the total mass of hot gas in a typical cluster is similar to the total mass in all the stars in all the galaxies in the cluster. The x-ray spectra of clusters show strong x-ray line emission from iron and other heavy elements; this indicates that a significant portion of the intracluster gas must have been ejected from galaxies in the cluster. Recent x-ray observations from the *Einstein* x-ray satellite show that intracluster gas is cooling in some clusters and being accreted onto large, central galaxies. X-ray images from *Einstein* also suggest that the morphology of the gas mirrors the dynamical state of the cluster. In this paper the x-ray observations of clusters of galaxies are reviewed. Related optical and radio measurements of clusters are also summarized. Theories for the physical state, distribution, origin, and evolution of the intracluster medium are extensively discussed. Finally, the author comments on the prospects for future x-ray observations.

CONTENTS

I. Introduction	2	2. Perseus	43
II. Optical Observations	4	3. M87/Virgo	45
A. Catalogs	4	4. A1367	47
B. Redshifts	5	F. X-ray—optical correlations	47
C. Richness—the number of galaxies in a cluster	6	G. Poor clusters	50
D. Luminosity function of galaxies	6	H. High-redshift clusters and x-ray cluster evolution	51
E. Morphological classification of clusters	10	IV. Radio Observations	52
F. Velocity distribution of galaxies	12	A. General radio properties	52
G. Spatial distribution of galaxies	12	B. Correlations between x-ray and radio emission	53
1. Models for galaxy distributions	12	C. Head-tail and other distorted radio structures	55
2. Core radii	14	D. Cluster radio halos	58
3. Other parameters and sizes	16	E. Cosmic microwave diminution (Sunyaev-Zel'dovich effect)	59
4. Elongation, alignment, and other complications	16	F. Faraday rotation	62
H. Cluster masses—the missing mass problem	17	G. 21-cm line observations of clusters	63
I. Dynamics of galaxies in clusters	19	V. Theoretical Progress	63
1. Two-body relaxation	20	A. Emission mechanisms	63
2. Violent relaxation	20	1. Inverse Compton emission	63
3. Ellipsoidal clusters	21	2. Individual stellar x-ray sources	65
4. Dynamical friction	21	3. Thermal bremsstrahlung from intracluster gas	65
J. Galactic content of clusters	23	B. Ionization and x-ray emission from hot, diffuse plasma	66
1. cD galaxies	23	1. Ionization equilibrium	67
2. Proportion of spiral, SO, and elliptical galaxies	27	2. X-ray emission	67
K. Extensions of clustering	30	3. Resulting spectra	68
1. Poor clusters	30	C. Heating and cooling of the intracluster gas	68
2. Superclusters and voids	30	1. Cooling	68
III. X-ray Observations	30	2. Infall and compressional heating	69
A. Detections and identifications	30	3. Heating by ejection from galaxies	70
B. X-ray luminosities and luminosity functions	32	4. Heating by galaxy motions	70
C. X-ray spectra	32	5. Heating by relativistic electrons	71
1. Continuum features in the spectrum	33	D. Transport processes	72
2. Line features—the 7-keV iron line	35	1. Mean free paths and equilibration time scales	72
3. Lower-energy lines	37	2. Thermal conduction	73
D. The spatial distribution of x-ray emission	39	3. Effects of the magnetic field	74
1. X-ray centers, sizes, and masses	39	4. Viscosity	75
2. X-ray images of clusters and the morphology of the intracluster gas	40	5. Diffusion and settling of heavy ions	75
E. Individual clusters	43	6. Convection and mixing	76
1. Coma	43		

*Permanent address.

E. Distribution of the intracluster gas—hydrostatic models	77
1. Isothermal distributions	78
2. Adiabatic and polytropic distributions	80
3. More complicated distributions	80
4. Empirical gas distributions derived by surface brightness deconvolution	81
5. Chemically inhomogeneous equilibrium models	82
F. Wind models for the intracluster gas	83
G. Cooling flows and accretion by cD's	84
1. Cooling flows	84
2. Accretion by central galaxies	87
3. Optical filamentation	88
4. Accretion-driven star formation on cD's	89
H. X-ray emission from individual galaxies	92
1. Massive halos around M87 and other central galaxies	92
2. Other models for M87 and other central galaxies	93
3. X-ray emission from noncentral cluster galaxies	94
I. Stripping of gas from galaxies in clusters	95
J. The origin and evolution of the intracluster medium	98
1. Infall models	98
2. Ejection from galaxies	100
VI. Prospects for the future and <i>AXAF</i>	103
Acknowledgments	104
References	105

I. INTRODUCTION

Regular clusters of galaxies are the largest organized structures in the universe. They typically contain hundreds of galaxies, spread over a region whose size is roughly 10^{25} cm. Their total masses exceed 10^{48} g. They were first studied in detail by Wolf (1906), although the tendency for galaxies to cluster on the sky had been noted long before this. A great advance in the systematic study of the properties of clusters occurred when Abell compiled an extensive, statistically complete catalog of rich clusters of galaxies (Abell, 1958). For the last quarter century, this catalog has been the most important resource in the study of galaxy clusters. Optical photographs of some of the best studied clusters of galaxies are shown in Fig. 1 (see also footnote 1). The Virgo cluster [Fig. 1(a)] is the nearest rich cluster to our own galaxy; the Coma cluster [Fig. 1(b)] is the nearest very regular cluster.

In 1966, x-ray emission was detected from the region around the galaxy M87 in the center of the Virgo cluster

[Byram *et al.*, 1966; Bradt *et al.*, 1967; Fig. 1(a)]. In fact, M87 was the first object outside of our galaxy to be identified as a source of astronomical x-ray emission. Five years later, x-ray sources were also detected in the directions of the Coma [Fig. 1(b)] and Perseus [Fig. 1(c)] clusters (Fritz *et al.*, 1971; Gursky *et al.*, 1971a, 1971b; Meekins *et al.*, 1971). Since these are three of the nearest rich clusters, it was suggested that clusters of galaxies might generally be x-ray sources (Cavaliere *et al.*, 1971). The launch of the *Uhuru* x-ray astronomy satellite permitted a survey of the entire sky for x-ray emission (Giacconi *et al.*, 1972) and established that this was indeed the case. These early *Uhuru* observations indicated that many clusters were bright x-ray sources, with luminosities typically in the range of 10^{43-45} ergs/sec. The x-ray sources associated with clusters were found to be spatially extended; their sizes were comparable to the size of the galaxy distribution in the clusters (Kellogg *et al.*, 1972; Forman *et al.*, 1972). Unlike other bright x-ray sources but consistent with their spatial extents, cluster x-ray sources did not vary temporally in their brightness (Elvis, 1976). Although several emission mechanisms were proposed, the x-ray spectra of clusters were most consistent with thermal bremsstrahlung from hot gas.

This interpretation requires that the space between galaxies in clusters be filled with very hot ($\sim 10^8$ K), low-density ($\sim 10^{-3}$ atoms/cm³) gas. Remarkably, the total mass in this intracluster medium is comparable to the total mass in all the stars in all the galaxies in the cluster. As to the origin of this gas, it was widely assumed that it had simply fallen into the clusters from the great volumes of space between them, where it had been stored since the formation of the universe (Gunn and Gott, 1972).

In 1976, x-ray line emission from iron was detected from the Perseus cluster of galaxies (Mitchell *et al.*, 1976), and shortly thereafter from Coma and Virgo as well (Serlemitsos *et al.*, 1977). The emission mechanism for this line is thermal, and its detection confirmed the thermal interpretation of cluster x-ray sources. However, the only known sources for significant quantities of iron or any other heavy element in astronomy are nuclear reactions in stars, and no significant population of stars has been observed which does not reside in galaxies. Since the abundance of iron in the intracluster gas was observed to be similar to the abundance in stars, a substantial portion of this gas must have been ejected from stars in galaxies in the cluster (Bahcall and Sarazin, 1977). This is despite the fact that the total mass of intracluster gas is on the same order as the total mass of stars presently observed in the clusters. Obviously, these x-ray observations suggest that galaxies in clusters have had more interesting histories than might otherwise have been assumed.

In this paper, the x-ray observations of clusters of galaxies and the theories for the intracluster gas will be reviewed. Because clusters are still largely defined by their optical properties, I shall first review the optical observations of clusters (Sec. II). I shall particularly emphasize information on their dynamical state, and the possibility that the galaxy population has been affected by

¹Unless otherwise indicated, all the figures showing optical, x-ray, or radio brightness on the sky have north at the top and east at the left. When coordinates are given, the east-west coordinate is right ascension (in hours, minutes, and seconds; a full circle equals 24 h) and the north-south coordinate is declination (in degrees, minutes, and seconds of arc; a full circle equals 360 deg).

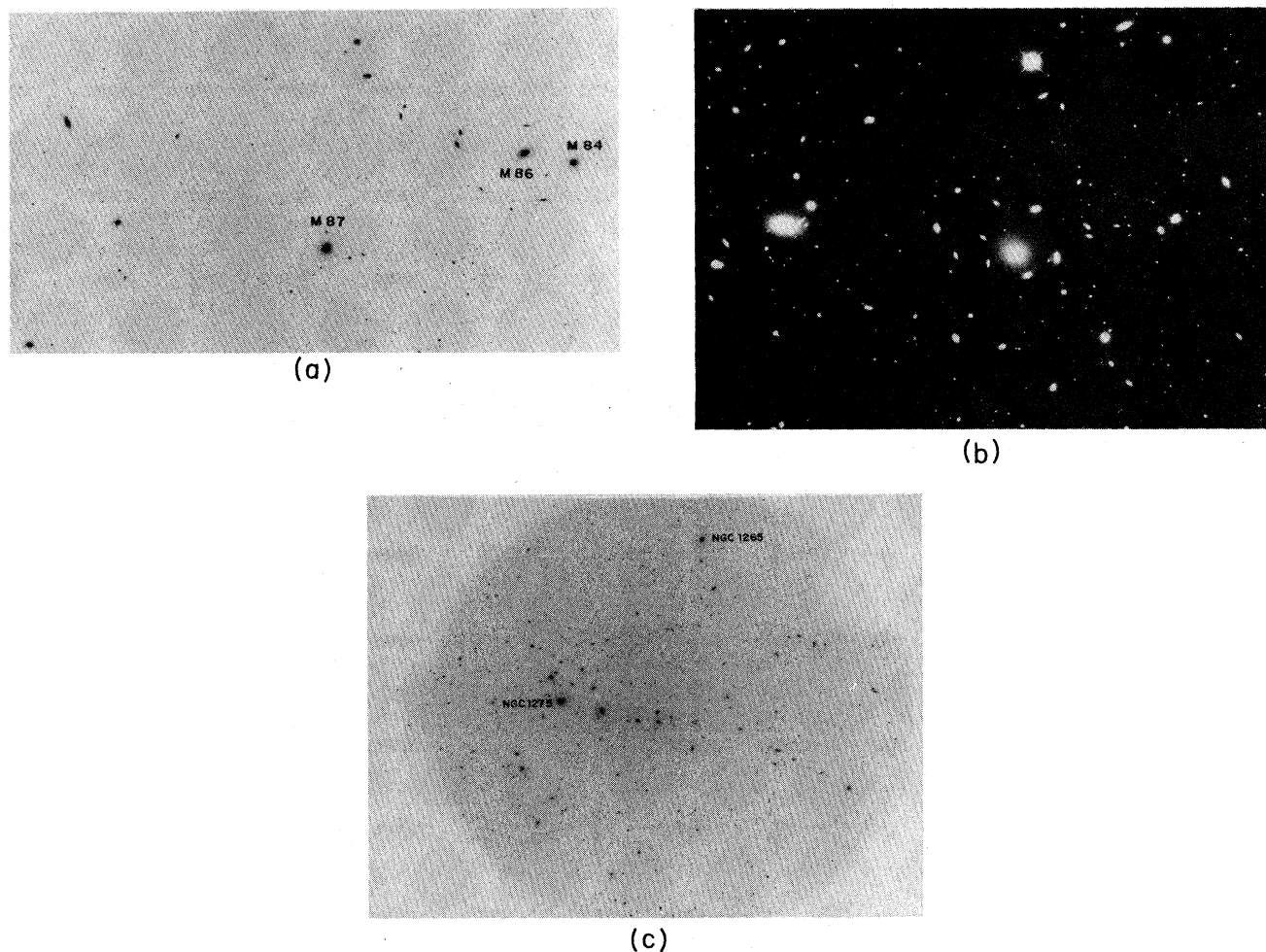
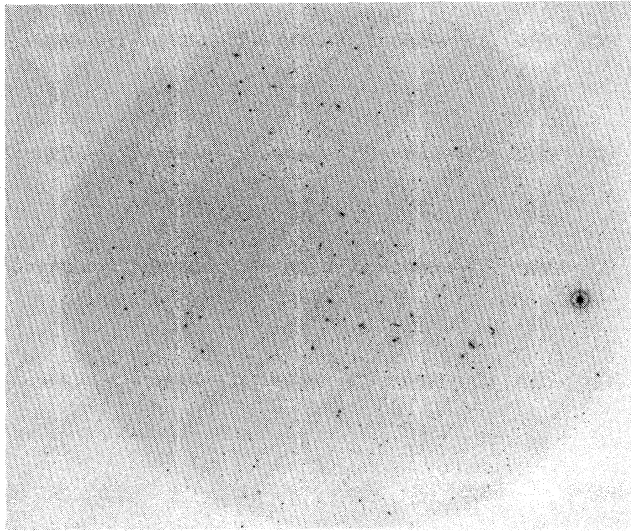


FIG. 1. Optical photographs of clusters of galaxies. (a) The Virgo cluster of galaxies, an irregular cluster that is the nearest cluster to our galaxy. The galaxy M87, on which the x-ray emission is centered, is marked, as are the two bright galaxies M84 and M86. Photograph from the Palomar Observatory Sky Survey (Minkowski and Abell, 1963). (b) The Coma cluster of galaxies (Abell 1656), showing the two dominant D galaxies. Coma is one of the nearest rich, regular clusters. Photograph copyright 1973 The National Optical Astronomy Observatories. (c) The Perseus cluster of galaxies (Abell 476), showing the line of bright galaxies. NGC1275 is the brightest galaxy, on the east (left) end of the chain. NGC1265 is a head-tail radio galaxy. Photograph from Strom and Strom (1978c). (d) The irregular Hercules cluster (Abell 2151), which contains a large number of spiral galaxies. Photograph from Strom and Strom (1978b). (e) The irregular cluster Abell 1367. Photograph from Strom and Strom (1978c). (f) The regular cluster Abell 2199, showing the dominant cD galaxy NGC6166 at its center. Photograph from Strom and Strom (1978b).

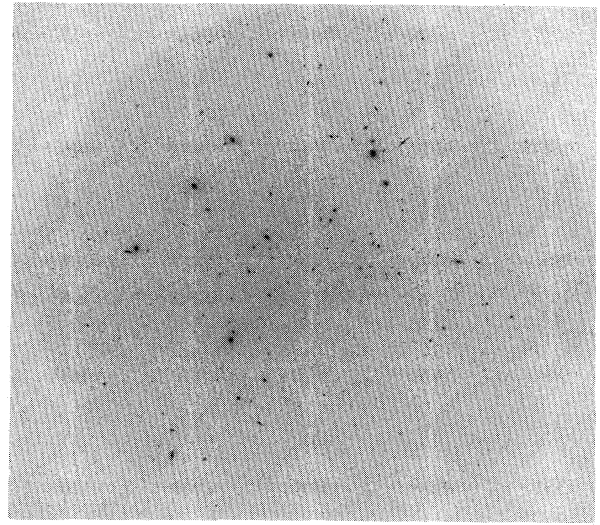
the intracluster gas. Then the x-ray observations will be reviewed (Sec. III), including the recent results of x-ray imaging and spectroscopy from the *Einstein* x-ray satellite. Radio observations of clusters also provide information on the intracluster gas, which is summarized in Sec. IV. For example, certain distortions seen in radio sources in clusters are most naturally explained as arising from interactions with this gas. Moreover, extensive searches have been made for "shadows" in the cosmic microwave radiation due to electron scattering by intracluster gas. In Sec. V theories for the x-ray emission mechanism, the physical state, the distribution, the origin, and the history of the intracluster medium will be reviewed. Finally, I shall comment briefly on the prospects for further obser-

vations of x-ray clusters, particularly with the *AXAF* satellite, in Sec. VI.

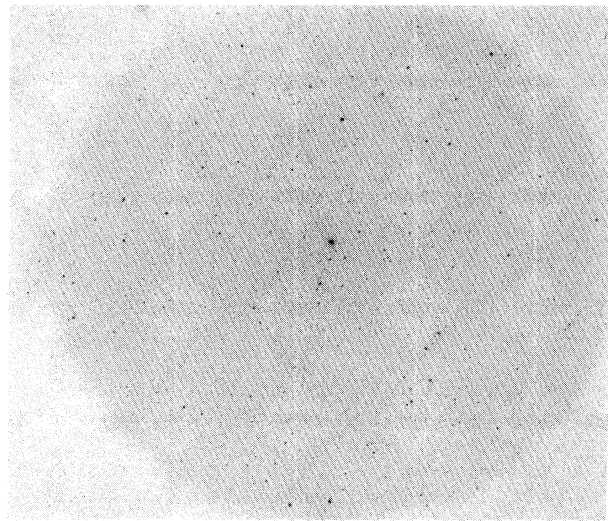
Previous reviews of clusters of galaxies emphasizing their optical properties include Abell (1965,1975), van den Bergh (1977b), Bahcall (1977a), Rood (1981), White (1982), and particularly Dressler (1984). Superclusters of galaxies are reviewed by Oort (1983). Some recent reviews which include the x-ray properties of clusters are Gursky and Schwartz (1977), Binney (1980), Cavaliere (1980), Cowie (1981), Canizares (1981), and Holt and McCray (1982). Fabian *et al.* (1984) give an excellent review of cooling flows in x-ray clusters (see Sec. V.G). An up-to-date review of the spectroscopic properties of x-ray clusters is that of Mushotzky (1984). Forman and Jones



(d)



(e)



(f)

FIG. 1. (*Continued*).

(1982) give a comprehensive review of the x-ray images of clusters.

II. OPTICAL OBSERVATIONS

A. Catalogs

The two most extensive and often cited catalogs of rich clusters of galaxies are those of Abell (1958) and Zwicky and his collaborators (Zwicky *et al.*, 1961–1968). In this paper, Abell clusters will be denoted by giving A and then the number of the cluster in Abell's list. Both catalogs were constructed by identifying clusters as enhancements in the surface number density of galaxies on the National

Geographic Society–Palomar Observatory Sky Survey (Minkowski and Abell, 1963) and thus are confined to northern areas of sky (declination greater than -20° for Abell and -3° for Zwicky). Abell surveyed only clusters away from the plane of our galaxy.

As clustering exists on a very wide range of angular and intensity scales (Peebles, 1974), it is not possible to give a unique and unambiguous definition of a "rich cluster." Thus the membership of a catalog of clusters is determined by the criteria used to define a "rich cluster." These criteria must specify the required surface number density enhancement for inclusion and the linear or angular scale of the enhancement. The scale is necessary in order to exclude small groupings of galaxies; for example, a close pair of galaxies can represent a very large enhance-

ment above the background galaxy density on a small angular scale. Alternatively, specifying the surface density and scale is equivalent to specifying the number of galaxies (the "richness" of the cluster) and the scale size. Because the number of galaxies observed increases as their brightness diminishes (Sec. II.D.), one must also specify the range of magnitudes² of the galaxies included in determining the cluster richness. Finally, because galaxies grow fainter with increasing distance, the catalog can only be statistically complete out to a limiting distance or redshift, and only clusters within this distance range should be included in a statistically complete sample.

Abell's criteria were basically (1) that the cluster contain at least 50 galaxies in the magnitude range m_3 to $m_3 + 2$, where m_3 is the magnitude of the third brightest galaxy; (2) that these galaxies be contained within a circle of radius $R_A = 1.7/z$ minutes of arc or $3h_{50}^{-1}$ megaparsecs (Mpc),^{3,4} where z is the estimated redshift of the cluster (Sec. II.B); (3) that the estimated cluster redshift be in the range $0.02 \leq z \leq 0.20$. R_A is called the Abell radius of the cluster. The Abell catalog contains 2712 clusters, of which 1682 satisfy all these criteria. The other 1030 were discovered during the search and were included to provide a more extensive finding list for clusters. The Abell catalog gives estimates of the cluster center positions (see also Sastry and Rood, 1971), distance, and richness of the clusters, as well as the magnitude of the tenth brightest galaxy m_{10} .

²The magnitude of an object is a logarithmic measure of its faintness. If f is the flux from the object observed at Earth, then its magnitude is $m \equiv -2.5 \ln(f/f_0)$; the flux standards f_0 at various wavelengths are given in many astronomical references (see, for example, Allen, 1973).

³A parsec is 3.086×10^{18} cm.

⁴All objects sufficiently distant from our galaxy are observed to be receding from us at a speed which increases with their distance. The Hubble constant H_0 is the coefficient of proportionality between the recession velocity v_r and the distance d : $v_r = H_0 d$. Because of difficulties in calibrating the extragalactic distance scale, H_0 is uncertain by about a factor of 2, $H_0 = 50-100$ km/sec/Mpc. For convenience, in this paper H_0 will be parametrized as $H_0 = 50 h_{50}$ km/sec/Mpc. The redshift z of an extragalactic object is the shift in the observed wavelength λ_{obs} of any feature in the spectrum of the object relative to the laboratory wavelength λ_{lab} : $z \equiv (\lambda_{\text{obs}} - \lambda_{\text{lab}}) / \lambda_{\text{lab}}$. If the redshift results from a Doppler shift and the redshift is small $z \ll 1$, then $z = v_r/c$, where v_r is the radial component of velocity of the object away from the observer. If the velocity is due to the universal cosmic expansion and, again, z is low, the distance to the object is $d = 6 \times 10^3 z / h_{50}$ Mpc.

For the Zwicky catalog, the criteria were as follows: (1) the boundary (scale size) of the cluster was determined by the contour (or isopleth) where the galaxy surface density fell to twice the local background density; (2) this isopleth had to contain at least 50 galaxies in the magnitude range m_1 to $m_1 + 3$, where m_1 is the magnitude of the first brightest galaxy. No distance limits were specified, although in practice, very nearby clusters, such as Virgo [Fig. 1(a)], were not included because they extended over several Sky Survey plates. Obviously, the Zwicky catalog criteria are much less strict than Abell's, and the Zwicky catalog thus contains many more clusters that are less rich. For each cluster, the Zwicky catalog gives a classification (Sec. II.E) and estimates of the coordinates of the center, the diameter, the richness, and the redshift. Finding charts showing the cluster isopleths and positions of brighter galaxies and stars are also presented.

A number of smaller catalogs have been compiled, consisting of clusters in the southern sky or clusters at higher redshifts ($z \geq 0.2$). Early southern cluster catalogs or lists include those of de Vaucouleurs (1956), Klemola (1969), Snow (1970), Sersic (1974), and Rose (1976). Until recently, the search for southern clusters was severely handicapped by the lack of deep survey plates. The first deep optical survey of the south, the European Southern Observatory Quick Blue Survey (ESO-B), was completed in 1978 (West, 1974; Holmberg *et al.*, 1974). A catalog of southern clusters from the first portion of this survey was prepared by Duus and Newell (1977), and a list of southern clusters near x-ray sources was given by Lugger (1978). More recently, portions of the ESO/SRC-J survey of very deep blue plates have been used to compile southern cluster catalogs by Braid and MacGillivray (1978) and White and Quintana (1985). Before his untimely death, Abell was preparing a southern continuation of the Abell catalog in collaboration with Corwin. The red portion of the ESO/SRC survey is currently being done, and these plates are being used to detect high-redshift clusters (West and Frandsen, 1981).

The discovery of higher-redshift clusters ($z \geq 0.2$) is of great importance to cosmological studies; lists of such clusters include Humason and Sandage (1957), Gunn and Oke (1975), Sandage, Kristian, and Westphal (1976), Spinrad *et al.* (1985), and Vidal (1980). In addition, the lists of southern clusters from the ESO/SRC surveys discussed in the last paragraph contain many high-redshift clusters.

B. Redshifts

The clusters in the Abell (1958) catalog were assigned to distance groups, based on the redshift (see also footnote 4) estimated from the magnitude of the tenth brightest galaxy in the cluster. Leir and van den Bergh (1977) have given improved estimates of redshifts for 1889 rich Abell clusters, using the magnitudes of the first and tenth brightest galaxies, and an estimate of the cluster radius. Their distance scale is calibrated using measured redshifts for 101 clusters. Photometric distance estimators derived

from a larger sample of redshifts have been given by Sarazin *et al.* (1982). Similarly, clusters in the Zwicky catalog were placed in distance groups, based on the magnitudes and sizes of the brightest cluster galaxies.

Spectroscopic redshifts are now available for about 500 Abell clusters. Table I lists the redshifts for Abell clusters known to the author at the time of writing, and is taken primarily from Sarazin *et al.* (1982). Table I includes the redshifts compiled by Noonan (1981) and Struble and Rood (1982,1984), and the list of redshifts for all rich, high-galactic-latitude, nearby Abell clusters from Hoessel, Gunn, and Thuan (1980). Some of the redshifts are ambiguous, mainly because of possible foreground contamination. Ambiguous redshifts are marked with a star; notes on these cases are given in Sarazin *et al.* (1982).

Of course, many redshifts are known for non-Abell clusters as well. The compilation of Noonan (1981) includes many such redshifts.

C. Richness—the number of galaxies in a cluster

The “richness” of a cluster is a measure of the number of galaxies associated with that cluster. Because of the presence of background galaxies, it is not possible to state with absolute confidence that any given galaxy belongs to a given cluster. Thus one cannot give an exact tally of the number of galaxies in a cluster. Richness is a statistical measure of the population of a cluster, based on some operational definition of cluster membership. The richness will be more useful if it is defined in such a way as to be reasonably independent of the distance to and morphology of a cluster.

Zwicky *et al.* (1961–1968) define the richness of their clusters as the total number of galaxies visible on the red Sky Survey plates within the cluster isopleth (Sec. II.A); the number of background galaxies expected is subtracted from the richness. These richnesses are clearly very dependent on a cluster redshift (Abell, 1962; Scott, 1962). First, a wider magnitude range is counted for nearby clusters, because the magnitude of the first brightest galaxy is further from the plate limit. Second, a larger area of the cluster is counted for nearby clusters, because the point at which the surface density is twice that of the background will be farther out in the cluster.

Abell (1958) has divided his clusters into richness groups using criteria that are nearly independent of distance (see Sec. II.A); that is, the magnitude range and area considered do not vary with redshift. Just (1959) has found a slight richness-distance correlation in Abell’s catalog; however, the effect is small and is probably explained by a slight incompleteness (10%) of the catalog for distant clusters (Paal, 1964). When more accurate determinations have been made, it has been found that the Abell richness generally correlated well with the number of galaxies, but that the Abell richness may be significantly in error in some individual cases (Mottmann and Abell,

1977; Dressler, 1980a). Thus the Abell richnesses are very useful for statistical studies, but must be used with caution in studies of individual clusters. Note also that it is generally preferable to use the actual Abell counts rather than just the richness group (Abell, 1982).

D. Luminosity function of galaxies

The luminosity function of galaxies in a cluster gives the number distribution of the luminosities of the galaxies. The integrated luminosity function $N(L)$ is the number of galaxies with luminosities greater than L , while the differential luminosity function $n(L)dL$ is the number of galaxies with luminosities in the range L to $L + dL$. Obviously, $n(L) \equiv -dN(L)/dL$. Luminosity functions are often defined in terms of galaxy magnitudes $m \propto -2.5 \log_{10}(L)$ (see footnote 2); $N(\leq m)$ is the number of galaxies in a cluster brighter than magnitude m . Observational studies of the luminosity functions of clusters include Zwicky (1957), Kiang (1961), van den Bergh (1961a), Abell (1962,1975,1977), Rood (1969), Gudehus (1973), Bautz and Abell (1973), Austin and Peach (1974b), Oemler (1974), Krupp (1974), Austin *et al.* (1975), Godwin and Peach (1977), Mottmann and Abell (1977), Dressler (1978b), Bucknell *et al.* (1979), Carter and Godwin (1979), Thompson and Gregory (1980), and Kraan-Korteweg (1981). Figure 2 gives the observed integrated luminosity function for a composite of 13 rich clusters as derived by Schechter (1976) from Oemler’s (1974) data.

Three types of functions are commonly used for fitting the luminosity function. Zwicky (1957) proposed the form

$$N(\leq m) = K (10^{0.2(m-m_1)} - 1), \quad (2.1)$$

where K is a constant and m_1 is the magnitude of the

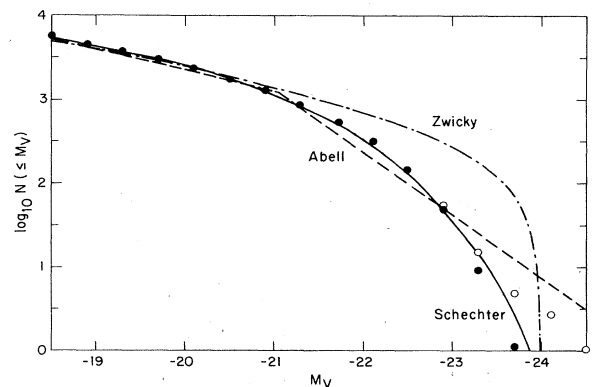


FIG. 2. The luminosity function of galaxies in clusters. $N(\leq M_V)$ is the number of galaxies brighter than absolute magnitude M_V . The circles are the composite observed luminosity function derived by Schechter (1976). The solid circles exclude cD galaxies, while the open circles show the changes when they are included. The solid, dashed, and dash-dotted curves are the fitting functions of Schechter, Abell, and Zwicky, as discussed in the text.

TABLE I. The redshifts of Abell clusters. Each entry gives the Abell number of the cluster and its redshift, corrected to the local group. The references and notes are given in Sarazin *et al.* (1982) except where indicated. A * means that the redshift may be ambiguous, and the notes in Sarazin *et al.* should be checked.

Cluster	z										
14	0.064	439	0.1072	1060	0.0114	1571	0.209	2006	0.1166 ^c	2249	0.0808
15	0.121	458	0.1050 ^a	1069	0.063	1589	0.0718	2008	0.1818 ^c	2250	0.0654
21	0.0948	465*	0.0855	1081	0.1588 ^a	1609	0.0891	2009	0.1532 ^c	2252	0.1147
22	0.1432 ^a	468	0.1325	1093	0.226	1630	0.0649 ^a	2012	0.1513 ^c	2255*	0.0810
24	0.1338	478	0.09	1123	0.1235 ^a	1631*	0.053	2021	0.0996 ^c	2256	0.0601
31	0.1596	480*	0.0473	1126	0.0831	1643	0.1981	2022	0.0564	2257	0.1054
34*	0.0410 ^a	496	0.0316	1132	0.1363	1644	0.0453	2028	0.0772	2263	0.1051 ^a
41	0.275	500	0.0666	1139	0.0376	1651	0.0825	2029	0.0767	2266	0.1671
42	0.1087 ^a	505	0.0543	1142	0.0373	1656	0.0235	2036	0.1163 ^a	2270	0.2377
43	0.1114 ^a	508	0.1479	1146	0.141	1667*	0.1648	2040	0.0456	2283	0.183
46	0.150	509*	0.2356	1149	0.0710 ^a	1674	0.1055 ^a	2048	0.0945	2295	0.0508
76	0.0377	514*	0.0697	1155	0.0738 ^a	1675	0.184	2050	0.1183	2301	0.0874
77	0.0719 ^a	518	0.1795	1169	0.0582 ^a	1677	0.1832	2052	0.0345	2317	0.211
79	0.0927	520	0.203	1170	0.1620 ^a	1685	0.197	2053	0.1127	2319*	0.0529
84	0.119	539	0.0267	1185	0.0349	1689	0.1747	2055	0.0530	2320	0.171
85	0.0518	545	0.153	1186	0.0791	1691	0.0722	2056	0.0763	2328	0.1470
86	0.0610	548	0.0390	1187	0.0791	1736	0.0431	2061	0.0768	2330	0.1138
88	0.1086	553	0.0670	1190	0.0738	1738	0.1146 ^a	2063	0.0337	2339	0.1128
96	0.1344	566	0.0957	1213	0.0469	1749	0.059	2065	0.0721	2344	0.1447
98	0.1054	568	0.0780	1216*	0.0524	1750	0.086	2067	0.0732	2347	0.1196
104	0.0822	569	0.0193	1224	0.2897 ^a	1758	0.2800	2069	0.116	2355*	0.2311
114	0.0566	576	0.0392	1225	0.1033	1759*	0.168	2079	0.0662	2356	0.1161
115	0.1959	586	0.171	1227	0.1117 ^a	1760*	0.168	2083	0.1143	2377	0.0808 ^a
119	0.0437	592	0.0624	1228	0.0344	1763	0.187	2084*	0.342	2382	0.0648
121	0.1048	593	0.226	1232*	0.1676	1767	0.0756	2089	0.0743	2384	0.0943
133	0.06	623	0.0871	1235	0.1036 ^a	1773	0.0776	2092	0.0669	2388*	0.0615 ^a
136	0.1569 ^a	629	0.138	1238	0.0716	1775	0.0709	2100	0.1533	2397	0.224
140	0.149	634	0.0266	1246*	0.216	1781	0.0762	2107	0.0421	2399	0.0587
141	0.230	639	0.291	1254*	0.0628	1785*	0.0792 ^a	2108	0.0919	2400	0.0881 ^a
147	0.0438	644	0.0781	1257	0.0339	1793	0.0849	2110	0.0978 ^a	2410	0.0806
151	0.0526	646	0.1303	1264	0.1267 ^a	1795	0.0621	2111	0.229	2420	0.0838 ^a
154	0.0658	652	0.1938	1278	0.129	1800	0.0724	2124	0.0669	2440*	0.0873
160	0.0450	655	0.1267	1291	0.0586	1809	0.0788	2125	0.2472	2443	0.108
166	0.1156	665	0.1816	1308	0.0481	1825	0.0632 ^a	2142	0.0904	2457	0.0597
168	0.0452	671	0.0497	1314	0.0341	1827	0.0668 ^a	2147	0.0356	2459	0.0736 ^a

TABLE I. (Continued).

Cluster	z										
171	0.0729	680*	0.079	1318*	0.0189	1831	0.0749	2148	0.0442	2462	0.0755 ^a
180	0.135	695*	0.0694	1337*	0.1442	1837	0.0376	2151*	0.0371	2469*	0.0656 ^b
186	0.1066 ^a	732	0.2030	1342*	0.1061	1840	0.1104	2152*	0.0383	2496	0.1233 ^a
189	0.0349	733	0.1159 ^a	1345	0.1095	1878*	0.254	2158*	0.1355 ^c	2521	0.1359 ^a
193	0.0478	744	0.0768	1346	0.0970 ^a	1880	0.1413 ^a	2162	0.0318	2534	0.196 ^d
194	0.0186	750	0.162	1354*	0.1128	1890	0.084	2163	0.1698	2550	0.1543
195	0.0437	754	0.0528	1356*	0.1167	1904	0.0714	2165	0.1286	2554	0.106
209	0.213	777	0.226	1360	0.1535	1913	0.0533	2172	0.1393 ^c	2556	0.0851
222	0.211	779	0.0226	1364	0.1070	1918	0.1400	2175	0.0978	2559	0.0796 ^a
223	0.207	780	0.0522	1365	0.0763	1921	0.1352 ^a	2177*	0.1606	2572	0.0395
225	0.0692	784	0.1236	1367	0.0213	1927	0.0740	2178	0.0928	2584	0.1196
234	0.1731	787	0.1355	1372	0.1126	1930	0.1313	2179	0.1366 ^c	2589	0.0421
246	0.0753	795	0.1357	1373	0.1314 ^a	1934	0.2195 ^a	2183	0.1371 ^c	2593	0.0440
262	0.0164	801	0.1918	1377	0.0509	1939	0.0883	2184	0.0546	2597	0.0852
272	0.0878	819	0.0759 ^a	1382	0.1053	1940	0.1396	2187	0.1835 ^c	2622	0.0615
274	0.1290	838	0.0507	1383	0.0598	1942	0.224	2192	0.1874 ^c	2626	0.0562
277	0.0947	854	0.2069	1385*	0.1563	1952	0.248	2196	0.1338 ^c	2632	0.1860
278	0.0896	858	0.0881 ^a	1392	0.1382	1957	0.241	2197	0.0303	2634	0.0322
279*	0.0797 ^a	868	0.153	1399*	0.0913	1960	0.1878 ^c	2198*	0.1702 ^c	2638*	0.0825
326*	0.0558 ^a	873	0.182	1401	0.1670 ^a	1961	0.232	2199	0.0305	2645*	0.246
347	0.0198	882	0.1408 ^a	1412	0.0839	1972	0.1191 ^c	2204	0.1524	2646	0.193
348	0.274	910	0.201	1413	0.1427	1976	0.1171 ^c	2210	0.1465	2657	0.0414
370*	0.373	912	0.0888	1436	0.0646	1980	0.1154 ^c	2211	0.1361 ^c	2658	0.185
376	0.0489	923	0.1162	1452	0.0631	1983	0.043	2213	0.1603 ^c	2666	0.0273
389	0.1160	924	0.0989	1461*	0.0538 ^a	1984	0.1265	2218	0.175 ^b	2670	0.0749
397	0.0325	951	0.1427	1468	0.0853	1986	0.1184 ^c	2219	0.224 ^b	2675	0.0726
399	0.0715	957	0.0437	1474	0.0791	1988	0.1162 ^c	2220	0.1106	2686	0.1124 ^a
400	0.0232	963	0.206	1496	0.0961	1990	0.2432 ^c	2224	0.1504	2694	0.0958 ^a
401	0.0748	978	0.0527	1514	0.200	1991	0.0589	2235	0.1511	2700	0.0978
403	0.107	979	0.055	1525	0.3687	1997	0.2502 ^c	2240	0.138	2703	0.1144
407	0.0472	991	0.0880	1541*	0.0892	1999	0.1032	2241*	0.0635		
410	0.0897 ^a	993	0.0533	1548	0.1608 ^a	2001*	0.111	2244	0.0997		
419	0.0406	1018	0.297 ^a	1550	0.254	2003*	0.2174 ^c	2246	0.225 ^a		
423	0.0797 ^a	1020	0.0650	1553	0.1652	2004*	0.1368 ^c	2246*	0.125 ^b		
426	0.0183	1035	0.0799	1559	0.1042 ^a	2005	0.1251	2247	0.0392		

^aSchneider et al. (1983). ^bSpinrad (1985). ^cCiardullo et al. (1983). ^dSteiner et al. (1982).

first brightest galaxy. In general, the Zwicky function fits the faint end of the luminosity function adequately, but does not fall off rapidly enough for brighter galaxies (see Fig. 2). Clearly, Eq. (2.1) implies that $N(L) = K[(L_1/L)^{1/2} - 1]$, where L_1 is the luminosity of the first brightest galaxy and K is the expected number of galaxies in the range $\frac{1}{4}L_1 \leq L \leq L_1$.

Abell (1975) has suggested that the luminosity function $N(L)$ be fit by two intersecting power laws; $N(L) = N^*(L/L^*)^{-\alpha}$, where $\alpha \approx \frac{5}{8}$ for $L < L^*$, and $\alpha \approx \frac{15}{8}$ for $L > L^*$. L^* is the luminosity at which the two power laws cross, and N^* is the expected number of galaxies with $L \geq L^*$. Of course, this form is intended only as a simple and practical fit to the data; the real luminosity function certainly has a continuous derivative $n(L)$, unlike Abell's function. The magnitude luminosity function corresponding to Abell's form is often written as

$$\log_{10} N(\leq m) = \begin{cases} K_1 + s_1 m, & m \leq m^* \\ K_2 + s_2 m, & m > m^* \end{cases}, \quad (2.2)$$

where K_1 and K_2 are constants. The slopes are approximately $s_1 \approx 0.75$ and $s_2 \approx 0.25$, and the power laws cross at $m = m^*$, so that $K_1 + s_1 m^* = K_2 + s_2 m^*$. As shown in Fig. 2, the Abell form fits both the bright and faint ends of the luminosity function adequately.

Schechter (1976) proposed an analytic approximation for the differential luminosity function

$$n(L)dL = N^*(L/L^*)^{-\alpha} \exp(-L/L^*) d(L/L^*), \quad (2.3)$$

where L^* is a characteristic luminosity, $N^*\Gamma(1-\alpha, 1)$ is the number of galaxies with $L > L^*$, and $\Gamma(\alpha, x)$ is the incomplete gamma function; Schechter derives a value for the faint end slope of $\alpha = \frac{5}{4}$. The integrated luminosity function corresponding to Eq. (2.3) is $N(L) = N^*\Gamma(1-\alpha, L/L^*)$.

The advantages of the Schechter function are that it is analytic and continuous, unlike Abell's form, and that it is a real statistical distribution function, unlike Zwicky's form, which requires that the magnitude of the first brightest galaxy (which ought to be a random variable) be specified. An expression similar to the Schechter form was predicted by a simple analytical model for galaxy formation (Press and Schechter, 1974). The Schechter function is steeper than Abell's function at the bright end because it contains an exponential. The Schechter differential luminosity function decreases monotonically with luminosity, while the Abell function has a local maximum at $L = L^*$ (Abell, 1975); there is some weak evidence for such a peak, especially near the centers of rich clusters (Rood and Abell, 1973).

The Schechter function fits the observed distribution in many clusters reasonably well from the faint to the bright end (Fig. 2), as long as the very brightest galaxies, the cD galaxies, are excluded (Schechter, 1976). These can have luminosities as large as $10L^*$, and thus are extremely improbable if Eq. (2.3) holds exactly. However, cD galaxies have a number of distinctive morphological characteristics which suggest that they were formed by special pro-

cesses which occur primarily in the centers of rich clusters (see Sec. II.J.1). In any case, they apparently can be excluded by morphological (as opposed to luminosity) criteria, and Eq. (2.3) can be taken to be the non-cD luminosity function.

The parameter N^* in the Abell or Schechter functions is a useful measure of the richness of the cluster. If these luminosity functions are adequate approximations, then fitting the luminosity function to determine N^* ought to give a more accurate measure of richness than counting galaxies in magnitude ranges. Note that while the total number of galaxies predicted by Abell's, Zwicky's, or Schechter's functions diverges at the faint end, the total luminosity is finite; for example, the total cluster optical luminosity is $L_{\text{opt}} = N^*\Gamma(2-\alpha)L^*$ for the Schechter function, and N^* thus measures the total cluster luminosity.

Because of the break in the luminosity function near L^* , this parameter represents a characteristic luminosity of cluster galaxies. Moreover, L^* is nearly the same for many clusters; it corresponds to an absolute visual magnitude⁵ $M_V^* \approx -21.2 + 5 \log_{10} h_{50}$ for Abell's form (Austin *et al.*, 1975), and $M_V^* \approx -21.9 + 5 \log_{10} h_{50}$ for Schechter's form (Schechter, 1976). By comparing these values with the apparent magnitude m^* derived from the observed luminosity function of a cluster, one can derive a distance estimate for the cluster (Bautz and Abell, 1973; Schechter and Press, 1976). Unfortunately, this requires that magnitudes be available for a large number of galaxies.

The magnitude of the brightest galaxy in a cluster has often been used as a distance indicator in cosmological studies (see, for example, Hoessel, Gunn, and Thuan, 1980). It is obviously easier to determine observationally than the luminosity function. Moreover, the luminosities of the brightest cluster galaxies show a very small variation from cluster to cluster (Sandage, 1976) and depend only weakly on richness. There has been a controversy concerning whether the luminosities of these brightest galaxies are determined statistically by the cluster luminosity function, or whether the brightest galaxies are produced by some special physical processes operating in clusters (see Dressler, 1984, for a review). Under the statistical hypothesis, all of the galaxy luminosities are random variables drawn from the luminosity function (Geller and Peebles, 1976). Then, the observed number of galaxies in any luminosity range will have a Poisson distribution about the expectation given by the luminosity function, and the luminosity L_1 of the brightest galaxy will thus be distributed as $\exp[-N(L_1)]n(L_1)dL_1$. As $N(L_1)$ is proportional to richness, the statistical model

⁵The absolute magnitude is the magnitude an object would have if it were moved to a distance of 10 parsecs (3.086×10^{19} cm) from the Earth. See footnotes 2, 3, and 4.

predicts that L_1 increases with cluster richness, which is not really observed (Sandage, 1976). However, Schechter and Peebles (1976) have argued that the near constancy of L_1 results from a selection effect (that is, the observed sample is biased), and that the statistical hypothesis may still be valid.

Alternatively, the brightest cluster galaxies may be affected by special physical processes, such as the tidal interactions or mergers of galaxies (Peach, 1969; Ostriker and Tremaine, 1975; Richstone, 1975; Hausman and Ostriker, 1978). Evidence that this may indeed be the case is given in Sec. II.J.1.

While the luminosity functions of many clusters are reasonably well represented by the Schechter or Abell form with a universal value of M^* , significant departures exist in a number of clusters (Oemler, 1974; Mottmann and Abell, 1977; Dressler, 1978b). These departures include variations in the value of M^* , variations in the slope of the faint end of the luminosity function [α in Schechter's form, Eq. (2.3)], and variations in the steepness of the bright end of the luminosity function (Dressler, 1978b). These variations are, in many cases, correlated with cluster morphology (Sec. II.E). The variations in M^* and α probably reflect variations in the conditions in the cluster at its formation, while the variations in the bright end slope may result from evolutionary changes, such as the tidal interaction or merging of massive galaxies (Richstone, 1975; Hausman and Ostriker, 1978). In particular, the clusters with the steepest luminosity functions at the bright end often contain cD galaxies (Dressler, 1978b); this may indicate that the brighter galaxies were either eliminated by mergers to form the cD or diminished in brightness through tidal stripping (Sec. II.J.1).

Turner and Gott (1976a) have shown that the luminosity function of galaxies in small groups is well represented by Eq. (2.3). In fact, Bahcall (1979a) has suggested that the luminosity function of all galaxian systems—from single galaxies (in or out of clusters) to the groups and clusters themselves—can be fit in a single function similar to the Schechter form [Eq. (2.3)].

E. Morphological classification of clusters

A number of different cluster properties have been used to construct morphological classification systems for clusters. Somewhat surprisingly, these different systems are highly correlated, and it appears that clusters can be represented very crudely as a one-dimensional sequence, running from *regular* to *irregular* clusters (Abell, 1965, 1975). There is considerable evidence that the regular clusters are dynamically more evolved and relaxed than the irregular clusters. The various morphological classification schemes are described below, and the way in which they fit into the one-dimensional sequence is summarized in Table II, which is adapted from Abell (1975) and Bahcall (1977a).

Zwicky *et al.* (1961–1968) classified clusters as *compact*, *medium compact*, or *open*. A *compact* cluster has a single pronounced concentration of galaxies, with more than ten galaxies appearing in contact as seen on the plate. A *medium compact* cluster has either a single concentration with ten galaxies separated by roughly their own diameters, or several concentrations. An *open* cluster lacks any pronounced concentration of galaxies.

Bautz and Morgan (1970) give a classification system based on the degree to which the cluster is dominated by its brightest galaxies. Bautz-Morgan *type I* clusters are dominated by a single, central cD galaxy; cD galaxies have the most luminous and extensive optical emission found in galaxies (see Sec. II.J.1). In *type II* clusters, the brightest galaxies are intermediate between cD and normal giant ellipticals, while in *type III*, there are no dominating cluster galaxies. *Type I-II* and *type II-III* are intermediates. Leir and van den Bergh (1977) have classified 1889 rich Abell clusters on the Bautz-Morgan system, and some of the newer southern catalogs (e.g., White and Quintana, 1985) give Bautz-Morgan types for their clusters.

The original Rood-Sastry (1971) classification system is based on the nature and distribution of the ten brightest cluster galaxies. Basically, the six Rood-Sastry (RS) classes are defined as follows:

TABLE II. Properties of morphological classes of clusters.

Property	Regular	Intermediate	Irregular
Zwicky type	compact	medium-compact	open
Bautz-Morgan type	I, I-II, II	II, II-III	II-III, III
Rood-Sastry type	cD, B, L, C	L, C, F	F, I
Galactic Content	elliptical rich	spiral poor	spiral rich
E:SO:Sp	3:4:2	1:4:2	1:2:3
Morgan type	ii	i-ii	i
Oemler type	cD, spiral poor	spiral poor	spiral rich
Symmetry	spherical	intermediate	irregular
Central concentration	high	moderate	low
Subclustering	absent	moderate	significant
Richness	rich $n^* \approx 10^2$	rich-moderate $n^* \geq 10^1$	rich-poor $n^* \geq 10^0$

cD: the cluster is dominated by a central cD galaxy (example: A2199). cD galaxies were defined by Mathews, Morgan, and Schmidt (1964) as galaxies with the nucleus of a very luminous elliptical galaxy embedded in an extended, amorphous optical halo of low surface brightness. They are generally found near the center of dense clusters and groups of galaxies. They are, as a class, the most luminous galaxies known if one excludes nuclear sources, such as quasars. cD galaxies are discussed extensively in Sec. II.J.1.

B: binary—the cluster is dominated by a pair of luminous galaxies [example: A1656 (Coma)].

L: line—at least three of the brightest galaxies appear to be in a straight line [example: A426 (Perseus)].

C: core—four or more of the ten brightest galaxies form a cluster core, with comparable galaxy separations [example: A2065 (Corona Borealis)].

F: flat—the brightest galaxies form a flattened distribution on the sky [example: A2151 (Hercules)].

I: irregular—the distribution of brightest galaxies is irregular, with no obvious center or core (example: A400).

Rood and Sastry (1971) give classifications for low-redshift Abell clusters on this system. They show that these classifications form a bifurcated sequence, which can be represented by a “tuning-fork” diagram [Fig. 3(a)]. This sequence is correlated with the sequence of *regular* to *irregular* clusters in the sense that clusters on the left of the diagram (cD and B) are regular and those to the

right (F and I) are irregular. Rich clusters are more or less equally distributed among the three arms of the diagram.

Recently, Struble and Rood (1982,1984) have proposed a revised version of the RS classification system. The definitions have been revised slightly, and a number of subclasses of the main RS classes have been proposed. More significantly, Struble and Rood have rearranged the “tuning fork” diagram into a “split linear” diagram [Fig. 3(b)], based on systematic trends in the galaxy distribution and content of clusters. This new scheme was devised in part from a comparison to numerical N -body simulations of the collapse of clusters (White, 1976c; Carnevali *et al.*, 1981; Farouki *et al.*, 1983; also see Fig. 4 below). Struble and Rood propose that this sequence represents an evolutionary sequence of clusters from irregular I to cD clusters.

Morgan (1961) and Oemler (1974) have constructed classification systems based on the galactic content of clusters [that is, the fraction of cluster galaxies which are spirals (Sp's), disk galaxies without spiral structure (SO's), or elliptical (E's)]. Morgan (1961) classified clusters as *type i* if they contained large numbers of spirals and as *type ii* if they contained few spirals. Oemler (1974) has refined this system, defining three classes of clusters: *spiral-rich* clusters, in which spirals (Sp) are the most common galaxies; *spiral-poor* clusters, in which spirals are less common and SO's are the most common galaxies; and *cD* clusters, which are dominated by a central cD galaxy and in which the great majority of galaxies are ellipticals or SO's.

These systems of classification are empirically found to be highly correlated, and can roughly be mapped into a one-dimensional sequence running from *regular* clusters to *irregular* clusters (Abell, 1965,1975). As shown in Table II, *regular* clusters are highly symmetric in shape and have a core with a high concentration of galaxies toward the center. Subclustering is weak or absent in *regular* clusters. In contrast, *irregular* clusters have little symmetry or central concentration and often show significant subclustering. This suggests that the *regular* clusters are, in some sense, dynamically relaxed systems, while the *irregular* clusters are dynamically less evolved and have preserved roughly their distribution of formation. Additional evidence that regular clusters are dynamically relaxed is provided in Secs. II.F, II.G, and II.J.1, and the nature of the dynamical processes that might produce this relaxation is discussed in Sec. II.I.

Regular clusters tend to be *compact* (Zwicky type), Bautz-Morgan *type I* to *II*, Rood-Sastry types *cD* or *B*, Morgan *type ii*, Oemler *spiral-poor* or *cD* clusters. These last four correlations indicate a connection between the dynamical state and galactic content of clusters. There is no one-to-one correlation between the morphology of a cluster and its richness; *regular* clusters are always rich, while *irregular* clusters may be either rich or sparse. However, *regular* clusters tend to have higher central galaxy densities than *irregular* clusters, because they are at least as rich and more compact.

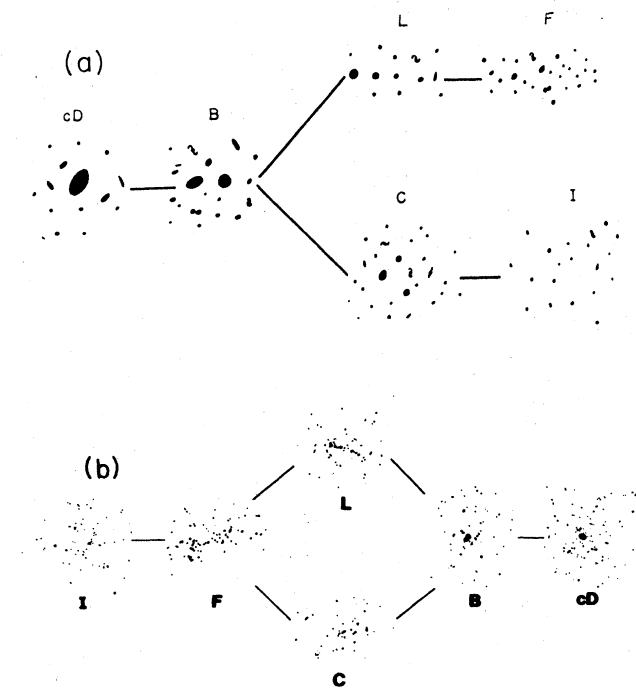


FIG. 3. (a) The Rood-Sastry (1971) cluster classification scheme. (b) The revised Rood-Sastry classes from Struble and Rood (1982).

F. Velocity distribution of galaxies

The existence of the morphological sequence of clusters from irregular to regular clusters (Sec. II.E) suggests that the regular clusters may have undergone some sort of dynamical relaxation. The nature of this relaxed distribution is examined in the next two sections through the distribution of cluster galaxy velocities and positions.

The redshifts in Sec. II.B are determined from the mean radial velocity of galaxies in a cluster; in fact, the radial velocities of individual galaxies are distributed around this mean. It has been conventional to characterize this distribution by the dispersion σ_r of radial velocities about the mean

$$\sigma_r = \langle (v_r - \langle v_r \rangle)^2 \rangle^{1/2}, \quad (2.4)$$

where v_r is the radial velocity, which is the component of the galaxy velocity along the line of sight. The dispersion completely characterizes the radial velocity distribution function if it is Gaussian:

$$p(v_r) dv_r = \frac{1}{\sigma_r \sqrt{2\pi}} \exp[-(v_r - \langle v_r \rangle)^2 / 2\sigma_r^2] dv_r. \quad (2.5)$$

Here, $p(v_r)dv_r$ is the probability that an individual cluster galaxy has a radial velocity in the range v_r to $v_r + dv_r$. While the Gaussian distribution has usually been adopted simply for convenience, statistical tests reveal that it is a consistent fit to the observed total distribution function in many clusters, at least if high velocities ($|v_r - \langle v_r \rangle| > 3\sigma_r$) are excluded (Yahil and Vidal, 1977). However, the velocity dispersion in a given cluster generally decreases with distance from the cluster center; in Coma and Perseus the decline is about a factor of 2 from the center to the outer edge (Rood *et al.*, 1972; Kent and Gunn, 1982; Kent and Sargent, 1983). Moreover, the velocity dispersion can differ in different clumps of an irregular cluster showing subclustering (Geller and Beers, 1982; Bothun *et al.*, 1983).

A Gaussian distribution for a single component of the velocity obtains for a system of nonidentical particles in thermodynamic equilibrium, in which case we identify the velocity dispersion with $\sigma_r \equiv (kT/m)^{1/2}$, where T is the galaxy "temperature" and m the galaxy mass. While the Gaussian velocity distribution found in clusters suggests that they are at least partially relaxed systems, they are not fully relaxed to thermodynamic equilibrium. In thermodynamic equilibrium, all components of the cluster would have equal temperatures; what is observed is that it is the velocity dispersion (not temperature) which is nearly independent of galaxy mass and position (Rood *et al.*, 1972; Kent and Gunn, 1982; Kent and Sargent, 1983).

Some variation of the velocity dispersion with galaxy mass or cluster position is observed (Rood *et al.*, 1972; Kent and Gunn, 1982; Kent and Sargent, 1983). In the Coma and Perseus clusters, the most luminous galaxies have a somewhat smaller velocity dispersion than the less luminous galaxies, and the velocity dispersion decreases

with increasing projected distance from the cluster center. In fact, the latter effect must necessarily occur if clusters are finite, bound systems. Then, the velocities of bound galaxies at any point in the cluster cannot exceed the escape velocity at that position. As the escape velocity decreases with increasing distance from the cluster center, the velocity dispersion must also decrease with projected distance from the cluster center.

The observed mean galaxy velocity $\langle v_r \rangle$ will depend on the projected position in the cluster if the cluster is rotating. The projected shapes of many clusters are substantially flattened. Of course, this is true of the L (line) and F (flat) clusters (Sec. II.E); however, many regular (cD and B) clusters are also significantly flattened (Abell, 1965; Dressler, 1981). If these clusters are actually oblate in shape due to significant rotational support, the variation in $\langle v_r \rangle$ across the cluster would be expected to be comparable to σ_r . In fact, such large velocity gradients are not observed (Rood *et al.*, 1972; Gregory and Tifft, 1976; Schipper and King, 1978; Dressler, 1981); apparently, the flattening of clusters is not due to rotation.

Useful compilations of velocity dispersions for clusters have been given by Hintzen and Scott (1979), Danese *et al.* (1980), and particularly Noonan (1981).

G. Spatial distribution of galaxies

1. Models for galaxy distributions

The most regular clusters show a smooth galaxy distribution with a concentrated core (Table II). In general, models to describe the galaxy distribution in these clusters will possess at least five parameters, which can be taken to be the position of the cluster center on the sky, the central projected density of galaxies per unit area of the sky σ_0 , and two distance scales r_c and R_h . The core radius r_c is a measure of the size of the central core, and is usually defined so that the projected galaxy density at a distance r_c from the cluster center is one-half of the central density σ_0 . The halo radius R_h measures the maximum radial extent of the cluster. If the cluster is elongated, at least two more parameters are necessary; these can be taken to be the orientation of the semimajor axis of the cluster on the sky, and the ratio of semimajor to semiminor axes.

Of course, the observed value of the central density σ_0 must depend on the range of galaxy magnitudes observed, and the values of other parameters may also depend on galaxy magnitude. However, spherically symmetric galaxy distributions will be discussed first, and r_c and R_h will be assumed to be independent of galaxy mass or luminosity. Then, one can write

$$\begin{aligned} n(r) &= n_0 f(r/r_c, r/R_h), \\ \sigma(b) &= \sigma_0 F(b/r_c, b/R_h), \end{aligned} \quad (2.6)$$

where $n(r)$ is the spatial volume density of galaxies at a

distance r from the cluster center, n_0 is the central ($r = 0$) density, $\sigma(b)$ is the projected surface density at a projected radius b , and f and F are two dimensionless functions. Obviously,

$$\sigma(b) = 2 \int_b^{R_h} \frac{n(r)r dr}{(r^2 - b^2)^{1/2}}. \quad (2.7)$$

A number of models have been proposed to fit the distribution of galaxies. Among the simplest are the isothermal models, which assume a Gaussian radial velocity distribution for galaxies [Eq. (2.5)]. If one further assumes that the velocity distribution is isotropic and independent of position, that the galaxy distribution is stationary, and that galaxy positions are uncorrelated, then one can write the galaxy phase-space density $f(\mathbf{r}, \mathbf{v})$ as

$$f(\mathbf{r}, \mathbf{v}) d^3r d^3v = n(r) (2\pi\sigma_r^2)^{-3/2} \times \exp \left[-\frac{1}{2} \left(\frac{v}{\sigma_r} \right)^2 \right] d^3v d^3r. \quad (2.8)$$

Now, the time scale for two-body gravitational interactions in a cluster is much longer than the time for a galaxy to cross the cluster (see Sec. II.I). Thus the galaxies can be considered to be a collisionless gas, and the phase-space density f is conserved along particle trajectories (Liouville's theorem); f is then a function of only the integrals of the motion ("Jeans's theorem"). If the velocity distribution is isotropic, f does not depend on the orbital angular momentum of the galaxies, and can only depend on the energy per unit mass $\epsilon = \frac{1}{2}v^2 + \phi(r)$, where $\phi(r)$ is the gravitational potential of the cluster. If we measure $\phi(r)$ relative to the cluster center, the galaxy spatial distribution is thus $n(r) = n_0 \exp[-\phi(r)/\sigma_r^2]$. If the mass in the cluster is distributed in the same way as the galaxies, then Poisson's equation for the gravitational potential becomes

$$\frac{1}{r^2} \frac{d}{dr} \left[r^2 \frac{d\phi}{dr} \right] = 4\pi G n_0 m \exp(-\phi/\sigma_r^2), \quad (2.9)$$

where m is the mass per galaxy (Chandrasekhar, 1942). It is conventional to make the change of variables $\psi \equiv \phi/\sigma_r^2$, $\xi \equiv r/\beta$, $\beta \equiv \sigma_r/(4\pi G n_0 m)^{1/2}$. Then the equation for ψ is

$$\frac{1}{\xi^2} \frac{d}{d\xi} \left[\xi^2 \frac{d\psi}{d\xi} \right] = e^{-\psi}, \quad (2.10)$$

subject to the boundary conditions (assuming the density is regular at the cluster center) of $\psi = 0$, $d\psi/d\xi = 0$ at $\xi = 0$. Equation (2.10) is identical to the equation for an isothermal gas sphere in hydrostatic equilibrium (Chandrasekhar, 1939).

The galaxy density distribution in this isothermal sphere model is then $n(\xi) = n_0 \exp[-\psi(\xi)]$. The projected galaxy density can be calculated from Eq. (2.7) and written as $\sigma(b) = \sigma_0 F_{\text{isot}}(b/\beta)$. For convenience, the core radius r_c is defined as $r_c \equiv 3\beta$, because $F_{\text{isot}}(3) \approx 0.502$, which is sufficiently close to one-half. The central volume density and projected density are re-

lated by $\sigma_0 \approx 6.06 n_0 \beta = 2.02 n_0 r_c$. Unfortunately, neither $\psi(\xi)$ nor F_{isot} can be represented by simple analytic functions. Relatively inaccurate tables of these functions are given in Zwicky (1957, p. 139), and more accurate economized analytic approximations to ψ and F_{isot} have been given by Flannery and Krook (1978) and Sarazin (1980), respectively.

At large radii $\xi \gg 1$, $n(\xi) \approx 2 n_0 / \xi^2$, and the total number of galaxies and total mass diverge in proportion to r . Thus the isothermal sphere cannot accurately represent the outer regions of a finite cluster. A number of methods to truncate the isothermal distribution have been used. If one is primarily concerned with representing the galaxy distribution near the core, and if one is not concerned with determining dynamically consistent velocity and spatial distributions, one can simply truncate the isothermal distribution at some radius. Zwicky (1957, p. 140) and Bahcall (1973a) have truncated the isothermal distribution with a uniform surface density cutoff C :

$$\sigma(b) = \frac{\sigma_0 [F_{\text{isot}}(b/\beta) - C/6.06]}{1 - C/6.06}. \quad (2.11)$$

The cluster galaxy density then falls to zero at a radius R_h given by $F_{\text{isot}}(R_h/\beta) = C/6.06$. Bahcall (1973a) also defines a modified central surface density parameter $\alpha \equiv \sigma_0/(6.06 - C)$; then, for small $C \ll 2\pi$, the central volume density is just $n_0 \approx \sigma_0 [1 - (C/2\pi)^2]/(6.06\beta) \approx \alpha/\beta$.

King (1966) has developed self-consistent truncated density distributions for clusters. The phase-space density he assumes is

$$f(\mathbf{r}, \mathbf{v}) d^3r d^3v \propto \exp \left[\frac{\phi(0) - \phi(r)}{\sigma_{r\infty}^2} \right] \times \left[\exp \left[-\frac{v^2}{2\sigma_{r\infty}^2} \right] - \exp \left[\frac{\phi(r)}{\sigma_{r\infty}^2} \right] \right] d^3r d^3v, \quad (2.12)$$

where $\sigma_{r\infty}$ is the radial velocity dispersion in an untruncated cluster. The velocity distribution is thus truncated at the escape velocity v_e : $f(\mathbf{r}, |\mathbf{v}| \geq v_e) = 0$ where $v_e^2 = -2\phi(r)$, and the potential goes to zero at infinity $\phi(\infty) = 0$. King showed that Eq. (2.12) gave an approximate solution to the Fokker-Planck equation for a finite cluster subject to two-body gravitational encounters. As shown in Sec. II.I, galaxy clusters are nearly collisionless; however, it is possible that Eq. (2.12) is a reasonable approximation for the truncated phase-space density. The phase-space density f in Eq. (2.12) is a function of only the energy per unit mass ϵ and the parameter $\sigma_{r\infty}^2$, and thus satisfies Jeans's theorem. King integrates Eq. (2.12) over all velocities to give the density $n(r)$ as a function of the potential $\phi(r)$, and then solves Poisson's equation to give a self-consistent potential. The density $n(r)$ in these models falls continuously to zero at a finite radius R_h . The models can be scaled in distance and central density

as with the unbounded isothermal models described earlier. The only characteristic parameter is $\sigma_r(0)/\sigma_{r\infty}$ or equivalently R_H/r_c (where r_c is again the core radius). King prefers to use the potential difference between cluster center and edge, $W_0 \equiv [\phi(R_h) - \phi(0)]/\sigma_{r\infty}^2$. These models predict that the velocity dispersion declines in the outer portions of the cluster, as is observed in Coma (Rood *et al.*, 1972).

Unfortunately, none of these bounded or unbounded isothermal models can be represented exactly in terms of simple analytic functions. However, King (1962) showed that the following analytic functions were a reasonable approximation to the inner portions of an isothermal function:

$$\begin{aligned} n(r) &= n_0[1+(r/r_c)^2]^{-3/2}, \\ \sigma(b) &= \sigma_0[1+(b/r_c)^2]^{-1}, \end{aligned} \quad (2.13)$$

where $\sigma_0 = 2n_0r_c$. At large radii $r \gg r_c$, $n(r) \approx n_0(r_c/r)^3$ in the analytic King model; thus the cluster mass and galaxy number diverge as $\ln(r/r_c)$. Although this is a slower divergence than the unbounded isothermal model, this analytic King model also must be truncated at some finite radius R_h .

Another analytic model is that of de Vaucouleurs (1948a), which was proposed to fit the distribution of surface brightness in elliptical galaxies. However, this distribution also fits many regular clusters (de Vaucouleurs, 1948b). The projected density is

$$\sigma(b) = \sigma_0 \exp[-7.67(b/r_e)^{1/4}], \quad (2.14)$$

where r_e is an effective radius such that one-half of the galaxies lie at projected radii $b \leq r_e$. Accurate tables of the three-dimensional density and potential for this model have been given by Young (1976). The de Vaucouleurs law has a density spike at the cluster center; in fact, some clusters show such a spike, which much be removed in order to fit isothermal sphere models to the galaxy distribution (see Table III below). The de Vaucouleurs form has several other advantages; first, it has only one distance scale, the effective radius r_e . It also converges to a finite total number of galaxies and cluster mass without a cut-off radius. Finally, numerical simulations of the collapse of clusters seem to lead to distributions similar to this form (see Sec. II.1.2). Unfortunately, the de Vaucouleurs form has not been widely used to fit galaxy distributions in clusters, and there have been few attempts to determine objectively whether it or the isothermal models give better fits to the actual distributions.

Another useful fitting form is the Hubble (1930) profile, which is sometimes used to fit the light distribution in elliptical galaxies. It is

$$\sigma(b) = \sigma_0 \left[1 + \frac{b}{r_c} \right]^{-2}, \quad (2.15)$$

which has the same asymptotic distribution as Eq. (2.13).

2. Core radii

These models [Eqs. (2.11)–(2.15)] have been used to fit the projected distribution of galaxies (see the references to Table III). In most cases, the galaxy distributions have been fit to the truncated isothermal model [Eq. (2.11)]. The derived values of the core radii for a sample of clusters are given in Table III; the numerical values assume a Hubble constant of $H_0 = 50$ km/sec/Mpc. For a number of clusters, there have been several determinations of the core radius, as shown in the table. These determinations often do not agree within the estimated errors. Because values of the core radius are essential to the detailed modeling of x-ray emission from clusters (Sec. V.E), the methods of determining core radii and possible explanations of this discrepancy will be discussed.

Most of the galaxy distributions in Table III have been derived using the method of radial binning and χ^2 fitting. This standard method (Zwicky, 1957; Bahcall, 1973a; Avni and Bahcall, 1976) consists of first projecting the galaxy distribution separately in two orthogonal directions. The separate maxima in these directions give the coordinates of the cluster center. Then, the galaxies are binned in rings centered on this cluster center, and the radial distribution is determined by fitting the ring counts to the hypothetical distribution while minimizing χ^2 . There are a number of problems with this standard method of analysis. First, it necessarily involves binning the data, in order to convert a multivariate distribution into one which is univariate. Second, the standard method cannot simultaneously fit all of the cluster parameters; the separate determinations of the two cluster center coordinates and the radial distribution may not be consistent. Finally, it is rather difficult to apply the standard method to clusters that are not axially symmetric (Bahcall, 1974a).

Sarazin (1980) proposed that the maximum likelihood (ML) method be applied directly to the distribution of individual galaxies, rather than applying it to the numbers of galaxies in bins (the standard χ^2 method). This technique has substantial advantages when compared to the standard method. It involves no binning of the data, so that it makes full use of all the positional information on the galaxies, and no artificial scale is introduced by the rings. The ML method can simultaneously determine all parameters of a cluster, or if desired, any subset of parameters with the others held fixed. It does not assume that the cluster is axially symmetric; it can fit any given cluster distribution function to the observed galaxy positions. It has a number of very favorable statistical properties; the ML method is asymptotically unbiased, minimum variance, and normally distributed. Thus the ML method provides the most accurate and precise estimate of the cluster parameters possible with the given data when applied to a sufficiently large data set.

The maximum likelihood method has been applied to determine galaxy distributions in a number of clusters (Sarazin, 1980; Johnston *et al.*, 1981; Sarazin and Quintana, 1985); clusters analyzed in this fashion are marked

TABLE III. Core radii of galaxy distributions in clusters in Mpc, for cosmological parameters $H_0=50$ km/sec/Mpc and $q_0=0$. First, Abell clusters are given, and then other clusters listed in order of increasing redshift. Non-Abell clusters are listed either by their name in the Zwicky catalog or by their right ascension and declination (see footnote 1 in the text). References are listed at the bottom.

Cluster	r_c	Ref.	Cluster	r_c	Ref.	Cluster	r_c	Ref.
A31	0.28±0.08	B	A1139	0.48±0.05	BS	A2165	0.39±0.10	BS
	0.49±0.08 ^b	B	A1146	0.61±0.20	BS	A2197	0.44±0.05	BS
A98	0.40±0.11 ^a	SQ	A1185	0.48±0.04	BS	A2199	0.22±0.15	B
	0.48	D	A1228	0.64±0.11	BS	A2218	0.27±0.07 ^a	SQ
A119	0.54±0.11	BS	A1257	0.41±0.04	BS		0.15±0.02	Bi
A147	0.51±0.07	BS	A1314	0.51±0.10	BS		0.40	D
A154	0.17±0.06 ^{a,b}	SQ	A1367	0.34±0.10	B	A2256	0.20±0.09	B
	0.19	D	A1413	0.46±0.11 ^a	SQ		0.24±0.07 ^a	SQ
	0.44 ^b	D		0.57	D		0.49	D
A168	0.30±0.19 ^a	SQ		0.52±0.11	AP	A2319	0.22±0.12	B
	0.55	D	A1553	0.41±0.06	AP		0.39±0.06	Bi
A194	0.23±0.15	B	A1589	0.46±0.08	BS	A2593	0.32±0.11	BS
A195	0.38±0.07	BS	A1643	0.37±0.06	AP	A2597	0.50±0.07	BS
A272	0.49±0.15	BS	A1656	0.25±0.10	B	A2634	0.54±0.09	BS
A274	0.24±0.20 ^{a,b}	SQ		0.31±0.06 ^a	S	A2657	0.47±0.07	BS
	0.30	D		0.22	Z	A2666	0.37±0.08	BS
A400	0.46±0.08	BS		0.50±0.10	BS	A2670	0.24±0.08 ^a	SQ
A401	0.42±0.11 ^a	SQ		0.45±0.09	Q		0.62±0.15	BS
	0.40	D		0.53±0.09 ^b	Q		0.31	D
	0.24±0.12	B		0.84	A			
A426	0.22±0.07	B		1.30±0.2	dF	0818 + 2106	0.15	Z
	0.31	Z	A1677	0.25±0.12	AP	ZW478-5	0.23±0.10	BS
A478	0.20±0.08	BaS	A1736	0.51±0.07	BS	ZW211-58	0.29±0.10	BS
A505	0.65±0.16	BS	A1775	0.26±0.19	B	ZW499-13	0.34±0.10	BS
A520	0.57±0.27	BS	A1795	0.25±0.08	B	1359-1128	0.49±0.09	BS
A539	0.46±0.06	BS	A1904	0.24±0.11	B	ZW430-21	0.50±0.09	BS
A548	0.33±0.06	BS	A1930	0.57±0.09	AP	1709-233	0.30±0.18 ^a	J
A576	0.48±0.04	BS	A1940	0.48±0.16 ^a	SQ	ZW406-13	0.35±0.07	BS
	0.31±0.03	Bi		0.52	D	0627-5426	0.42	M
A634	0.51±0.05	BS	A1983	0.53±0.13	BS	0340-538	0.34±0.03	HQ
A665	1.07±0.28	SQ	A2029	0.27±0.16	B	0431-6133	0.45	M
	0.55	D		0.59±0.15 ^{a,b}	SQ	0106 + 1304	0.54±0.09	BS
A732	0.44±0.26	BS		0.35	D	2122 + 1549	0.51±0.12	BS
	0.23±0.08	AP		0.68 ^b	D	0237-0147	0.38±0.13	BS
A754	0.38±0.09	BS	A2048	0.35±0.06	BS	0024 + 1654	0.23±0.02	B
A801	0.47±0.09	AP	A2052	0.28±0.08	B	0949 + 4409	0.58±0.12	BS
A838	0.51±0.08	BS	A2065	0.29±0.08	B	0024 + 1654	0.37±0.11	BS
A1020	0.75±0.19	BS		0.39±0.03	BS	1410 + 5224	0.45±0.17	BS
A1060	0.24	Z	A2100	0.47±0.06	BS	0016 + 16	0.38	K
A1132	0.21±0.03	B		0.36±0.10		1609 + 6605	0.53±0.19	BS
	0.53±0.25	BS	A2151	0.47±0.05	BS	1305 + 2952	0.58±0.22	BS
	0.37±0.06	AP	A2162	0.59±0.13	BS			

References

A	Abell (1977)	AP	Austin and Peach (1974a,1974b)
B	Bahcall (1973a,1973b,1975)	BaS	Bahcall and Sargent (1977)
Bi	Birkinshaw (1979)	BS	Bruzual A. and Spinrad (1978)
dF	des Forets <i>et al.</i> (1984)	D	Dressler (1978c)
HQ	Havlen and Quintana (1978)	J	Johnston <i>et al.</i> (1981)
K	Koo (1981)	M	Materne <i>et al.</i> (1982)
Q	Quintana (1979)	S	Sarazin (1980)
SQ	Sarazin and Quintana (1985)	Z	Zwicky (1957)

^aUses maximum likelihood method.

^bA central spike in the galaxy distribution was removed.

with a superscript a in Table III.

Sarazin and Quintana (1985) found that the discrepancies in previous results were due in part to binning problems, to problems with not fitting the cluster center simultaneously, and also to differences in the background correction. In general, clusters are not well fit by a truncated isothermal sphere plus a universal background. The background determined by fitting the galaxy distribution in the clusters was often a factor of 3 higher than the standard galaxy background. Apparently, clusters either have extended envelopes or are usually contained in extended regions of higher density (i.e., superclusters, Sec. II.K.2). If a lower general value for the background is assumed, the core size is artificially inflated to fit the higher background, and this effect operates most strongly at larger magnitudes, where the background correction is more significant. This increase in the core radius with magnitude has previously been taken as evidence for mass segregation in clusters (Quintana, 1979; Capelato *et al.*, 1980). However, when the background is determined by the data and independent magnitude samples are used (Sarazin, 1980), only weak evidence for mass segregation is found. A more fundamental problem is that many clusters show strong subclustering (Geller and Beers, 1982) and are not well fit by a single isothermal sphere.

Bahcall (1975) has suggested that the core radii of regular clusters are all very similar, with an average value

$$r_c = (0.25 \pm 0.04) h_{50}^{-1} \text{ Mpc}. \quad (2.16)$$

Sarazin and Quintana (1985) find that this may be true for the most compact, regular clusters. However, they also find that the core radius and galaxy distribution depend on the morphology of the cluster (Sec. II.E).

3. Other parameters and sizes

The statistical uncertainty in the determination of the core radius or central density of a cluster tends to be rather large ($\geq 30\%$), because even in a rich cluster only a small fraction of the galaxies are within the core. However, the errors in σ_0 and r_c are highly anticorrelated, so that the product $(\sigma_0 r_c)$ is relatively well determined. The reason for this is that the number of galaxies within a projected radius b such that $r_c < b \ll R_h$ is roughly $N(b) \approx 2.17 (\sigma_0 r_c) b$ for an isothermal model. Thus the uncertainty in the product $(\sigma_0 r_c)$ tends to be determined by Poisson statistics on the total number of cluster galaxies observed, and not just by the smaller number in the core (Sarazin and Quintana, 1985). Bahcall (1977b, 1981) has defined a related quantity \bar{N}_0 as the number of "bright galaxies" with projected positions within 0.5 Mpc of the cluster center. Here, "bright galaxies" are those no more than two magnitudes fainter than the third brightest galaxy ($m \leq m_3 + 2$). Of course, the magnitude of the third brightest galaxy m_3 itself depends on richness; \bar{N}_0 is the number corrected for richness assuming a universal luminosity function (Sec. II.D). From the discussion above, it is clear that $\bar{N}_0 \propto (\sigma_0 r_c)$, if σ_0 is taken at a

standard luminosity level [for example, L^* (Sec. II.D)], and if $r_c \lesssim 0.5 \text{ Mpc} \ll R_h$.

Because they are better determined statistically than the core radius r_c or center surface density σ_0 , $(\sigma_0 r_c)$ and \bar{N}_0 are often more useful as richness parameters when searching for correlations of integral properties of clusters in the optical, radio, and x ray. However, when comparing detailed spatial distributions the core radius is needed.

For example, from the arguments given above $\sigma_0 r_c \propto \bar{N}_0 \propto n_0 r_c^2$, if σ_0 and n_0 are taken at a standard luminosity level. From Eq. (2.9), $r_c^2 = 9 \sigma_r^2 / 4\pi G n_0 m$, where m is the average galaxy mass $m \equiv \rho_0 / n_0$, and ρ_0 is the central mass density. As n_0 is defined at a fixed luminosity level, this gives $(\sigma_0 r_c) \propto \bar{N}_0 \propto (M/L)^{-1} \sigma_r^2$, where (M/L) is the mass-to-light ratio of the cluster (Sec. II.H). Bahcall (1981) finds the empirical correlation $\bar{N}_0 \approx 21 (\sigma_r / 10^3 \text{ km sec}^{-1})^{2.2}$, which suggests that cluster mass-to-light ratios decrease with σ_r . This relationship may be useful for providing quick estimates of the velocity dispersions of clusters.

Several other size scales can be determined for clusters. The halo radius R_h gives the outermost limit of the cluster. Unfortunately, this is very poorly determined, because it depends critically on the assumed background. Moreover, clusters often have very extended halos or are embedded in extended regions of enhanced density (superclusters). For Coma, the main isothermal distribution of galaxies extends to roughly $4 h_{50}^{-1} \text{ Mpc}$; there is then a low-density halo extending to $\sim 10 h_{50}^{-1} \text{ Mpc}$, which blends into the Coma supercluster which extends to a radius of about $35 h_{50}^{-1} \text{ Mpc}$ (Rood *et al.*, 1972; Rood, 1975; Chincarini and Rood, 1976; Abell, 1977; Gregory and Thompson, 1978; Shectman, 1982). However, studies of the galaxy covariance function (Peebles, 1974) suggest that there are no preferred scales for galaxy clustering and that the outer regions of clusters and superclusters represent a continuous distribution of clustering.

Other size scales for clusters have been measured that are intermediate between the core and halo size; they include the harmonic mean galaxy separation (Hickson, 1977), which is related to the gravitational radius R_G of a cluster (Sec. II.H), the de Vaucouleurs effective radius r_e defined by Eq. (2.14), the mean projected distance from the cluster center (Noonan, 1974; Capelato *et al.*, 1980), and the Leir and van den Bergh radius (1977).

4. Elongation, alignment, and other complications

While the distribution functions for galaxies discussed above are spherically symmetric, most clusters appear to be at least slightly elongated, and some are highly elongated (Sastry, 1968; Rood and Sastry, 1972; Rood *et al.*, 1972; Bahcall, 1974a; MacGillivray *et al.*, 1976; Thompson and Gregory, 1978; Carter and Metcalfe, 1980; Dressler, 1981; Binggeli, 1982). Carter and Metcalfe (1980) and Binggeli (1982) give ellipticities and position angles for samples of Abell clusters. Their results suggest

that clusters have average intrinsic ellipticities of $\sim 0.5-0.7$; thus clusters are actually much more elongated on average than elliptical galaxies.

Carter and Metcalfe (1980) and Binggeli (1982) find that the position angles for the long axes of clusters are significantly aligned with the axis of the first brightest cluster galaxy. In Secs. II.I.3 and II.J.1, it is shown that such alignments may result if the first brightest galaxies are produced by the merger of smaller galaxies through dynamical friction. They might also be produced during the collapse of the cluster.

Thompson (1976) has suggested that the axes of many of the elliptical galaxies in clusters may be aligned with the cluster axis; Adams *et al.* (1980) find a similar effect in two linear (L; see Sec. II.E) clusters. Helou and Salpeter (1982) and Salpeter and Dickey (1985) do not find such alignments for the axes of spiral galaxies in the Virgo or Hercules clusters.

Binggeli (1982) finds that the long axes of Abell clusters tend to point at one another, even when the clusters are separated by as much as $\sim 30 h_{50}^{-1}$ Mpc. The alignments of nearby clusters were found to show evidence of a correlation even up to distances a factor of 3 larger.

The fact that clusters may be more elongated than galaxies and aligned on large scales suggests that structure in the universe may be built in on the largest scales, and cascade down to smaller scales. This will tend to occur if structure grows by the gravitational instability of initially small-amplitude, *adiabatic* perturbations in a uniform-density, expanding universe (Doroshkevich *et al.*, 1978). These perturbations are damped on all but the largest scales and are expected to collapse one-dimensionally to produce "pancakes." These pancakes might be associated with superclusters (see Sec. II.K.2); the plane of the pancake might give the direction for the alignment of cluster axes.

In the previous discussion, it has been assumed that the galaxy density decreases monotonically with distance from the cluster center. However, Oemler (1974) found a plateau or local minimum in the projected distribution of galaxies in many clusters at a radius of about $0.4R_G$ (where R_G is the gravitational radius). These features would imply the existence of significant oscillations in the three-dimensional galaxy density, although the process of deprojecting to counts is rather unstable (Press, 1976). Although these features are not statistically very significant in any one case, they do appear in a large number of clusters (Omer *et al.*, 1965; Bahcall, 1971; Austin and Peach, 1974a).

H. Cluster masses—the missing mass problem

The masses of clusters of galaxies can be determined if it is assumed that they are bound, self-gravitating systems. Cluster masses were first derived by Zwicky (1933) and Smith (1936). They found that the masses greatly exceed those which would be expected by summing the

masses of all the cluster galaxies. Recent reviews of cluster mass determinations include Faber and Gallagher (1979) and Rood (1981).

If clusters were not bound systems, they would disperse rather quickly (in a crossing time $t_{cr} \sim 10^9$ yr). Because many clusters appear regular and relaxed, and because their galactic content is quite different from that of the field, it is very unlikely that the regular compact clusters are flying apart. Assuming they are held together by gravity, one limit on the mass of clusters comes from the binding condition,

$$E = T + W < 0. \quad (2.17)$$

Here E is the total energy, T the kinetic energy, and W the gravitational potential energy:

$$T = \frac{1}{2} \sum_i m_i v_i^2, \quad (2.18)$$

$$W = -\frac{1}{2} \sum_{i \neq j} \frac{G m_i m_j}{r_{ij}},$$

where the sum is over all galaxies, m_i and v_i are the galaxy mass and velocity, and r_{ij} is the separation of galaxies i and j .

A stronger mass limit results if we assume that the cluster distribution is stationary. The equations of motion of galaxies can be integrated to give

$$\frac{1}{2} \frac{d^2 I}{dt^2} = 2T + W, \quad (2.19)$$

where $I = \sum m_i r_i^2$ is the moment of inertia measured from the center of mass. For a stationary configuration, the left-hand side of Eq. (2.19) is zero, and

$$W = -2T, \quad E = -T. \quad (2.20)$$

This is the virial theorem. The total cluster mass is $M_{tot} = \sum m_i$; we can define a mass-weighted velocity dispersion $\langle v^2 \rangle \equiv \sum m_i v_i^2 / M_{tot}$, and gravitational radius

$$R_G \equiv 2M_{tot}^2 \left[\sum_{i \neq j} m_i m_j / r_{ij} \right]^{-1}. \quad (2.21)$$

Then, the virial theorem gives

$$M_{tot} = \frac{R_G \langle v^2 \rangle}{G}. \quad (2.22)$$

Now, $\langle v^2 \rangle$ and R_G can be evaluated from the radial velocity distribution and the projected spatial distribution of a fair sample of galaxies if one assumes that the positions of galaxies and the orientation of their velocity vectors are uncorrelated. Then, $\langle v^2 \rangle = 3\sigma_r^2$, where σ_r is the (mass-weighted) radial velocity dispersion, and $R_G = (\pi/2) b_G$ (Limber and Mathews, 1960), where

$$b_G = 2M_{tot}^2 \left[\sum m_i m_j / b_{ij} \right]^{-1} \quad (2.23)$$

and b_{ij} is the projected separation of galaxies i and j . Alternatively, R_G can be calculated from a fit to the galaxy distribution (as in Sec. II.G) or from strip counts of galax-

ies (Schwarzschild, 1954). Combining these we have

$$M_{\text{tot}} = \frac{3 R_G \sigma_r^2}{G} \\ = 7.0 \times 10^{14} M_{\odot} \left[\frac{\sigma_r}{1000 \text{ km/sec}} \right]^2 \left[\frac{R_G}{\text{Mpc}} \right]. \quad (2.24)$$

Since $\sigma_r \sim 10^3$ km/sec and $R_G \sim 1$ Mpc for an average rich cluster, one finds $M_{\text{tot}} \sim 10^{15} M_{\odot}$ typically.

The virial theorem requires that one sum over all the particles in a cluster; it can only be directly applied to galaxies alone if they contain all of the mass in the cluster. One can also derive the mass of a cluster by treating the galaxies as test particles in dynamical equilibrium in the gravitational potential of the cluster. Such calculations generally give results for the total mass which are consistent with the virial theorem determinations; usually, one must assume that the galaxies and the total mass have the same spatial distribution. The most accurate of these determinations involve comparing numerical or analytical models for the galaxy distribution in a cluster with the observed spatial and velocity distributions (White, 1976c; Kent and Gunn, 1982; Kent and Sargent, 1983). The best data exist for the Coma and Perseus clusters; the masses for both these clusters are about $3 \times 10^{15} M_{\odot}$ within a projected radius of 3° from the cluster center (Kent and Gunn, 1982; Kent and Sargent, 1983).

These analyses give surprisingly large masses for clusters, particularly when compared to the total luminosity of a cluster $L_{\text{tot}} \sim 10^{13} L_{\odot}$. The conventional method of quantifying this comparison is to calculate the mass-to-light ratio of a system in solar units $(M_{\text{tot}}/L_{\text{tot}})/(M_{\odot}/L_{\odot})$. Obviously, any system composed solely of stars like our sun would have a mass-to-light ratio of unity. Mass-to-light ratios have been derived for a number of clusters using the virial theorem and the measured magnitudes of the galaxies at visual (V) or blue (B) magnitudes.⁶ Typically (see Faber and Gallagher, 1979, and Rood, 1981, and references in these reviews) one finds

$$(M/L_V)_{\text{tot}} \approx 250 h_{50} M_{\odot}/L_{\odot}, \\ (M/L_B)_{\text{tot}} \approx 325 h_{50} M_{\odot}/L_{\odot}. \quad (2.25)$$

The mass-to-light ratios found for the luminous portions of galaxies range from $(M/L_B)_{\text{gal}} \approx (1-12) h_{50} M_{\odot}/L_{\odot}$, with the large values corresponding to the E and SO galaxies which predominate in compact regular clusters. Thus only about 10% of the mass in clusters can be accounted for by material within the luminous portions of

galaxies. This is the so-called "missing mass" problem, although this is something of a misnomer. It is not the mass which is missing; what is missing is any other evidence for this invisible matter. The application of the virial theorem to clusters and the discovery that most of their mass was nonluminous was first made by Zwicky (1933) and Smith (1936).

How secure are these mass determinations for clusters? As long as a fair sample of galaxies are observed, the virial theorem masses are insensitive to velocity anisotropies, although this can be a problem if only galaxies near the cluster center are used. The dynamical model estimates for the masses are also not affected much by velocity anisotropies (Kent and Gunn, 1982). The virial theorem applies even if most galaxies are bound in binaries or subclusters, as long as the velocities and positions are measured for a fair sample of galaxies and R_G is computed directly from the galaxy positions. However, galaxies are not generally bound in binaries in regular clusters (Abell, Neyman, and Scott, 1964), and in any case typical binary or group velocities are too small to contribute significantly to σ_r (however, see Noonan, 1975). If the clusters are bound but not relaxed, Eq. (2.17) would give a mass lower by only a factor of 2 than Eq. (2.20). The velocity dispersion and R_G of a cluster might be contaminated by field galaxies. This background contamination problem can be reduced by determining the mass-to-light ratio for the core of a regular cluster, using the core parameters of an isothermal model fit (Sec. II.G). Again, one typically finds $(M/L_V)_{\text{core}} \approx 300 h_{50} M_{\odot}/L_{\odot}$ (Rood *et al.*, 1972; Bahcall, 1977a; Dressler, 1978b).

In principle, the "missing mass" could be associated with a large number of low-luminosity, large M/L galaxies (see Noonan, 1976; Sec. II.D). Such galaxies could affect the mass-to-light ratio if they made a significant contribution to the total light of a cluster which was not included in the usual determinations of the total luminosity because the galaxies were too faint to be detected individually. However, these galaxies would then produce a significant amount of diffuse light between galaxies in a cluster. Observations of the diffuse light in the Coma cluster show that its luminosity is at most comparable to that in bright galaxies (de Vaucouleurs and de Vaucouleurs, 1970; Melnick *et al.*, 1977; Thuan and Kormendy, 1977). Thus the required mass-to-light ratios cannot be greatly affected by low-mass galaxies. Abell (1977) included a large number of low-mass galaxies in his determination of the mass-to-light ratio in Coma, and found a value a factor of about 2 smaller than that in Eq. (2.25).

There is now considerable direct and indirect evidence for invisible matter associated directly with individual galaxies as well as clusters (see Faber and Gallagher, 1979, and Rood, 1981, for extensive reviews). It has been suggested that the invisible matter forms an extended halo around noncluster galaxies, extending significantly further than the luminous material and having at least several times more mass (Einasto *et al.*, 1974; Ostriker *et al.*, 1974).

The nature of this "missing mass" component in clus-

⁶Visual (V) and blue (B) magnitudes are based on the measured optical fluxes at wavelengths near 5500 and 4400 Å, respectively. For a more precise definition of these or other astronomical color magnitudes, see a general astronomy reference book such as Allen (1973).

ters and galaxies remains one of the most important unsolved problems in astrophysics. Careful searches have been made for diffuse radiation in clusters, which might be produced if the missing mass were gaseous or stellar. These have included searches for radio free-free emission (Davidsen and Welch, 1974), optical and uv line emission (Bohlin *et al.*, 1973; Crane and Tyson, 1975), optical continuum emission (de Vaucouleurs and de Vaucouleurs, 1970; Melnick *et al.*, 1977; Thuan and Kormendy, 1977); and 21-cm radio emission from neutral hydrogen (Shostak *et al.*, 1980). The observations of x-ray emission from clusters, which are the subject of this review, also give limits on the mass of hot gas (Sec. V.D.1). These studies and other similar searches have shown that the missing mass is not diffuse gas at any temperature, not dust grains of the type found in the interstellar medium, and not luminous stars.

In general, most suggestions as to the identity of the "missing mass" fall into three categories:

(1) substellar mass condensations, such as stars with mass $< 0.1M_{\odot}$ (Ostriker, Peebles, and Yahil, 1974), planetary size bodies, or comets (Tinsley and Cameron, 1974);

(2) invisible remnants of massive stars (black holes, neutron stars, or cool white dwarfs);

(3) stable, weakly interacting elementary particles, such as massive neutrinos, magnetic monopoles, axions, photons, etc. (Blumenthal *et al.*, 1984).

Where is this missing mass located? A number of arguments suggest that the total mass distribution is similar to the galaxy distribution (Rood *et al.*, 1972). The fact that the galaxy distributions in compact, regular clusters are reasonably represented by isothermal spheres and that core and total mass-to-light ratios are equal within the errors supports this view. On the other hand, H. Smith *et al.* (1979) and H. Smith (1980) have argued that the galaxy and mass distributions can be very dissimilar if the galaxies collapsed after the cluster potential was established. However, in this case violent relaxation (Sec. II.I.2) is not effective, clusters could not have compact cores, and the mass-to-light ratio in the inner regions would not be the same as that for the entire cluster.

Is the missing mass bound to individual galaxies in clusters? Probably not. The rate of two-body relaxation (dynamical friction) of galaxies in clusters is proportional to galaxy masses (Sec. II.I.1). If the missing mass were distributed among galaxies in proportion to their luminosity, very significant mass segregation would be expected (Rood, 1965; White, 1977b), which is not seen (Sec. II.G). Moreover, if the missing mass were bound to galaxies in halos having velocity dispersions similar to those in their visible portions, then the halos would have to extend roughly 0.5 Mpc from the galaxy center (White, 1985). This is much larger than the typical separations of galaxies in the cores of clusters. Thus the missing mass probably forms a continuum, occupying the entire volume of the cluster, but with an overall density distribution fairly similar to that of the galaxies.

Although the missing mass is probably not currently

bound to individual galaxies, it may initially have formed massive halos around individual galaxies, which were stripped by tidal interactions during and after the formation of the cluster (Richstone, 1976, and Sec. II.J.1). As mentioned above, there is considerable evidence that more isolated galaxies are immersed in extensive massive halos (see reviews by Faber and Gallagher, 1979, and Rood, 1981). However, the time scales for tidal interactions and dynamical friction are similar; it is not clear, therefore, that tidal interactions will strip the massive halos before galaxies merge. The problem of the competition between tidal forces and dynamical friction is the subject of a number of recent investigations (Richstone and Malumuth, 1983; Merritt, 1983, 1984; Miller, 1983; Malumuth and Richstone, 1984), which unfortunately reach contradictory conclusions (Sec. II.J.1). This problem is particularly serious for the massive binary galaxies which dominate B clusters (Sec. II.E).

Alternatively, the missing mass in clusters may never have been associated with galaxies. For example, the missing mass may be more extensive than the luminous material; the luminous matter, may only be the "tip of the iceberg" of the real mass distribution. Rood *et al.* (1970) found that M/L increased with the scale size of the system (see also Rood, 1981), which supports this hypothesis; however, Turner and Sargent (1974) have argued that this was an artifact of calculating M from Eq. (2.22).

I. Dynamics of galaxies in clusters

In Secs. II.E, II.F, and II.G, evidence was presented indicating that the velocity and spatial distribution of galaxies in regular, compact clusters are in a relaxed, quasistationary state. In this section, the nature of the relaxation processes of galaxies in clusters will be briefly discussed.

If clusters result from the gravitational growth of initially small perturbations, we expect the initial state of material in the protocluster to be irregular. The relaxation of the cluster thus involves the spatial motion of the galaxies, and a lower limit to the relaxation time is the crossing time

$$t_{cr}(r) \equiv r/v_r \approx 10^9 \text{ yr} \left[\frac{r}{\text{Mpc}} \right] \left[\frac{\sigma_r}{10^3 \text{ km/sec}} \right]^{-1}, \quad (2.26)$$

where the radial velocity dispersion σ_r has been substituted for the radial velocity v_r . An upper limit on the age of the cluster is the Hubble time (age of the universe)

$$t_H \sim (1.3 - 2.0) h_{50}^{-1} \times 10^{10} \text{ yr}, \quad (2.27)$$

where the numerical coefficient depends on the cosmological model. Thus the outer parts of a cluster or surrounding supercluster for which $r \geq 10$ Mpc cannot possibly

have relaxed and are expected to be irregular, as is observed (Secs. II.G and II.K.2).

1. Two-body relaxation

The phase-space distribution of galaxies in the central parts of spherical regular clusters can be represented as $f(\mathbf{r}, \mathbf{v}) \propto \exp(-\epsilon/\sigma_r^2)$, where $\epsilon \equiv \frac{1}{2}v^2 + \phi(r)$ is the energy per unit mass in the cluster (Sec. II.G). This is very similar to a Maxwell-Boltzmann distribution, except that it is the energy per unit mass (velocity dispersion) which is determined, and not the energy (temperature). We first consider the possibility that clusters have relaxed thermodynamically.

Thermodynamic equilibrium could result from elastic collisions between galaxies, and would be expected if the time scale for energy transfer in such collisions were shorter than the age of the cluster or the time scale for the loss of kinetic energy through dissipative processes. The most important elastic two-body collisions in a cluster are gravitational. The resulting relaxation times have been calculated analytically by Chandrasekhar (1942) and Spitzer and Harm (1958), and numerically through N -body simulations, including a realistic luminosity function for galaxies by White (1976c, 1977b) and Farouki and Salpeter (1982). A useful characteristic time scale (0.94 times the Spitzer "reference time") is

$$t_{\text{rel}} = \frac{3\sigma_r^3}{4\sqrt{\pi}G^2mm_f n_f \ln \Lambda} \quad (2.28)$$

for the relaxation of a galaxy of mass m in a background field of galaxies of mass m_f and number density n_f . Λ is the ratio of maximum to minimum impact parameters of collisions which contribute to the relaxation; the maximum impact parameter is on the order of half the gravitation radius of the cluster R_G [Eq. (2.21)], while the minimum impact parameter is roughly the larger of the galaxy radius r_g or "turning radius" $G m_f / 3\sigma_r^2$ (White, 1976b). Thus

$$\Lambda \approx \min \left[\left[\frac{3R_G\sigma_r^2}{2G m_f} \right], \left[\frac{R_G}{2r_g} \right] \right]. \quad (2.29)$$

Usually, the second value applies. Thus, for $r_g \sim 20$ kpc, $R_G \sim 1$ Mpc, $\ln \Lambda \sim 3$.

In order to give a lower limit to the relaxation time, we assume for the moment that all the mass in a cluster [including the "missing mass" (Sec. II.H)] is bound to individual galaxies; we later show that this is unlikely to be the case. Then, we define an average density $\langle \rho \rangle \equiv 3M_{\text{tot}} / (4\pi R_G^3)$, where M_{tot} is the total mass of the cluster. If we assume a Schechter luminosity function [Eq. (2.3)], and a fixed galaxy mass-to-light ratio, we find

$$t_{\text{rel}}(m, r) \geq 0.24 t_{\text{cr}}(R_G) N^* \times \left[\left[\frac{m}{m^*} \right] \left[\frac{\rho(r)}{\langle \rho \rangle} \right] \ln \Lambda \right]^{-1}, \quad (2.30)$$

where m^* is the characteristic galaxy mass (corresponding to L^*), N^* is the characteristic galaxy number (richness), t_{cr} is the cluster crossing time [Eq. (2.26)], and $\rho(r)$ is the total cluster density at r . Equation (2.30) is a lower limit because it assumes that all the cluster mass is bound to individual galaxies. Typically, $R_G \sim \text{Mpc}$, $\sigma_r \sim 1000$ km/sec, $N^* \sim 1000$, and $\ln \Lambda \approx 3$, giving $t_{\text{cr}}(R_G) \sim 10^9$ yr and $t_{\text{rel}}(m^*, R_G) \geq 3 \times 10^{11}$ yr. This is much longer than a Hubble time [Eq. (2.27)]; it is therefore unlikely that the apparently relaxed state of regular clusters results from two-body collisions. However, two-body relaxation processes can affect the more massive galaxies ($m \gg m^*$) near the cluster center [$\rho(r) \gg \langle \rho \rangle$], as is discussed below.

2. Violent relaxation

The fact that clusters exhibit a nearly constant velocity dispersion (rather than kinetic temperature) suggests that the relaxation is produced by collective gravitational effects. Lynden-Bell (1967) showed that collective relaxation effects can result in a very rapid quasirelaxation ("violent relaxation"). The existence of these effects involves a somewhat subtle point; collective relaxation develops through collisionless interactions, and thus the detailed ("fine-grain") phase-space distribution of galaxies is conserved. However, if the relaxation is sufficiently violent (for example, the energy of particles is changed by a significant fraction), then initially adjoining units of phase space will be widely separated in the final state (phase mixing). Thus, if one averages the "fine-grain" phase-space density over any observable volume to give a "coarse-grain" distribution, this "coarse-grain" distribution can be an equilibrium distribution and independent of the details of the initial state.

If clusters were formed by the growth and collapse of initial perturbations, then during the collapse the gravitational potential ϕ fluctuated violently. This would cause a change in the energy per unit mass $\epsilon \equiv \frac{1}{2}v^2 + \phi(r)$ of

$$\frac{D\epsilon}{Dt} \approx \frac{\partial \phi}{\partial t}. \quad (2.31)$$

For example, if the cluster collapsed from a stationary state ($v = 0$) to a virialized final state (Sec. II.H), then $\Delta\epsilon \sim \Delta\phi \sim \epsilon$. The time scale for collapse t_{coll} is roughly a dynamical time scale or crossing time

$$t_{\text{coll}} \sim (G\langle \rho \rangle)^{-1/2} \sim (R_G^3/GM_{\text{tot}})^{1/2} \sim t_{\text{cr}}(R_G). \quad (2.32)$$

As the energy of a galaxy changes by $\sim 100\%$ during a collapse time, violent relaxation can be completed during the collapse of the cluster, after which time the potential is constant, and the galaxy distribution is in stationary virial equilibrium.

Since the equation of motion of a particle in the cluster's mean gravitational field is independent of mass [Eq. (2.31)], the equilibrium is independent of mass. Lynden-Bell (1967) derived an equilibrium state by assuming that the system relaxed to the most probable

coarse-grained phase-space state subject to conservation of energy, particle number, and fine-grain phase density. This equilibrium state was found to be a Fermi-Dirac distribution that reduces to the Maxwell-Boltzmann distribution for the appropriate number densities in clusters (see also Shu, 1978),

$$f(\mathbf{r}, \mathbf{v}) \propto \exp(-\epsilon/\sigma_r^2). \quad (2.33)$$

This phase-space density produces a Gaussian velocity distribution and isothermal spatial distribution of galaxies, which are roughly consistent with the observed distributions in the inner parts of clusters (Secs. II.F and II.G). The distribution is also independent of mass, roughly as observed. If Eq. (2.33) held for all radii, the cluster mass would be infinite (Sec. II.G). However, galaxies at large radii or with large energies never reach equilibrium because their crossing times [Eq. (2.26)] are longer than the Hubble or collapse times [Eq. (2.27) and (2.32)]. Because the relaxation occurs only while the cluster is collapsing, it is not clear that this equilibrium state can ever be achieved in any real collapsing system.

The state of equilibrium of a collisionless, gravitationally collapsing system can be studied directly through numerical N -body experiments. These experiments do show that isolated collapsing or merging systems relax rapidly (in a few crossing times), and they agree roughly on the nature of the equilibrium state. In general, they *do not* find that the systems become isothermal spheres; instead they find spatial distributions that are reasonably represented by the de Vaucouleurs [1948a, 1948b; Eq. (2.14)] or Hubble [1930; Eq. (2.15)] forms (White, 1979; Villumsen, 1982; van Albada, 1982). These distributions are more centrally condensed and fall off more rapidly at large radii than the isothermal sphere. However, it is possible that the subsequent collapse of surrounding material can increase the density at large distances; Gunn (1977) has shown that for some initial conditions this process can lead to nearly isothermal mass distributions.

The idea that the distribution of galaxies in clusters is determined by violent relaxation during the formation of the cluster provides a simple explanation for the one-dimensional morphological sequence of clusters running from irregular to regular (Table II; Gunn and Gott, 1972; Jones *et al.*, 1979; Dressler, 1984). The regular clusters are those old enough to have collapsed and relaxed, while the irregular ones have not. As the collapse time is $t_{\text{coll}} \sim (R_h^3/GM_{\text{tot}})^{1/2} \sim (G\rho_i)^{-1/2}$, where ρ_i is the initial density, higher-density protoclusters will collapse more rapidly. Since the age of clusters is limited by the Hubble time t_H , *regular clusters will be produced by higher-density protoclusters, and irregular clusters by lower-density protoclusters.* Thus we expect regular clusters to have higher densities than irregular clusters, as is observed. Moreover, violent relaxation and phase mixing will eliminate subclustering and produce a centrally condensed, symmetric distribution, as observed in regular clusters.

White (1976c) has followed the collapse of a model cluster numerically, with an N -body code; the results are

shown in Fig. 4. He finds that the cluster first forms irregular subcondensations around massive galaxies (like an I cluster). These continually merge until the galaxy distribution is elongated and has two large clumps (like an F cluster), which merge to form a smooth, regular cluster with a prominent core (a C cluster) (see also Henry *et al.*, 1981; Forman and Jones, 1982). Recently, Cavaliere *et al.* (1983) have produced many similar models for cluster collapse.

The other aspects of the morphological sequence have to do with galactic content—the fractions of spiral, SO, and elliptical galaxies, or domination by supergiant (B, D, and cD) galaxies. In Sec. II.J evidence is presented which suggests that the galactic content of clusters is also determined by the density of the cluster, although the mechanism is still controversial.

3. Ellipsoidal clusters

The distribution in Eq. (2.33) is isotropic in velocity space and spherically symmetric in real space. However, many of the most regular clusters have observed galaxy distributions that are not symmetric on the sky (Sec. II.G). This asymmetry could be due to rotation; however, the velocity fields in clusters show no evidence for dynamically significant rotation (Sec. II.F).

Numerical N -body simulations of the formation of clusters show that if the initial distribution of galaxies is aspherical, the final distribution after violent relaxation will be aspherical [Fig. 4(d); Aarseth and Binney, 1978]. The most general final configurations have compact cores and are regular, but the surfaces of constant density are basically triaxial ellipsoids rather than spheres. The triaxial shape is maintained by an ellipsoidal Gaussian velocity distribution $p(v) \propto \exp[-(\Sigma_{ij})^{-1}v_i v_j]$, where Σ is the velocity dispersion tensor. The principal axes of Σ and the spatial figure of the galaxy are parallel and nearly proportional to one another (Binney, 1977), as expected from the tensor virial theorem (Chandrasekhar, 1968). Thus the velocity dispersion is largest parallel to the longest diameter of the cluster.

4. Dynamical friction

Once the collapse of a cluster is completed, violent relaxation is ineffective, and further relaxation occurs through two-body interactions. As shown above, these effects are probably not important for a typical galaxy at an average position in the cluster, but they can be significant for a more massive galaxy ($m \gg m^*$) in the cluster core [$\rho \gg \langle \rho \rangle$; see Eq. (2.30)]. Chandrasekhar (1942) showed that a massive object of mass m moving at velocity \mathbf{v} through a homogeneous, isotropic, Maxwellian distribution of lighter, collisionless particles suffers a drag force given by

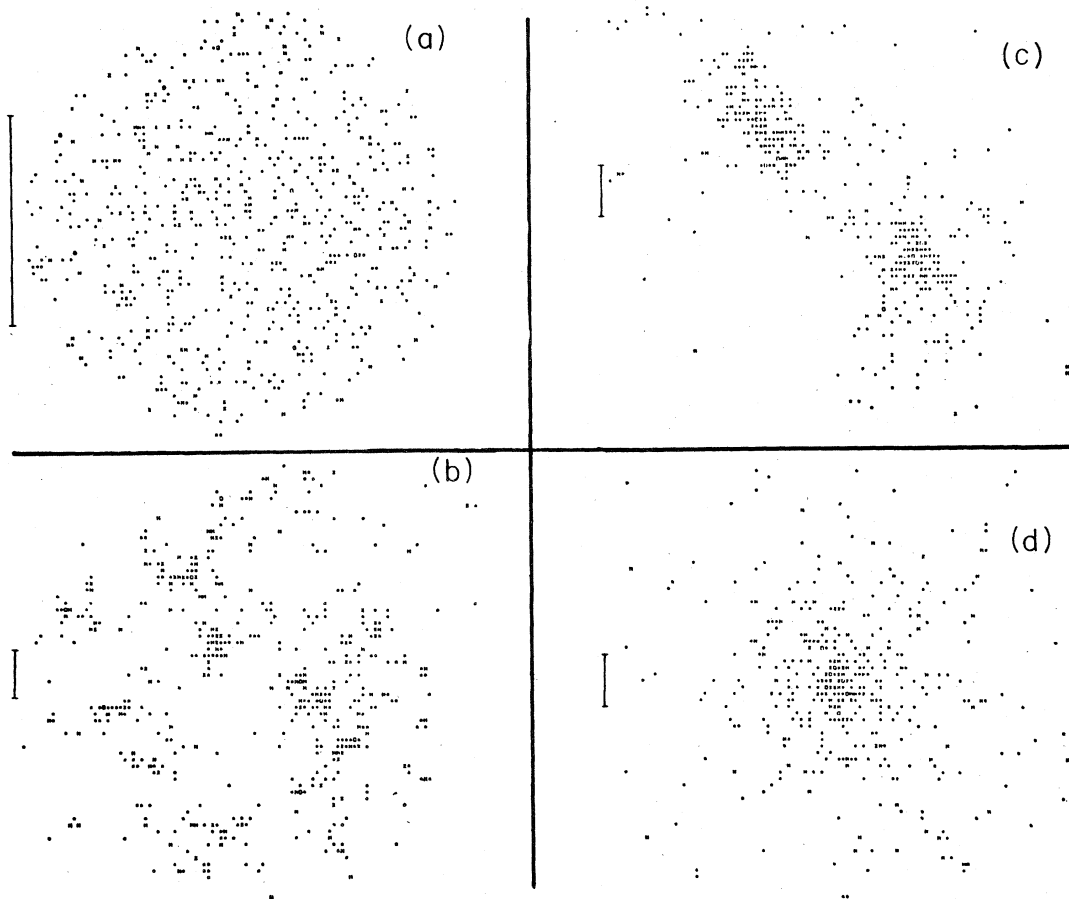


FIG. 4. The projected galaxy distributions in White's (1976c) N -body calculations of the evolution of a collapsing cluster. Each symbol represents a galaxy. In each figure, the bar represents a fixed length scale, one-half of the gravitational radius R_G [(Eq. (2.21)]. The times t are given in units of the initial collapse time of the cluster. (a) The initial configuration ($t=0$). (b) An irregular distribution with subclustering at $t=0.19$. (c) A bimodal distribution in the cluster at $t=0.97$. (d) The final relaxed configuration at $t=2.66$.

$$\frac{d\mathbf{v}}{dt} = -\mathbf{v} \left[\frac{4\pi G^2 m}{v^3} \times \ln(\Lambda) \rho_{\text{tot}} [\text{erf}(x) - x \times \text{erf}'(x)] \right], \quad (2.34)$$

where $x \equiv v/(\sqrt{2} \sigma_r)$, σ_r is the radial velocity dispersion of the lighter particles, ρ_{tot} is their total mass density, erf is the error function, and Λ is given by Eq. (2.29). Note that this "dynamical friction" force is independent of the mass of the lighter particles, and thus depends only on the total density ρ_{tot} of such particles (regardless of whether they are galaxies or collisionless "missing mass" particles).

The relaxation time in the cluster core can be evaluated by noting that, for an isothermal cluster distribution (Sec. II.G), the central density ρ_0 , velocity dispersion σ_r , and core radius r_c are related by

$$4\pi G \rho_0 r_c^2 = 9 \sigma_r^2. \quad (2.35)$$

Let $m = (m/m^*)m^* = (m/m^*)(M/L_V)_{\text{gal}}L_V^*$, where L_V^* and m^* are the characteristic visual luminosity and corresponding mass of galaxies in the Schechter luminosity function (Schechter, 1976, and Sec. II.D), and M/L_V is the visual mass-to-light ratio. Schechter finds $L_V^* \approx 4.9 \times 10^{10} L_\odot$. Substituting this value, $\ln \Lambda \approx 3$, and the ρ_0 from Eq. (2.35) into Eq. (2.28) gives for the dynamical friction time scale

$$t_{\text{rel}}(m, r=0) \approx 6 \times 10^9 \text{ yr} \left[\frac{\sigma_r}{1000 \text{ km/sec}} \right] \times \left[\frac{r_c}{0.25 \text{ Mpc}} \right]^2 \left[\frac{m}{m^*} \right]^{-1} \times \left[\frac{(M/L_V)_{\text{gal}}}{10 M_\odot/L_\odot} \right]^{-1}. \quad (2.36)$$

Dynamical friction slows down the more massive galaxies near the center of a spherical cluster; they spiral in toward the cluster center (Lecar, 1975). The kinetic energy removed from the massive galaxies is transferred to the lighter particles (galaxies or "missing mass" components), which then expand. Thus dynamical friction produces mass segregation in a cluster; more massive galaxies are found preferentially at smaller radii. Moreover, at a fixed radius the velocity dispersion of the more massive galaxies will be lower, as they have been slowed down.

If the cluster is aspherical because of an anisotropic velocity dispersion, the dynamical friction force will not be parallel to the velocity (Binney, 1977). Because the force depends inversely on velocity, it is strongest along the shortest axis of the cluster. Thus dynamical friction increases the anisotropy of the most massive galaxies in a cluster. This can explain the formation of L clusters such as Perseus, in which the brightest galaxies form a narrow chain along the long axis of the cluster (Binney, 1977).

The massive galaxies that spiral into the cluster center will eventually merge to form a single supergiant galaxy if they are not tidally disrupted first. In Sec. II.J.1 evidence is given which suggests that this is the mechanism by which cD galaxies form; however, there are also strong arguments that galaxies lose mass due to tidal effects so rapidly that dynamical friction is not important (Merritt, 1984). The merger of the most massive and therefore brightest galaxies in the cluster core might cause the luminosity function to fall off more rapidly at high luminosities, as may have been observed in some cD clusters (Dressler, 1978b), and might produce a deficiency of brighter galaxies (other than the cD) in the cluster core (White, 1976a).

The fact that the dynamical friction time scale depends inversely on galaxy mass provides a method to measure the mass bound to individual galaxies in a cluster, as opposed to the total virial mass of the cluster. If the mass-to-light ratio derived for the cluster as a whole [typically $(M/L_V) \approx 250M_\odot/L_\odot$; Eq. (2.25)] is substituted in Eq. (2.36), $t_{\text{rel}} \sim 2 \times 10^8 \text{ yr } (m/m^*)^{-1}$, which is much smaller than the probable age of a cluster of about a Hubble time $t_H \sim 10^{10} \text{ yr}$ (for typical parameters for a compact, regular cluster). Thus, if the "missing mass" in clusters were bound to individual galaxies, the massive galaxies $m \geq m^*$ would be highly relaxed (at least in the cluster core). All of these galaxies would have segregated into a very small core and possibly merged to form a single galaxy. Observations of the degree of mass segregation, luminosity function, and luminosity of the brightest galaxies in well-studied clusters are all inconsistent with this much relaxation. From the observations one can limit the mass-to-light ratios of massive galaxies in cluster cores to $(M/L_V) \lesssim 30M_\odot/L_\odot$. This indicates that the "missing mass" cannot be bound to individual, massive galaxies, but rather must form a continuum. This important result was first given by Rood (1965), and has been verified by numerical integration of Eq. (2.34) and N -body models by White (1976a, 1977b) and Merritt (1983).

J. Galactic content of clusters

In the discussion of the morphological classification of clusters (Sec. II.E), it was noted that the regular, compact clusters have a galactic content that differs markedly from that of the field. First, these clusters are often dominated by a single very luminous (cD) galaxy, or by a pair of very bright galaxies. Second, elliptical and SO galaxies predominate over spiral galaxies in regular, compact clusters, where the opposite is true in the field. In this section possible origins for these differences are described and are related to the overall picture of cluster evolution given in the preceding section.

1. cD galaxies

cD galaxies were defined by Mathews, Morgan, and Schmidt (1964) as galaxies with a nucleus of a very luminous elliptical galaxy embedded in an extended amorphous halo of low surface brightness. They are usually found at the center of regular, compact clusters of galaxies (Morgan and Lesh, 1965; Bautz and Morgan, 1970), and about 20% of all rich clusters contain cD galaxies. However, some galaxies that appear to be cD's have been found in poor clusters and groups (Morgan, Kayser, and White, 1975; Albert, White, and Morgan, 1977).

cD galaxies are extremely luminous; if one excludes nuclear sources (Seyfert galaxies, N galaxies, and quasars), they are, as a class, the most luminous galaxies known. Sandage (1976) and Hoessel (1980) find average absolute magnitudes $\langle M_V \rangle_{\text{cD}} \approx -23.7 + 5 \log h_{50}$ and $-22.7 + 5 \log h_{50}$ for apertures of $43/h_{50}$ kpc and $19/h_{50}$ kpc, respectively. Since the galaxies extend well beyond this, total luminosities are at least a magnitude brighter. Moreover, the magnitudes of cD's show a rather small dispersion (~ 0.3 mag) and are only weakly dependent on cluster richness (Sandage, 1976). cD galaxies are usually considerably brighter (often by a full magnitude) than other galaxies in the same cluster.

The question naturally arises as to whether cD galaxy luminosities simply represent the high end of the normal galaxy luminosity function, or whether cD's are "special." The distribution of brightest galaxy luminosities L_1 in a cluster would be $p(L_1)dL_1 = \exp[-N(L_1)]dN(L_1)$ if the brightest galaxies were drawn at random from the integrated luminosity function $N(L)$ (Sec. II.D). This distribution would produce a large dispersion in L_1 and a strong dependence on cluster richness (neither of which are observed), unless the luminosity function were much steeper than is observed at the bright end (Sandage, 1976). However, cD luminosities themselves are too high to be drawn from the galaxy luminosity function (Schechter, 1976), unless it were less steep than is observed. While selection effects may account for the small dispersion of brightest elliptical and SO galaxies in groups and clusters (Schechter and Peebles, 1976), it does not appear that this can explain the high luminosities of cD galaxies. A number of statistical tests (Sandage, 1976; Tremaine and Rich-

stone, 1977; Dressler, 1978a) indicate that the magnitudes of cD galaxies cannot be drawn statistically from a general galaxy luminosity function.

cD galaxies are more extended than the other giant elliptical galaxies in two ways [see Figs. 5(a) and 5(b) where the surface brightness of the cD in A1413 is compared to the giant elliptical NGC1278 in the Perseus cluster]. First, the core regions of cD's are apparently larger. Hoessel (1980) finds that cD galaxies have core radii that average $\langle r_c(\text{gal}) \rangle \sim 4/h_{50}$ kpc, while typical giant elliptical galaxies have $\langle r_c(\text{gal}) \rangle \sim 0.4/h_{50}$ kpc (here, the surface brightness of the galaxy at projected radius b is assumed to vary as $\{1 + [b/r_c(\text{gal})]^2\}^{-1}$). Unfortunately, these core radii represent fairly small angles and their determination may be ambiguous (Dressler, 1984). If one fits galaxy surface brightnesses to a de Vaucouleurs (1948a) form [Eq. (2.14)], the effective radii r_e of cD galaxies are roughly a factor of 2 larger than the effective radii of normal giant elliptical galaxies. Alternatively, one can define the integrated luminosity slope

$$\alpha \equiv \frac{d \ln L(b)}{d \ln b}, \quad (2.37)$$

where $L(b)$ is the luminosity observed within the projected radius b . Hoessel (1980) finds $\langle \alpha \rangle_{\text{cD}} \approx 0.59$ for $b = 19/h_{50}$ kpc, which is about twice the value found for typical giant ellipticals.

In cD galaxies in rich clusters, the giant elliptical-like core of the galaxy is embedded in a very extended low-surface-brightness halo (Oemler, 1973,1976; Carter, 1977; Dressler, 1979). In Figs. 5(a) and 5(b) the surface brightness of the very extended cD in the cluster A1413 is compared to that of a typical giant elliptical galaxy NGC1278 in the Perseus cluster (Oemler, 1976). The solid line shows a de Vaucouleurs fit [Eq. (2.14)] to each galaxy. This profile fits the inner parts of either galaxy reasonably well, but the cD in A1413 has a halo of low surface brightness extending to beyond 1 Mpc from the galactic center. The surface brightness in cD halos generally falls off as roughly the $\frac{3}{2}$ power of projected distance from the galaxy center.

Masses of cD galaxies have been estimated by a measurement of the stellar velocity dispersion in the outer parts of the cD in A2029 (Dressler, 1979) and by measurements of the velocities of smaller companion galaxies which are assumed to be bound to the cD (Wolf and Bahcall, 1972; Jenner, 1974). Typically, one finds $M \sim 10^{13} M_{\odot}$, but it is difficult to separate the galaxy and cluster mass distributions in the outermost parts of the cD (Dressler, 1979). For the same central velocity dispersion, cD galaxies are about 60% brighter than other giant ellipticals (Malumuth and Kirshner, 1981).

cD galaxies are usually found very near the centers of compact clusters (Morgan and Lesh, 1965; Leir and van den Bergh, 1977; R. A. White, 1978). They also have velocities very near the mean velocity of galaxies in the cluster (Quintana and Lawrie, 1982), and may in fact give a better estimate of the cluster mean velocity than the average value for a few bright galaxies. These results suggest

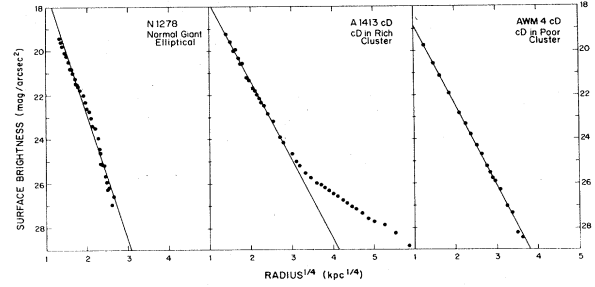


FIG. 5. The surface photometry of cD galaxies. The surface brightness in magnitudes per square second of arc is plotted against the one-fourth power of the radius. The dots are the observed points, and the straight lines are de Vaucouleurs fits to the inner points. NGC1278 (Oemler, 1976) is a normal giant elliptical galaxy, showing no extended halo. The middle figure shows the cD in the cluster A1413 (Oemler, 1976), with a more extended central de Vaucouleurs profile and a very extended halo. The right panel is the cD in the poor cluster AWM4 (Thuan and Romanishin, 1981), which has an even more extensive de Vaucouleurs profile, but no apparent halo.

that cD's are usually sitting at rest at the bottom of the cluster gravitational potential well.

cD galaxies often have double or multiple nuclei (Minkowski, 1961; Morgan and Lesh, 1965; Hoessel, 1980; Schneider and Gunn, 1982); that is, there are several peaks in the surface brightness within the central part of the cD. Many cD's are in binary or multiple galaxy systems (Leir and van den Bergh, 1977; Rood and Leir, 1979; Struble and Rood, 1981); when the two cD nuclei are surrounded by a common halo, these are referred to as "dumbbell" galaxies.

The special structural and kinematic properties of cD galaxies suggest that they have been formed or modified by dynamical processes in clusters. Gallagher and Ostriker (1972) and Richstone (1975,1976) have suggested that cD's consist of the debris from galaxy collisions. In a rich cluster, the outer envelopes of galaxies will be stripped by tidal effects during these collisions. The rate of mass loss due to tidal collisions in a cluster was derived by Richstone (1976); if his rate is integrated over a Schechter luminosity function (Sec. II.D) and an isothermal galaxy density function with core radius r_c (Sec. II.G), one finds

$$\left(\frac{dM}{dt} \right)_{\text{tidal}} \approx 3 \times 10^4 M_{\odot} \text{ yr}^{-1} \left[\frac{\sigma_r}{10^3 \text{ km/sec}} \right]^4 \times \left[\frac{\sigma_*}{200 \text{ km/sec}} \right]^{-1} \left[\frac{r_t}{r_c} \right], \quad (2.38)$$

where σ_r is the cluster line-of-sight velocity dispersion (Sec. II.F), and r_t and σ_{gal} are the tidal (outermost) radius and line-of-sight stellar velocity dispersion of a typical galaxy ($L = L^*$; see Sec. II.D). Equation (2.38) assumes

that all the cluster mass is in galaxies; if this is not the case, then the rate of mass loss from galaxies is reduced by the square of the fraction of mass in galaxies.

Knobloch (1978a,1978b) and Da Costa and Knobloch (1979) have argued that Richstone's expression overestimates the rate of mass loss, because the tidal stripping of a galaxy halo is limited by the rate of diffusion of stars into the halo. However, they take as their basic model a galaxy in which the halo mass is very small; this does not agree with the determinations of the mass distributions in galaxies (see, for example, Faber and Gallagher, 1979). For realistic mass models, it appears that the claimed discrepancy is a factor of roughly (σ_*/σ_r) .

If most of the mass in a cluster were initially in extended ($r_t \sim r_c \sim 300$ kpc) halos of dark material bound to individual galaxies, Eq. (2.38) shows that these dark halos could have been stripped by tidal interactions within the age of a cluster, as was suggested in Sec. II.H.

The outer portions of the luminous material would also be stripped (Strom and Strom, 1978a,1979); if we assume a tidal radius of $r_t \sim 0.1 r_c \sim 30$ kpc, we would expect $\geq 10^{12} L_\odot$ of luminous material to be stripped from galaxies in a compact cluster. The stripped material would settle to the center of the cluster gravitational potential; because of the dependence of the collision rate on the square of galaxy density, the stripped material would probably be somewhat more centrally condensed than the galaxy distribution in the cluster. This tidal debris might thus be observed as the extended halo about a central cD galaxy. The stripped material would be centered on the cluster center, be at rest (on average) relative to the cluster center of mass, and have a mass and spatial distribution similar to that observed for cD halos. This model for the formation of cD halos (Gallagher and Ostriker, 1972; Richstone, 1975,1976) predicts that they have high velocity dispersions, as has been observed for the cD in A2029 by Dressler (1979). This tidal debris model may explain the observed properties of cD halos; however, it cannot naturally explain the giant elliptical galaxy nucleus of the cD.

Ostriker and Tremaine (1975), Gunn and Tinsley (1976), and White (1976a,1977a) have suggested that cD galaxies are produced by the merger of massive galaxies within the core of a cluster. As discussed in Sec. II.I, dynamical friction causes the orbits of massive cluster galaxies to decay. As such galaxies reach the cluster center, they merge to form a single supergiant galaxy, which swallows any galaxies that subsequently pass through the cluster center. The merger hypothesis (called "galactic cannibalism" by Ostriker and Hausman, 1977) provides an attractive explanation for the formation of cD galaxies in a cluster.

First of all, since a cD galaxy would be produced by the merger of many of the more luminous galaxies in a cluster, the high luminosities of cD's (in excess of that expected from the galaxy luminosity function) is naturally explained. Once a massive galaxy reaches the cluster center, it will swallow other galaxies. Initially, its luminosity will increase at the rate (Ostriker and Tremaine, 1975)

$$\frac{d(L_{cD}/L^*)}{d(t/10^{10} \text{ yr})} \approx 13 h_{50}^{-1} \left[\frac{r_t}{100 \text{ kpc}} \right]^3 \left[\frac{r_c}{250 \text{ kpc}} \right]^{-4} \times \left[\frac{\sigma_r}{10^3 \text{ km/sec}} \right] \left[\frac{M/L_V}{30M_\odot/L_\odot} \right], \quad (2.39)$$

where r_t is the tidal radius of the central galaxy, r_c and σ_r are the core radius and velocity dispersion of the cluster, and M/L_V is the visual mass-to-light ratio of all galaxies in the cluster. [Very recently, Merritt (1985) has shown that Eq. (2.39) greatly overestimates the actual merger rate at early times in a cluster.] Once most of the massive galaxies within the core have been accreted, the luminosity grows as $t^{1/2}$ rather than as t (Ostriker and Tremaine, 1975):

$$\left[\frac{L_{cD}}{L^*} \right] \approx 8 \left[\frac{\sigma_r}{10^3 \text{ km/sec}} \right]^{3/2} \times \left[\frac{M/L_V}{30M_\odot/L_\odot} \right]^{1/2} \left[\frac{t}{10^{10} \text{ yr}} \right]^{1/2}. \quad (2.40)$$

Thus luminosities of $L_{cD} \sim 10L^*$ can be produced during the lifetime of a compact cluster.

The merger product should be larger than the initial galaxy, because the kinetic energy of the merging galaxies "heats" and inflates the final product (Ostriker and Hausman, 1977; Hausman and Ostriker, 1978). Hausman and Ostriker (1978) argue that the galaxy core radius $r_c(\text{gal})$ will increase by roughly a factor of 10, and the structure parameter α by a factor of at least 2, in rough agreement with the observations (Hoessel, 1980).

With the large increase in the luminosity of the first brightest galaxy through mergers [Eq. (2.40)], it might seem surprising that these galaxies show a rather small dispersion in absolute magnitude (Sandage, 1976). The observed magnitudes are for fixed measuring apertures, which are generally much smaller than the halo size of the cD; depending on the amount of swelling the cD undergoes, the observed magnitude may either increase or decrease (Gunn and Tinsley, 1976). In the simulations of Hausman and Ostriker (1978), the apparent magnitude within an aperture of 16 kpc remains roughly constant once the massive galaxies in the core of the cluster have been swallowed. This may explain the small dispersion in observed cD absolute magnitudes.

The first brightest galaxy grows in luminosity by swallowing other massive galaxies; this increases the contrast between the first brightest and the other bright galaxies (Gunn and Tinsley, 1976; Hausman and Ostriker, 1978), as is observed (Sandage, 1976; Tremaine and Richstone, 1977; Dressler, 1978a; McGlynn and Ostriker, 1980).

Of course, the process of dynamical friction and merging leaves the merger product nearly at rest relative to the average cluster galaxy and nearly at the center of the cluster, as is observed for cD's.

If a cluster is elongated, then the merger product at its center will tend to be elongated in the same direction. In general, cD galaxies are more highly flattened than other ellipticals (Leir and van den Bergh, 1977; Dressler, 1978c), and the axes of the cD's align with those of their clusters, as predicted (Sastry, 1968; Rood and Sastry, 1972; Dressler, 1978c, 1981; Carter and Metcalfe, 1980; Binggeli, 1982).

If cD galaxies are produced by mergers of massive galaxies, one expects mergers to take place roughly every 10^9 yr (Ostriker and Hausman, 1977). The actual merger will occur over roughly an orbital period in the cD galaxy $\sim 3 \times 10^8$ yr (S. D. M. White, 1978), and for this period the nucleus of the merging galaxy will be visible within the cD envelope. Thus one would expect about $\frac{1}{4}$ of cD galaxies to have multiple nuclei, roughly as is observed (Hoessel, 1980). However, a major problem with this interpretation of multiple nuclei in cD's is that these nuclei, in many cases, have rather large velocities relative to the cD (Jenner, 1974). This suggests that they are not bound to the cD, but might only be cluster galaxies seen in projection against the cD.

Rood and Leir (1979) find that about $\frac{1}{4}$ of all cD galaxies are binaries (actually dumbbells); they argue that this fraction is much larger than is expected due to dynamical friction and merging. The reason is that in these systems the two galaxies in the binary differ by less than a magnitude in apparent luminosity. However, the primary component of the system would have swallowed roughly five other galaxies in the merger picture, and therefore should be much brighter than its companion. Since one magnitude corresponds to a factor of 2.5 in brightness, and magnitudes at a fixed aperture do not increase directly with total luminosity because of swelling, it is not clear how serious a discrepancy this is (see also Tremaine, 1981).

The dynamical friction and merger theory may explain most of the observed properties of cD galaxies except for their very extended halos. The tidal debris theory explains the extended halos, but not the properties of the inner elliptical galaxy. It seems natural to suggest that cD galaxies result from the action of both types of processes. Although the impression is sometimes given in the literature that these two processes are alternative and exclusive explanations for cD galaxies, both must occur to some extent in clusters, and cD's are better explained by their mutual action.

However, Merritt (1983, 1984, 1985) has recently pointed out some very serious problems with this simple picture of cD formation. He argues that the tidal effect of the global cluster potential (as opposed to that due to individual galaxy interactions) dominates the evolution of cluster galaxies. Tidal stripping of galaxies would then lower their masses and prevent any mergers. If this argument is correct and if mergers formed cD's, then the mergers must have occurred before the cluster collapsed, perhaps in smaller subclusters or groups (Carnevali *et al.*, 1981; van den Bergh, 1983a; Dressler, 1984).

Theories of the origin of cD galaxies can be tested

through observations of the apparent cD galaxies in 23 poor clusters which were discovered by Morgan, Kayser, and White (1975) (hereafter MKW) and Albert, White, and Morgan (1977) (hereafter AWM). These clusters range in Abell richness (Sec. II.C) from < 10 to ~ 50 galaxies; none are richer than Abell richness class zero (Bahcall, 1980). These clusters have velocity dispersions σ_r (Stauffer and Spinrad, 1978) and core radii r_c (Bahcall, 1980) which are probably about $\frac{1}{2}$ of those of rich, compact clusters. Since the dynamical friction rate (when summed over all galaxies) varies as σ_r/r_c [Eq. (2.30)], and the merger rate varies as σ_r/r_c^4 [Eq. (2.39)], one expects mergers to form remnants in these poor clusters even larger than those in rich clusters. On the other hand, the tidal stripping rate [Eq. (2.38)] varies as σ_r^4/r_c , and is thus much lower in poor clusters. If mergers form the extended elliptical galaxy body of a cD and tidal debris makes up the very extended halo, the cD's in poor clusters should lack such halos. Surface photometry of the cD's in poor clusters (Oemler, 1976; Stauffer and Spinrad, 1980; Thuan and Romanishin, 1981) indicates that this is indeed the case. In Fig. 5(c), the surface photometry of the cD in the poor cluster AWM4 as observed by Thuan and Romanishin (1981) is shown.

While the processes of merging and tidal stripping, perhaps in preexisting subclusters and groups, seem to provide a possible explanation of many of the unusual properties of cD galaxies, the core of a rich compact cluster is a very active physical environment in which many other processes may be important. For example, recent x-ray and optical observations suggest that central, dominant galaxies are accreting vast quantities of gas, as much as $400M_\odot/\text{yr}$ in the case of NGC1275 in the Perseus cluster (Secs. III.C.3 and V.G). The accreting galaxies include a number of cD's. There are several arguments which suggest that the accreted gas is being converted into low-mass stars (Cowie and Binney, 1977; Fabian, Atherton, Taylor, and Nulsen, 1982; Sarazin and O'Connell, 1983); if so, accretion can significantly increase the core luminosities of cD's (Fabian, Atherton, Taylor, and Nulsen, 1982; Sarazin and O'Connell, 1983).

Finally, I would like to comment on a semantic issue that has arisen concerning cD's and other similar galaxies. It should be clear from the discussion above that cD's represent the extreme result of a number of dynamical processes, which must be occurring continuously in clusters and groups. There are a number of related types of galaxies which share many but not all of the properties of cD's; they may be extended, and be the brightest galaxy in a cluster (or nearly so), and be located at the spatial and velocity center of the cluster. In Sec. III.D.2 we shall see that such galaxies may affect the x-ray morphology of clusters, even if they do not satisfy the technical definition of a cD galaxy; examples are M87 in the Virgo cluster and NGC1275 in the Perseus cluster. It has sometimes been argued that the definition of cD galaxies should be extended in some way to include all such objects. It seems to me that this is not a good idea; it is more useful to retain the degree of specificity in the origi-

nal definition of cD galaxies, based on their optical properties as defined by Morgan and his collaborators (Mathews, Morgan, and Schmidt, 1964). I suggest that a new term, "central dominant galaxy" (abbreviated cd?) be used for galaxies that are the brightest cluster member or within 0.5 magnitudes of the brightest, and that appear to be at rest at the cluster center.

2. Proportion of spiral, SO, and elliptical galaxies

Elliptical and SO galaxies are more common than spiral galaxies in the inner portions of regular compact clusters, while the opposite is true in irregular clusters and in the field (Table II). Many explanations have been proposed for the origin of this systematic variation in galactic content. In general, these theories fall into two broad classes. In the first class, the proportion of galaxy types is set by the conditions when the galaxies form, and once the galaxies form they do not alter their morphology. Thus, in regions that are or will become regular clusters, more ellipticals are formed. In the second group of theories, galaxies may form with the same distribution of morphological types everywhere, but physical processes that depend on environment cause galaxies to alter their morphology. That is, in compact regular clusters, spirals become SO's or ellipticals, and SO's become ellipticals. Often an analogy is made between the generation of variations in the character of galaxy populations and human populations; in the first case, galaxy morphology is determined at conception (the "heredity" hypothesis), while in the second case it is influenced primarily by the "environment" in later life.

From the point of view of the "environment" theories, the primary difference between spiral galaxies and SO or elliptical galaxies is that spirals contain much more gas. As a result, spirals have active star formation, and the gas allows shocks, which delineate the spiral structure. The basic idea behind most of the environment theories, first suggested by Spitzer and Baade (1951), is that spiral galaxies would become SO galaxies if their gas were removed. A number of mechanisms have been proposed to remove the gas from spiral galaxies in clusters; these are reviewed in detail in Sec. V.I.

Spitzer and Baade (1951) suggested that collisions between spiral galaxies in the cores of compact clusters remove the interstellar medium from the disks of these galaxies. Subsequent increases in the estimates of the distance scale to clusters have had the effect of seriously reducing the efficiency of this process (Sec. V.I). It certainly could strip some of the spirals in a cluster. However, if the cluster has a significant amount of intracluster gas, there are several other processes which are more efficient.

Gunn and Gott (1972) suggested that SO galaxies are formed when spiral galaxies lose their interstellar medium through ram pressure ablation on intracluster gas. This process has now been studied fairly extensively, and is re-

viewed in Sec. V.I. In general, these studies indicate that a galaxy will be stripped almost completely during a single passage through the core of a cluster if the intracluster gas density exceeds roughly 3×10^{-4} atoms cm^{-3} .

Another mechanism for removing gas from galaxies, which can operate even when the galaxies are moving slowly through the intracluster gas, is evaporation (Cowie and Songaila, 1977; Secs. V.I and V.D.2). Heat is conducted into the cooler galactic gas from the hotter intracluster gas, and if the rate of heat conduction exceeds the cooling rate, the galactic gas will heat up and flow out of the galaxy [Eq. (5.118)]. The evaporation rate can be significantly reduced if the conductivity saturates (Sec. V.D.2), or because of the magnetic field (Sec. V.D.3). If the conductivity is not suppressed by these effects, this mechanism can play an important role in stripping gas from galaxies.

The x-ray observations that are the subject of this review have shown that many clusters have intracluster gas densities high enough to make ram pressure stripping effective [Sec. V.I; Eq. (5.115)]. In addition, there is a strong inverse correlation between the x-ray luminosity and the fraction of spiral galaxies in a cluster [Bahcall, 1977c; Melnick and Sargent, 1977; Tytler and Vidal, 1979; Eq. (3.9)]. The spiral fraction also decreases as the velocity dispersion of the cluster increases, as required for ram pressure ablation, and the spirals that are observed in x-ray clusters are on average at large projected distances from the cluster center (Gregory, 1975; Melnick and Sargent, 1977), where the intracluster gas density is presumably much lower than in the cluster core. Although not directly connected with stripping from spiral galaxies, the x-ray observations of M86 (an elliptical galaxy in the Virgo cluster) suggest that it is currently undergoing ram pressure ablation (Forman *et al.*, 1979; Fabian *et al.*, 1980).

Ram pressure ablation or evaporation removes the gas from cluster galaxies, and this prevents ongoing star formation. Thus one would expect that even when spiral galaxies do occur in a cluster, they will have less gas than field spirals and less active star formation. Studies of the 21-cm radio line of hydrogen from spiral galaxies in clusters indicate that they have considerably less gas than field spirals (Davies and Lewis, 1973; Krumm and Salpeter, 1976, 1979; Huchtmeier *et al.*, 1976; Sullivan and Johnson, 1978; Chamaraux *et al.*, 1980; Giovanelli *et al.*, 1981, 1982; Sullivan *et al.*, 1981) and that the amount of gas present increases with distance from the cluster center. Spirals in clusters also show weaker optical line emission than those in the field, which also suggests they have less gas (Gisler, 1978; but see Stauffer, 1983); the same is apparently true of cluster ellipticals and SO's (Davies and Lewis, 1973; Gisler, 1978). Moreover, many of the spirals in clusters have poorly defined spiral arms; they are classed as "anemic" spirals by van den Bergh (1976). These anemic cluster spirals are intermediate in appearance and in color between field spirals and SO's, which suggests that they have less active star formation than the field spirals. Cluster spirals may also be smaller

than field spirals (Peterson *et al.*, 1979). Finally, Gallagher (1978) and Kotanyi *et al.* (1983) present possible examples of spiral galaxies currently undergoing stripping.

Of course, the most direct test of the hypothesis that spiral galaxies evolve to become elliptical galaxies is the observation of spiral galaxies in high-redshift clusters which may be undergoing this transformation. Unfortunately, the image sizes of galaxies in high-redshift clusters (with ground-based telescopes) are so small that the galaxies cannot be directly classified. However, Butcher and Oemler (1978a) showed that a number of moderately high-redshift ($z \sim 0.4$) clusters apparently contained a high proportion of blue galaxies. The blue galaxies lie at larger projected distances from the cluster center than the redder galaxies. When redshift effects were removed, these blue galaxies had colors indistinguishable from those of nearby spiral galaxies. No such population of blue galaxies occurs in nearby compact clusters (Butcher and Oemler, 1978b). These blue galaxies in high-redshift clusters probably contain substantial quantities of gas and may be undergoing star formation; they may indeed be spiral galaxies. If so, we would have fairly direct evidence that galactic populations evolve in rich clusters.

There are, however, a number of problems associated with this interpretation of the "Butcher-Oemler effect." First, Mathieu and Spinrad (1981) and van den Bergh (1983b) have argued, based on the photometry and positions of the blue galaxies in the Butcher-Oemler cluster about 3C295, that the cluster is actually relatively poor, and that the blue galaxies are primarily background and foreground field galaxies; they claim that the actual cluster members have a more normal color distribution. Redshifts and spectra now exist for a reasonably large sample of galaxies in the Butcher-Oemler clusters (Dressler and Gunn, 1982; Dressler, 1984); they show that some of the blue galaxies are cluster members, although many are foreground galaxies. The blue galaxies that are cluster members do have colors which might suggest that they are spirals. However, the spectra and surface brightnesses of these blue galaxies are very different from those of present-day spiral galaxies; they appear to consist of Seyfert-like active galaxies and galaxies that have recently undergone or are undergoing very large bursts of star formation. The present rather uncertain situation concerning the Butcher-Oemler effect has been reviewed recently by Dressler (1984). Second, the effect is not at all universal; high-redshift clusters are known which do not contain such a blue population (see, for example, Koo, 1981). Third, x-ray observations show that the Butcher-Oemler clusters contain significant quantities of intracluster gas (Sec. III.H). The ram pressure ablation time scales are thus rather short ($\leq 10^9$ yr). It seems unlikely that the clusters formed such a short time before they were observed; how then have the spirals survived? It is possible, given the fact that the blue galaxies lie in the outer parts of the clusters, that they have not passed through the cluster core yet. Another possibility, suggested by Gisler (1979), is that the rate of formation of interstellar gas in

galaxies was higher at these redshifts. This could make it considerably more difficult to strip the galaxies through ram pressure ablation. (However, also see Livio *et al.*, 1980.) Finally, the redshifts of the clusters observed by Butcher and Oemler are not that large; why is it that similar clusters are not found at the present time?

Norman and Silk (1979) and Sarazin (1979) have suggested that nearly all the gas in a cluster was initially in the form of gaseous halos around galaxies. These halos would be stripped rather slowly by collisions until sufficient gas built up in the cluster core for ram pressure ablation to become effective. In this way, the stripping of spiral galaxies could be delayed for a significant fraction of a Hubble time, in agreement with the Butcher-Oemler effect. Larson *et al.* (1980) argued that the gaseous disks of galaxies are supplied by the continual infall of gas from the gaseous halos proposed by Norman and Silk (1979) and Sarazin (1979). In this scenario, a galaxy will be transformed from a spiral into an SO following the removal of its gaseous halo; star formation will then exhaust the interstellar medium in the disk in a few billion years. The Butcher-Oemler clusters might be in the midst of this transformation.

The stripping mechanisms described above (ram pressure ablation, evaporation, or the Spitzer-Baade effect) remove the gas from galaxies, but probably would not seriously affect the distribution of the stars because the mass fraction of gas in typical spirals is not terribly large (Farouki and Shapiro, 1980). Unfortunately, simply removing the gas from a spiral would leave behind a thin stellar disk; thus a stripped spiral galaxy might resemble an SO galaxy, but never an elliptical galaxy. As the fraction of elliptical galaxies is higher in the centers of compact clusters than in the field (Table II), the difference in galactic population between these two environments cannot result solely from the transformation of spirals into SO's. Moreover, SO's appear to have thicker disks than spirals (Burstein, 1979b). If galactic populations have evolved since formation, the stellar distribution in galaxies must have been modified during this evolution.

Of course, the process of gas removal could directly affect the stellar distribution if, during the removal of the gas, a significant portion were converted into stars which remained bound to the galaxy. This might produce the "thick disk" component seen in SO's by Burstein (1979b).

Tidal gravitational effects during galaxy collisions can alter the stellar and mass distributions in galaxies. The possibility that massive halos around galaxies might be removed by tidal collisions in clusters has already been discussed in Secs. II.H and II.J.1. Such tidal encounters might also puff up the disks of spiral galaxies and transform them into SO or elliptical galaxies (Richstone, 1976). Unfortunately, detailed numerical simulations suggest that tidal interactions are not capable of transforming disk galaxies into ellipticals unless they do so before the cluster collapses (Da Costa and Knobloch, 1979; Farouki and Shapiro, 1981).

Another possibility is that elliptical galaxies are formed by the merger of spiral galaxies in clusters (Toomre and

Toomre, 1972; White, 1979). There are a number of serious problems with this hypothesis, which have been summarized by Ostriker (1980) and Tremaine (1981). Most of these objections disappear if the mergers occur in subclusters before the formation of the cluster (see White, 1982).

Evidence given in support of the "heredity hypothesis" (the theory that galaxy morphology is determined at the time of galaxy formation) is primarily in the form of evidence against the "environment hypothesis." Specifically, most of these arguments attack the extreme suggestion that the differences in galaxy morphology are determined solely by some environmental mechanism which removes the gaseous content of galaxies.

First, the total fraction of disk galaxies ($Sp+SO$)/($Sp+SO+E$) is not fixed, but varies from regular clusters to the field (Faber and Gallagher, 1976; Table II). If the only change in galaxy morphology were the conversion of spirals into SO's, this ratio would be a constant. Second, some SO and E galaxies are sometimes found in low-density regions (the field), where ram pressure ablation and other environmental influences should be very weak (Sandage and Visvanathan, 1978; Dressler, 1980b), and these field SO's and E's have the same color distribution as the cluster SO's and E's. Third, Dressler (1980b) has found that distribution of galaxy morphologies correlates most strongly with the local galaxy density, and not as strongly with the global environment (which probably determines the density of intracluster gas). Fourth, the properties of SO galaxies (colors, bulge-to-disk ratios, gaseous content, etc.) are generally intermediate between Sp and E galaxies (Sandage *et al.*, 1970; Faber and Gallagher, 1976). This would not necessarily be true if SO's were stripped Sp's, but would be explained under the "heredity hypothesis" if the nature of galaxy formation were characterized by a single parameter, which is often taken to be the density of the region in which galaxy formation occurs (see below). Fifth, SO galaxies have larger ratios of bulge to disk luminosity than spirals (Burstein, 1979a), and also absolutely larger and more luminous bulges (Dressler, 1980b). This would not be expected if SO's were simply spirals with their gas removed. Finally, SO galaxies appear to have a thick, boxy component to the disk, which is not present in spirals (Burstein, 1979b). Of course, one could argue that these thick disks actually arise during the process of stripping the gaseous disks from spirals; for example, the stripping process might induce star formation in the gas while it is being stripped, and produce a thick disk of stars supported by large-velocity components perpendicular to the disk.

If galaxy morphology is determined by the conditions at the time of galaxy formation, what is the mechanism and to what conditions is it responsive? Most theories of galaxy formation assume that galaxies form by the collapse of initially gaseous matter (Eggen *et al.*, 1962; Gott, 1977). The stellar bulge components of galaxies all have distributions similar to the de Vaucouleurs profile [Eq. (2.14)], which suggests that they have relaxed violently (Sec. II.I) during the collapse. As discussed in Sec. II.I, this implies that the collapse takes place in nearly a free-

fall time [Eq. (2.32)]. If, prior to this collapse, most of the gas in the galaxy were converted to stars, these stars would act as a collisionless, dissipationless fluid, and only violent relaxation would occur. This would produce an ellipsoidal distribution of stars—that is, an elliptical galaxy. On the other hand, if star formation were ineffective, and most of the collapsing material remained gaseous, it would dissipate through radiation much of its energy, while maintaining its net angular momentum, and collapse to form a disk. With this hypothesis one can understand why the galaxies that contain significant quantities of gas are the disk-dominated spirals, and why the galaxies that lack gas are ellipticals and SO's.

Moreover, if galaxies initially have little gas compared to their stellar content, it is easier for them to remain free of gas. First, the stripping processes discussed above (ram pressure ablation, evaporation, etc.) are more effective if the density of interstellar gas is low. Second, even in the absence of such external mechanisms for removing gas, a galaxy with a high ratio of the density of stars to gas can clean itself of interstellar medium through the formation of a galactic wind (Mathews and Baker, 1971). The interstellar gas in a galaxy is heated by the stars, through supernovae, stellar winds, ionizing radiation, and the motion of mass-losing stars at high velocity through the ambient gas. If the gas density is sufficiently high compared to the stellar density, the gas will be able to cool efficiently, and the energy input from stars will be radiated away. Conversely, if the gas density is low compared to the stellar density, the gas will heat up until thermal velocities in the gas exceed the escape velocity from the galaxy, and the gas leaves the galaxy in a transonic wind. Thus, if a galaxy starts with a small proportion of gas to stars, it can keep itself free of gas. Since the standard hypothesis is that E and SO galaxies start with little gas, one can understand how they have managed to stay relatively gas free.

If it is the efficiency of star formation during the collapse of a protogalaxy which determines its morphology, what determines the efficiency of star formation? Why does it depend on the location of the protogalaxy? Two attempts to answer these questions have received particular attention. First, Sandage, Freeman, and Stokes (1970) argued that the efficiency of star formation in a protogalaxy is determined by the specific angular momentum content of the gas. If the angular momentum content of the gas is high, the collapse of protostars will be halted or delayed by centrifugal forces. Thus one would expect protogalaxies with a high angular momentum content to form spirals, and those with low angular momentum to form ellipticals. This hypothesis is in agreement with the observation that the specific angular momentum of disks significantly exceeds that of ellipsoidal components of galaxies.

Alternatively, Gott and Thuan (1976) have argued that the efficiency of star formation during the collapse of a galaxy is set by the density in the protogalaxy. Star formation requires that gas cool. Cooling processes generally involve two-body collisions. Therefore it is reasonable

to assume that the cooling rate increases with density [see Eq. (5.23) for example]. In protogalaxies with a sufficiently high initial density, the gas will be largely converted to stars during the collapse. If the initial density is sufficiently low, star formation is not effective and the gas collapses to a disk.

In Sec. II.I evidence was presented which indicated that the sequence of cluster morphology, from the field to irregular clusters to regular clusters, was a dynamical sequence resulting from increasing initial density. Thus regular, compact clusters formed from regions of high density, and irregular clusters from lower-density regions. If density is also the factor that determines galaxy morphology, the relationship of galaxy morphology and cluster morphology can be understood.

In summary, it remains controversial whether galaxy morphology is determined primarily by conditions at the time of galaxy formation, or whether galaxy morphology evolves in response to the environment after formation. It seems unlikely that *all* galaxies have identical forms at birth, and that *all* the variation in galaxy morphology is due to environment. It seems reasonable that environment has played *some* role in determining galaxy morphology; surely, somewhere at least one spiral galaxy has blundered into a core of a rich, compact cluster and been stripped. Thus I believe both mechanisms have probably significantly affected galaxy morphology. Note that two other possibilities further obscure the distinction between these two hypotheses. First, galaxies may have formed before clusters; then, the galaxies might have evolved in an environment different from that observed today (Roos and Norman, 1979). Second, the formation of disks in galaxies might be a slow and ongoing process (Larson *et al.*, 1980); then, there is no real distinction between the "heredity" and "environment" hypotheses, at least to the origin of disks.

Ultimately, the Hubble Space Telescope (Hall, 1982) will permit structural studies of galaxies in and out of clusters at large redshifts. These studies will show whether morphological evolution has occurred in galaxies, at least over the last half of the age of the universe.

K. Extensions of clustering

Rich clusters of galaxies represent only a portion of a spectrum of clustering (Peebles, 1974), which ranges from individual galaxies and binary galaxies to enormous regions of enhanced density ("superclusters") or reduced density ("voids").

1. Poor clusters

Lists of poor clusters and groups have been given by Sandage and Tammann (1975), de Vaucouleurs (1975), Turner and Gott (1976b), Hickson (1982), Beers *et al.* (1982), and Huchra and Geller (1982). Of particular interest are the poor clusters containing possible cD galaxies which have been cataloged by Morgan, Kayser, and White

(1975) and Albert, White, and Morgan (1977); these are generally referred to as MKW and AWM, respectively. In Sec. II.J.1 observations of the cD's in these poor clusters were used to constrain models for the formation of cD galaxies. Bahcall (1980) has studied the optical properties (richness, galaxy distribution, and galactic content) and finds that they represent a smooth continuation to lower richness of the properties of the Abell clusters.

2. Superclusters and voids

Clustering does not stop at the well-defined rich clusters, but extends to a much larger scale (Peebles, 1974). These superclusters appear in the distribution of galaxies, or in the distribution of clusters of galaxies. Recent reviews of superclustering include those of Rood (1981) and Oort (1983). Our own galaxy appears to lie within the Local Supercluster, a flattened system dominated by the Virgo cluster (de Vaucouleurs, 1953).

The recognition of distinct superclusters and of voids (nearly empty regions between superclusters) has largely become possible as larger samples of redshifts have become available for galaxies and clusters. With redshifts, one can study the three-dimensional distribution of galaxies, rather than just their angular distribution on the sky, and the confusing effects of projection can be reduced. Such studies have shown that Coma (A1656) and A1367 form part of a large (≥ 30 Mpc) Coma supercluster (Rood *et al.*, 1972; Chincarini and Rood, 1976; Tifft and Gregory, 1976; Gregory and Thompson, 1978), and that the Perseus cluster is embedded in the Perseus supercluster (Gregory *et al.*, 1981). Other possible superclusters identified as groupings of clusters have been cataloged by Abell (1961), Rood (1976), Murray *et al.* (1978), and Thuan (1980).

Similar large-scale clustering is observed directly in the distribution of galaxies in redshift surveys in small regions of the sky by Kirshner, Oemler, and Schechter (1978) and by the more extensive survey of Davis *et al.* (1982). Many of the superclusters appear to be highly elongated.

Large voids have also been found to lie between the superclusters. Such voids appear in front of the Coma, Perseus, and Hercules superclusters (Rood, 1981). An extremely large void (100–200 Mpc in size) in the galaxy distribution in the direction of Bootes has been discovered by Kirshner *et al.* (1981). A similarly large void in the distribution of Abell clusters was discovered recently by Bahcall and Soneira (1982).

III. X-RAY OBSERVATIONS

A. Detections and identifications

The first extragalactic object to be detected as an x-ray source was M87 in the Virgo cluster (Byram *et al.*, 1966; Bradt *et al.*, 1967). Sources associated with the Perseus cluster (Fritz *et al.*, 1971; Gursky *et al.*, 1971a) and the

Coma cluster (Meekins *et al.*, 1971; Gursky *et al.*, 1971b) were detected next. The idea that extragalactic x-ray sources were generally associated with groups or clusters of galaxies was suggested by Cavaliere *et al.* (1971). While the early detections were made with balloon- or rocket-borne detectors, a major advance in the study of x-ray clusters (and all of x-ray astronomy) came with the launch of the *Uhuru* x-ray satellite, which permitted more extended observations of individual sources and a complete survey of the sky in x rays, the *Uhuru* Catalog (Giacconi *et al.*, 1972, 1974; Forman, Jones, Cominsky, Julien, Murray, Peters, Tananbaum, and Giacconi, 1978).

The early *Uhuru* observations established a number of properties of the x-ray sources associated with clusters. First, clusters of galaxies are the most common bright extragalactic x-ray sources. Second, clusters are extremely luminous in their x-ray emission, with luminosities $\sim 10^{43-45}$ ergs sec⁻¹, and they have a wide range of luminosities. This makes clusters as a class the most luminous x-ray sources in the universe, with the exception of quasars. Third, the x-ray sources associated with clusters are extended (Kellogg *et al.*, 1972; Forman *et al.*, 1972); the sizes found from the *Uhuru* data range from about 200 to 3000 kpc. Fourth, the clusters have x-ray spectra that show no strong evidence for low-energy photoabsorption, unlike the spectra of the compact sources associated with discrete sources either in the nuclei of galaxies or stellar sources within our own galaxy. Fifth, the x-ray emission from clusters is not time variable, as is the emission from many point sources of x rays in our galaxy or in the nuclei of other galaxies (Elvis, 1976). These last three results suggest that the emission is truly diffuse, and not the result of one or many compact sources. Many of the early *Uhuru* results are presented in several review papers by Kellogg (1973, 1974, 1975).

The original identifications of clusters with *Uhuru* sources were made by Gursky *et al.* (1972) and Kellogg *et al.* (1971, 1973). Other identifications of clusters as *Uhuru* sources were made by Bahcall (1974c), Disney (1974), Rowan-Robinson and Fabian (1975), Elvis *et al.* (1975), Melnick and Quintana (1975), Vidal (1975a, 1975b), Bahcall *et al.* (1976), Ives and Sanford (1976), Pye and Cooke (1976), Lugger (1978), and Johnston *et al.* (1981). The situation on the identifications of clusters was summarized by Bahcall and Bahcall (1975), who argued that the many unidentified *Uhuru* sources at high galactic latitude were probably also clusters of galaxies. A systematic search for Abell cluster identifications in the *Uhuru* catalog was made by Kellogg *et al.* (1973). Cluster x-ray sources were also identified in surveys made with the *Ariel 5* satellite (Elvis *et al.*, 1975; Cooke and Maccagni, 1976; Maccacaro *et al.*, 1977; Mitchell *et al.*, 1977; McHardy, 1978a; Ricketts, 1978; McHardy *et al.*, 1981) and *SAS-C* satellite (Markert *et al.*, 1976, 1979). A combined sample of x-ray identification from the *Uhuru* and *Ariel* surveys was given by Jones and Forman (1978), and the pre-*HEAO* cluster identifications have been reviewed by Gursky and Schwartz (1977).

The next major advance in sensitivity came with the

launch of the *HEAO-1* x-ray observatory, with proportional counters with a very large collecting area. Identifications of clusters with hard x-ray sources detected in sky surveys with the *HEAO A-2* instrument have been given by Marshall *et al.* (1979) and by Piccinotti *et al.* (1982) for high-galactic-latitude x-ray sources. Searches for x-ray emission from the richest Abell clusters were made by Pravdo *et al.* (1979). A soft x-ray survey of a few clusters was made by Reichert *et al.* (1981), and a complete soft x-ray catalog is given by Nugent *et al.* (1983). A statistically complete sample of Abell clusters was surveyed with the *HEAO-1 A-2* instrument by McKee *et al.* (1980). A survey of a large sample (~ 1900) of Abell clusters with the *HEAO-1 A-1* was made by Ulmer *et al.* (1981) and Johnson *et al.* (1983), while a survey of the most distant Abell clusters with the *HEAO-1 A-1* detector (Ulmer, Shulman *et al.*, 1980) detected 11 such clusters, suggesting that many of them are extremely luminous.

X-ray astronomy made a quantum leap forward with the launch of the *Einstein* observatory. This was the first satellite with focusing optics for extrasolar x-ray observing. Because of its focusing capability, the sensitivity of this instrument to small sources was orders of magnitude higher than that for any previous x-ray detector. At the time of writing, the analysis of the data from many of the extensive surveys of x-ray emission from clusters had not been completed. (However, as this review was being completed, two large surveys appeared: Abramopoulos and Ku, 1983; Jones and Forman, 1984.) Undoubtedly, the number of detected x-ray clusters will increase greatly. The currently available x-ray cluster detections with *Einstein* include those of Jones *et al.* (1979), Henry *et al.* (1979, 1982), Burns, Gregory, and Holman (1981), Forman *et al.* (1981), Maccagni and Tarengi (1981), Perrenod and Henry (1981), R. A. White *et al.* (1981, 1985), S. D. M. White *et al.* (1981), Abramopoulos and Ku (1983), Bechtold *et al.* (1983), Soltan and Henry (1983), and Jones and Forman (1984).

Compact, poor clusters were detected as x-ray sources by Schwartz, Davis, Doxsey, Griffiths, Huchra, Johnston, Mushotzky, Swank, and Tonry (1980), Schwartz, Schwarz, and Tucker (1980), and Kriss *et al.* (1980, 1981, 1983), and will be discussed in more detail in Sec. III.G.

Murray *et al.* (1978) suggested that a number of sources in the 4U *Uhuru* catalog were associated intrinsically with superclusters (that is, there was more emission than could be accounted for simply by the sum of the emissions from the number of x-ray clusters one would have expected to find in the supercluster). Kellogg (1978) presented evidence that x-ray clusters were located in superclusters, but did not suggest that there was any intrinsic emission associated with the supercluster itself. Subsequent observations have not confirmed the detections of superclusters as a distinct class of x-ray sources (Ricketts, 1978; Pravdo *et al.*, 1979). Forman, Jones, Murray, and Giacconi (1978) claimed to have detected very large and luminous halos of x-ray emission about clusters of galaxies, and argued that the extra emission seen by Murray *et*

al. from superclusters might really be the sum of the halos of the clusters in the superclusters. In general, subsequent observations have not confirmed the presence of these luminous and extensive halos (Pravdo *et al.*, 1979; Nulsen *et al.*, 1979; Ulmer, Cruddace, Wood, Meekins, Yentis, Evans, Smathers, Byram, Chubb, and Friedman, 1980; Nulsen and Fabian, 1980).

B. X-ray luminosities and luminosity functions

The number of clusters per unit volume with x-ray luminosities in the range L_x to $L_x + dL_x$ is defined as $f(L_x)dL_x$, where $f(L_x)$ is the x-ray luminosity function. In general, the luminosity function will depend on the method used to select the clusters. One can begin with a statistically complete catalog of optically detected clusters (such as the "statistical sample" of Abell clusters; see Sec. II.A), which is surveyed for x-ray emission. Alternatively, a complete catalog of x-ray sources can be examined optically to determine which sources are associated with clusters of galaxies. In addition to reproducing the observed statistics of x-ray cluster identifications, the x-ray luminosity function is subject to the additional constraints that the total number of x-ray clusters not exceed the total number of all clusters, and the total emissivity of x-ray clusters not produce a larger x-ray background than is observed. Most data on cluster luminosities have been fit to either an exponential or a power-law form of the luminosity function. Thus we define

$$f(L_x) = A_e h_{50}^5 \exp(-L_x/L_{x0}) \times (10^{44} \text{ ergs sec}^{-1})^{-1} \text{ Mpc}^{-3}, \quad (3.1)$$

$$f(L_x) = A_p h_{50}^5 \left[\frac{L_x}{10^{44} h_{50}^{-2} \text{ ergs sec}^{-1}} \right]^{-p} \times (10^{44} \text{ ergs sec}^{-1})^{-1} \text{ Mpc}^{-3}. \quad (3.2)$$

All luminosities in this section are given for the photon energy range of 2–10 keV. It is convenient to define $L_{44} \equiv L_x/10^{44} \text{ ergs sec}^{-1}$.

Schwartz (1978) derived an estimate of the luminosity function for a sample of 14 Abell clusters in distance class three or less, which were detected with the *Uhuru*, *Ariel 5*, or *SAS-C* satellites. More distant clusters are used only to give an upper limit to the luminosity function at high luminosities. This sample is only expected to be complete for $1 \leq L_{44} \leq 10$. Schwartz found that the best fit exponential luminosity function has $A_e = 4.5 \times 10^{-7}$ and $L_{x0} = 2.0 \times 10^{44} h_{50} \text{ ergs sec}^{-1}$, although a power law with $A_p = 7.9 \times 10^{-7}$ and $p \approx 2.45$ would also fit the data if suitably truncated at high and low luminosities.

McHardy (1978a) derived an x-ray luminosity function from the *Ariel 5* fluxes for Abell clusters of distance class three or less; he argued that the *Uhuru* fluxes are unreliable for weak sources. While he did not fit his numerical

luminosity function to any analytic expression, a suitable fit is given by a power law with $A_p = 2.5 \times 10^{-7}$ and $p \approx 2$ for $0.2 \leq L_{44} \leq 20$.

The *HEAO-1* satellite provided a much more extensive data base for determining the luminosity function of clusters. Both the A-1 and A-2 experiments were used to survey the Abell clusters. A luminosity function was derived for a significant portion of the "statistical sample" of Abell clusters (Sec. II.A), using the A-1 data by Ulmer *et al.* (1981). Exponential and power-law fits to these data gave $A_e = 0.49 \times 10^{-7}$, $L_{x0} = 2.9 \times 10^{44} h_{50}^{-2} \text{ ergs sec}^{-1}$, and $A_p = 1.1 \times 10^{-8}$, $p = 1.7$, respectively. When the sample was extended to all Abell clusters and luminosities, the normalization A_e and the characteristic luminosity L_{x0} both were roughly doubled.

The *HEAO-1* A-2 data were used to derive a luminosity function both by surveying the Abell clusters (McKee *et al.*, 1980; Hintzen *et al.*, 1980) and by identifying a complete sample of x-ray sources in a flux-limited survey at high galactic latitude (Piccinotti *et al.*, 1982). The Abell cluster survey included all richness classes and all distance classes less than five. The luminosity function could be fit adequately with either an exponential or power-law form, and the coefficients in Eqs. (3.1) and (3.2) were $A_e \approx 2.5 \times 10^{-7}$, $L_{x0} \approx 1.8 \times 10^{44} h_{50}^{-2} \text{ ergs sec}^{-1}$, $A_p \approx 3.8 \times 10^{-7}$, and $p \approx 2.2$. The cluster luminosity from the high-latitude survey was not well represented by an exponential; a power-law fit gave $A_p \approx 3.6 \times 10^{-7}$ and $p \approx 2.15$, which agrees well with the A-2 Abell survey result.

Bahcall (1979b) has attempted to predict the x-ray luminosity function of clusters from their optical luminosity function by assuming a one-to-one correspondence between the optical and x-ray luminosity of clusters. She predicts that clusters have a luminosity function that can be represented by two intersecting power laws with $p \approx 2.5$ for $L_{44} \geq 1$ and $p \approx 1.3$ for $L_{44} \leq 1$. While the *HEAO-1* data do not show any clear evidence for a change in the slope of the luminosity function at $L_{44} \approx 1$, they are probably not inconsistent with such a change because they do not extend much below this luminosity.

One important application of cluster luminosity functions is in determining the contribution of clusters to the hard x-ray background (see Field, 1980, for a review of its properties). From the estimates of the luminosity function of clusters discussed above, it appears that clusters probably provide only about 3–10% of the x-ray background in the (2–10)-keV photon energy band, assuming they do not evolve rapidly with time (Rowan-Robinson and Fabian, 1975; Gursky and Schwartz, 1977; McKee *et al.*, 1980; Hintzen *et al.*, 1980; Piccinotti *et al.*, 1982; Ulmer *et al.*, 1981).

C. X-ray spectra

Observations of the x-ray spectra of clusters of galaxies have played a critical role in establishing the primary emission mechanism (thermal emission from diffuse hot

intracluster gas) and in testing models for the origin of this gas. Models in which the emission comes from diffuse thermal gas predict (1) that the spectrum will be roughly exponential [the intensity I_ν (ergs per cm^2 per sec per hertz) varies as $\sim \exp(-h\nu/kT_g)$ where T_g is the gas temperature]; (2) that the gas temperature will be such that the thermal velocity of protons in the gas $\sim (kT_g/m_p)^{1/2}$ will be comparable to the velocity of the galaxies in the cluster, as both are bound by the same gravitational potential; (3) that there will be no strong low-energy photoabsorption; and (4) that emission lines will be present if the gas contains a significant contamination of heavy elements like iron. Alternatively, models in which the emission is due to relativistic nonthermal electrons predict a power-law spectrum $I_\nu \propto \nu^{-\alpha}$, which implies an excess at low and high energies when compared to an exponential spectrum; no line emission would be expected for a nonthermal emission process. As another possibility, the emission might be thermal emission from a number of compact sources, such as galactic nuclei or the binary stellar x-ray sources which dominate the x-ray sky within our own galaxy; however, such sources are generally optically thick at low x-ray energies ($\lesssim 1$ keV). The theories for each of these classes of emission processes and the basis for these predictions are discussed in Sec. V.A.

The first three of the predictions given above concern the broad-band form of the spectrum (the continuum), while the last prediction concerns lines. Accordingly, the properties of the continuum spectra will first be reviewed, and then those of the line spectra. Reviews devoted primarily to the observations of the x-ray spectra of clusters have been given recently by Canizares (1981) and Mushotzky (1980,1984), while Holt and McCray (1982) review all of x-ray spectroscopy.

1. Continuum features in the spectrum

If the x-ray emission from clusters is due to a diffuse plasma of either thermal or nonthermal electrons, the optical depth of the gas should be quite low. On the other hand, compact x-ray sources (such as galactic nuclei or binary stellar x-ray sources) often contain significant quantities of relatively cool neutral gas, which absorbs soft x rays through photoionization. Because the fluorescent yield of the light elements is low, the absorbed x rays are not reemitted and are lost from the spectrum. This low-energy photoabsorption occurs in a series of edges which correspond to the absorption edges of cosmically abundant elements. The opacity of a solar abundance,⁷ low-density, cold neutral gas has been calculated, for example, by Brown and Gould (1970). It is conventional to

parametrize the absorption observed in an x-ray spectrum by the column density of hydrogen N_H in a gas with assumed solar abundances required to produce the observed absorption. Typically, compact sources have $N_H \gtrsim 10^{22} \text{ cm}^{-2}$. Even the earliest x-ray spectra of clusters suggested that they had rather weak low-energy absorption (Catura *et al.*, 1972; Kellogg, 1973; Davidsen *et al.*, 1975; Kellogg *et al.*, 1975; Margon *et al.*, 1975; Avni, 1976), with column densities $N_H \lesssim 10^{22} \text{ cm}^{-2}$, which were generally consistent with the amount of neutral hydrogen in our own galaxy along the line of sight to the cluster. This indicated that the emission from clusters comes from a diffuse, ionized plasma.

Initially, there were two competing models for the nature of this ionized plasma (see Sec. V.A). It could be a hot, thermal plasma with a temperature $T_g \sim 10^8$ K, or it could be a relativistic, nonthermal plasma with a power-law electron energy distribution, such as the plasma responsible for the radio emission observed in clusters (see Sec. IV.A). In the first case, the x-ray continuum would be primarily due to thermal bremsstrahlung (see Sec. V.A.3), with a spectrum given by Eq. (5.11). If the frequency variation of the Gaunt factor $g_{ff}(\nu, kT_g)$ is ignored and the gas is all at a single temperature, the spectrum is exponential $I_\nu \propto \exp(-h\nu/kT_g)$. In the second case, the emission is primarily due to the inverse Compton process (the scattering of low-energy photons to x-ray energies by the relativistic electrons; see Sec. V.A.1), and the expected spectrum is a power law $I_\nu \propto \nu^{-\alpha}$.

Unfortunately, proportional counters have rather poor spectral resolution, and it is therefore difficult to distinguish between thermal and nonthermal spectra. Moreover, any sufficiently smooth and monotonic spectrum can be produced by the combination of the thermal spectra with varying temperatures, or nonthermal spectra with varying spectral indices α ; thus the distinction between thermal and nonthermal spectra cannot be made unambiguously. It is not surprising, therefore, that the early proportional counter spectra of clusters could be fit consistently by either thermal (exponential) or nonthermal (power-law) spectra (for example, Kellogg *et al.*, 1975). However, spectra over a large energy range were better fit by the thermal model (Davidsen *et al.*, 1975; Scheepmaker *et al.*, 1976).

The first large surveys of cluster spectra came from observations with *OSO-8* and *Ariel 5*. These satellites observed individual clusters for longer periods of time than had been possible with previous sky survey instruments, and had detectors that were optimized for spectral resolution. The spectra of clusters observed with *OSO-8* and *Ariel 5* were significantly better fit by the thermal bremsstrahlung model than by the nonthermal model (Mushotzky *et al.*, 1978; Mitchell *et al.*, 1979). The required temperatures for the cluster gas were found to range from about 2×10^7 to 2×10^8 K from cluster to cluster, and some of the clusters required gas at several temperatures to fit the spectrum. Recently, a more extensive survey of x-ray cluster spectra was made with the *A-2* experiment on the *HEAO-1* satellite (Mushotzky,

⁷The "solar abundance" of an element is usually taken to be its abundance relative to hydrogen in the solar system at its formation. See, for example, Allen (1973).

1980,1984).

The two properties that can be derived most easily from the continuum x-ray spectrum are the gas temperature T_g and the emission integral

$$EI \equiv \int n_p n_e dV, \quad (3.3)$$

where n_p is the proton density, n_e is the electron density, and V is the volume of the gas in the cluster. The x-ray luminosity of a cluster is proportional to EI [Eq. (3.11)]. The x-ray luminosity (or EI) and gas temperature are strongly correlated (Mitchell *et al.*, 1977,1979; Mushotzky *et al.*, 1978). The *HEAO-1 A-2* sample (Fig. 6) gives $L_x \sim T_g^3$ (Mushotzky, 1984). The *OSO-8*, *Ariel 5*, and *HEAO-1 A-2* spectral surveys established a number of correlations between these x-ray spectral parameters and the optical properties of x-ray clusters, which are discussed in Sec. III.F below.

There was also some evidence from the *OSO-8* survey that the gas in clusters was isothermal; that is, the range of temperatures within the gas in a single cluster was relatively small. However, in many cases the *OSO-8* and *Ariel 5* temperatures were not in agreement within the errors; if these differences are real, they suggest that there are multiple temperature components to the emission. If that were the case, the *OSO-8* and *Ariel 5* detectors, which have different spectral and spatial sensitivities, might give different weights to the different components, and produce different average temperatures.

The *HEAO-1 A-2* detector has provided much more data on the spectra of clusters in the photon energy range 2–60 keV (Mushotzky, 1980,1984). There is now evidence that many clusters contain several temperature components, with typical temperatures of $T_g \sim 2 \times 10^7$ and 8×10^7 K. (This probably does not mean that there are two discrete temperatures in these clusters; rather, the spectrum cannot be fit by a single temperature.) These multiple temperature components appeared to be most significant in clusters with low x-ray luminosities, al-

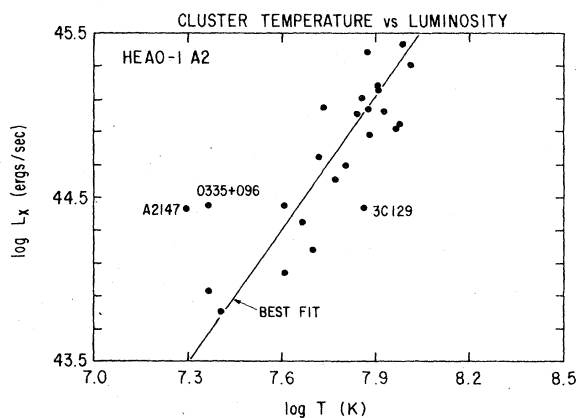


FIG. 6. The correlation between the gas temperatures derived from x-ray spectra with *HEAO-1 A-2* and the cluster x-ray luminosities, from Mushotzky (1984).

though it is possible that similar low-luminosity cool components might remain undetected if hidden in the spectrum of clusters with high-luminosity high-temperature emission. The information on the spatial distribution of the x-ray emission in clusters (Sec. III.D) suggests two locations for this cool gas. First, in low-luminosity clusters, the x-ray emission is often inhomogeneous, with clumps of emission being associated, in some cases, with individual galaxies. These clumps may contain cooler gas. Second, in some clusters there are enhancements in the x-ray surface brightness at the position of the cD or other centrally located dominant galaxy in the cluster. X-ray line observations suggest that these are regions at which the hot intracluster gas is cooling and being accreted by the central dominant galaxy (Sec. V.G).

The *Einstein* x-ray observatory had two instruments capable of providing information on the continuum spectra of clusters. First, there was the Imaging Proportional Counter (IPC), which provided low-resolution spatial and spectral information. Initially there were problems with the calibration of the energy scale of the spectra due to gain variations. While these problems have now apparently been resolved, there are few cluster spectra from this instrument available in the literature at the present time (see, however, Fabricant *et al.*, 1980; Perrenod and Henry, 1981; Fabricant and Gorenstein, 1983; White *et al.*, 1985). The second instrument was the Solid State Spectrometer (SSS), which had considerably better spectral resolution, but had no spatial resolution and less sensitivity than the IPC. Because of its small field of view (6 arcmin), it could only observe a small portion of nearby clusters. Thus it was used primarily to determine spectra for the central regions of nearby clusters. It provided strong evidence for the presence of cool gas at the centers of a number of clusters (Mushotzky, 1980,1984; Mushotzky *et al.*, 1981; Lea *et al.*, 1982); these observations are discussed further below. One problem with *Einstein* as an instrument for x-ray cluster spectroscopy is that the telescope was only sensitive to photons with energies of about 0.1–4.0 keV. With the typical temperatures of the gas in clusters being $kT_g \sim 8$ keV, observations with *Einstein* could not determine the thermal structure in this hot gas. However, the *Einstein* detectors were very sensitive to the presence of low-temperature components to the emission.

Detections or limits on the hard x-ray spectrum and flux of clusters have been useful in limiting the contribution of nonthermal processes to their luminosity. As mentioned above, spectra extending into the hard x-ray region ($h\nu > 20$ keV) gave the first direct, strong indication that the primary emission mechanism was thermal, rather than nonthermal (Davidsen *et al.*, 1975; Scheepmaker *et al.*, 1976). Subsequently, stronger limits on the hard x-ray emission have shown that nonthermal emission makes at most a very small contribution to the x-ray luminosity of clusters (Mushotzky *et al.*, 1977; Lea *et al.*, 1981). When combined with observations of the diffuse radio emission in the cluster (Sec. III.D), these hard x-ray

limits can be used to give lower limits on the magnetic field in the cluster, because the synchrotron radio emissivity is proportional to the product of the density of relativistic electrons and the magnetic field strength, while the inverse Compton x-ray emission depends only on the density of relativistic particles (see Sec. V.A.1 for a more detailed discussion of this point). Typically, these limits are $B \gtrsim 10^{-7}$ G (Lea *et al.*, 1981; Primini *et al.*, 1981).

In the Perseus cluster, a power-law hard x-ray component with $\alpha \approx 2.25$ has been detected; it varies on a time scale of about a year, and the x-ray variations are correlated with variations in the radio flux of the compact radio source at the nucleus of the galaxy NGC1275 (Primini *et al.*, 1981; Rothschild *et al.*, 1981). Much weaker variable power-law sources may also have been detected in the M87/Virgo and A2142 clusters (Lea *et al.*, 1981).

2. Line features—the 7-keV iron line

In many ways, the most significant observational discovery concerning x-ray clusters (following their identification as x-ray sources) was the detection of line emission due to highly ionized iron as a strong feature in their x-ray spectra. Immediately, this discovery established that the primary emission mechanism in x-ray clusters was thermal, and that the hot intracluster gas contained at least a significant portion of processed gas, which had at some point been ejected from stars. This line feature was first detected in the spectrum of the Perseus cluster by Mitchell *et al.* (1976) and shortly thereafter in the spectra of the Coma and Perseus clusters by Serlemitsos *et al.* (1977). It has subsequently been detected in the spectra of a total of about thirty clusters (Mitchell and Culhane, 1977; Mushotzky *et al.*, 1978; Malina *et al.*, 1978; Berthelsdorf and Culhane, 1979; Mitchell *et al.*, 1979; Mushotzky, 1980,1984). Figure 7 gives the *HEAO-1* A-2 spectra of the Coma and Perseus clusters, showing these line features.

The line feature that was detected is actually a blend of lines from iron ions (mainly Fe^{24+} and Fe^{25+}) and weaker lines from nickel ions (see Sec. V.B). These lines are mainly at photon energies between 6.5 and 7.0 keV; for convenience, this blend will be referred to as the “7-keV Fe line.” The resolution of this component structure and the measurement of the relative intensities of the various components can provide a wealth of diagnostic information on the physical state and environment of the x-ray-emitting gas (Sarazin and Bahcall, 1977; Bahcall and Sarazin, 1978). Unfortunately, while the *Einstein* observatory contained a number of high-resolution spectrometers, none were sensitive to the 7-keV Fe lines because the mirror in *Einstein* was ineffective for photon energies greater than about 4 keV. The application of the *Einstein* spectrometers to lower-energy lines is discussed below. However, the proportional counters on the *HEAO-1* A-2 experiment had sufficient spectral resolution to resolve

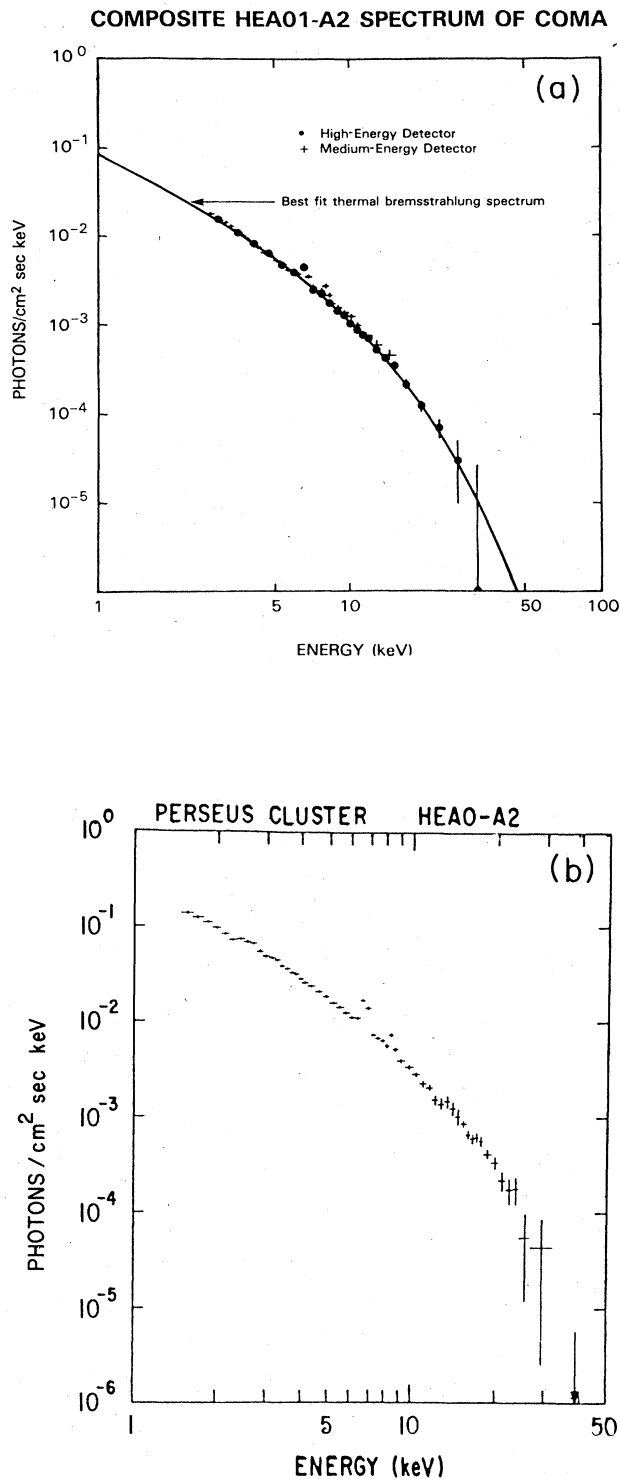


FIG. 7. *HEAO-1* A-2 low-resolution x-ray spectra of clusters, showing the Fe K line at about 7 keV. The plots give the number flux of x-ray photons per $\text{cm}^2 \text{sec keV}$ vs photon energy in keV, for the (a) Coma (Henriksen, and Mushotzky, 1985) and (b) Perseus (Henriksen, 1985) clusters.

er been bound in stars or even in galaxies (Gunn and Gott, 1972). During the formation of the universe (the "big bang"), hydrogen and helium were formed, but it is generally believed that no heavier elements could have been produced because of the lack of any stable isotopes with atomic weights of 5 or 8 (see, for example, Weinberg, 1972). The only sources that have been suggested for the formation of iron involve processing in stars. Moreover, the observed abundance in the intracluster gas is nearly the same as that in the solar system. The solar system is a second-generation stellar system (the sun is a Population I star). Thus it is possible that much of the intracluster gas has been processed through stars.

At the present epoch, there is no significant population of stars known that are not bound to galaxies. This may indicate that part of the intracluster gas may originally have been located within the galaxies. Alternatively, it is possible that there was a "pregalactic" generation of stars (sometimes referred to as Population III stars; see, for example, Carr *et al.*, 1984). Now, the mass of intracluster gas implied by the x-ray observations is nearly as large as the total mass of the galaxies in the cluster (see Sec. III.D.1). If the intracluster gas did originate in part in galaxies, there has been a considerable exchange of gas between stars, galaxies, and the intracluster medium. Thus we are led by the x-ray line observations to a much more complicated picture of galaxy formation and evolution than we might have envisioned without this crucial piece of information. Theories of the origin of the intracluster gas and the formation of galaxies and clusters are discussed in more detail in Sec. V.J.

The 7-keV Fe line can be used to determine the redshift of a cluster with moderate accuracy from even low-resolution x-ray spectra (Boldt, 1976; Bahcall and Sarazin, 1978). Over a wide range of temperatures, the equivalent width of the 7-keV Fe line is at least an order of magnitude larger than that of any other feature in the spectrum of a hot plasma. Thus the detection of a strong feature at photon energies below 7 keV, coupled with the failure to detect a feature at higher energies up to 7 keV, permits the immediate identification of the feature with the 7-keV Fe line and the determination of a single-line redshift. This application of the 7-keV line has not been useful thus far because the *Einstein* x-ray observatory could not detect hard x rays and had too little sensitivity to measure spectra from high-redshift clusters. However, it promises to be of great importance in the future (see Sec. VI).

3. Lower-energy lines

In addition to the 7-keV Fe line complex, the x-ray spectrum of a solar abundance low-density plasma contains a large number of lower-energy lines (Sarazin and Bahcall, 1977). These include the *K* lines of the common elements lighter than iron, such as C, N, O, Ne, Mg, Si, S, Ar, and Ca, as well as the *L* lines of Fe and Ni. Although the Fe *L* line complex was tentatively identified in proportional counter spectra of the M87/Virgo cluster by

Fabricant *et al.* (1978) and Lea *et al.* (1979), the capability for detecting these lines was greatly increased with the launch of the *Einstein* x-ray observatory with its moderate-resolution Solid-State Spectrometer (SSS) and its high-resolution Focal Plane Crystal Spectrometer (FPCS); see Giacconi *et al.* (1979) for a description of the satellite and its capabilities.

The SSS has detected the *K* lines from Mg, Si, and S and the *L* lines from Fe in the spectra of M87/Virgo, Perseus, A496, and A576 (Mushotzky, 1980,1984; Mushotzky *et al.*, 1981; Lea *et al.*, 1982; Nulsen *et al.*, 1982; Rothenflug *et al.*, 1984). Figure 9 shows the SSS spectrum from Virgo. In general, line emission from both the heliumlike and hydrogenic ions of Si and S is seen, indicating that the emission occurs at relatively low temperatures $T_g \sim 2 \times 10^7$ K. The observations in M87/Virgo are consistent with nearly solar abundances of Si, S, and Mg, while the observation in A576 may require lower abundances. Observations of SSS spectra away from the center of M87/Virgo show that the heavy-element abundances are roughly constant throughout the gas (Lea *et al.*, 1982).

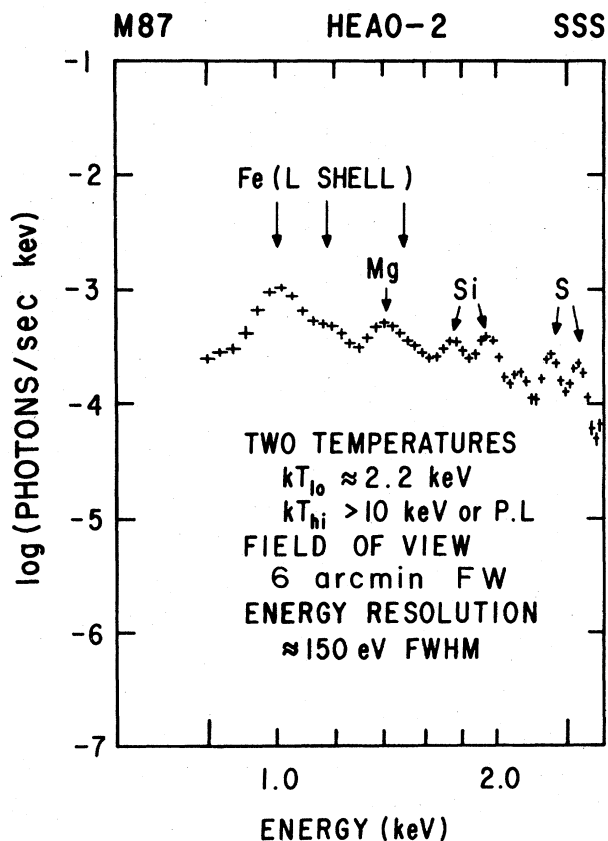


FIG. 9. The moderate-resolution x-ray spectrum of the M87/Virgo cluster taken with the Solid State Spectrometer on the *Einstein* satellite (Lea *et al.*, 1982). The spectral lines of Mg, Si, S, and the lower-energy (*L*-shell) lines of Fe are marked.

In Perseus, the SSS observations of the Fe *L* lines imply that the iron abundance is about one-half of the solar value (Mushotzky *et al.*, 1981), which agrees with the abundance derived from the 7-keV Fe line in proportional counter spectra. However, the SSS observations were made with a very small (~ 6 -arcmin) aperture centered on the cluster center, while the proportional counter observations determine the spectrum of the entire cluster. The approximate agreement of the two abundances suggests that the iron is well mixed throughout the cluster, and not just concentrated in the cluster core.

In general, the SSS spectral line observations seem to imply that many clusters contain cooler gas than was required to explain their continuum spectra. Because the SSS has a small field of view and was centered on the cluster center in these observations, this cool gas must be concentrated at the center of the cluster; in the case of the Virgo and Perseus clusters, the center coincides with the central dominant galaxies M87 and NGC1275. In Perseus, this cool gas has a cooling time (see Sec. V.C.1) of less than 2×10^9 yr, which is considerably less than the probable age of the cluster. It therefore seems likely that the cool gas observed is part of a steady-state cooling flow (see Sec. V.G for a discussion of the theory of such flows). From the observed line intensities, Mushotzky *et al.* (1981) determined that about $300M_{\odot}$ per year of gas must currently be cooling onto NGC1275 in the Perseus cluster, and Nulsen *et al.* (1982) found that about $200M_{\odot}$ per year must be accreting onto the cD in A496. These rates assume that the gas is not being heated.

The FPCS has also provided strong evidence for the cooling and accretion of gas onto M87 in the Virgo cluster and NGC1275 in the Perseus cluster (Canizares *et al.*, 1979,1982; Canizares, 1981). In M87, the FPCS has detected the $O^{7+} K\alpha$ line, as well as blends of the $Fe^{16+}-Fe^{23+} L$ lines and the $Ne^{9+} K\alpha$ line. Figure 10 shows the FPCS detection of the $O^{7+} K\alpha$ line in M87. The ratio of the abundance of oxygen to iron is apparently 3–5 times higher than the solar ratio. The relative strengths of the various Fe *L* line blends cannot result from gas at any single temperature. Apparently, a range of temperatures is necessary, with the x-ray luminosity originating from gas in any range of temperature dT_g being roughly proportional to dT_g . This is just what is predicted if the cool gas results from the cooling and accretion of hotter gas onto the center of M87 (Cowie, 1981). Canizares *et al.* (1979,1982) and Canizares (1981) show that the spectra are consistent with radiative accretion at a rate of $\sim 3-10M_{\odot}$ per year. Similar results were found for the Perseus cluster, except that the required accretion rate is very large $\sim 300M_{\odot}$ per year (Canizares, 1981), in agreement with the results from the SSS. The SSS spectra of about a half dozen other clusters also show evidence for such accretion flow, with rates between those of the M87/Virgo cluster and the Perseus cluster (Fabian, Ku, Malin, Mushotzky, Nulsen, and Stewart, 1981; Mushotzky, 1984).

Thus the two primary observational results of the *Einstein* spectrometers are these: first, the intracluster gas

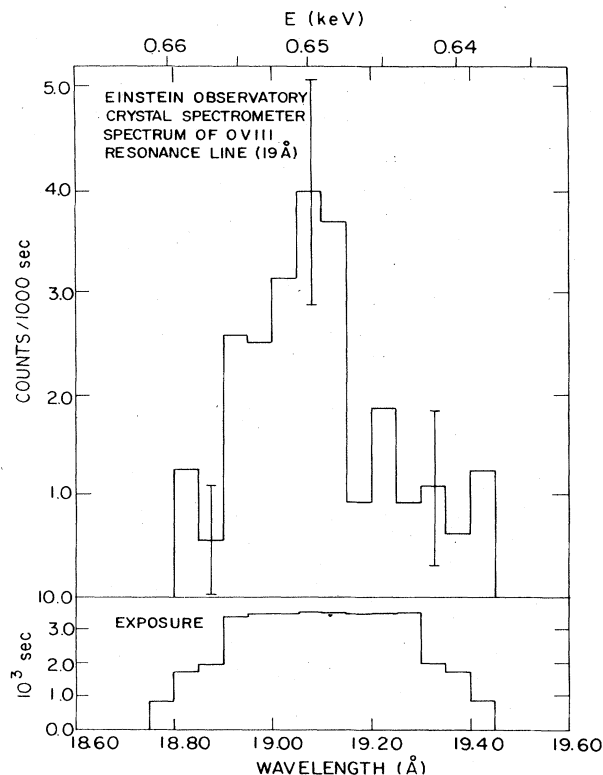


FIG. 10. The very high-resolution x-ray spectrum of the M87/Virgo cluster, showing the O VIII *K* line, from Canizares *et al.* (1979) using the Focal Plane Crystal Spectrometer on the *Einstein* satellite.

contains the heavy elements oxygen, magnesium, silicon, and sulfur, as well as iron; second, gas is cooling and being accreted onto central dominant galaxies in many clusters at rather high rates ($3-400M_{\odot} \text{ yr}^{-1}$). Such accretion had been predicted by Cowie and Binney (1977), Fabian and Nulsen (1977), and Mathews and Bregman (1978); models for the accretion flows are discussed in Sec. V.G. The rates of accretion are so high that if they have persisted for the age of the cluster, the entire mass of the inner portions of the central dominant galaxies might be due to accretion. Models for central dominant galaxies based on this idea have been given by Fabian, Atherton, Taylor, and Nulsen (1982) and Sarazin and O'Connell (1983), who argue that the majority of the accreted gas is converted into low-mass stars.

X-ray line observations have established that the primary emission mechanism of x-ray clusters is thermal emission from hot, diffuse intracluster gas. They have also shown that at least part of that gas has been ejected from stars and presumably from galaxies. Apparently, some of this intracluster gas is now completing the cycle and returning to the central galaxies, and possibly being formed into stars.

D. The spatial distribution of x-ray emission

1. X-ray centers, sizes, and masses

Early *Uhuru* observations indicated that the x-ray sources were centered on the cluster center, as determined from the galaxy distribution, or on an active galaxy in the cluster (Bahcall, 1977a). In many of the x-ray clusters, the cluster center also corresponds with the position of a cD or other central dominant galaxy.

The earliest x-ray observations showed that the x-ray sources in clusters were extended. With the nonimaging proportional counters used in these observations, the spatial resolution of the detectors was usually determined by mechanical collimators in front of the detectors and was therefore relatively crude (generally an angular resolution of $\sim 1^\circ$). Since this is comparable to the sizes of the x-ray emission regions in the nearest clusters, the distribution of emission could not generally be observed in any detail. Only estimates of the size could be determined by convolving a model for the distribution of the emission with the resolution of the detector and comparing the result to the observations.

Lea *et al.* (1973) derived sizes for the sources in the Virgo/M87, Coma, and Perseus clusters, assuming that the gas had the density distribution given by the King approximation to a self-gravitating isothermal sphere [Eqs. (2.9) and (2.13)],

$$\rho_g \propto \left[1 + \left(\frac{r}{r_x} \right)^2 \right]^{-3/2}. \quad (3.5)$$

Here, ρ_g is the gas density and r_x is the x-ray core radius. While this model is not physically consistent (see Sec. V.E.1), it does provide a convenient fitting form for comparison to the galaxy distribution, which is often fit by the same function. Values of r_x were derived from the x-ray distribution in nine clusters by Lea *et al.* (1973) and Kellogg and Murray (1974). Recently, Eq. (3.5) has been fit to the distribution of x-ray emission from 53 clusters detected in an extensive survey of clusters with the *Einstein* x-ray observatory (Abramopoulos and Ku, 1983). In general, these studies found that the x-ray core radii were significantly larger than the core radii of the galaxies (Sec. II.G). These results were fairly uncertain because of the difficulties in determining either of these radii accurately.

The thermal x-ray emission from intracluster gas is proportional to the emission integral EI [Eq. (3.3)], while the mass of intracluster gas is proportional to $\int n_p dV$. Thus, if the size and distribution of the x-ray-emitting gas can be determined from the x-ray surface brightness, the mass in intracluster gas can be estimated. Unfortunately, the estimate is very uncertain because the x-ray emission falls off rapidly as the density decreases in the outer parts of the cluster, where a large fraction of the mass of the intracluster gas may be located. Estimates of the mass of the intracluster gas based on the same self-gravitating isothermal model for the intracluster gas were

given in Lea *et al.* (1973). In general, the total mass of intracluster gas determined from the x-ray observations is similar to or somewhat larger than the total mass of the galaxies in the cluster estimated from their total luminosity and a typical galaxy mass-to-light ratio. However, this intracluster gas is still only 5–15% of the total virial mass of the cluster, and thus the discovery of the intracluster gas has not resolved the missing mass problem in clusters (Sec. II.H).

More physically consistent hydrostatic models for the intracluster gas have also been used to fit the observed x-ray distributions (Lea, 1975; Gull and Northover, 1975; Cavaliere and Fusco-Femiano, 1976; Bahcall and Sarazin, 1977; Cavaliere, 1980). These calculations all basically agree on the mass in intracluster gas required to explain the x-ray observations; on average, about 10% of the virial mass must be in the form of intracluster gas. One model that has been used extensively is the hydrostatic isothermal model for the intracluster gas (Cavaliere and Fusco-Femiano, 1976, 1981; Bahcall and Sarazin 1977, 1978; Sarazin and Bahcall, 1977; Gorenstein *et al.*, 1978; Jones and Forman, 1984; Sec. V.E.1). In this model, both the galaxies and the intracluster gas are assumed to be isothermal, bound to the cluster, and in equilibrium. The galaxies are assumed to have an isotropic velocity dispersion. However, the gas and galaxies are not assumed to have the same velocity dispersion; the square of the ratio of the galaxy-to-gas velocity dispersions is

$$\beta \equiv \frac{\mu m_p \sigma_r^2}{k T_g}, \quad (3.6)$$

where μ is the mean molecular weight in amu, m_p is the mass of the proton, σ_r is the one-dimensional velocity dispersion, and T_g is the gas temperature. Then, the gas and galaxy densities vary as $\rho_g \propto \rho_{gal}^\beta$. If the galaxy distribution is taken to be a King analytical form for the isothermal sphere [Eq. (2.13)], then the x-ray surface brightness $I_x(b)$ at a projected radius b varies as

$$I_x(b) \propto \left[1 + \left(\frac{b}{r_c} \right)^2 \right]^{-3\beta+1/2}, \quad (3.7)$$

where r_c is the galaxy core radius (Sec. II.G.2). The self-gravitating isothermal model [Eq. (3.5)] has the same surface brightness distribution if one makes the replacements $\beta = 1$ and $r_c = r_x$. These and other models for the distribution of the intracluster gas will be discussed in detail in Sec. V.E.

Observations with somewhat higher spatial resolution were made using detectors with modulation collimators (Schwarz *et al.*, 1979) or one-dimensional imaging detectors (Gorenstein *et al.*, 1973). Some clusters were found to contain compact x-ray sources associated with the central dominant galaxies in the cluster (Schnopper *et al.*, 1977), such as NGC1275 in the Perseus cluster (Wolff *et al.*, 1974, 1975, 1976; Cash *et al.*, 1976; Malina *et al.*, 1976; Helmken *et al.*, 1978). In Perseus, this point source contributes ~ 20 –25% of the x-ray luminosity at

moderate photon energies (\sim keV); at very high energies ≥ 20 keV the point source is dominant (Primini *et al.*, 1981; Rothschild *et al.*, 1981). The x-ray surface brightness of the Perseus cluster was shown to be extended in the east-west direction (Wolff *et al.*, 1974,1975,1976; Malina *et al.*, 1976; Cash *et al.*, 1976); this is the same direction as the line of bright galaxies seen optically in this L cluster. Later high-resolution observations of the center of the cluster by Branduardi-Raymont *et al.* (1981) show a smaller elongation. A similar but smaller elongation was observed in the x-ray emission from the Coma cluster (Johnson *et al.*, 1979; Gorenstein *et al.*, 1979).

Recently, moderate-resolution *Einstein* IPC images of the x-ray emission in 46 clusters have been fit by Eq. (3.7) (Jones and Forman, 1984). Because galaxy core radii, velocity dispersions, and x-ray temperatures are poorly determined for most of these clusters, both the core radius and β were derived from the observed x-ray surface brightness. Figure 11 shows the x-ray surface brightness as a function of radius from the center of the x-ray emission (in minutes of arc) for A400, A2063, and A1795 (Jones and Forman, 1984). The solid histogram is the data; the dots are the best fit using Eq. (3.6). About two-thirds of the clusters were fit quite well with this formula; however, one-third appeared to have an excess of emission near the cluster center. In Fig. 11, A400 and A2063 were reasonably fit by Eq. (3.6), while A1795 was not. The second panel on A1795 shows the fit to Eq. (3.6) if the central several minutes of arc are ignored. Jones and Forman suggest that this excess central x-ray emission correlates with the radio luminosity of the cluster, and that the excess emission may be due to a cooling flow in the cluster core (Sec. V.G). A1795 does in fact have a very large cooling flow (Table V, below).

A wide range of core radii ($0.07-0.9h_{50}^{-1}$ Mpc) were derived by Jones and Forman. They found a strong anticorrelation between the presence of a dominant cluster galaxy in the core and the size of the x-ray core radius. [Unfortunately, Abramopoulos and Ku (1983) found the opposite effect with a similar sample of clusters observed with *Einstein*.] The average value of β found by Jones and Forman from the x-ray distributions is $\beta = 0.65$, which implies that the gas is considerably more extensively distributed than the mass in the cluster. Using $\beta = 0.65$ increases the mass of the gas in a cluster significantly as compared to the $\beta = 1$ estimates described above. Unfortunately, the average value of β determined by applying Eq. (3.6) to those clusters with measured velocity dispersions and x-ray temperatures is $\beta = 1.1$. It is not clear whether this discrepancy results from errors in the measured cluster properties, velocity anisotropies, or a failure of the isothermal model (see Sec. V.E.1).

While in most clusters the x-ray emission was found to be as broadly distributed as the galaxy distribution, an exception was Virgo/M87. Here the soft x-ray emission comes from a small region around M87, while the galaxy core radius of this irregular cluster, although hard to define, is certainly much larger. However, there appeared to be weaker hard x-ray emission originating from a larger

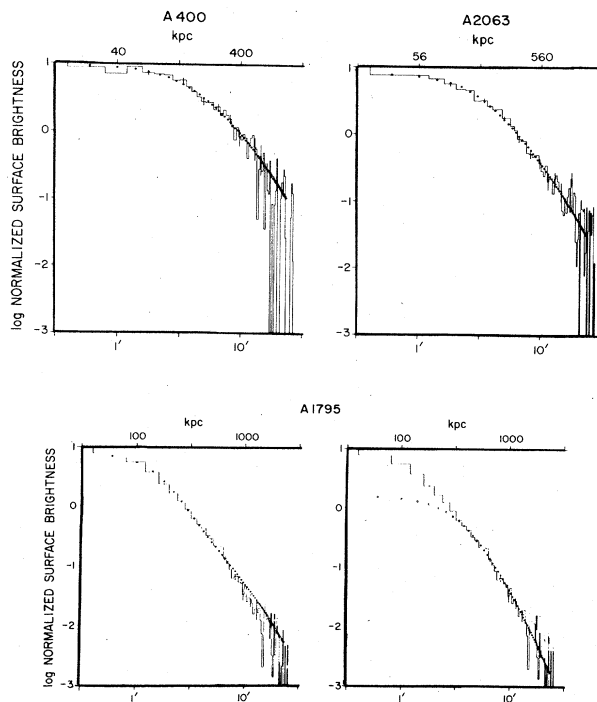


FIG. 11. The x-ray surface brightness of several clusters, as determined by the IPC on the *Einstein* satellite by Jones and Forman (1984). The surface brightness is normalized to its central value and is given as a function of the angular distance from the cluster center. The solid curves give the observed surface brightness, and the dots are the best fit using Eq. (3.7). The bottom two panels show the A1795 cluster with the inner eight data points either included in the fit (left) or removed (right). The improvement in the fit in the outer points when the inner regions are removed suggests excess emission in the center, due to a cooling flow.

region of the cluster (Davison, 1978; Lawrence, 1978), although recent observations suggest that this emission actually is due to the nucleus of M87 (Lea *et al.*, 1981, 1982).

2. X-ray images of clusters and the morphology of the intracluster gas

A tremendous increase in our understanding of the distribution of the x-ray-emitting gas in clusters has come about through imaging of the two-dimensional x-ray surface brightness. Such x-ray imaging observations became possible on a routine basis with the launch of the *Einstein* x-ray observatory satellite, although a rocket-borne x-ray mirror was used to image the x-ray emission from the Coma, Perseus, and M87/Virgo clusters prior to the launch of *Einstein* (Gorenstein *et al.*, 1977,1978,1979). The results of the x-ray imaging observations of clusters have been extensively reviewed recently by Forman and Jones (1982).

TABLE IV. Morphological classification of x-ray clusters, adapted from Forman and Jones (1982).

	Non-x-ray-dominant galaxy (nXD)	X-ray-dominant galaxy (XD)
Irregular	Low $L_x \leq 10^{44}$ ergs/sec Cool gas $T_g = 1-4$ keV X-ray emission around many galaxies Irregular x-ray distribution High spiral fraction $> 40\%$ Low central galaxy density Prototype: A1367	Low $L_x \leq 10^{44}$ ergs/sec Cool gas $T_g = 1-4$ keV Central galaxy x-ray halo Irregular x-ray distribution High spiral fraction $> 40\%$ Low central galaxy density Prototype: Virgo/M87
Regular	High $L_x \geq 10^{44}$ ergs/sec Hot gas $T_g \geq 6$ keV No cooling flow Smooth x-ray distribution Low spiral fraction $\leq 20\%$ High central galaxy density Prototype: Coma (A1656)	High $L_x \geq 3 \times 10^{44}$ ergs/sec Hot gas $T_g \geq 6$ keV Cooling flow onto central galaxy Compact, smooth x-ray distribution Low spiral fraction $\leq 20\%$ High central galaxy density Prototype: Perseus (A426)

Forman and Jones (1982; also Jones *et al.*, 1979) propose a two-dimensional classification scheme for the x-ray morphology of galaxies, which they relate to the evolutionary state of the cluster as determined by its optical properties (Secs. II.I and II.J). This scheme is presented in Table IV, which is taken in large part from Forman and Jones (1982). In Fig. 12 the x-ray surface brightness distributions from the Imaging Proportional Counter (IPC) on the *Einstein* x-ray observatory are shown for representative examples of clusters of each morphological type. The x-ray brightness distribution is shown as a contour plot, in which the lines are loci of constant x-ray surface brightness. The contours are superimposed on optical photographs of the cluster for comparison.

First of all, Forman and Jones classify the clusters as being irregular ("early") or regular ("evolved"), based on their overall x-ray distribution. The early clusters have irregular x-ray surface brightnesses, and often show small peaks in the x-ray surface brightness, many of which are associated with individual galaxies in the cluster. Their x-ray luminosities L_x and x-ray spectral temperatures T_g are low. Optically, these clusters tend to be irregular clusters (Table II). That is, they have irregular galaxy distributions with subclustering and with low central concentration. They are not generally very rich, and tend to be Bautz-Morgan types II to III and Rood-Sastry types F and I. They generally have low velocity dispersions σ_v . They are often, but not always, spiral rich.

On the other hand, the evolved clusters have regular, centrally condensed x-ray structures (Forman and Jones, 1982). The x-ray distribution is smooth, and x-ray emission peaks are not found associated with individual galaxies, except possibly with a central dominant galaxy at the cluster center. The evolved clusters have high x-ray luminosities and gas temperatures. Optically, these are regular, symmetric clusters, generally of Bautz-Morgan type I to II and Rood-Sastry types cD, B, L, or C. They are rich and have a high central concentration of galaxies. They have high velocity dispersions and are spiral poor in their

galaxy composition.

The second determinant of the x-ray morphology of clusters is the presence or absence of a central, dominant galaxy in the cluster. The x-ray emission from a cluster tends to peak at the position of such a galaxy. Clusters containing such central dominant galaxies are classified by Forman and Jones (1982) as x-ray dominant (XD); those without such a galaxy are classified as non-x-ray-dominant (nXD). The nXD clusters have larger x-ray

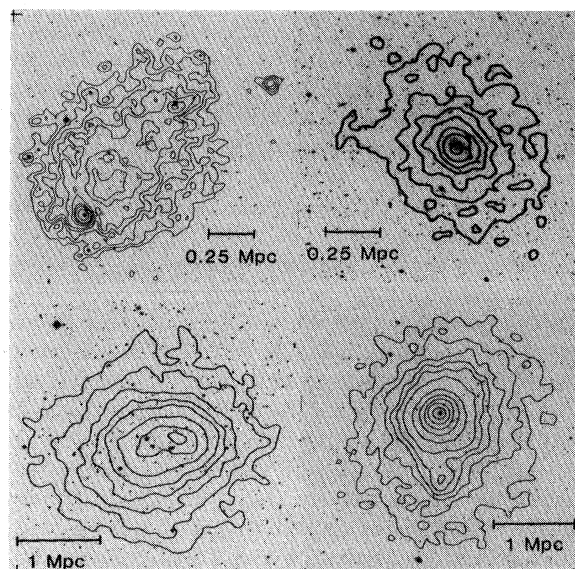


FIG. 12. The x-ray morphology of several clusters of galaxies from Jones and Forman (1984). Contours of constant x-ray surface brightness are shown superimposed on optical images of the clusters. (Top left), the prototypical irregular nXD cluster A1367. (Top right), the irregular XD cluster A262. (Bottom left), the regular nXD cluster A2256. (Bottom right), the regular XD cluster A85, showing the x-ray emission centered on the cD galaxy.

core radii $r_x \sim 500/h_{50}$ kpc. There is no strong x-ray emission associated with any individual galaxy in these systems.

The XD clusters have small x-ray core radii $r_x \sim 250/h_{50}$ kpc. The x-ray emission is strongly peaked on the central dominant galaxy. In many cases, spectral observations indicate that gas is cooling in this central peak and being accreted onto the central galaxy (Sec. III.C.3). Regular XD clusters have, on average, the highest x-ray luminosities of any clusters (Forman and Jones, 1982).

Examples of irregular nXD clusters include A1367 (Jones *et al.*, 1979; Bechtold *et al.*, 1983), A194 (Forman and Jones, 1982), A566 (Harris *et al.*, 1982), and A2069 (Gioia *et al.*, 1982). A1367, which is shown in Fig. 12(a), is the prototype of this class.

Virgo/M87 is the prototype of the irregular XD clusters, of which A262 (Forman and Jones, 1982), A347 (Maccagni and Tarengi, 1981), A2147 (Jones *et al.*, 1979), and A2384 (Ulmer and Cruddace, 1982) are also members. Figure 12(b) shows the x-ray image of A262.

Regular nXD clusters probably include Coma (A1656; Abramopoulos *et al.*, 1981; see Fig. 14 below), A576 (White and Silk, 1980), A1763 (Vallee, 1981), A2255, A2256 (Jones *et al.*, 1979; Forman and Jones, 1982), and CA0340-538 (Ku *et al.*, 1983). Figure 12(c) shows the x-ray image of A2256. Although the statistics are poor, it appears that clusters with radio halo emission (see Sec. IV.D) are primarily of this class.

The regular XD clusters include Perseus (A426, Branduardi-Raymont *et al.*, 1981; Fabian, Hu, Cowie, and Grindlay, 1981), A85, A1413, A1795 (Jones *et al.*, 1979), A478 (Schnopper *et al.*, 1977), A41a (Nulsen *et al.*, 1982), A2029 (Johnson *et al.*, 1980), A2218 (Boynton *et al.*, 1982), and possibly A2319 (White and Silk, 1980). Figure 12(d) shows the x-ray image of the cD cluster A85.

The prototypes of each of these classes (A1367, Virgo/M87, Coma, and Perseus) are discussed individually in Sec. III.E below.

Forman and Jones (1982) and Jones *et al.* (1979) argue that this classification scheme represents a sequence of cluster evolution, just as the sequence of cluster optical morphology (Sec. II.E) was related to the dynamical evolution of the cluster in Sec. II.I. Specifically, the evolution of the overall cluster distribution may be due to violent relaxation during the collapse of the cluster. This occurs on the dynamical time scale of the cluster, which depends only on its density [Eq. (2.32)]. On the other hand, the formation of central dominant galaxies may be due to mergers of galaxies; as demonstrated in Sec. II.J.1, this mechanism favors compact but poor regions. Thus, while both a regular overall distribution of a cluster and the presence of a central dominant galaxy may indicate that the cluster has undergone dynamical relaxation, the processes are different and depend in different ways on the size and mass of the region. This provides a possible qualitative explanation for this two-dimensional classification system of x-ray morphology.

Double-peaked x-ray emission has been seen in a num-

ber of clusters, of which the best studied example is A98 (Henry *et al.*, 1981; Forman *et al.*, 1981). Other possible examples include A115, A1750, SC0627-54 (Forman *et al.*, 1981), A1560, A2356 (Ulmer and Cruddace, 1982), A982, A2241 (Bijleveld and Valentijn, 1982), CA0329-527 (Ku *et al.*, 1983), and possibly A399/401 (Ulmer *et al.*, 1979; Ulmer and Cruddace, 1981). In Fig. 13, the x-ray distributions are shown for four double clusters observed by Forman *et al.* (1981). In most of these systems, the galaxy distribution is also double peaked (Dressler, 1978c; Henry *et al.*, 1981; Beers *et al.*, 1983), and the two peaks correspond to slightly different radial velocities (Faber and Dressler, 1977; Beers *et al.*, 1982). The small velocity differences indicate that the two subclusters are bound, and would be expected to collapse together and merge in a time of typically a few billion years.

These double systems may represent an intermediate stage in the evolution of clusters from irregular to regular distributions (Tables II and IV). In fact, numerical N -body simulations of cluster formation often show an intermediate bimodal stage to the galaxy distributions [see Fig. 4(c); White, 1976c; Ikeuchi and Hirayama, 1979; Carnevali *et al.*, 1981]. With the current (rather poor) statistics, the fraction of clusters detected in this double phase ($\sim 10\%$) is consistent with the relatively short lifetime of the phase.

In the irregular and double clusters, the gas distribution is correlated with the galaxy distribution. The gas is probably roughly in hydrostatic equilibrium with the cluster gravitational potential (Sec. V.E), which is primarily influenced by the distribution of the dynamically dominant missing mass component (Sec. II.H). The fact that the x-ray surface brightness and galaxy distribution corre-

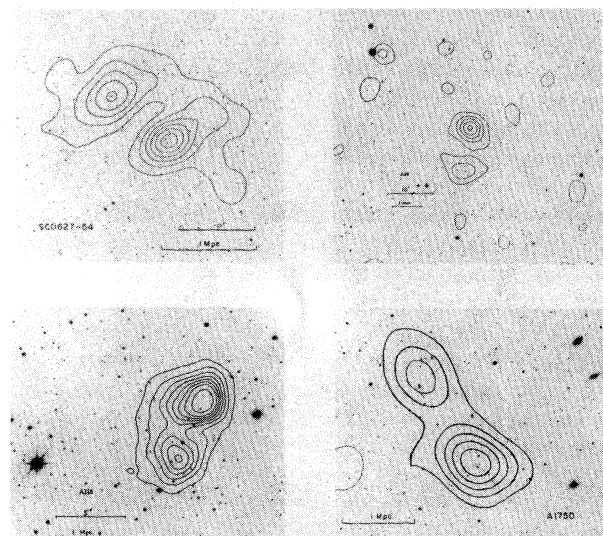


FIG. 13. The x-ray surface brightness in four double clusters, from Forman *et al.* (1981). Contours of constant x-ray surface brightness are shown superimposed on optical images of the clusters.

late suggests that the galaxies and the missing mass have a similar distribution in clusters; other evidence favoring this viewpoint was given in Sec. II.H.

E. Individual clusters

1. Coma

Coma is the prototype of the nXD regular cluster, and is often used as a general prototype for comparing models for relaxed clusters. Its optical image is given in Fig. 1(b). It is worthwhile noting that clusters as rich and compact as Coma are actually rather uncommon. Coma is also unusual in having the most prominent radio halo observed among clusters (Sec. IV.D). Coma and A1367 (see below) appear to be portions of a large supercluster system (Gregory and Thompson, 1978).

The x-ray image of Coma, which is shown in Fig. 14, shows that the x-ray emission is somewhat elongated (Johnson *et al.*, 1979; Gorenstein *et al.*, 1979; Helfand *et al.*, 1980) in the same direction as the galaxies in the cluster (Sec. II.G.4). The x-ray emission shows a central uniform core (Helfand *et al.*, 1980; Abramopoulos *et al.*, 1981) and falls off with radius more slowly than the galaxy distribution [$\beta \approx 0.8$ in Eq. (3.7)]. Coma has an unusually high x-ray temperature for its galaxy velocity dispersion (Mushotzky *et al.*, 1978), although this is consistent with its small value for β . The x-ray surface brightness from Coma is very smooth, and there is no apparent excess emission associated with the two central galaxies (Forman and Jones, 1982; Bechtold *et al.*, 1983).

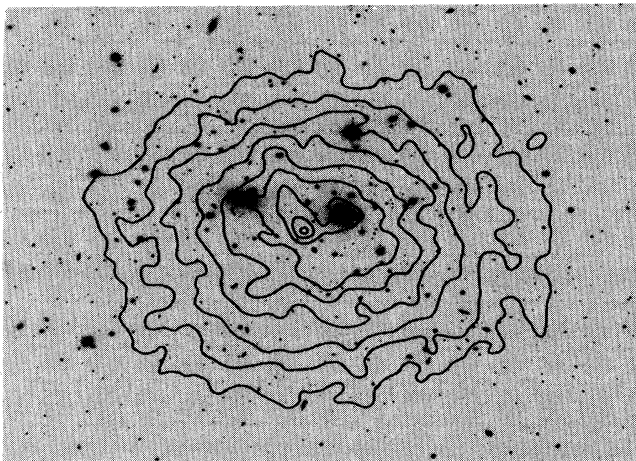


FIG. 14. The x-ray surface brightness of the Coma cluster of galaxies from the IPC on *Einstein*, kindly provided by Christine Jones and Bill Forman. Contours of constant x-ray surface brightness are shown superimposed on the optical image of the cluster.

2. Perseus

The Perseus cluster is one of the most luminous x-ray clusters known, and has an unusually high radio luminosity as well (Gisler and Miley, 1979). It may represent an extreme in the evolution of the gas component in clusters.

Optically, Perseus is an L cluster (Bahcall, 1974a); the brightest galaxies form a chain oriented roughly east-west [see Fig. 1(c)]. The very prominent and unusual galaxy NGC1275 (Fig. 15) is located near the east end of this chain. Together, Perseus, the clusters A262 and A347, and some smaller groups form the Perseus supercluster, which is also elongated in an east-west direction (Gregory *et al.*, 1981). On a moderately large scale, the x-ray emission from Perseus also appears to be elongated in the same direction as the galaxy distribution (Wolff *et al.*, 1974, 1976; Cash *et al.*, 1976; Malina *et al.*, 1976; Branduardi-Raymont *et al.*, 1981). The x-ray emission is peaked on NGC1275 and becomes more spherically symmetric near this galaxy (see Figs. 16 and 17). Oddly, the center of the extended x-ray emission in Perseus appears to lie slightly to the east of NGC1275, while the galaxy distribution is centered to the west (Fig. 16).

The x-ray emission from Perseus has been observed out to large distances ($\sim 2.5^\circ$) from the cluster core (Nulsen *et*

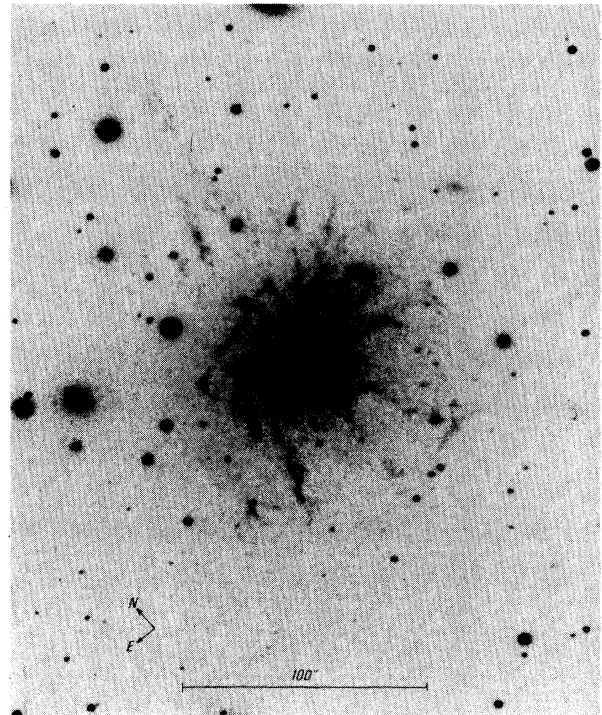


FIG. 15. An optical photograph of the spectacular galaxy NGC1275 in the Perseus cluster from Lynds (1970), copyright 1970 AURA, Inc., National Optical Astronomy Observatories, Kitt Peak. The photograph was taken with a filter sensitive to the $H\alpha$ emission line, and shows the prominent optical emission line filaments around this galaxy.

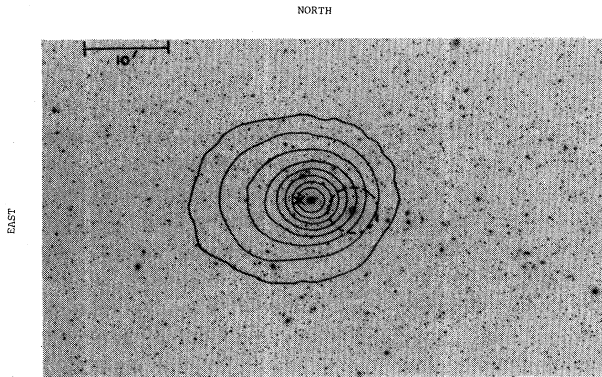


FIG. 16. The x-ray surface brightness of the Perseus cluster of galaxies, observed by Branduardi-Raymont *et al.* (1981) with the IPC on the *Einstein* satellite. Contours of constant x-ray surface brightness are shown superimposed on the optical image of the cluster. The center of the galaxy distribution in the cluster is shown as a dashed circle, while the centroid of the extended x-ray emission is the \times . The peak in the x-ray surface brightness is centered on the galaxy NGC1275.

al., 1979; Nulsen and Fabian, 1980; Ulmer, Cruddace, Wood, Meekins, Yentis, Evans, Smathers, Byram, Chubb, and Friedman, 1980), although the brightness observed is that expected from models of the inner x-ray emission. Unlike Coma, Perseus does not appear to have a significant radio halo (Gisler and Miley, 1979; Hanisch and

EINSTEIN X-RAY OBSERVATORY

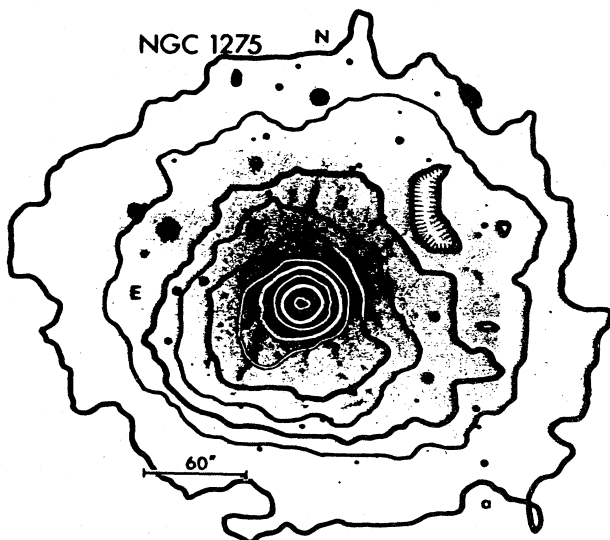


FIG. 17. A higher-resolution x-ray image of the Perseus cluster emission around the galaxy NGC1275, from Branduardi-Raymont *et al.* (1981) and Fabian *et al.* (1984), using the HRI on the *Einstein* satellite. Contours of constant x-ray surface brightness are shown superimposed on the optical image of the galaxy NGC1275.

Erickson, 1980; Birkinshaw, 1980). In the outer portions of the cluster, the radio galaxy NGC1265 is the classic example of a head-tail radio galaxy (see Sec. IV.C). The distortion in the radio morphology of the source indicates that it is passing at high velocity through moderately dense intracluster gas (Owen *et al.*, 1978).

Perseus was the first cluster to have an x-ray line detected in its spectrum (Mitchell *et al.*, 1976). The gas temperature in Perseus, derived from its spectrum (Mushotzky *et al.*, 1981), is smaller than one would expect, given the very large line-of-sight velocity dispersion in the cluster [Eq. (3.10)] or the extent of the gas distribution observed [Eq. (3.6)]. However, recent work on the galaxy spatial and velocity distribution by Kent and Sargent (1983) has reduced the discrepancy considerably.

The galaxy NGC1275 in the core of the Perseus cluster is one of the most unusual objects in the sky; it occupies a role in extragalactic astronomy similar to the position of the Crab Nebula (which it visually resembles) in galactic astronomy. The visual appearance of the galaxy (Fig. 15) is dominated by a complex network of filaments, which show an emission line spectrum (Kent and Sargent, 1979). These filaments form two distinct velocity systems (Rubin *et al.*, 1977, 1978): a "low-velocity" system with the same velocity as the stars in NGC1275, and a "high-velocity" system with a radial velocity about 3000 km/sec higher. Strangely enough, 21-cm absorption line measurements indicate that the high-velocity system lies between us and NGC1275 (Rubin *et al.*, 1977). Thus the velocity difference cannot be explained as a difference in the Hubble velocity due to differences in the distance to the two systems. At the moment, the leading suggestion appears to be that the high-velocity gas is in a spiral or irregular galaxy that is accidentally superposed on NGC1275 and that just happens to be moving towards the center of the Perseus cluster at 3000 km/sec. It is possible that this intervening galaxy is in the outer parts of the cluster or supercluster and is falling into the cluster on a nearly radial orbit. Alternatively, Hu *et al.* (1983) suggest that the high-velocity system is a spiral galaxy that is actually colliding with the x-ray-emitting gas around NGC1275 (Sec. V.G.3). Unfortunately, no stellar component of this possible intervening galaxy has ever been detected (Kent and Sargent, 1979; but see Adams, 1977), and the galaxy seems to have very little neutral hydrogen, given its strong line emission (van Gorkom and Ekers, 1983).

Although the spatial distribution of stellar light from NGC1275 is that of a giant elliptical galaxy (Oemler, 1976), the galaxy has very blue colors and an A-star stellar spectrum (Kent and Sargent, 1979), suggesting ongoing or recent star formation. The nucleus of the galaxy contains a very compact, highly variable, powerful non-thermal source of radiation with a spectrum that extends from radio to hard x-rays. Because of its line emission, filaments, blue color, and nuclear emission, NGC1275 was classified as a Seyfert galaxy, although Seyferts are generally spiral galaxies and are not usually located in compact cluster cores.

The diffuse cluster x-ray emission from Perseus is very

strongly peaked on the position of NGC1275 (Fabian, Hu, Cowie, and Grindlay, 1981; Branduardi-Raymont *et al.*, 1981; Figs. 16 and 17). This is in addition to the highly variable, very hard x-ray point source associated with the nucleus of NGC1275 (Primini *et al.*, 1981; Rothschild *et al.*, 1981). The gas around NGC1275 has a positive temperature gradient $dT_g/dr > 0$ (Ulmer and Jernigan, 1978), which is not expected if the gas is hydrostatic and not cooling. High-resolution x-ray spectra of the region about NGC1275 show the presence of significant quantities of cool gas in this region (Canizares *et al.*, 1979; Mushotzky *et al.*, 1981). Together, the x-ray surface brightness, x-ray spectra, and temperature gradients are best explained if gas is cooling onto NGC1275 at a rate of $\dot{M} \approx 400M_\odot/\text{yr}$ (Sec. V.G).

This cooling flow can provide an explanation of all the unusual properties of NGC1275 except the high-velocity filaments. As the gas continues to cool through lower temperatures, it could produce the optical line emission seen in the low-velocity filaments. The line emission becomes filamentary because the cooling is thermally unstable (Fabian and Nulsen, 1977; Mathews and Bregman, 1978; Cowie *et al.*, 1980; Sec. V.G.3). If a small fraction of the accreted mass reaches the nucleus, it could power the nonthermal nuclear emission. Over the age of the cluster of $\sim 10^{10}$ yr, roughly $3 \times 10^{12}M_\odot$ would have been accreted. There is no reasonable reservoir for this much mass except in low-mass star formation, which may be favored under the physical conditions in accretion flows (Fabian, Nulsen, and Canizares, 1982; Sarazin and O'Connell, 1983). Ongoing star formation would explain the blue color and A-star spectrum of NGC1275. Moreover, if accretion has been going on for the lifetime of the cluster, the entire luminous mass of NGC1275 might be due to accretion (Fabian, Nulsen, and Canizares, 1982; Sarazin and O'Connell, 1983; Wirth *et al.*, 1983).

3. M87/Virgo

Virgo is the nearest rich cluster to our galaxy. The cluster is quite irregular and spiral rich (de Vaucouleurs, 1961; Abell, 1975; Bautz and Morgan, 1970), although the x-ray emission comes from an elliptical-rich core surrounding the galaxy M87 [Fig. 1(a)].

M87 is classified as a peculiar elliptical galaxy. It has fairly extended optical emission (de Vaucouleurs and Nieto, 1978), but is not a cD. This galaxy is one of the brightest radio sources in the sky. Nonthermal radio emission is observed from the nucleus and from the prominent optical jet (see Fig. 18), and both the nucleus and jet also produce nonthermal x-ray emission (Schreier *et al.*, 1982; Fig. 20). There is also a larger-scale radio halo source with a size comparable to that of the entire galaxy (Andernach *et al.*, 1979; Hanisch and Erickson, 1980).

The x-ray emission from this cluster is strongly concentrated in the region around M87, and is much less broadly distributed than the galaxies in the cluster (Malina *et al.*,

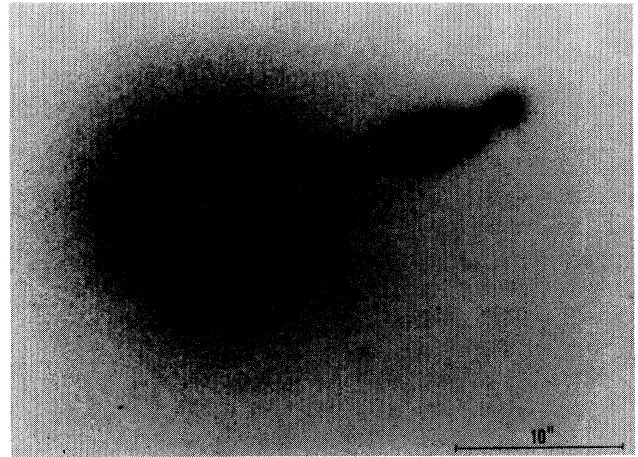


FIG. 18. An optical photograph of the elliptical galaxy M87 in the Virgo cluster, showing the jet in the interior of the galaxy (Arp and Lorre, 1976).

1976; Gorenstein *et al.*, 1977; Fabricant and Gorenstein, 1983). Figure 19 shows the *Einstein* IPC x-ray image of this cluster; Fig. 20 is the HRI image. The top panel shows the outer contours, while the bottom panel is an expanded view of the center, showing x-ray emission from the jet. The emission is also considerably cooler ($T_g \approx 2.5$ keV) than is usually associated with cluster emission (Lea *et al.*, 1982). Nearly all of the emission comes from a 1° region around M87, in which more than

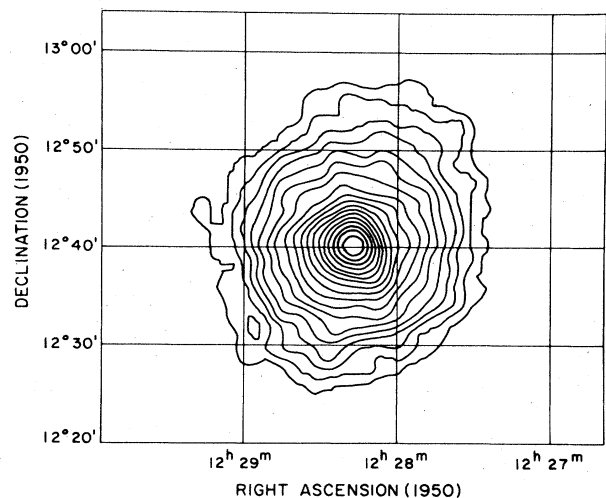


FIG. 19. The x-ray surface brightness of the M87/Virgo cluster of galaxies as observed by Fabricant and Gorenstein (1983) with the IPC on the *Einstein* satellite. The lines are contours of constant x-ray surface brightness. The x-ray emission is centered on M87.

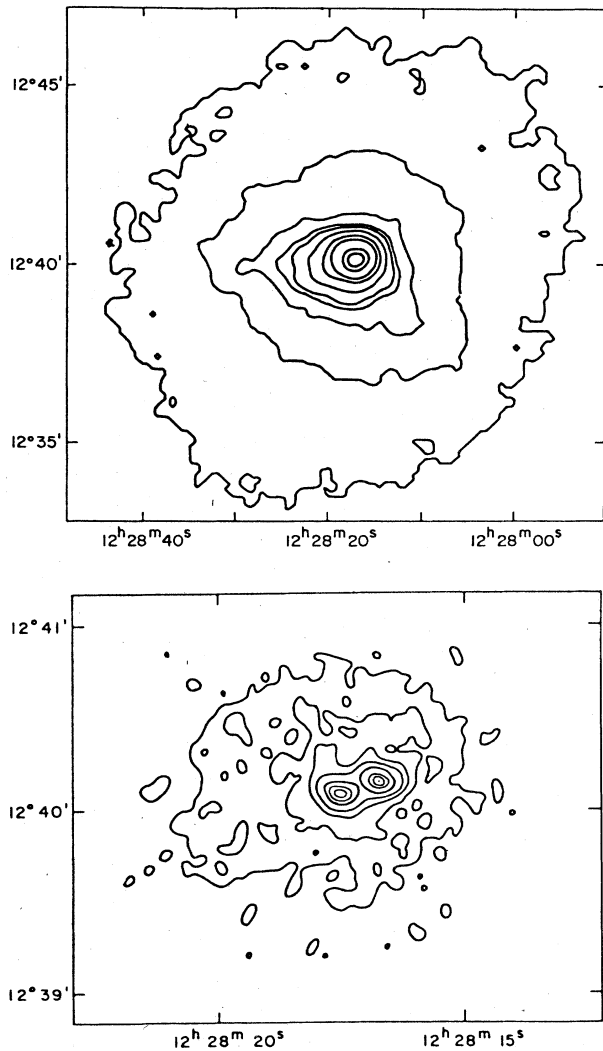


FIG. 20. A higher-resolution x-ray image of the M87/Virgo cluster emission centered on the galaxy M87, from Schreier *et al.* (1982). The lines are contours of constant x-ray surface brightness. (Upper), a lower-spatial-resolution version, showing the peaking of the emission on the center of M87, and its asymmetrical structure. (Lower), a blowup of the center of the galaxy, showing x-ray emission along the optical jet.

95% of the optical emission comes from M87. As a result, it seems reasonable to assume that the bulk of the emission is associated with M87 itself, rather than the cluster as a whole.

Similar arguments led Bahcall and Sarazin (1977) and Mathews (1978b) to suggest that the x-ray-emitting gas is gravitationally bound to M87 itself. Bahcall and Sarazin showed that M87 could only bind the gas if it had a very massive halo, with a total mass of $1-6 \times 10^{13} M_{\odot}$. This estimate was based on early low-resolution x-ray observations. More recent *Einstein* observations (Fabricant *et*

al., 1980; Fabricant and Gorenstein, 1983; Stewart, Canizares, Fabian, and Nulsen, 1984) appear to support this model and provide a more accurate estimate of the mass of $3-6 \times 10^{13} M_{\odot}$. These observations measure, at least approximately, the temperature gradient in M87 and allow a direct determination of the mass profile of the galaxy. The massive halo must extend out to roughly 1° from M87. The optical surface brightness of the galaxy is very low in this region, and thus the mass-to-light ratio of the material making up this halo must be rather large. These observations suggest that at least this one elliptical galaxy possesses a massive, dark "missing mass" halo of the type discussed in Sec. II.H. Whether this is typical of giant ellipticals or whether it is a consequence of M87's position at the center of the Virgo cluster is uncertain.

Alternatively, Binney and Cowie (1981) have suggested that the mass of M87 might actually be rather small. They argue that the cooler ($T_g \approx 2.5$ keV) gas providing the bulk of the x-ray emission is confined by the pressure of a hotter ($T_g \approx 8$ keV), lower-density, intracluster medium.

A key prediction of the Binney-Cowie model is the existence of a significant amount of hot gas ($T_g \approx 8$ keV) surrounding M87. The density of this gas is determined by the requirement of pressure equilibrium with the cooler gas in M87. Early observations (Davison, 1978; Lawrence, 1978) suggested that there was extended, hard x-ray emission in this cluster. More recent observations (Mushotzky *et al.*, 1977; Ulmer, Cruddace, Wood, Meekins, Yentis, Evans, Smathers, Byram, Chubb, and Friedman, 1980; Lea *et al.*, 1981, 1982) have not confirmed its existence, and it has been suggested that the previously observed hard x-ray emission is entirely from the nucleus of M87. The observed temperature gradient in M87 is apparently not consistent with the Binney-Cowie model (Fabricant *et al.*, 1980; Fabricant and Gorenstein, 1983; Stewart, Canizares, Fabian, and Nulsen, 1984).

A host of x-ray lines have been detected from M87 (see Sec. III.C). Both Fe *L* and *K* lines have been observed (Serlemitsos *et al.*, 1977; Lea *et al.*, 1979), as well as lines from lighter elements. The observations indicate that the abundance of these elements is reasonably uniform within M87 (Fabricant *et al.*, 1978; Lea *et al.*, 1982). The gas temperature appears to be roughly constant at projected radii of ≥ 5 arcmin, and decreases rapidly within this radius. In the inner regions, large amounts of emission by quite cool gas are observed in the higher-resolution spectra (Canizares *et al.*, 1979, 1982; Lea *et al.*, 1982). The x-ray surface brightness is also strongly peaked in this region.

The presence of a range of temperatures of cool gas and the central peak in the x-ray surface brightness both suggest that the gas in M87 is radiatively cooling and being accreted onto the center of the galaxy (Gorenstein *et al.*, 1977; Mathews, 1978b). Comparisons between models for the accretion (Mathews and Bregman, 1978; Binney and Cowie, 1981) and the observations suggest that the accretion rate is $\dot{M} \sim 3-20 M_{\odot}/\text{yr}$. Like NGC1275 in Perseus, M87 has optical-line-emitting filaments in its inner

regions (Ford and Butcher, 1979; Stauffer and Spinrad, 1979), which may be produced by thermal instabilities in the cooling gas (Fabian and Nulsen, 1977; Mathews and Bregman, 1978). As discussed above for NGC1275, the radio source may be powered by further accretion of a small fraction of the gas onto the nucleus (Mathews, 1978a), while the bulk of the accreted material may form low-mass stars (Sarazin and O'Connell, 1983). Both the line emission and halo radio emission are concentrated to the north side of M87. De Young *et al.* (1980) suggest that M87 is moving at ~ 200 km/sec relative to the intra-cluster gas it is accreting, but Dones and White (1985) show that the thermodynamic structure of the gas is inconsistent with this motion.

Recently, Tucker and Rosner (1983) have suggested a hydrostatic (no accretion) model for M87. The gas in the outer portions of the galaxy is heated by the nonthermal electrons that produce the halo radio emission. Heat is conducted from these hotter outer regions into the cooler central regions, where it is radiated away; unlike Binney and Cowie (1981), Tucker and Rosner assume full thermal conductivity. The heating by nonthermal electrons balances the cooling, and the gas is thermo- and hydrostatic. The radio source is itself powered by accretion; thus they argue that the behavior of the system is episodic, with alternating periods of accretion and nonthermal heating.

Many other galaxies in the central regions of the Virgo cluster have been detected as x-ray sources with luminosities in the range $L_x \sim 10^{39-41}$ ergs/sec (Forman *et al.*, 1979). Because no spectra are available for these galaxies, it is uncertain whether the x rays are due to thermal emission from hot gas or some other source. Figure 21 shows

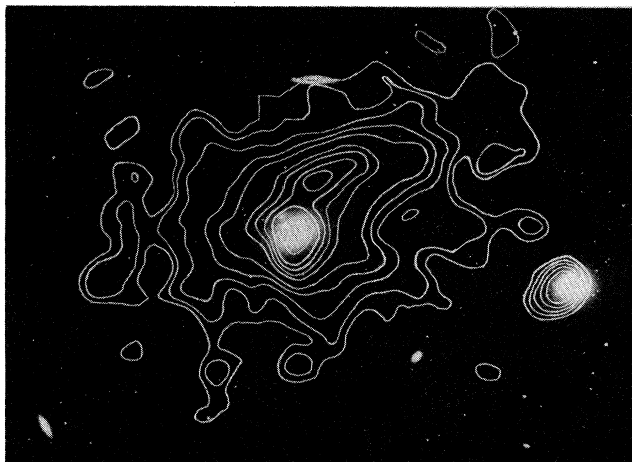


FIG. 21. The x-ray emission from the Virgo cluster galaxies M86 (east or left) and M84 (west or right) from Forman and Jones (1982). Contours of constant x-ray surface brightness are shown superimposed on an optical image of the galaxies. Note the plume of x-ray emission extending to the north of M86, which may indicate that this galaxy is currently being stripped of its gas.

the x-ray emission from the very optically luminous galaxy M84 and the galaxy M86, which has an x-ray plume extending away from M87. Fabian *et al.* (1980) suggest that M86 contains hot gas, which is currently being stripped by ram pressure as it moves into the core of the cluster (see Secs. II.J.2 and V.I). The interpretation of the x-ray emission from M87 and the other galaxies in the Virgo cluster is discussed in more detail in Sec. V.H.

4. A1367

A1367 is an irregular, BM type II-III cluster (Bautz and Morgan, 1970; Carter and Metcalfe, 1980) with a moderately high spiral fraction (Bahcall, 1977c). It has a low x-ray luminosity $L_x \approx 4 \times 10^{43} h_{50}^{-2}$ ergs/sec and a temperature $T_g \approx 3 \times 10^7$ K (Mushotzky, 1984). The x-ray emission is extended and elongated [Fig. 22(a)]; Bechtold *et al.* (1983) found an x-ray core radius [Eq. (3.7)] of $r_x = (0.8 \times 0.4) h_{50}^{-1}$ Mpc for the semimajor and semiminor axes of the distribution. In addition, 8 point sources and 13 resolved peaks in the x-ray emission (with typical sizes of an arcmin) were observed at higher spatial resolution [Fig. 22(b)], 11 of which were associated with cluster galaxies. These galaxies have x-ray luminosities in the range $10^{40-42} h_{50}^2$ ergs/sec. 21-cm observations indicate that some of these galaxies also contain neutral hydrogen (Chincarini *et al.*, 1983). A1367 is the only irregular cluster that appears to have an extended radio halo (Hanisch, 1980).

F. X-ray—optical correlations

A number of correlations between the optical and x-ray properties of clusters have been found (Bahcall, 1977a). The optical cluster properties that have been used to study x-ray clusters include the richness (Sec. II.C), morphology (RS or BM type; Sec. II.E), the galactic content (cD galaxies and spiral fractions; Sec. II.J), the core radius r_c (or other radii; Sec. II.G), the velocity dispersion σ_r (Sec. II.F), and the central galaxy density \bar{N}_0 of Bahcall (1977b; Sec. II.G). The largest x-ray surveys (Sec. III.B) provide only x-ray fluxes (and thus luminosities L_x) for a given x-ray photon energy range. In addition, there are now smaller samples of clusters with x-ray surface brightness determinations, giving r_x or β (Sec. III.D), and samples with x-ray spectra, yielding T_g and EI (Sec. III.C).

Solinger and Tucker (1972) first suggested that the x-ray luminosity of a cluster correlates with its velocity dispersion $L_x \propto \sigma_r^4$, based on the small sample of known x-ray clusters at that time. This sample included M87/Virgo, in which the x-ray emission comes from the galaxy M87 rather than the entire cluster, and several clusters having multiple velocity components, which probably cause the velocity dispersion to be overestimated. Solinger and Tucker gave a simple model to explain the correlation based on the assumption that the emission comes from intracluster gas. This correlation has been

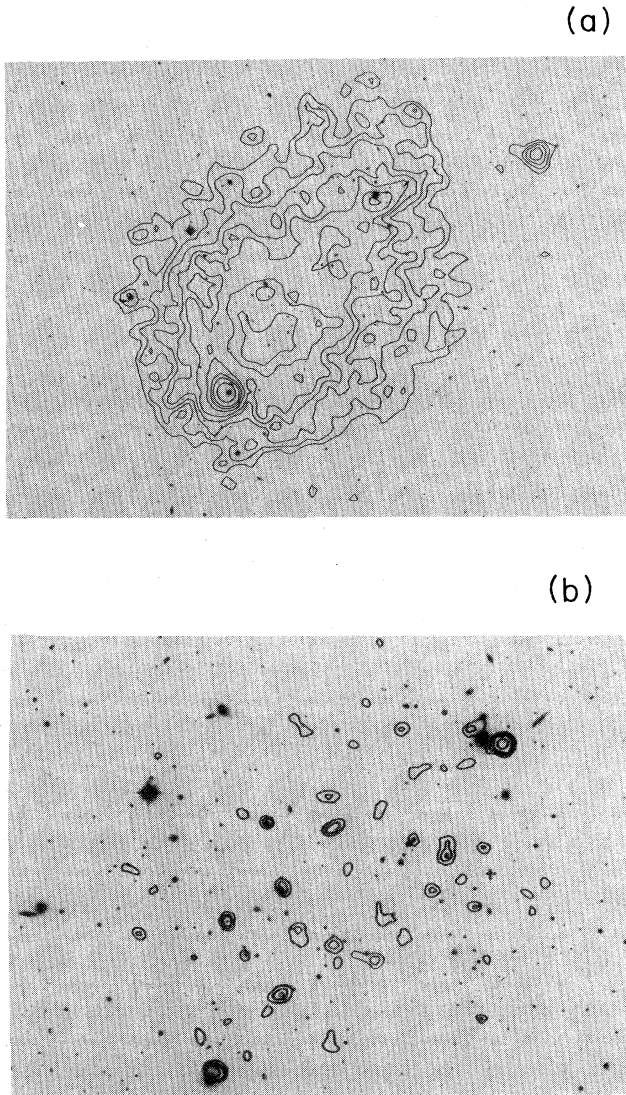


FIG. 22. The x-ray surface brightness of the A1367 cluster of galaxies, observed by Bechtold *et al.* (1983) with the *Einstein* satellite. Contours of constant x-ray surface brightness are shown superimposed on the optical image of the cluster. (a) The lower-resolution IPC image, showing the irregular cluster emission. (b) The higher-resolution HRI image, showing many discrete sources within the cluster, many of which are associated with individual cluster galaxies.

reexamined a number of times and other explanations of its physical significance have been given (Yahil and Ostriker, 1973; Katz, 1976; Silk, 1976). As the sample of x-ray clusters has grown, the correlation has become less convincing (McHardy, 1978a), and certainly there is a great deal of scatter about any such correlation. However, Quintana and Melnick (1982) find basically the same relationships for larger data samples from the *HEAO-1*

and *Einstein* observatories. Their relationship for the *HEAO-1* data is shown as Fig. 23; roughly, the correlation is

$$L_x(2-10 \text{ keV}) \approx 4.2 \times 10^{44} \text{ ergs sec}^{-1} \times \left[\frac{\sigma_r}{10^3 \text{ km sec}^{-1}} \right]^4 \quad (3.8)$$

For the lower-energy *Einstein* observations, the power in Eq. (3.8) is closer to three (Quintana and Melnick, 1982; Abramopoulos and Ku, 1983).

In some sense, the richness of a cluster (the number of galaxies in the cluster) and L_x measure the mass of stars and of diffuse gas in the cluster, respectively, and one might expect these to be related. Such a relationship does indeed appear in the data (Bahcall, 1974b; Jones and Forman, 1978; McHardy, 1978a; McKee *et al.*, 1980; Ulmer *et al.*, 1981; Abramopoulos and Ku, 1983; Johnson *et al.*, 1983). It is difficult to give a quantitative measure of the correlation because the richness class 0 clusters are incomplete in the Abell catalog, Abell richnesses are binned in the original catalog, and the higher-richness clusters are generally more distant. Abramopoulos and Ku (1983) find that the low-energy x-ray luminosity increases with richness to the 1.2 power. Recently this correlation has been shown to extend to the very richest Abell clusters by Soltan and Henry (1983; see also Pravdo *et al.*, 1979). Low-luminosity x-ray clusters are much less common among the richest clusters.

There appears to be a correlation between the optical morphology and x-ray luminosity of clusters. Bahcall (1974b), Owen (1974), Mushotzky *et al.* (1978), McKee *et*

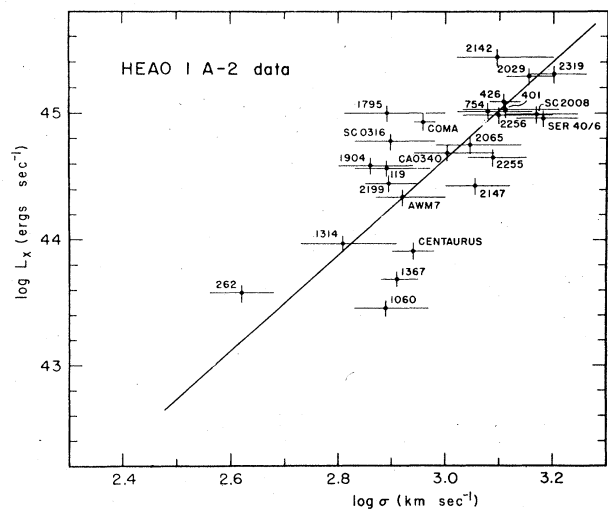


FIG. 23. The correlation between the x-ray luminosity of clusters observed with *HEAO-1* A-2 and their line-of-sight velocity dispersion, from Quintana and Melnick (1982).

al. (1980), and Abramopoulos and Ku (1983) found that the more regular Rood-Sastry types (cD, B) in general have higher x-ray luminosities than the less regular clusters. The reality of this correlation has been disputed by Jones and Forman (1978) and Lugger (1978), although it does appear in the larger *HEAO-1* and *Einstein* data samples. Bautz-Morgan type I clusters are found to be more luminous than the less regular clusters, although the correlation does not seem to continue to less regular BM types (McHardy, 1978a; McKee *et al.*, 1980; Ulmer *et al.*, 1981; Abramopoulos and Ku, 1983; Johnson *et al.*, 1983). Clusters that contain optically dominant galaxies near the cluster center tend to be stronger x-ray sources than those that do not (Bahcall, 1974b; Jones and Forman, 1984). (In the Jones-Forman classification scheme these are XD clusters; see Sec. III.D.)

Jones and Forman (1978) have argued that all of these x-ray-optical correlations are due to the correlation of x-ray luminosity and richness *plus* the tendency of rich clusters to be more regular (lower BM type, etc.). As the sample of x-ray clusters has enlarged, it has become possible to test this possibility by considering subsamples of fixed richness, and correlations with optical morphology appear in these samples as well (e.g., McHardy, 1978a).

Bahcall (1977b) showed that the x-ray luminosity of clusters was well correlated with the projected central galaxy density parameter \bar{N}_0 (Sec. II.G.3). This correlation is tighter than the richness correlation; an explanation of this may be that thermal x-ray emission depends on the square of the density of the gas, and thus is most sensitive to the deepest portion of the cluster potential. This correlation has been confirmed by Mushotzky *et al.* (1978), Mitchell *et al.* (1979), Abramopoulos and Ku (1983), and Mushotzky (1984). The correlation in the *HEAO-1* A-2 sample (Fig. 24) is consistent with $L_x \propto (\bar{N}_0)^{3.5}$, and is one power weaker in the lower-energy *Einstein* sample.

Bahcall (1977c) showed that the x-ray luminosity of a cluster correlated with its galactic content, in that luminous x-ray clusters generally have a small proportion of spiral galaxies. This correlation has been confirmed by

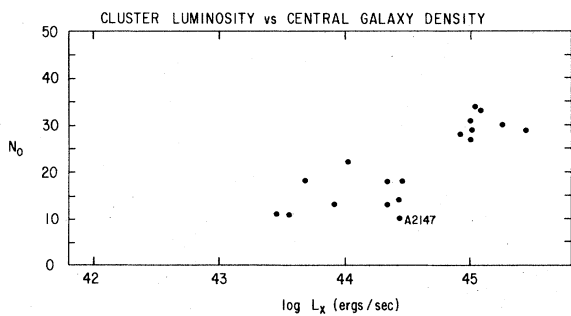


FIG. 24. The relationship between the x-ray luminosities of clusters observed with *HEAO-1* A-2 and the central galaxy density N_0 of Bahcall (1977b), from Mushotzky (1984).

McHardy (1978a), Mushotzky *et al.* (1978), Tyler and Vidal (1979), and Abramopoulos and Ku (1983). Melnick and Sargent (1977) showed that the spiral fraction increased with radius in x-ray clusters, and that the spiral fraction was inversely correlated to the velocity dispersion. These correlations are consistent with the theory that spiral galaxies formed in clusters are stripped of their gas content through interactions with the intracluster gas and become SO galaxies (Secs. II.J.2 and V.I), although they certainly do not prove that this has occurred. Let f_{sp} be the fraction of cluster galaxies that are spirals. This spiral fraction is plotted against the x-ray luminosity of clusters in Fig. 25. Bahcall (1977c) showed that the correlation could be represented as

$$f_{sp} \approx 0.37 - 0.26 \ln \left[\frac{L_x}{10^{44} \text{ ergs sec}^{-1}} \right], \quad (3.9)$$

which she derived based on a simple model for stripping of spirals in a cluster. An important counterexample to this correlation is A194, which has a low spiral fraction $f_{sp} \approx 0.27$ (Oemler, 1974; Dressler, 1980a). Yet this cluster has a very low x-ray luminosity (Jones and Forman, 1984) and low velocity dispersion, which make it unlikely that the spirals were stripped by the ram pressure of intracluster gas.

Kellogg and Murray (1974) suggested a correlation between the sizes of the x-ray sources in clusters and the galaxy core radii, $r_x \sim 2 r_c$, but very few clusters have accurately determined galaxy core radii (Sec. II.G). Ulmer *et al.* (1981) found that the x-ray luminosity of clusters in the *HEAO-1* A-1 survey correlated with the cluster radius R_{LV} as given by Leir and van den Bergh (1977; Sec. II.G.3), with $L_x \propto R_{LV}^2$. This correlation was confirmed in the *Einstein* data by Abramopoulos and Ku (1983).

The *OSO-8*, *Ariel 5*, and *HEAO-1* A-1 spectral surveys established a number of correlations between the x-ray

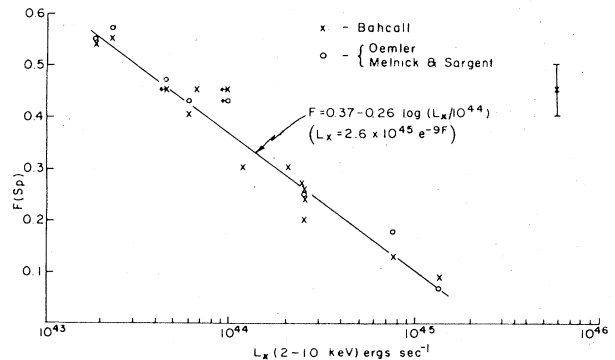


FIG. 25. The correlation between the spiral fraction in clusters and their x-ray luminosity, from Bahcall (1977c). The line shows the relation from Eq. (3.9).

spectral parameters and the optical properties of x-ray clusters (Mitchell *et al.*, 1977,1979; Mushotzky *et al.*, 1978; Smith, Mushotzky, and Serlemitsos, 1979; Mushotzky, 1980,1984). The two properties that can be derived most easily from a continuum x-ray spectrum are the gas temperature T_g and the emission integral EI [Eq. (3.3)]. The x-ray luminosity of a cluster is proportional to EI [Eq. (3.11)].

An important correlation was found between the gas temperatures T_g , determined from the x-ray spectra, and the velocity dispersion of the galaxies in the cluster (see Sec. II.F). The older surveys (Mushotzky *et al.*, 1978; Mitchell *et al.*, 1979; Smith, Mushotzky, and Serlemitsos, 1979) had found that, when cD clusters were excluded, the temperatures varied roughly as

$$T_g \approx 6 \times 10^7 \text{ K} \left[\frac{\sigma_r}{10^3 \text{ km sec}^{-1}} \right]^2. \quad (3.10)$$

As will be demonstrated in Sec. V.E, such a correlation would be expected if the gas were gravitationally bound to the cluster, because the velocity dispersion measures the depth of the cluster potential [Eq. (2.24)]. Moreover, this correlation between T_g and σ_r^2 supported the view that clusters must contain large masses of unseen material (the "missing mass" problem, Sec. II.H). The fact that the galaxy and gas velocity dispersions were similar and proportional to one another suggested that both gas and galaxies were bound by the same gravitational potential, which required a very large mass for the cluster. The cD clusters showed less of a correlation, which may indicate that in these systems there is a significant amount of gas bound to the cD itself, rather than to the entire cluster. Unfortunately, the *HEAO 1 A-2* data do not show a very tight correlation and give $T_g \propto \sigma_r$ (Mushotzky, 1984; Fig. 26).

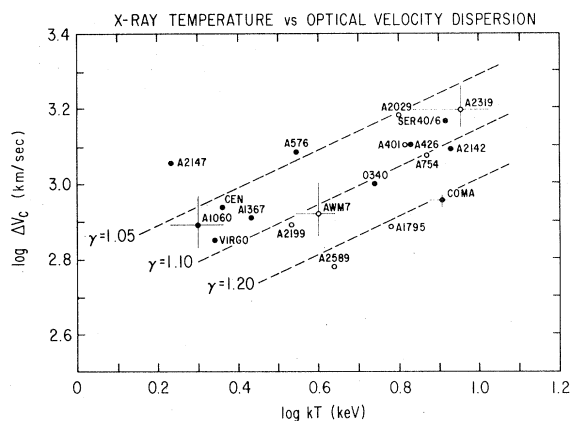


FIG. 26. The relationship between gas temperatures derived from x-ray spectral observations with *HEAO-1 A-2* and the central velocity dispersion ($\Delta V_c = \sigma_r$, at the cluster center), from Mushotzky (1984). The lines show the predictions of polytropic models with various indices (Sec. V.E.2). The dots are the data for non-cD clusters; the open circles are cD clusters.

The gas temperature correlates strongly with the central density \bar{N}_0 of Bahcall (1977b), with $T_g \propto \bar{N}_0$ (Mushotzky *et al.*, 1978; Mitchell *et al.*, 1979; Mushotzky, 1984). This correlation is shown in Fig. 27.

For thermal bremsstrahlung emission (Sec.V.A.3), the emission integral EI, x-ray luminosity L_x , and gas temperature T_g are related by

$$L_x \propto \text{EI } T_g^{1/2}, \quad (3.11)$$

and thus the correlations of L_x and T_g with optical properties imply correlations of EI with these properties as well.

G. Poor clusters

X-ray emission has also been detected associated with poor clusters of galaxies (Schwartz, Davis, Doxsey, Griffiths, Huchra, Johnston, Mushotzky, Swank, and Tonry, 1980; Schwartz, Schwarz, and Tucker, 1980; Kriss *et al.*, 1980,1981,1983). Of special interest are the poor clusters that contain D or cD galaxies, lists of which have been given by Morgan *et al.* (1975) and Albert *et al.* (1977); clusters from these two lists are identified as MKW and AWM clusters, respectively. The optical properties of these cD galaxies were discussed in Sec. II.J.1, where it was concluded that the cD's in poor clusters were similar to cD's in rich clusters, except that they lacked the very extended, low-surface-brightness envelopes seen in rich cluster cD's (Thuan and Romanishin, 1981; Oemler, 1976; van den Bergh, 1977a). This suggests that the main bodies of cD's are formed by a process, such as mergers, that is not strongly dependent on richness, while the halos are formed by a process, such as tidal interactions, that does depend strongly on richness.

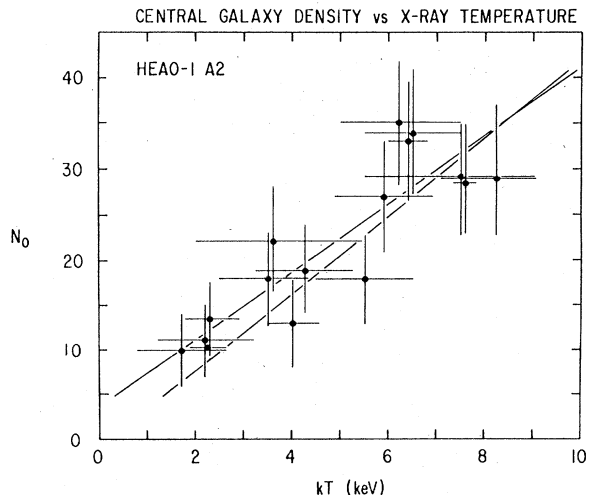


FIG. 27. The correlation between the gas temperatures derived from x-ray spectral measurements with *HEAO-1 A-2* and the central galaxy density of Bahcall (1977b), from Mushotzky (1984).

In general, the optical properties of the poor clusters appear to be simple extensions of the properties of rich clusters to lower richness (Stauffer and Spinrad, 1978; Thomas and Batchelor, 1978; Schild and Davis, 1979; Bahcall, 1980). The radio properties of the poor cluster cD's are also very similar to those of rich clusters (White and Burns, 1980; Burns *et al.*, 1980; Burns, White, and Hough, 1981).

The poor clusters containing cD galaxies are generally observed to be x-ray sources with luminosities of $\sim 10^{42-44}$ ergs/sec (Schwartz, Davis, Doxsey, Griffiths, Huchra, Johnston, Mushotzky, Swank, and Tonry, 1980; Schwartz, Schwarz, and Tucker, 1980; Kriss *et al.*, 1980, 1981, 1983). Recently Kriss *et al.* (1983) surveyed 16 MKW and AWM clusters, and detected x-ray emission from 12. In the brighter clusters, the x-ray emission was found to be smoothly distributed, relatively symmetrical, and fairly extended (out to radii of ~ 1 Mpc). Kriss *et al.* found that the x-ray temperatures in these poor clusters were fairly low $T_g \approx 1-5$ keV, in keeping with their low velocity dispersions [see Eq. (3.10)]. The x-ray emission is strongly peaked on the position of the cD galaxy (Canizares *et al.*, 1983; see the image of AWM4 in Fig. 28). This suggests that the cD's in poor clusters are located at the bottoms of cluster potential wells, as was shown to be the case for rich cluster cD's (Sec. II.J.1). In many ways, the bright poor cluster x-ray sources resemble the regular XD clusters discussed above. The x-ray emission in a number of cases is elongated in the same direction as the long axis of the cD galaxy (Kriss *et al.*, 1983; a similar effect is seen in rich clusters, as discussed in Secs. II.J.1 and III.E).

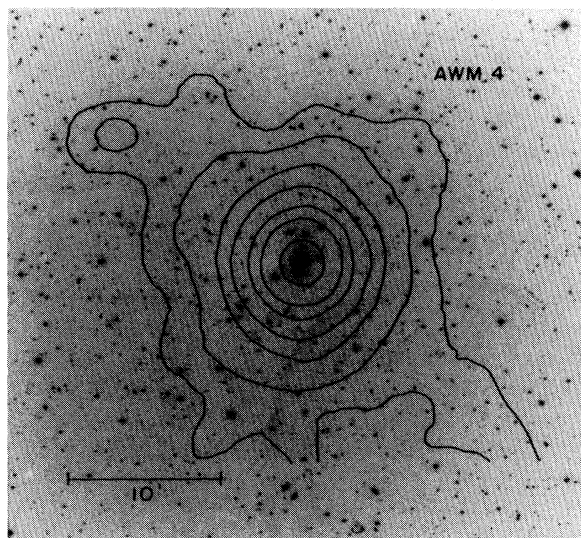


FIG. 28. The x-ray emission from the AWM4 poor cluster of galaxies, from Kriss *et al.* (1983) with the IPC on the *Einstein* satellite. Contours of constant x-ray surface brightness are shown superimposed on the optical image of the cluster. The emission is centered on the cD galaxy.

From the distribution of the gas in the cluster, the cluster gravitational potential and mass can be derived (Kriss *et al.*, 1983). When these are compared to the optical luminosity of the clusters, a considerable missing mass problem is found. The mass-to-light ratios in the inner parts of these clusters are found to be roughly $M/L_V \approx 100h_{50}M_{\odot}/L_{\odot}$. The x-ray-emitting gas makes up roughly 15% of the total cluster mass in these inner regions. Because the cD galaxy contributes a large fraction of the luminosity in these poor clusters, this dark matter can also be thought of as a massive halo around the central cD, as in the M87/Virgo cluster.

The x-ray emission is strongly peaked on the position of the cD in these poor clusters (Canizares *et al.*, 1983; Kriss *et al.*, 1983), and the cooling times in the central portions of the gas are generally estimated to be less than the probable age of the cluster (the Hubble time). This suggests that the x-ray-emitting gas forms a cooling accretion flow onto the cD (Canizares *et al.*, 1983), as has been observed in many rich clusters. The accretion rates in MKW4, MKW3s, AWM4, and AWM7 are estimated to be in the range of $20-100M_{\odot}/\text{yr}$ (Canizares *et al.*, 1983). It is possible that star formation from the accretion flow may provide a portion of the optical luminosity of the cD (Fabian, Nulsen, and Canizares, 1982; Sarazin and O'Connell, 1983). Very little cold gas (neutral hydrogen) is detected in these cD's (Burns, White, and Haynes, 1981; Valentijn and Giovanelli, 1982).

Poor clusters containing head-tail radio sources have also been detected in x rays (Burns and Owen, 1979; Holman and McKee, 1981). Head-tail radio sources are believed to be produced by galaxy motions through intra-cluster gas (Sec IV.C).

H. High-redshift clusters and x-ray cluster evolution

Observations of high-redshift x-ray clusters (taken here to mean clusters with $z \geq 0.2$) offer the possibility of studying the formation and evolution of clusters. At the moment this study is hampered by the small sample of clusters that have been observed and the difficulty in obtaining detailed information (spectra and spatial distributions) for these distant sources. Samples of high-redshift x-ray clusters have been given by Henry *et al.* (1979, 1982), Helfand *et al.* (1980), Perrenod and Henry (1981), White, Sarazin, Quintana, and Jaffe (1981), White, Silk, and Henry (1981), and White *et al.* (1985). These samples are based on lists of clusters detected initially through optical or radio emission.

One purpose of this study is to determine whether x-ray clusters have evolved in any detectable way over the cosmological time span represented by the redshift. Henry *et al.* (1979) compared a sample of six high-redshift clusters with more nearby clusters, and concluded that they were similar in many ways. They found marginal evidence that x-ray luminosities increase with time in accordance with the models of Perrenod (1978b) and Sara-

zin (1979), but the sample was too small to make any strong statements. Henry *et al.* (1982) studied the evolution of the slope of the x-ray luminosity function at redshifts $z < 0.5$. No significant evidence for evolution was found.

Perrenod and Henry (1981) estimated gas temperatures for a sample of seven high-redshift clusters observed with the *Einstein* observatory. With one exception (the remarkable cluster 0016 + 16 discussed below), the clusters with $z > 0.3$ all had $T_g < 4$ keV (a sample of six clusters). Nearby clusters of similar x-ray luminosity have average temperatures of $T_g \approx 7$ keV. Thus it appeared that gas temperatures in clusters might be increasing with time. Since the temperature of gas in a cluster reflects in part the depth of the cluster potential well (Sec. V.E), this suggested that clusters might be growing through the merger of smaller clusters, in accord with models developed by Perrenod (1978b). White, Sarazin, Quintana, and Jaffe (1981) also detected a fairly distant cluster (2059-247) with a very high x-ray luminosity and a low x-ray temperature. However, White *et al.* (1985) observed a sample of 10 high-redshift clusters; of the five detected cluster x-ray sources, all have reasonably high x-ray temperatures $T_g \geq 6$ keV. They suspect that the previous evidence for low x-ray temperatures by Perrenod and Henry was an artifact of the small size of the sample being discussed. They also point out that some high-luminosity, low-temperature clusters, such as 2059-247, may be extreme examples of clusters with cooling accretion flows at their centers.

Several of the high-redshift clusters that have been observed as x-ray sources (Henry *et al.*, 1979, 1982; Helfand *et al.*, 1980) are Butcher-Oemler clusters (Butcher and Oemler, 1978a). As discussed in Sec. II.J.2, these are high-redshift clusters that appear to contain blue galaxies with colors similar to those of spirals in nearby clusters. Prior to the x-ray observations, the most straightforward explanation of these clusters was that they did not contain enough gas to strip spiral galaxies effectively by ram pressure ablation (Norman and Silk, 1979; Sarazin, 1979). Obviously, the detection of large quantities of hot gas in these clusters has made that explanation untenable. Recently optical observations indicate that the blue galaxies in these clusters are not normal spirals and are unlike any class of present-day galaxies (Dressler and Gunn, 1982).

The most spectacular high-redshift cluster to be detected so far is the $z = 0.54$ cluster 0016 + 16 (White, Silk, and Henry, 1981). This cluster has one of the highest x-ray luminosities observed $L_x = 3 \times 10^{45} h_{50}^{-2}$ ergs/sec, and may have a high temperature, although this is very uncertain. The cluster is extremely rich (Koo, 1981); most of its properties can be viewed as an extrapolation of the Coma cluster to about twice Coma's richness. The cluster 0016 + 16 is also similar to nearby rich clusters in that it has predominately red galaxies—it does not show the Butcher-Oemler effect. A microwave decrement (Sec. IV.E) of -1.4 mK has been detected from the cluster (Birkinshaw, Gull, and Moffet, 1981). This effect has not been detected in many nearby clusters, and if the detec-

tion were confirmed it would demonstrate the extreme luminosity and temperature of 0016 + 16.

The tentative conclusion at this point is that the x-ray properties of clusters do not appear to evolve dramatically to redshifts of $z \approx 0.5$, and that evolution of the x-ray properties is probably not the explanation of the Butcher-Oemler effect.

IV. RADIO OBSERVATIONS

A. General radio properties

The association between radio sources and clusters of galaxies was first made by Mills (1960) and van den Bergh (1961b). Radio emission from clusters has been reviewed recently by Robertson (1985). A brief review of the radio properties of clusters relevant to their x-ray emission will be given in this section. First, the general radio luminosities and spectra will be summarized. Second, possible correlations between the radio and x-ray emissions of clusters will be discussed. Third, two classes of radio source morphology (head-tail radio sources and cluster halo sources) which are unique to the cluster environment will be described. Fourth, possible observations of the effect of the intracluster medium on radio emission due to the cosmic blackbody background or background source will be reviewed. Finally, the use of the 21-cm hyperfine line to detect neutral hydrogen gas in clusters will be briefly discussed.

Figure 29 shows a contour plot of the radio emission in the Perseus cluster, superimposed on an optical photograph. The very strong radio emission from the central galaxy NGC1275 (Sec. III.E.2) and the two head-tail radio galaxies NGC1265 and IC310 are shown.

The radio emission from clusters of galaxies (as well as most other extragalactic objects) is synchrotron emission due to the interaction of a nonthermal population of relativistic electrons (with a power-law energy distribution) with a magnetic field (Robertson, 1985). Such nonthermal synchrotron emission generally has a spectrum in which the intensity I_ν (ergs/cm² Hz sec) is well represented as a power law over a wide range of frequencies ν ,

$$I_\nu \propto \nu^{-\alpha_r}, \quad (4.1)$$

where α_r is the radio spectral index. Typical extragalactic radio sources have $\alpha_r \sim 0.8$. Most of the radio emission from clusters is due to discrete sources, which can be associated with individual galaxies within the cluster. The properties of the nonthermal radio emission from radio galaxies have been reviewed recently by Miley (1980).

Radio emission from Abell clusters at a frequency of 1400 MHz has been surveyed by Owen (1975), Jaffe and Perola (1975), and Owen *et al.* (1982). At lower frequencies there are a number of older surveys (e.g., Fomalont and Rogstad, 1966), as well as an extensive list based on the 4C Cambridge survey (Slingo, 1974a, 1974b; Riley, 1975; McHardy, 1978b). These observations suggested

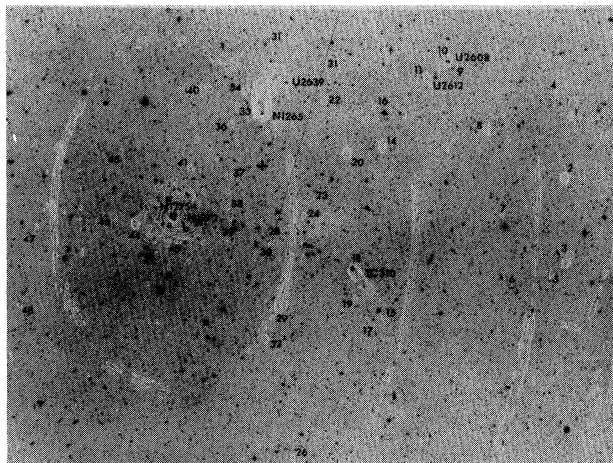


FIG. 29. A radio map of the Perseus cluster of galaxies from Gisler and Miley (1979). Contours of constant radio surface brightness at 610 MHz are shown superimposed on the optical image of the cluster. Note the very strong source associated with the galaxy NGC1275 (the highest contours associated with this source have been removed), and the two head-tail radio sources associated with NGC1265 and IC310. The rings are diffraction features due to NGC1275 and are not real.

that only sources detected in the inner portions (within $\frac{1}{3}$ Abell radii) of the Abell clusters were likely to belong to the cluster, the rest being background objects. Observations at higher frequencies have been made by Andernach *et al.* (1980,1981), Haslam *et al.* (1978), and Waldthausen *et al.* (1979). The more distant Abell clusters were searched for radio emission by Fanti *et al.* (1983), while the richest Abell clusters were observed by Birkinshaw (1978). Jaffe (1982) surveyed a sample of high-redshift clusters, and found evidence of evolution in the radio luminosity of clusters for the range of redshifts $0.25 < z < 0.95$.

In discussing the radio luminosity functions of clusters, it is important to distinguish the luminosity function of galaxies in clusters from the luminosity function of the cluster as a whole. The radio emission from clusters is mainly due to sources associated with individual radio galaxies. About 20% of the nearby strong radio galaxies are located in rich clusters of galaxies (McHardy, 1979). This appears to be mainly due to the fact that strong radio emission is primarily associated with giant elliptical galaxies, which occur preferentially in clusters. A galaxy of a given morphology (elliptical, for example) and optical luminosity apparently has the same radio luminosity function whether inside or outside of a cluster (Jaffe and Perola, 1976; Auriemma *et al.*, 1977; Guindon, 1979; McHardy, 1979). The radio luminosity function of the whole cluster can be fit as the result of superposing the

luminosity function of an average of ~ 5 radio galaxies per cluster (Owen, 1975). The cluster radio luminosity function does not appear to depend strongly on richness for the Abell clusters (Riley, 1975; Owen, 1975; McHardy, 1979).

There does appear to be a correlation between cluster radio emission and cluster morphology. Owen found that the more evolved RS types (cD, B, C, and L; see Sec. II.E) have stronger radio emission. McHardy (1979) found that more evolved BM types (I, I-II; see Sec. II.E) tend to contain stronger radio galaxies, at least at low frequencies.

Powerful radio sources are found most often near the cluster center (McHardy, 1979). They are usually associated with optically dominant galaxies, which often have multiple nuclei and are often cD galaxies (Guthrie, 1974; McHardy, 1974,1979; Riley, 1975).

Cluster radio sources generally have steeper radio spectra (values of $\alpha_r \geq 1$) than radio sources in the field (Costain *et al.*, 1972; Baldwin and Scott, 1973; Slingo, 1974a,1974b; McHardy, 1979). The steepness of the spectrum (the value of α_r) increases with cluster richness and decreases as the BM type increases (Roland *et al.*, 1976; McHardy, 1979). The steepest radio spectra ($\alpha_r \approx 1.3$) in clusters are associated with radio sources in optically dominant galaxies (Riley, 1975).

De Young (1972) claimed that cluster radio galaxies were generally smaller than those in the field; this claim was not supported by larger surveys (Hooley, 1974; McHardy, 1979). Owen and Rudnick (1976a) found that cluster radio sources generally had extended emission; unresolved sources seen towards clusters are usually background objects. Guindon (1979) found that, while the average size of double or triple radio sources in clusters was the same as those in the field, clusters did lack the very largest sources.

Differences in the morphology of cluster radio sources and field sources are discussed in Secs. IV.C and IV.D below.

Recently, the radio emission properties of poor clusters have been studied. In general, the sources in poor clusters also have steep spectra and show some of the same morphological distortions found in rich cluster sources (Burns and Owen, 1977). As in rich clusters, the strongest radio emission is associated with optically dominant galaxies near the cluster center, and these sources have especially steep spectra (White and Burns, 1980; Burns, White, and Hough, 1981; Hanisch and White, 1981). There is no apparent difference between the radio emission of poor and rich cD clusters beyond the direct effect of richness (Burns *et al.*, 1980).

B. Correlations between x-ray and radio emission

Based on the small sample of x-ray clusters known at that time, Owen (1974) argued that there was a strong correlation between the radio and x-ray luminosity of

clusters. Rowan-Robinson and Fabian (1975) did not find this correlation. Bahcall (1974b, 1977a) found that the x-ray emission of a cluster was increased if a strong radio source was located near the center of the cluster. McHardy (1978a) found that strong radio sources were more likely to be located in luminous x-ray clusters than in other clusters.

As discussed above, clusters generally contain steep-spectrum radio sources. It appears that radio sources in x-ray clusters have even steeper spectra, and that α_r correlates with x-ray luminosity (Erickson *et al.*, 1978; McHardy, 1978a; Cane *et al.*, 1981; Dagkesamansky *et al.*, 1982). This suggests that there might be a strong correlation between low-frequency radio flux and x-ray luminosity (Erickson *et al.*, 1978; Cane *et al.*, 1981). Such a correlation is not found in larger samples of x-ray clusters (Mitchell *et al.*, 1979; Ulmer *et al.*, 1981). X-ray selected cluster samples from the *Einstein* observatory do not show a strong x-ray—radio correlation (Feigelson *et al.*, 1982; Johnson, 1981).

A possible correlation between x-ray emission and radio emission in poor clusters has also been found (Burns, Gregory, and Holman, 1981).

There appears to be a strong correlation between radio emission by central dominant galaxies in clusters and the presence of cooling flows, as evidenced by soft x-ray line emission or central spikes in the x-ray surface brightness (Burns, White, and Haynes, 1981; Valentijn and Bijleveld, 1983; Jones and Forman, 1984; Sec. V.G.2).

To summarize, at present there may be a weak correlation between x-ray and radio luminosities, and there appears to be stronger correlation between the radio spectral index α_r and the x-ray luminosity L_x . Because of the many interrelationships between cluster properties, it is difficult to decide whether these possible correlations are primary or reflect other correlations (see Sec. III.F). For example, the relationship between L_x and α_r may be a result of the fact that L_x correlates with cluster optical morphology (Sec. III.F), as does α_r . Moreover, it is difficult to establish a clear causal basis for these correlations.

Costain *et al.* (1972) and Owen (1974) argued that the correlation between x-ray and radio emission implied that the same population of relativistic electrons produced both radio emission and x-ray emission. The radio emission is synchrotron emission; in this model the x-ray emission would be inverse Compton scattering of cosmic radiation photons by the same relativistic electrons. This "inverse Compton" (IC) theory is described in more detail in Sec. V.A.1. The IC model does require that cluster radio sources have steep spectra, as observed. However, the evidence against the IC model is now overwhelmingly strong (Secs. III.C and V.A). Thermal emission by diffuse gas provides the main x-ray emission from clusters.

Another direct connection between the radio-emitting electrons and the x-ray-emitting thermal gas would be established if the thermal gas were heated by the relativistic electrons and/or any associated "cosmic ray" nuclei. Such heating would occur through Coulomb interactions (Lea and Holman, 1978) and might be enhanced by plas-

ma interactions (Scott *et al.*, 1980; see Sec. V.C.5 for more details). The heating is strongest for the lower-energy electrons which produce very low-frequency radio emission, and thus the heating requires that the radio sources in clusters have steep spectra, as observed. However, it is not clear that any ongoing heating of the thermal gas either is needed or does occur in the majority of x-ray clusters. First of all, there exist a reasonable number of strong x-ray clusters that do not have strong steep-spectrum radio sources. Second, the thermal energy per unit mass in the hot gas is roughly the same as the kinetic energy per unit mass in the galaxies. Thus the gas could have been heated initially by thermalizing its kinetic energy when it either was ejected from galaxies or fell into the cluster. In typical clusters, the cooling time in most of the gas is longer than the probable age of the cluster (the Hubble time), and no further heating of the gas would necessarily be required (Sec. V.C).

A connection between the x-ray and radio luminosity of clusters might be produced if the radio emission were powered by accretion of gas which was initially part of the hot intracluster medium. In Secs. III.C and V.G evidence is presented indicating that intracluster gas is cooling and being accreted by central dominant galaxies in many x-ray clusters. As mentioned previously, there is a correlation between radio emission by central dominant galaxies in clusters and the presence of these cooling flows (Burns, White, and Haynes, 1981; Valentijn and Bijleveld, 1983; Jones and Forman, 1984). The further accretion of this cooling gas onto a central massive object in the galaxy might produce the radio emission.

It is likely that the most important connection between the x-ray-emitting gas in clusters and the relativistic electrons that produce the radio emission is dynamical. The hot gas provides pressure forces that can control the dynamics of the plasma of relativistic electrons. The current evidence suggests that radio emission from galaxies occurs when streams or blobs of relativistic non-thermal plasma are ejected from the nucleus of the galaxy (Miley, 1980). If the pressure and density of any surrounding medium is sufficiently large, the bulk motion and expansion of the radio-emitting plasma will be retarded. This could explain the absence of very large radio galaxy sources associated with clusters. Moreover, the intracluster gas may confine the radio-emitting plasma and prevent its adiabatic expansion. Expansion and synchrotron emission provide two competing energy-loss mechanisms for the relativistic plasma. If expansion occurs, it weakens the radio emission but generally will not affect its spectrum. If the expansion is retarded by the pressure of a confining medium, synchrotron losses become important. These losses are most important for the highest-energy electrons, and thus they cause the spectrum of the radio source to steepen. This mechanism probably provides the most plausible explanation of the steep spectrum of cluster radio sources.

Additional evidence for the dynamical effect of the hot intracluster gas on radio galaxies comes from distortions in the structure of the radio source produced if the radio

galaxy is moving relative to the intracluster medium, as discussed below.

C. Head-tail and other distorted radio structures

There are two general types of radio source structures that occur predominantly in clusters of galaxies. In this section, distortions in the structures of single radio galaxies are discussed. In Sec. IV.D cluster-sized radio halo sources are reviewed.

A large proportion of relatively isolated radio galaxies have a fairly simple and symmetrical radio structure; for a review of the properties of radio galaxies see Miley (1980). Many of these galaxies have a compact radio source associated with the nucleus of the galaxy. There is also extended radio emission, generally in the form of double radio "lobes," which lie on either side of the galaxy. These lobes are often of comparable brightness and projected distance from the nucleus, and most importantly, lie on a line through the nucleus of the galaxy. Recently observations have detected jets of radio emission originating at the nucleus and extending out to the radio lobes; in some cases only one jet on one side of the galaxy has been found. The conventional theoretical scenario for the origin and energetics of these radio galaxies contains the following elements (Miley, 1980). First, the ultimate energy source for the radio emission (and all other non-thermal galaxy emission) is thought to be a very compact object in the nucleus of the galaxy. Energy is carried from this nonthermal engine out to the radio lobes by twin "beams" of plasma; this plasma probably contains a mixture of thermal gas and relativistic nonthermal particles, which cause the beams to be observable in some cases as radio jets. The beams may be more or less continuous, or may consist of blobs of plasma ("plasmoids"). The beams probably move outwards until they encounter a sufficient quantity of intergalactic (or intragalactic) gas, at which point their bulk kinetic energy of motion is converted into thermal energy and into the disordered relativistic motion of particles of nonthermal plasma. This non-thermal plasma produces the emission from the radio lobes.

Radio galaxies in clusters show more complex radio structures, which generally tend to lack the symmetrical, aligned double structure of standard radio galaxies. These range from double-lobed radio sources in which the lobes are not aligned with the galaxy nucleus ("bent-doubles" or "wide-angle tails") to sources in which all the radio emission lies in a tail on one side of the galaxy, and the galaxy itself forms the head of the tail ("head-tail" radio galaxies).

The first head-tail (HT) radio galaxies discovered were NGC1265 and IC310 in the Perseus cluster (Ryle and Windram, 1968; see Fig. 29), followed by the discovery of head-tail radio galaxies in Coma (Willson, 1970) and the 3C129 cluster (MacDonald *et al.*, 1968). Figure 30 shows a radio map of NGC1265, which is the archetypical

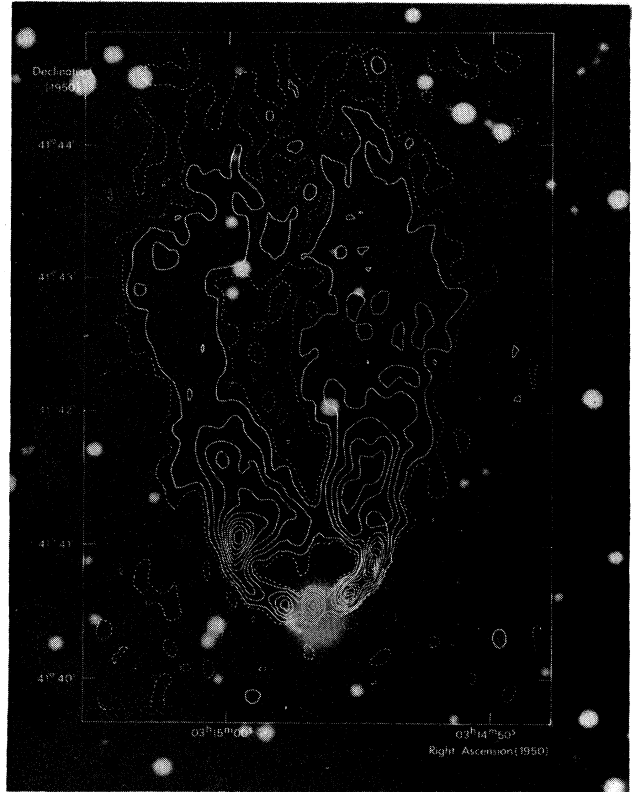


FIG. 30. A low-resolution radio map at a frequency of 5 GHz of the head-tail radio source associated with the galaxy NGC1265 in the Perseus cluster, from Wellington *et al.* (1973). Contours of constant radio surface brightness are shown superimposed on the optical image of the galaxy.

head-tail radio galaxy. Some lists of head-tail radio galaxies and other distorted radio sources are those of Rudnick and Owen (1976a, 1976b), Simon (1978, 1979), and Valentijn (1979a), and other observations of head-tail radio galaxies in rich clusters are given in Hill and Longair (1971), Vallee and Wilson (1976), Miley and Harris (1977), Gisler and Miley (1979), Burns and Ulmer (1980), Hintzen and Scott (1980), Bridle and Vallee (1981), Gavazzi *et al.* (1981), Vallee *et al.* (1981), and Dickey and Salpeter (1984).

NGC1265 and IC310, the first two head-tail radio galaxies discovered, are both in the Perseus cluster and have tails that lie on the line from the galaxy to the powerful radio galaxy NGC1275 at the cluster center (Fig. 29). Ryle and Windram (1968) suggested that the radio emission from these galaxies was activated by a wind of relativistic particles from NGC1275, which also determined the directions of the tails. However, subsequent head-tail radio galaxies have not been found to show any alignment with the direction to powerful radio galaxies or the cluster center. The accepted explanation of head-tail radio galaxies, originally due to Miley *et al.* (1972), is that they are conventional radio galaxies moving at a high velocity through a static intracluster gas. The

radio-emitting beams or plasmoids are decelerated by the ram pressure of the intracluster gas and form a wake behind the galaxy. The high velocity of the galaxy is a result of the gravitational potential of the cluster (that is, the velocity v is comparable to the cluster velocity dispersion). The ram pressure acting on the radio blobs or beams is then

$$P_r = \rho_g v^2, \quad (4.2)$$

where ρ_g is the intracluster gas density (Sec. V.I).

Miley (1973) found that the spectral index α_r and the fractional polarization of the radio emission increased with distance away from the galaxy along the tail. Synchrotron emission energy losses will steepen a radio spectrum, so the spectral variations are consistent with injection of particles at the galaxy. The polarization indicates that the magnetic field is highly ordered and directed along the direction of the tail, probably by the sweeping of the radio-emitting plasma behind the galaxy. There are some indications that head-tail radio galaxies are more rapidly moving than typical cluster galaxies (Guindon and Bridle, 1978), but the effect is not very large (Ulrich, 1978), and in any case, only one component of the velocity can be measured. Head-tail radio galaxies are never cD galaxies and are seldom among the most luminous galaxies in a cluster, either at radio or at optical wavelengths (Rudnick and Owen, 1976a, 1976b; Simon, 1978; McHardy, 1979; Valentijn, 1979c). Since cD galaxies are nearly at rest in the cluster potential (Sec. II.J.1), they would not be expected to form head-tail radio galaxies.

Of course, the intracluster gas that produces the head-tail radio galaxies also produces x-ray emission; in general, the densities of intracluster gas ρ_g derived from x-ray observations are consistent with those needed to give a ram pressure sufficient to produce the observed radio structures (see, for example, Simon, 1979).

The first detailed theoretical work on head-tail radio galaxies was done by Jaffe and Perola (1973). They suggested two models; in the first, blobs of plasma were ejected in opposite directions (taken to be perpendicular to the direction of motion of the galaxy). They gave several arguments against this model. First, the adiabatic expansion of the blobs would produce large losses in their energy; if these losses exceeded losses due to synchrotron emission, the spectrum would not vary as observed. Second, they argued that the magnetic field was too well ordered to be an initially disordered field. Thus they proposed a second model, in which the radio galaxy possessed an extensive magnetosphere, which was swept behind the galaxy. The magnetosphere provided an ordered magnetic field, and they argued that it could confine the adiabatic expansion of the radio-emitting blobs. This second argument was shown to be incorrect by Cowie and McKee (1975) and Pacholczyk and Scott (1976). Cowie and McKee showed that the large adiabatic losses found by Jaffe and Perola were due in part to the assumption of high-Mach-number flow, which is not correct for the temperatures of the intracluster gas derived from x-ray observations (Sec. III.C). As a result,

subsequent theoretical work has largely been devoted to models for the interaction of free plasmoids (the first Jaffe-Perola model) or twin beams with intracluster gas (Cowie and McKee, 1975; Pacholczyk and Scott, 1976; Begelman *et al.*, 1979; Christiansen *et al.*, 1981).

One important problem with this model is that in many sources the age of the tail (projected length divided by the estimated galaxy velocity) is much longer than the lifetimes of the emitting electrons against synchrotron losses (Wilson and Vallee, 1977). Pacholczyk and Scott (1976) and Christiansen *et al.* (1981) have argued that these particles are reaccelerated by turbulence in the tails.

Recent high-resolution radio observations have detected well-defined radio jets leading out from the nucleus of the head-tail radio galaxy to the start of the tails (Owen *et al.*, 1978, 1979; Burns and Owen, 1980). Figure 31 shows these jets in NGC1265. Begelman *et al.* (1979) presented a twin-jet theory for the formation of HT's. Because the observed jets are narrow and follow well-defined curved paths, it is unlikely that they consist of independent plasmoids, because these plasmoids would most likely have different masses and surface areas and would be bent by different amounts by the ram pressure force. The transition from a collimated jet into the swept-back tail is fairly abrupt. Jones and Owen (1979) argued that the jets in the inner parts of the galaxies are protected from the ram pressure of the intracluster gas. They suggested that the head-tail radio galaxies contain regions of gas that are bound to the galaxy and too dense to be stripped by ram pressure (Sec. V.I). The jets propagate through and are confined by this gas until they reach the intracluster gas and are swept back. However, the jets are curved in this inner region (Fig. 31), which is difficult to understand if they propagate through static intragalactic gas (although the curvature could be due to buoyancy force if the intragalactic gas is compressed by ram pressure from the intracluster gas). In any case, Begelman *et al.* (1979) are able

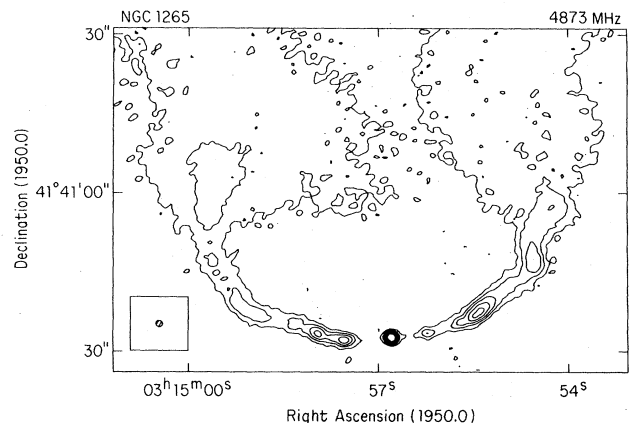


FIG. 31. A high-resolution Very Large Array radio map at a frequency of 4.9 GHz of the head-tail radio galaxy NGC1265, from O'Dea and Owen (1985). Note the twin radio jets leading from the nucleus of the galaxy out to the radio tails.

to fit the observed shape of the jets assuming ram pressure from intracluster gas and no intragalactic gas.

In some cases the tails in head-tail radio galaxies are observed to be curved or bent. Jaffe and Perola (1973), Miley and Harris (1977), and Vallee *et al.* (1979,1981) suggested that the curvature reflects nonlinear galaxy motion, due to the orbit of the head-tail radio galaxies in the cluster potential, or due to a binary orbit. Jaffe and Perola (1973) also suggested that there might be an intracluster gas wind with shear. Cowie and McKee (1975) suggested that the bending might be due to buoyancy forces; the bendings in a number of head-tail radio galaxies are consistent with this (Gisler and Miley, 1979).

Another common morphological type of cluster radio source is the "wide-angle tail" or WAT. These resemble classical double radio sources in which the two radio lobes and/or jets are not oppositely aligned, but lie at an angle. Figure 32 shows the radio image of the WAT 1919 + 479, which is in a Zwicky cluster. Some lists of these sources include those of Owen and Rudnick (1976b), Simon (1978), Guindon and Bridle (1978), Valentijn and Perola (1978), Valentijn (1979b,1979c), and van Breugel (1980). WAT's are generally associated with optically dominant cluster galaxies, often cD galaxies (Owen and Rudnick, 1976b; Simon, 1978; Valentijn, 1979c), and tend to be more luminous radio sources than head-tail radio galaxies. They tend to be slower moving galaxies than those containing head-tail radio galaxies (Guindon and Bridle, 1978).

A major theoretical question about WAT's is whether



FIG. 32. A Very Large Array radio image at a frequency of 1420 MHz of the wide-angle-tail (WAT) radio galaxy 1919 + 479 associated with a cD galaxy in a Zwicky cluster, from Burns *et al.* (1985).

they are the result of the same physical process (ram pressure by intracluster gas) as head-tail radio galaxies. Owen and Rudnick (1976b) suggested that ram pressure was the mechanism behind WAT's; since the WAT's occur in slow moving (cD) galaxies, the ram pressure is less, and the radio structure is bent at a smaller angle. Another possible reason that WAT's might be less bent is that they are associated with stronger radio sources. The plasmoids or beams associated with these sources may have more momentum than those in weaker radio sources, and may be harder to deflect. Valentijn and Perola (1978) and Valentijn (1979b) suggested that WAT's were similar to HT's, except that the ejection angle of the beams or plasmoids was not nearly perpendicular to the velocity of the galaxy. This would not, by itself, explain why WAT's occur in galaxies that are more prominent optically and in radio emission. Valentijn (1979b) also invokes the smaller galaxy velocity and more rigid beams discussed above, and suggests that these brighter galaxies may have more intragalactic gas, which shields the beams from the intracluster gas.

Burns (1981) and Burns *et al.* (1982) suggest that the WAT's are bent mainly by buoyancy forces and *not* ram pressure forces. Of course, if the galaxy associated with the WAT were a cD galaxy located at the center of the cluster potential and if the intracluster gas density were spherically symmetric about this center, no bending due to buoyancy could occur. Burns *et al.* (1982) argue that the cD associated with a WAT may not be exactly at the cluster center, and that accretion by the slowly moving cD may produce an aspherical density distribution in the intracluster gas.

Sparke (1983) argues that WAT's and other distorted radio sources associated with cD's are indications that the clusters are in the process of collapsing. She notes that many of the WAT's are associated with irregular clusters with clumpy x-ray emission and low x-ray temperatures (the irregular x-ray clusters of Table IV).

The association between these distorted radio morphologies and clusters of galaxies containing intracluster gas has been used to detect previously unobserved clusters and cluster x-ray sources. Burns and Owen (1979) found a number of distorted radio sources associated with poor Zwicky clusters, and suggested they might be x-ray sources. This conjecture was confirmed by Holman and McKee (1981). Fomalont and Bridle (1978) discovered a number of WAT's in groups of galaxies.

Hintzen and Scott (1978) suggested that quasars with distorted radio structure were likely to be members of clusters of galaxies, and that radio observations of quasars could be used to detect high-redshift clusters of galaxies and cluster x-ray sources. In general, optical studies have not found that quasars are associated with rich clusters, and any method that selected quasars in clusters or any type of high-redshift clusters would be very useful. This method has in fact been used to detect clusters around several quasars (Hintzen *et al.*, 1981; Harris *et al.*, 1983) and to provide a list of other candidates (Hintzen *et al.*, 1983).

D. Cluster radio halos

The second type of radio morphology distinctly associated with clusters of galaxies is the cluster radio halo. They are diffuse, extended radio sources whose sizes are generally considerably larger than the cluster galaxy core radius, and smaller than the overall cluster size (say an Abell radius). The best studied example is Coma C, the halo source in the Coma cluster, which was first shown to be diffuse by Willson (1970), and which was studied further by Jaffe *et al.* (1976), Jaffe (1977), Valentijn (1978), Hanisch *et al.* (1979), Hanisch (1980), and Hanisch and Erickson (1980). Other clusters in which halo sources have probably been detected include A401 (Harris *et al.*, 1980; Roland *et al.*, 1981; but see Hanisch and Erickson, 1980), A1367 (Gavazzi, 1978; Hanisch, 1980; but this halo is considerably weaker and smaller than the others), A2255 (Harris *et al.*, 1980), A2256 (Bridle and Fomalont, 1976; Bridle *et al.*, 1979; but this is a very messy radio cluster), and A2319 (Grindlay *et al.*, 1977; Harris and Miley, 1978; Andernach *et al.*, 1980). While Ryle and Windram (1968) reported a rather large radio halo in the Perseus cluster, it does not appear to be a real source (Gisler and Miley, 1979; Jaffe and Rudnick, 1979; Birkinshaw, 1980; Hanisch and Erickson, 1980), although a smaller halo source has been reported recently (Noordam and de Bruyn, 1982).

Radio halos do not appear to be very common, as a large number of surveys of clusters have failed to find them (Jaffe and Rudnick, 1979; Cane *et al.*, 1981; Andernach *et al.*, 1981; Hanisch, 1982a).

The cluster radio halos have very steep power-law radio spectra, with $\alpha_r \approx 1.2$. The power-law spectrum and some indications of polarization suggest that the emission process is synchrotron emission by nonthermal relativistic electrons, as in radio galaxies. The halo in Coma has a diameter [full width at half maximum (FWHM)] of $\sim 1 \text{ Mpc}/h_{50}$, which is typical. In Coma, the spectrum of the halo is relatively uniform spatially (Jaffe, 1977). Although the sample of known radio halos is small, they appear to be associated with clusters of intermediate optical morphology (BM II; RS B, C, L) (Hanisch, 1982b). These clusters are relaxed, but do not have a dominant cD galaxy (an exception may be A2319). The halos are generally associated with clusters having a regular nXD x-ray morphology (Vestrand, 1982); Vestrand notes that many of these clusters have particularly luminous and extended x-ray emission and may have unusually high x-ray temperatures (see also Forman and Jones, 1982). In making these comparisons, the unusually weak and small halo associated with A1367 has not been included.

There is currently no consensus as to the origin of these halos. Jaffe (1977) discussed observational and theoretical constraints on the origin of the nonthermal electrons producing the emission in the Coma cluster, and proposed that the electrons originate at strong radio sources in the cluster and diffuse out to form the halo. The observed spectral index α_r is about 0.5 larger than the spectral in-

dexes of strong cluster radio sources; such an increase occurs if there is a steady state between the input of relativistic nonthermal electrons and synchrotron losses. Moreover, the number of electrons produced in strong radio sources is sufficient to explain the halo radio emission if the magnetic field in the cluster is $B_c \sim 1 \mu\text{G}$, which is consistent with limits on the hard x-ray emission from clusters (Sec. III.C.1). However, the halo radio emission is less strongly peaked at the cluster center than the distribution of galaxies, particularly of strong radio galaxies (Jaffe, 1977). Thus the nonthermal electrons must be transported out from the cluster core. In order that synchrotron losses not affect the spectrum of the electrons and cause the halo radio spectrum to steepen dramatically with radius (which is not observed; Jaffe, 1977), the particles must be transported at a velocity $\gtrsim 2000 \text{ km/sec}$. Convective fluid motions of this order would be supersonic and would involve a very high rate of energy dissipation. Thus Jaffe argued that the relativistic electrons must diffuse out into the cluster.

As discussed extensively by Jaffe, a diffusion velocity $\gtrsim 2000 \text{ km/sec}$ would greatly exceed the Alfvén velocity

$$v_A \equiv \left[\frac{B_c^2}{4\pi\rho_g} \right]^{1/2} \quad (4.3)$$

in the intracluster plasma. (Here, ρ_g is the density of intracluster gas.) For typical values of the gas density from x-ray observations and the required magnetic field discussed above, $v_A \lesssim 100 \text{ km/sec}$. Particles that diffuse through a plasma faster than the Alfvén speed excite plasma waves, which rapidly slow down the diffusion of the particles, and thus Jaffe argued that the Alfvén speed acts as an upper limit on the diffusion speed of the relativistic electrons in radio halos. This velocity is much too small to allow the particles to diffuse without losses. A possible solution to this Alfvén speed limit problem, suggested by Holman *et al.* (1979), is that the plasma waves generated by electrons diffusing at speeds greater than v_A may be damped by ions in the background thermal plasma. This would allow diffusion at speeds up to the speed of these background ions, essentially the sound speed in the intracluster gas.

Another solution to the Alfvén speed problem was suggested by Dennison (1980b). He noted that the flux of relativistic, nonthermal particles at the Earth (cosmic rays) is dominated by protons, and suggested that this might also be true in radio sources. The protons would diffuse away from cluster radio galaxies at the Alfvén speed, but suffer no significant synchrotron losses because of their rigidity. In the cluster they would collide with thermal protons and produce secondary electrons by a number of processes. These relativistic, nonthermal secondaries would then produce the observed radio halos in this model.

Harris and Miley (1978) suggested that the radio halos are remnants of previous head-tail radio galaxies, whose spectra have steepened due to synchrotron losses. One problem with this idea is that HT's are typically not very

luminous, and the clusters with radio halos therefore would be required to have had a large number of bright radio galaxies in the past. However, radio halos are rare, so this may not be a serious objection.

Jaffe (1977) considered the possibility that the non-thermal electrons are accelerated to relativistic energies within the cluster by turbulence in the intracluster gas. Roland *et al.* (1981) suggested that the turbulence was generated by the wakes of galaxies moving through the intracluster medium. Based on the small available sample, they suggested that the luminosity of radio halos increases with the cluster x-ray luminosity L_x (a measure of the amount of gas in the cluster) and the velocity dispersion of galaxies σ_r , with $L_{\text{halo}} \propto L_x \sigma_r^2$. There are several problems with this hypothesis; first, unless the acceleration of relativistic electrons is very efficient, the rate of dissipation of the turbulent energy is unacceptably large (Jaffe, 1977). Second, no galactic wake has been detected as a radio source. They ought to appear as tailed galaxies without heads (no radio source in the nucleus of the galaxy).

The cluster A401 has been observed to possess a radio halo. With A399, this cluster forms a possible merging double system (Ulmer and Cruddace, 1981; Sec. III.D). Harris *et al.* (1980) suggested that radio halos form during the coalescence of subclusters, possibly by the acceleration of relativistic particles in shocks which form in the intracluster gas. However, there are a reasonable number of other double clusters that do not show radio halos.

Observations of radio halos are important to the understanding of x-ray cluster emission because the nonthermal radio-emitting electrons and x-ray-emitting thermal plasma coexist and may interact. Initially, it had been suggested that the x-ray emission might be inverse Compton emission from the nonthermal electrons (Sec. V.A.1). However, the frequency of occurrence of x-ray emission and rarity of radio halos is one of the many arguments against this theory. On the other hand, the nonthermal electrons may heat the thermal plasma and contribute to the x-ray emission indirectly (Lea and Holman, 1978; Rephaeli, 1979; Scott *et al.*, 1980; see also Secs. IV.B and V.C.5). Vestrand (1982) has pointed out that radio halo clusters have extended x-ray emission and may have higher x-ray temperatures than nonhalo clusters; he attributes this difference to the heating of intracluster gas by nonthermal electrons.

E. Cosmic microwave diminution (Sunyaev-Zel'dovich effect)

X-ray observations indicate that clusters of galaxies contain significant amounts of diffuse, hot gas. In this section and the next, the effect of this gas on sources of radio emission lying behind the cluster will be discussed. The free electrons in this intracluster plasma will have an optical depth for scattering low-frequency photons given by

$$\tau_T = \int \sigma_T n_e dl, \quad (4.4)$$

where

$$\sigma_T = \frac{8\pi}{3} \left[\frac{e^2}{m_e c^2} \right]^2$$

is the Thompson electron scattering cross section, n_e is the electron density, and l is the path length along any line of sight through the gas. For a typical x-ray cluster, $n_e \sim 10^{-3} \text{ cm}^{-3}$ and $l \sim 1 \text{ Mpc}$, and thus $\tau_T \sim 10^{-(2-3)}$. Thus a fraction τ_T of the photons from any radio source behind a cluster will be scattered as the radiation passes through the cluster.

One "source" of radio emission which lies "behind" everything is the cosmic radiation that is a relic of the big bang formation of the universe (Sunyaev and Zel'dovich, 1980a). This radiation has a spectrum that is nearly a blackbody, with a temperature of $T_r \approx 2.7 \text{ K}$. Because this radiation is nearly isotropic, simply scattering the radiation would not have an observable effect. However, because the electrons in the intracluster gas are hotter than the cosmic radiation photons, they heat the cosmic radiation photons and change the spectrum of the cosmic radiation observed in the direction of a cluster of galaxies. This effect was first suggested by Zel'dovich and Sunyaev (1969; Sunyaev and Zel'dovich, 1972). Reviews of the theory and current observational status of this Sunyaev-Zel'dovich effect have been given recently by Sunyaev and Zel'dovich (1980a, 1981).

During an average scattering, a photon with frequency ν has its frequency changed by an amount $\Delta\nu/\nu = 4kT_g/m_e c^2$, where T_g is the electron temperature of the intracluster gas. In calculating the effect this has on the radiation spectrum, it is conventional to measure the intensity in terms of a "brightness temperature" T_r ; this is defined as the temperature of a blackbody having the same intensity. Then, the change in the brightness temperature of the cosmic radiation due to passage through the intracluster gas is given by

$$\frac{\Delta T_r}{T_r} = \frac{\Delta I_\nu}{I_\nu} \frac{d \ln T_r}{d \ln I_\nu} = \tau_T \frac{kT_g}{m_e c^2} [x \coth(x/2) - 4], \quad (4.5)$$

where I_ν is the radiation intensity and $x \equiv h\nu/kT_r$. This expression is actually derived in the diffusion limit and is valid only for sufficiently small $x \lesssim 10$ (Sunyaev, 1981). The change in brightness temperature or intensity is negative for low frequencies $x < 3.83$ and positive for higher frequencies. This change occurs at a wavelength $\lambda_0 = 0.14 \text{ cm}$ ($2.7 \text{ K}/T_r$). It is somewhat paradoxical that heating the background radiation lowers its brightness temperature at low frequencies. This is because Compton scattering conserves the number of photons, and shifting lower-frequency photons to higher energies lowers the intensity at low frequencies.

Nearly all of the measurements that have been made of

this effect have been at relatively low frequencies; taking the limit $x \rightarrow 0$ in Eq. (4.5) gives

$$\frac{\Delta T_r}{T_r} = - \int \frac{2kT_g}{m_e c^2} d\tau_T. \quad (4.6)$$

This reduction in the cosmic radiation in the direction of clusters of galaxies in the microwave region is often referred to as the "microwave diminution." Calculations of ΔT_r and its variation with projected position for a large set of models for the intracluster gas have been given by Sarazin and Bahcall (1977), and specific predictions of the size of the effect for the Coma, Perseus, and Virgo/M87 clusters are given in Bahcall and Sarazin (1977). Models for the Coma cluster have been given by Gould and Rephaeli (1978; but note that their basic model for the intracluster gas is not physically consistent) and Stimpel and Binney (1979; these models included the effect of cluster ellipticity).

Unfortunately, it has proved to be very difficult to make reliable measurements of this very small microwave diminution effect. Pariiskii (1973) claimed to have detected a microwave diminution from the Coma cluster. Gull and Northover (1976) claimed to have detected both Coma and A2218, and found very small diminutions towards four other clusters. The claimed detections of Coma were at a level much too high to be consistent with models for the x-ray emission from this well-studied cluster (Bahcall and Sarazin, 1977; Gould and Rephaeli, 1978), and subsequent observations have not confirmed the microwave diminution in Coma. Rudnick (1978) gave upper limits for five clusters, including Coma; his limits were consistent with models for the x-ray emission, but inconsistent with the previously claimed detections of Coma. Lake and Partridge (1977) claimed three detections of very rich clusters, but later withdrew the claim, saying that the measurements were undermined by systematic problems with the telescope. In a later survey of 16 clusters (Lake and Partridge, 1980), they detected only A576 at a level of $\Delta T_r = -1.3 \pm 0.3$ mK. (Note that $1 \text{ mK} \equiv 10^{-3} \text{ K}$.) Birkinshaw *et al.* (1978; Birkinshaw, Gull, and Northover, 1981) surveyed 10 clusters, detecting microwave diminutions in A576 ($\Delta T_r = -1.12 \pm 0.17$ mK), A2218 ($\Delta T_r = -1.05 \pm 0.21$ mK), and possibly A665 and A2319. A2218 was *not* detected by Lake and Partridge (1978); in fact, their measurements have the opposite *sign*. Perrenod and Lada (1979) made measurement at higher frequencies ($\lambda = 9 \text{ mm} \gg \lambda_0$) in order to reduce the effects of contamination by radio galaxies and beam smearing. They detected A2218 at the same level as Birkinshaw *et al.*, and also had a marginal detection of A665 at $\Delta T_r = -1.3 \pm 0.6$ mK (A665 is the richest cluster in the Abell catalog). Lasenby and Davies (1983) did not detect either A576 or A2218.

The apparent microwave diminutions from A576 and A2218 require very large masses of gas (comparable to the virial masses) at very high temperatures $T_g \gtrsim 3 \times 10^8 \text{ K}$. X-ray observations of A576 are completely inconsistent with this much gas at these temperatures (Pravdo *et al.*, 1979; White and Silk, 1980), and thus the measured mi-

crowave reductions must be due to some other effect. While earlier low-spatial-resolution studies of A2218 suggested that it was too weak an x-ray source to produce the claimed microwave diminution (Ulmer *et al.*, 1981), a detailed high-spatial-resolution study of the x-ray emission from A2218 with the *Einstein* observatory (Boydton *et al.*, 1982) indicates that the required amounts of gas are present in this cluster at the required temperatures $T_g = 10\text{--}30 \text{ keV}$.

From Eq. (4.6), the microwave diminution effect is independent of distance as long as the cluster can be resolved. In fact, Birkinshaw, Gull, and Moffet (1981) have measured a diminution of $\Delta T_r = -1.4 \pm 0.3$ mK from the distant ($z = 0.541$) cluster 0016 + 16. Optically, this is a very rich cluster (Koo, 1981), and it is also extremely luminous in x rays (White, Silk, and Henry, 1981). In some ways, microwave diminution observations of distant clusters are more straightforward than observations of nearby clusters, because the reference positions are further outside the cluster core.

As this review was being completed, a new set of observations of the microwave diminution were published by Birkinshaw *et al.* (1984; see also Birkinshaw and Gull, 1984). These observations used the Owens Valley Radio Observatory and are apparently less subject to systematic effects than earlier observations. They confirm the detections of 0016 + 16 ($\Delta T_r = -1.40 \pm 0.17$ mK), A665 ($\Delta T_r = -0.69 \pm 0.10$ mK), and A2218 ($\Delta T_r = -0.70 \pm 0.10$ mK). Several of these detections have also been confirmed by Uson and Wilkinson (1985). Since there are now several confirming observations of the microwave diminution in these three clusters, it may be that the effect has finally been observed unambiguously. However, in view of the disagreements between different observers in the past, the withdrawal of previously claimed detections, and the inconsistency of some of the radio results with x-ray measurements of the amount of gas present, I do not feel completely confident that the current microwave diminution results are conclusive. It is clear that the major sources of errors in the measurements are not statistical but systematic. These include very low-level systematic problems with the response of the radio telescopes used (Lake and Partridge, 1980).

One major source of problems is the possible presence of radio sources in the cluster. If these are concentrated at the cluster core, they will increase the radio brightness of the cluster and mask the microwave diminution. All of the observations are corrected for the presence of strong radio sources, and the observers generally avoid observing clusters, such as Perseus, which contain very strong radio sources. There is still the danger that a larger number of harder to detect, weaker radio sources will make a significant contribution to the cluster radio brightness. Birkinshaw (1978) surveyed six clusters, including A576 and A2218, for weak radio source emission, and concluded that it was unlikely to affect the microwave diminution measurements. Schallwisch and Wielebinski (1978) detected a weak radio source in the direction of A2218, and corrected the microwave diminu-

tion measurement of Birkinshaw *et al.* (1978) for this cluster. Unfortunately, this correction would destroy the agreement of this measurement with the shorter-wavelength measurement of Perrenod and Lada (1979), because the radio source and microwave diminution have different spectral variations. Tarter (1978) has suggested that if clusters contained a small amount of ionized gas at a cooler temperature than the x-ray-emitting gas, the free-free radio emission from this gas could mask the microwave diminution. All of these radio source problems would generally mask the microwave diminution and might explain why some clusters that are predicted to have very strong diminutions, such as A2319, are in fact observed to have *positive* ΔT_r .

What about A576, in which a strong microwave diminution was initially observed, although very little gas is observed in x rays? The microwave diminution measurements are generally relative measurements, in which one compares the cosmic microwave brightness in the direction of the cluster core with the brightness at one or more positions away from the cluster core. A negative ΔT_r at the cluster core cannot be distinguished from a positive ΔT_r in these reference positions, which are generally not far outside the cluster core. Thus the observation of a negative ΔT_r in A576 may indicate that there is excess radio emission in the outer parts of the cluster. Cavallo and Mandolesi (1982) have suggested that this radio emission is produced by the stripping of gas from spiral galaxies in the outer parts of the cluster.

The microwave and x-ray observations of a cluster can be used to derive a distance to the cluster which is independent of the redshift (Cavaliere *et al.*, 1977, 1979; Gunn, 1978; Silk and White, 1978). From Eq. (4.6), ΔT_r depends on the electron density n_e , the gas temperature T_g , and the size of the emitting region. The x-ray flux f_x from the cluster depends on all of these, but also decreases with the inverse square of the distance to the cluster. Thus the distance can be determined by comparing the x-ray flux and the microwave diminution:

$$D_A \propto \left[\frac{\Delta T_r}{T_r} \right]^2 f_x^{-1} [T_g(0)]^{-3/2} \theta_c (1+z)^{-4}, \quad (4.7)$$

where D_A is the angular diameter distance (Weinberg, 1972), z is the redshift, θ_c is the angular radius of the cluster core (Sec. II.G), $T_g(0)$ is the gas temperature at the cluster center, and the coefficient of proportionality depends on the distribution of gas in the cluster and the x-ray detector response (Cavaliere *et al.*, 1979). In fact, any assumptions about the gas distribution can be avoided by mapping the variation of both the x-ray surface brightness I_x and the microwave diminution as a function of the angle away from the cluster center θ . Silk and White (1978) find

$$D_A = \frac{F[T_g(0)]}{\pi(1+z)^4} \frac{\left[\int_0^\infty [\Delta T_r(0) - \Delta T_r(\theta)] \frac{d\theta}{\theta^2} \right]^2}{\int_0^\infty [I_x(0) - I_x(\theta)] \frac{d\theta}{\theta^2}}, \quad (4.8)$$

where F is a known function of gas temperature, which for a hot solar abundance plasma contains only atomic constants. This determination of the distance to the cluster is independent of the distribution of the gas as long as it is spherically symmetric. Applying this method to nearby clusters and comparing the distances with the redshift would allow the determination of Hubble's constant H_0 (Sec. II.B, footnote 4). Mapping high-redshift clusters ($z \sim 1$) would give the cosmological deceleration parameter q_0 ; together, these two parameters determine the structure, dynamics, and age of the universe (Weinberg, 1972), yet remain very poorly determined after a half-century of observational cosmology research.

Unfortunately, the difficulty of obtaining reliable microwave diminution measurements has made it impossible to apply this method at the present time (Birkinshaw, 1979; Boynton *et al.*, 1982). In general, cluster microwave diminutions have not been mapped with sufficient accuracy to allow the distance to be determined from Eq. (4.8). Even the optical data on clusters are not accurate enough to allow an accurate distance determination. In addition, the cause of false detections, such as A576, must be determined so that they can be weeded out of cluster samples. For example, if the detection of A576 were taken seriously, it would imply a distance to this cluster at least an order of magnitude more than its redshift distance (White and Silk, 1980).

Gould and Rephaeli (1978) suggested that it might be easier to detect the Sunyaev-Zel'dovich effect unambiguously at high frequencies ($\lambda < \lambda_0$) at which ΔT_r is positive. Some observations have been attempted at $\lambda = 1-3$ mm (Meyer *et al.*, 1983), but no cluster diminutions were detected, and this wavelength range straddles λ_0 . Observations at shorter wavelengths must be made from satellites.

Sunyaev and Zel'dovich (1981) point out that although their effect is often thought of as a small change in the cosmic microwave background, at $\lambda < \lambda_0$ the effect may also be considered as an enormous source of submillimeter luminosity for the cluster. Because the surface brightness of the submillimeter emission is proportional to $\tau_T \propto n_e l$, where $l \sim r$ is the path length through the cluster and r is the radius of the gas, and the surface area is proportional to r^2 , the luminosity is proportional to $n_e r^3$ or the mass of the gas M_g in the cluster. The submillimeter luminosity at frequencies above the critical frequency ($\lambda < \lambda_0$) is given by

$$L^+ = 8.7 \times 10^{43} \left[\frac{T_g}{10^8 \text{ K}} \right] \left[\frac{T_r}{2.7 \text{ K}} \right]^4 \left[\frac{M_g}{10^{14} M_\odot} \right] \\ \times (1+z)^4 \text{ ergs sec}^{-1}, \quad (4.9)$$

where the factor $[T_r(1+z)]^4$ gives the cosmic radiation density at the redshift of the cluster. Thus clusters could be among the strongest sources of submillimeter radiation in the universe. Other strong submillimeter sources, such

as quasars, would have different spectra, be more compact, and probably be variable.

The variation in the cosmic microwave intensity and polarization toward a cluster can also be used to determine the velocity of the cluster relative to the average of all material in that region of the universe (Sunyaev and Zel'dovich, 1980b). This velocity, measured relative to the local comoving cosmological reference frame, is as near as one can come to an absolute measure of motion in a relativistically invariant universe. In a sense, the cosmic background radiation acts as an "ether." Just as the thermal motion of electrons in a cluster changes the wavelength of the cosmic background radiation during scattering, their bulk motion has a similar effect. As long as $\tau_T \ll 1$, the variation in the brightness temperature due to cluster motion is independent of frequency and is given by

$$\frac{\Delta T_r}{T_r} = -\frac{v_r}{c} \tau_T, \quad (4.10)$$

where v_r is the radial component of the velocity. The tangential component of velocity (the component in the plane of the sky) can be detected if the polarization of the microwave background in the direction of clusters can be measured to very high accuracy. At low frequencies ($x \ll 1$), the polarization (which is in the direction of motion) is

$$p = \frac{1}{10} \beta_t^2 \tau_T + \frac{1}{40} \beta_t \tau_T^2 \quad (4.11)$$

to lowest order in τ_T , and $\beta_t \equiv v_t/c$, where v_t is the tangential velocity.

The Sunyaev-Zel'dovich effect can also be used to determine the spectrum and angular distribution of the cosmic background radiation itself (Sunyaev and Zel'dovich, 1972; Fabbri *et al.*, 1978; Rephaeli, 1980, 1981; Sunyaev, 1981; Zel'dovich and Sunyaev, 1981). In principle, the different causes of variations in ΔT_r towards clusters (thermal motions of electrons, bulk motions, and variations in the cosmic background radiation itself) can be separated because they have different spectral variations (Sunyaev and Zel'dovich, 1981).

To summarize, the Sunyaev-Zel'dovich effect has a tremendous potential for providing information about the properties of hot gas in clusters and the nature of the universe as a whole. Unambiguous detections of this effect in clusters have proved elusive, but this situation may be improving.

F. Faraday rotation

A plasma containing a magnetic field is birefringent; the speed of propagation of an electromagnetic wave depends on its circular polarization (Spitzer, 1978). While natural sources of circularly polarized radiation are rare, synchrotron emission in an ordered magnetic field produces linearly polarized radiation, and many radio galaxies and quasars produce radio emission that is somewhat linearly polarized. The plane of polarization of linearly

polarized radiation is rotated during passage through a birefringent medium. For a magnetized plasma, the angle of rotation ϕ is

$$\phi = R_m \lambda_m^2, \quad (4.12)$$

where it is conventional to give the wavelength λ_m of the radiation in meters. The rotation measure R_m is given by

$$\begin{aligned} R_m &= \frac{e^3}{2\pi m_e^2 c^4} \int n_e B_{\parallel} dl \\ &= 8.12 \times 10^5 \int n_e B_{\parallel} dl_{\text{pc}} \text{ cm}^3 \text{ m}^{-2} \text{ G}^{-1} \text{ pc}^{-1}, \end{aligned} \quad (4.13)$$

where l is the path length through the medium, B_{\parallel} is the component of the magnetic field parallel to the direction of propagation of the radiation, and n_e is the electron density. In the lower right of Eq. (4.13), l is given in pc, n_e in cm^{-3} , and B_{\parallel} in gauss (G). The wavelength dependence of the rotation is the feature that allows the observational separation of the initial polarization angle and the amount of rotation.

The rotation measures to radio sources lying within or behind clusters can be used to constrain the magnitude of the intracluster magnetic field and its geometry (Dennison, 1980a; Jaffe, 1980; Lawler and Dennison, 1982). One problem with these determinations is that the rotation measure due to other plasma along the line of sight to the radio source must be removed. If this can be done, and the electron density and path length through the gas are determined from x-ray observations of the cluster, the average value of B_{\parallel} can be determined. Since this average of a single component of B must be less than the average magnitude of B , this gives a lower limit to the intracluster magnetic field. The Faraday rotation of the halo radio source in M87 in the Virgo cluster has been used to give a lower limit $B \gtrsim 2 \mu\text{G}$ ($\mu\text{G} \equiv 10^{-6}$ gauss) on the magnetic field in the gaseous halo around M87 (Andernach *et al.*, 1979; Dennison, 1980a). This limit implies that very little of the x-ray emission from M87 can be nonthermal.

Jaffe (1980) noted that the rotation measures to radio sources within or behind clusters are generally small $R_m \lesssim 100 \text{ m}^{-2}$, which for a cluster with $n_e \approx 3 \times 10^{-3} \text{ cm}^{-3}$ and a path length of 500 kpc gives $B_{\parallel} \lesssim 0.1 \mu\text{G}$. On the other hand, the halo radio emission observed in some clusters (Sec. IV.D) implies that the intracluster magnetic field strengths are $B \gtrsim 1 \mu\text{G}$. Since it is unlikely that the fields are preferentially ordered perpendicular to our line-of-sight to each cluster, the difference in these two limits must be due to the cancellation of components of B_{\parallel} along the path through the cluster. Jaffe argues that this implies that the field is tangled. If this tangled field can be thought of as consisting of cells of ordered field of size l_B randomly oriented along the path length l through the cluster, then statistically $\langle B_{\parallel} \rangle \sim B (l_B/l)^{1/2}$. Noting that only a portion of the rotation measure can be associated with the intracluster gas, Jaffe argued that the coherence length l_B of the intraclus-

ter magnetic field must be $l_B \lesssim 10$ kpc. Since tangled fields in a static medium can straighten and decay rapidly, he suggests that the fields are tangled by the turbulent wakes produced behind galaxies as they move through the intracluster gas.

With a larger sample of radio sources and clusters, Lawler and Dennison (1982) claimed that the sources seen through rich clusters had slightly larger rotation measures, although the two distributions only differ at the 80% confidence level. Attributing the difference to intracluster Faraday rotation, they derived an average rotation measure of $R_m \sim 130 \text{ m}^{-2}$ through the cluster center, which implies $l_B \gtrsim 20$ kpc; this is not inconsistent with the galactic wake model.

These limits on the strength and geometry of the intracluster B field are important to models for the x-ray emission for two reasons. First, the halo radio emission from a cluster depends on the product of the number of relativistic electrons and the magnetic field, and the relativistic electrons may heat the intracluster gas (Sec. V.C.5). Second, the effectiveness of transport processes in the intracluster gas (such as thermal conduction) is determined by the geometry of the magnetic field because the gyroradius of electrons in even a very weak intracluster B field is very much less than the size of the cluster (Sec. V.D.3).

G. 21-cm line observations of clusters

The 21-cm hyperfine line in hydrogen allows one to measure the mass of neutral hydrogen in galaxies or clusters of galaxies. There are an enormous number of 21-cm observations of galaxies, which would require an entire review to discuss. The main results for clusters are negative, and I shall briefly summarize these. The H I observations of clusters and superclusters have been reviewed recently by Chincarini (1984).

The 21-cm line observations have shown that the galaxies that make up clusters are deficient in neutral hydrogen gas. First, many observations have shown that elliptical and SO galaxies in clusters have very little neutral hydrogen gas (Sec. II.J.2; Davies and Lewis, 1973; Krumm and Salpeter, 1976; Biegging and Bierman, 1977). Similarly, spiral galaxies in clusters generally have less neutral hydrogen than spirals found in the field (Huchtmeier *et al.*, 1976; Sullivan and Johnson, 1978; Helou *et al.*, 1979; Krumm and Salpeter 1979; Chamaraux *et al.*, 1980; Giovanelli *et al.*, 1981; Sullivan *et al.*, 1981), and the deficiency is stronger near the cluster center (Giovanelli *et al.*, 1982; Giovanardi *et al.*, 1983). As discussed in Sec. II.J.2, these observations have been used to argue that stripping of gas from galaxies through ram pressure ablation or some other mechanism is an important process in clusters, and that SO galaxies may be produced by this process.

Observations indicate that cD galaxies, including those accreting large amounts of intracluster gas (Secs. III.C.3 and V.G.2), contain very little neutral hydrogen (less than $10^9 M_\odot$; Burns, White, and Haynes, 1981; Valentijn and

Giovanelli, 1982). This indicates that the accreted gas is not all stored as neutral hydrogen gas.

Finally, 21-cm observations of clusters as a whole indicate that the missing mass component (Sec. II.H) is not neutral hydrogen gas (Goldstein, 1966; Haynes *et al.*, 1978; Peterson, 1978; Baan *et al.*, 1978; Shostak *et al.*, 1980).

V. THEORETICAL PROGRESS

A. Emission mechanisms

When clusters of galaxies were found to be an important class of x-ray sources, there were a number of suggestions as to the primary x-ray emission mechanism. The three most prominent ideas were that the emission resulted from thermal bremsstrahlung from a hot diffuse intracluster gas (Felten *et al.*, 1966), or that the emission resulted from inverse Compton scattering of cosmic background photons up to x-ray energies by relativistic electrons within the cluster (Brecher and Burbidge, 1972; Bridle and Feldman, 1972; Costain *et al.*, 1972; Perola and Reinhardt, 1972; Harris and Romanishin, 1974; Rephaeli, 1977a, 1977b), or that the emission was due to a population of individual stellar x-ray sources, like those found in our galaxy (Katz, 1976; Fabian *et al.*, 1976). Subsequent observations have provided a great deal of support for the thermal bremsstrahlung model, and have generally not supported the other two suggestions. These three emission mechanisms will be briefly reviewed, and a few of the arguments in favor of thermal bremsstrahlung and against the other two models will be cited.

1. Inverse Compton emission

As noted in Sec. IV.B, many x-ray clusters also have strong radio emission, and cluster radio emission is distinguished by having a large spectral index α_r . This led to the idea that the x-ray emission might be produced by the same relativistic electrons that produce the synchrotron radio emission. Very high-energy electrons, with very short lifetimes, would be required to produce the emission by synchrotron emission, but much lower-energy electrons could scatter low-energy background photons up to x-ray energies (Felten and Morrison, 1966). If the electrons are extremely relativistic, with energies $E_e = \gamma m_e c^2$ for $\gamma \gg 1$, and the initial frequency of the background photon is ν_b , then on average the frequency after the scattering will be

$$\nu_x = \frac{4\gamma^2 \nu_b}{3} \quad (5.1)$$

Because the cluster radio spectra vary as power laws, it is generally assumed that the relativistic electrons have a power-law energy distribution

$$N_e(\gamma) d\gamma = N \gamma^{-p} d\gamma, \quad \gamma_l < \gamma < \gamma_u, \quad (5.2)$$

where $N_e d\gamma$ is the number of electrons with energies between γ and $\gamma + d\gamma$. Then, the resulting inverse Compton (IC) radiation has a spectrum given by

$$\frac{dL_x}{dv_x} = 3\sigma_T ch 2^p N \frac{p^2 + 4p + 11}{(p+3)^2(p+1)(p+5)} \times \left[\int v_b^{\alpha_x} n_b(v_b) dv_b \right] v_x^{-\alpha_x}, \quad (5.3)$$

where L_x is the x-ray luminosity, n_b is the number density of background photons as a function of frequency v_b , σ_T is the Thomson cross section, and the x-ray spectral index is

$$\alpha_x = \frac{p-1}{2}. \quad (5.4)$$

A source of low-energy photons that is present everywhere and dominates the overall photon density in the universe is the 3-K cosmic background radiation. If the background is taken to be a blackbody radiation field at a temperature T_r , then

$$\frac{dL_x}{dv_x} = \frac{3\pi\sigma_T}{h^2c^2} b(p) N (kT_r)^3 \left(\frac{kT_r}{h\nu_x} \right)^{\alpha_x} \quad (5.5)$$

for frequencies in the range $\gamma_l^2 \ll (h\nu_x/kT_r) \ll \gamma_u^2$. Here

$$b(n) = \frac{2^{p+3}(p^2+4p+11)\Gamma[(p+5)/2]\zeta[(p+5)/2]}{(p+3)^2(p+1)(p+5)}, \quad (5.6)$$

and Γ and ζ are the gamma and Riemann zeta functions.

Now, the synchrotron radio luminosity L_r produced by the same electron population is given by

$$\frac{dL_r}{dv_r} = \frac{8\pi^2 e^2 v_B N}{c} a(p) \left(\frac{3v_B}{2v_r} \right)^{\alpha_r}, \quad (5.7)$$

where $v_B \equiv (eB/2\pi m_e c)$ is the gyrofrequency in the magnetic field B , and

$$a(p) = 2^{(p-7)/2} \left[\frac{3}{\pi} \right]^{1/2} \frac{\Gamma\left[\frac{3p-1}{12}\right] \Gamma\left[\frac{3p+19}{12}\right] \Gamma\left[\frac{p+5}{4}\right]}{(p+1) \Gamma\left[\frac{p+7}{4}\right]}. \quad (5.8)$$

Equation (5.8) assumes that the electron distribution is isotropic and that the frequency is in the range $\gamma_l^2 \ll (v_r/v_B) \ll \gamma_u^2$. The radio spectral index α_r is equal to the x-ray spectral index α_x .

Thus the synchrotron radio and IC x-ray emission from the same relativistic electrons will have the same spectral shape, and the luminosities in the two spectral regimes are also very simply related:

$$\frac{L_x}{L_r} = \frac{U_r}{U_B}, \quad (5.9)$$

where U_r and $U_B = (B^2/8\pi)$ are the energy densities of the background radiation and the magnetic field, respectively. Because fluxes (f_x, f_r) at single frequencies are easier to measure than integrated luminosities, it is useful to note that (in cgs units)

$$\left(\frac{f_x}{f_r} \right) \left(\frac{v_x}{v_r} \right)^{\alpha_x} = \frac{2.47 \times 10^{-19} T_r^3 b(p)}{B a(p)} \times \left[\frac{4960 T_r}{B} \right]^{\alpha_x}. \quad (5.10)$$

Since the temperature of the cosmic background radiation is known, the ratio of radio and IC x-ray fluxes determines the magnetic field strength (Harris and Romanishin, 1974). If the x-ray emission from clusters were due to inverse Compton emission, the magnetic field would typically be $B \sim 0.1 \mu\text{G}$. Fields at least ten times larger than this are expected if the relativistic electrons and the magnetic field have equal energy densities; the small magnetic fields required by the IC model would increase the energy requirements for cluster radio sources by about 2 orders of magnitude. On the other hand, if the x-rays are not due to IC emission, then this value is a lower limit to the magnetic field strength in the radio-emitting region (Sec. III.C.1).

For a magnetic field of $B \sim 1 \mu\text{G}$, radio photons at a frequency of 1 GHz are produced by electrons with $\gamma \sim 2 \times 10^4$. Similarly, IC x-ray emission at a photon energy of 1 keV is produced by electrons with $\gamma \sim 10^3$. Thus the electrons that could produce the observed x-ray emission would produce very low frequency radio emission, typically at a frequency of 20 MHz if $B \sim 1 \mu\text{G}$, and at an even lower frequency if B is lower, as required in this model. Such low-frequency radio emission generally cannot be detected from the Earth. However, one argument in favor of the IC model of cluster x-ray emission was that cluster radio sources have steep spectra (Sec. IV.A), indicating that they have many lower-energy relativistic electrons, as required to explain their x-ray emission.

There is now considerable evidence against the IC model. In this model, one would expect a very strong correlation between the low-frequency radio flux and the x-ray flux [Eq. (5.10)]. The reality of any radio-x-ray correlation is questionable (Sec. IV.B), and recent larger samples of x-ray clusters from *HEAO-1* and *Einstein* do not support such a strong correlation. In the IC model, the radio and x-ray emission would come from identical spatial regions and would therefore have identical distributions on the sky. However, while the x-ray emission is extended and diffuse (Sec. III.D), the radio emission comes primarily from individual radio galaxies. Only a very small fraction of clusters appear to have significant diffuse radio halo emission (Sec. IV.D). The IC model predicts that clusters have power-law x-ray spectra, which is not consistent with the best x-ray spectral observations (Sec. II.C.1); one clear distinction is that a power law provides much more high-energy x-ray emission than an exponential thermal spectrum (Sec. V.A.3), and such emis-

sion is either not seen or very weak. The IC model would not produce any of the x-ray line emission that is seen universally in clusters that have been observed with reasonable sensitivity (Secs. III.C.2 and III.C.3). The magnetic field is required to be much weaker than would be favored by radio observations. The distorted radio morphologies in clusters would not be explained in this model. Finally, most of the x-ray–optical correlations could not be accounted for naturally in the IC model.

2. Individual stellar x-ray sources

Katz (1976) suggested that the x-ray emission from clusters was produced by a large number of individual cluster stellar x-ray sources, located either in galactic halos or in intracluster space. He suggested that these sources might be similar to the binary x-ray sources found in our galaxy, and assumed that the x-ray luminosity-to-virial-mass ratio would be the same for our galaxy and for clusters of galaxies. This predicts too little x-ray emission from clusters (see also Felten *et al.*, 1966); however, globular clusters within our galaxy have a much higher x-ray luminosity-to-mass ratio, and so they might be used as a model for cluster x-ray sources (Fabian *et al.*, 1976). In fact, M87 and some other central dominant galaxies are known to possess very extensive systems of globular star clusters.

Katz argued that the observed x-ray luminosities of clusters were consistent (in 1976) with a fixed x-ray luminosity-to-virial-mass ratio; the current data would appear to rule out such a correlation (Sec. III.F). It is difficult to see how this model could produce the variation in x-ray emission properties of clusters, or the optical–x-ray and radio–x-ray correlations. Of course, if the properties of the individual stellar x-ray sources are not constrained in any manner, any x-ray observations could be explained, but the model has no predictive power. The granularity in the cluster x-ray emission produced by these individual sources should have been detected in M87/Virgo, but has not been seen (Schreier *et al.*, 1982). Finally, we note that luminous stellar x-ray sources are generally very optically thick. As a result, they do not show any x-ray line emission except for the fluorescence line of low-ionization iron (which is probably produced by reprocessing of x-ray radiation in other parts of the binary star system). In particular, they do not show lines from highly ionized iron (Fe^{24+} and Fe^{25+}) or from lighter elements (for which the fluorescent yields are low). Clusters, on the other hand, do show strong lines from Fe^{24+} and Fe^{25+} , as well as lines from lighter elements (Secs. III.C.2 and III.C.3).

In short, there is no real evidence in favor of the individual stellar source model, and considerable evidence against it.

3. Thermal bremsstrahlung from intracluster gas

Felten *et al.* (1966) first suggested that the x-ray emission from clusters (the Coma cluster in particular) was

due to diffuse intracluster gas at a temperature of $T_g \sim 10^8$ K and an atomic density of $n \sim 10^{-3} \text{ cm}^{-3}$. (Unfortunately, the early x-ray detection of Coma that they sought to explain was spurious.) At such temperatures and densities, the primary emission process for a gas composed mainly of hydrogen is thermal bremsstrahlung (free-free) emission. The emissivity at a frequency ν of an ion of charge Z in a plasma with an electron temperature T_g is given by

$$\epsilon_{\nu}^{ff} = \frac{2^5 \pi e^6}{3 m_e c^3} \left[\frac{2\pi}{3 m_e k} \right]^{1/2} Z^2 n_e n_i g_{ff}(Z, T_g, \nu) T_g^{-1/2} \times \exp(-h\nu/kT_g), \quad (5.11)$$

where n_i and n_e are the number density of ions and electrons, respectively. The emissivity is defined as the emitted energy per unit time, frequency, and volume V ,

$$\epsilon_{\nu} \equiv \frac{dL}{dV d\nu}. \quad (5.12)$$

The Gaunt factor $g_{ff}(Z, T_g, \nu)$ corrects for quantum-mechanical effects and for the effect of distant collisions, and is a slowly varying function of frequency and temperature given in Karzas and Latter (1961) and Kellogg *et al.* (1975). If the intracluster gas is mainly at a single temperature, then Eq. (5.11) indicates that the x-ray spectrum should be close to an exponential of the frequency. In fact, the observed x-ray spectra are generally fit fairly well by this equation (Sec. III.C.1), with gas temperatures of 2×10^7 to 10^8 K. This equation predicts that the emission from clusters should fall off rapidly at high frequencies, as is observed.

As first noted by Felten *et al.* (1966), if the intracluster gas either came out of galaxies or fell into the cluster from intergalactic space, it would have a temperature such that the typical atomic velocity was similar to the velocity of galaxies in the cluster. That is,

$$\frac{kT_g}{\mu m_p} \approx \sigma_r^2, \quad (5.13)$$

where μ is the mean molecular weight in amu, m_p is the proton mass, and σ_r is the line-of-sight velocity dispersion of galaxies in the cluster. If the gas came out of galaxies, it would have the same energy per unit mass as the matter in galaxies. If it fell into clusters, it has roughly the same velocity dispersion because it responds to the same gravitational potential as the galaxies. Finally, if the gas were heated so that its initial energy per mass were much greater than that given by Eq. (5.13), it would not be bound to the cluster and would escape as a wind. Even in this situation, most of the extra energy would go into the kinetic energy of the wind (Sec. V.F), and the gas temperature would stay within a factor of 3 or so of Eq. (5.13). Thus this model predicts

$$T_g \approx 7 \times 10^7 \text{ K} \left[\frac{\sigma_r}{1000 \text{ km sec}^{-1}} \right]^2 \quad (5.14)$$

for a solar abundance plasma, in reasonable agreement with the temperatures required to explain the x-ray spectra [see Eq. (3.10)].

If the intracluster gas is in hydrostatic equilibrium in the cluster potential, and if the gas temperature is given roughly by Eq. (5.14), then the spatial distribution of the gas and galaxies will be similar. In fact, the observed x-ray surface brightness of clusters is similar to the projected distribution of galaxies, with the gas distribution being slightly more extended in the inner regions (Sec. III.D). The thermal emission model thus explains the extent of the x-ray emission from clusters (more detailed models and comparisons are given in Sec. V.E). Moreover, gas at these temperatures and densities has a very long cooling time, and the time for sound waves to cross a cluster is much less than its probable age. These conditions imply that the gas distribution should be smooth, as observed (Jones and Forman, 1984).

Given the extent of the x-ray emission, the gas temperature derived from the spectrum, and the observed x-ray flux, Eq. (5.11) gives the atomic number density if the emission is assumed to come mainly from hydrogen. As discussed in Sec. III.C, the required mass of gas is less than the total virial mass of the cluster, as required for consistency with this model for the emission. Moreover, the derived densities are very similar to those required to explain the distortions of radio sources in clusters of galaxies (Sec. IV.C) as the result of ram pressure by intracluster gas.

Whether the intracluster gas came out of galaxies or fell into the cluster, the mass of this gas should increase as the total mass of the cluster increases, and as a result the x-ray luminosity should increase with the virial mass. Solinger and Tucker (1972) first pointed out that the x-ray luminosity (L_x) does appear to increase with the velocity dispersion of clusters, in a way consistent with a constant fraction of the total cluster mass being intracluster gas. They found $L_x \propto \sigma_v^4$, and were able to predict x-ray emission successfully in a number of clusters based on this relationship. As discussed in Sec. III.F, there are many other correlations observed between L_x or T_g and optical properties such as richness, velocity dispersion, and projected central galaxy density \bar{N}_0 . These correlations are generally consistent with the hypothesis that the mass of intracluster gas increases with the virial mass of the cluster, and that the temperature of the gas increases with the velocity dispersion (depth of the cluster gravitational potential well). There is also an inverse correlation between L_x and the fraction of spirals in the cluster, which may reflect the stripping of spiral galaxies by the intracluster gas. All of these optical-x-ray correlations have natural explanations if the cluster x-ray emission is due to intracluster gas, but not if it is due to the other two mechanisms discussed above.

The clearest evidence in favor of the thermal bremsstrahlung model is the detection of strong x-ray line emission from clusters (Secs. III.C.2 and II.C.3). This emission occurs naturally in the intracluster gas model if the abundances of heavy elements are roughly solar (see Sec.

V.B.2 below). However, it is not at all expected in the IC model and unlikely in the individual stellar source model because such sources are generally optically thick. Only a small portion of the x-ray luminosity of a typical cluster is emitted in these lines, so it is possible, in principal, that the lines might come from a different source than the majority of the x-ray emission. Several considerations show that this is extremely unlikely. First of all, the required abundances in the intracluster gas are nearly solar, and thus very high abundances would be needed if the lines were to come from gas that provided only a small fraction of the continuum x-ray emission. Second, the abundances derived for all the observed clusters are essentially the same within the errors (Sec. III.C.2), although the clusters span a wide range in optical and x-ray properties. A very odd coincidence would be required to produce the appearance of constant abundances in such varied clusters, if the x-ray lines and continuum came from two distinct sources.

B. Ionization and x-ray emission from hot, diffuse plasma

The ionization state and x-ray line and continuum emission from a low-density ($n \sim 10^{-3} \text{ cm}^{-3}$), hot ($T \sim 10^8 \text{ K}$) plasma will now be discussed. Several simple assumptions will be made. First, the time scale for elastic Coulomb collisions between particles in the plasma is much shorter than the age or cooling time of the plasma, and thus the free particles will be assumed to have a Maxwell-Boltzmann distribution at the temperature T_g (Sec. V.D.1). This is the kinetic temperature of electrons, and therefore determines the rates of all excitation and ionization processes. Second, at these low densities collisional excitation and deexcitation processes are much slower than radiative decays, and thus any ionization or excitation process will be assumed to be initiated from the ground state of an ion. Three-body (or more) collisional processes will be ignored because of the low density. Third, the radiation field in a cluster is sufficiently dilute that stimulated radiative transitions are not important, and the effect of the radiation field on the gas is insignificant. Fourth, at these low densities, the gas is optically thin and the transport of the radiation field can therefore be ignored. These assumptions together constitute the "coronal limit." Under these conditions, ionization and emission result primarily from collisions of ions with electrons, and collisions with ions can be ignored. Finally, the time scales for ionization and recombination are generally considerably less than the age of the cluster or any relevant hydrodynamic time scale, and the plasma will therefore be assumed to be in ionization equilibrium.

In nearly all astrophysical plasmas, hydrogen is the most common element and helium is the next commonest, with all the heavier elements being considerably less abundant. For example, this is true of the abundances of elements observed on the surface of the sun. It is conventional to use these solar abundances as a standard of com-

parison when studying other astrophysical systems. Since most of the electrons originate in hydrogen and helium atoms, and they are fully ionized under the conditions considered here, the electron density is nearly independent of the state of ionization and is given by $n_e = 1.21 n_p$, where n_p is the density of hydrogen.

1. Ionization equilibrium

In equilibrium, the ionization state is determined by the balance between processes that produce or destroy each ion:

$$\begin{aligned} [C(X^i, T_g) + \alpha(X^{i-1}, T_g)] n(X^i) n_e \\ = C(X^{i-1}, T_g) n(X^{i-1}) n_e + \alpha(X^i, T_g) n(X^{i+1}) n_e. \end{aligned} \quad (5.15)$$

Here $n(X^i)$ is the number density of the ion X^i (X is the element), T_g is the electron temperature, and $C(X^i, T_g)$ and $\alpha(X^i, T_g)$ are the rate coefficients for collisional ionization out of ion X^i and recombination into ion X^i , respectively.

The collisional ionization rate is the sum of two processes: direct collisional ionization and collisional excitation of inner-shell electrons to autoionizing levels which decay to the continuum. This last process is often re-

ferred to as autoionization. Recombination is also the sum of two processes, radiative and dielectronic recombination. Recent compilations of ionization and recombination rates and discussions of their accuracy include Mewe and Gronenschild (1981), Shull and Van Steenberg (1982), and Hamilton *et al.* (1983).

The electron density dependence drops out of Eq. (5.15), and the equilibrium ionization state of a diffuse plasma depends only on the electron temperature. Tables of ionization fractions of various elements are given by Shull and Van Steenberg (1982). Generally, each ionization fraction reaches a maximum at a temperature that is some fraction of its ionization potential. At the temperatures which predominate in clusters, iron is mainly in the fully stripped, hydrogenic, or heliumlike stages.

2. X-ray emission

The x-ray continuum emission from a hot diffuse plasma is due primarily to three processes, thermal bremsstrahlung (free-free emission), recombination (free-bound) emission, and two-photon decay of metastable levels. The emissivity for thermal bremsstrahlung is given by Eq. (5.11) above. The radiative recombination (bound-free) continuum emissivity is usually calculated by applying the Milne relation for detailed balance to the photoionization cross sections, which gives (Osterbrock, 1974)

$$\epsilon_v^{bf}(X^i) d\nu = n(X^{i+1}) n_e \sum_l \frac{\omega_l(X^i)}{\omega_{gs}(X^{i+1})} a_v^l(X^i) \frac{h^4 \nu^3}{c^2} \left[\frac{2}{\pi(m_e k T_g)^3} \right]^{1/2} \exp \left[- \left[\frac{h\nu - \chi_l(X^i)}{k T_g} \right] \right] d\nu. \quad (5.16)$$

Here, l sums over all of the energy levels of the ion X^i , gs refers to the ground state of the recombining ion X^{i+1} , ω are the statistical weights of the levels, a_v^l is the photoionization cross section, and $\chi_l(X^i)$ is the ionization potential for each energy level in the ion.

The two-photon continuum comes from the metastable $2s$ states of hydrogenic and heliumlike ions. These levels are excited by the same processes, discussed below, that excite line emission from less forbidden transitions. For hydrogenic ions, the spectral distribution of two-photon emission is given by Spitzer and Greenstein (1951).

At the high temperatures which predominate in clusters (outside of accretion flows), thermal bremsstrahlung is the predominant x-ray emission process. For solar abundances, the emission is primarily from hydrogen and helium.

Processes that contribute to the x-ray line emission from a diffuse plasma include collisional excitation of valence or inner-shell electrons, radiative and dielectronic recombination, inner-shell collisional ionization, and radiative cascades following any of these processes. The emissivity due to a collisionally excited line is usually written (Osterbrock, 1974)

$$\begin{aligned} \int \epsilon_v^{line} d\nu = n(X^i) n_e \frac{h^3 \nu \Omega(T_g) B}{4\omega_{gs}(X^i)} \left[\frac{2}{\pi^3 m_e^3 k T_g} \right]^{1/2} \\ \times e^{-\Delta E/k T_g}, \end{aligned} \quad (5.17)$$

where $h\nu$ is the energy of the transition, ΔE is the excitation energy above the ground state of the excited level, B is the branching ratio for the line (the probability that the upper state decays through this transition), and Ω is the "collision strength," which is often a slowly varying function of temperature. Recent compilations of emissivities for x-ray lines and continua include Kato (1976), Raymond and Smith (1977), Mewe and Gronenschild (1981), Shull (1981), Hamilton *et al.* (1983), and Gaetz and Salpeter (1983). Lines and line ratios that are particularly suited for determining the temperature, ionization state, and elemental abundances in the intracluster gas are described in Bahcall and Sarazin (1978).

Shapiro and Bahcall (1980) and Basko *et al.* (1981) have suggested that x-ray absorption lines due to intracluster gas might be observed in the spectra of background quasars.

3. Resulting spectra

All of these emission processes give emissivities that increase in proportion with the ion and electron densities, and otherwise depend only on the temperature, so that

$$\epsilon_v = \sum_{X,i} \Lambda_v(X^i, T_g) n(X^i) n_e, \quad (5.18)$$

where Λ is the emission per ion at unit electron density. If $n(X)$ is the total density of the element X , then in equilibrium the ionization fractions $f(X^i) \equiv n(X^i)/n(X)$ depend only on the temperature, and Eq. (5.18) becomes

$$\epsilon_v = n_p n_e \sum_{X,i} \frac{n(X)}{n(H)} [f(X^i, T_g) \Lambda_v(X^i, T_g)]. \quad (5.19)$$

As previously noted [Eq. (3.3)], it is useful to define the emission integral EI as

$$EI \equiv \int n_p n_e dV, \quad (5.20)$$

where V is the volume of the cluster. Then the shape of the spectrum depends only on the abundances of elements $n(X)/n(H)$ and the distribution of temperatures $d(EI)/dT_g$. The normalization of the spectrum (the overall level or luminosity) is set by EI.

Detailed calculations of the x-ray spectra predicted by different models of the intracluster gas have been given by Sarazin and Bahcall (1977) and Bahcall and Sarazin (1977,1978). Figure 33 gives the x-ray spectrum for isothermal (T_g constant) models for the intracluster gas at a variety of different temperatures, showing the continuum and x-ray emission. The emission integral for these models was taken to be $6.3 \times 10^{-7} \text{ cm}^{-6} \text{ Mpc}^3$.

In these models most of the x-ray emission is thermal bremsstrahlung continuum, and the strongest lines (highest equivalent width) are in the 7-keV iron line complex. This line complex is a blend of K lines from many stages of ionization, although Fe^{24+} and Fe^{25+} predominate at typical cluster temperatures. As noted in Sec. III.C.2, the 7-keV iron line is indeed the strongest line feature observed from clusters. Weaker lines at lower energies from lighter elements, such as oxygen, silicon, and sulfur, as well as from L shell transitions in less ionized iron, were also predicted to be present in the spectra of clusters, particularly at lower temperatures. Such low-energy lines have recently been detected (Sec. III.C.3).

Because the line intensities depend on the abundances of heavy elements, while the continuum intensity is mainly due to hydrogen, the line-to-continuum ratio of a line is proportional to the abundance of the element responsible. This ratio is given by the "equivalent width" [Eq. (3.4)]. Figure 34 gives the equivalent width of the iron 7-keV line complex as a function of temperature in a gas with solar abundances. Comparison of these models to the observed strengths of the lines from clusters leads to the determination that the iron abundances are roughly one-half of solar (Sec. III.C.2).

The spectral observations of clusters also indicate that

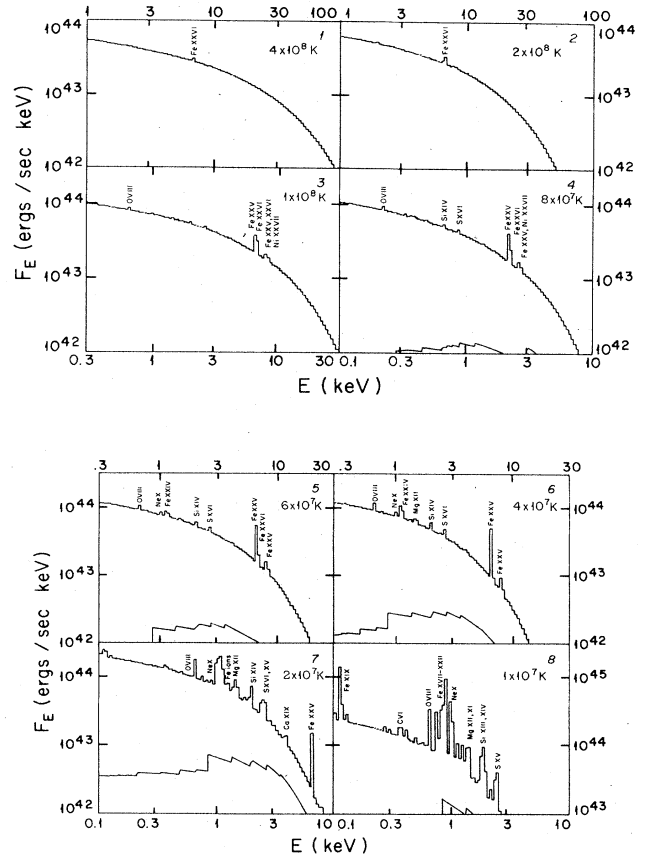


FIG. 33. The predicted x-ray spectra of intracluster gas at various gas temperatures (shown at the upper right of each panel) from Sarazin and Bahcall (1977). The calculations assume the gas is isothermal, and the intensities are normalized to a sphere of gas with a proton number density of 0.001 cm^{-3} and a radius of 0.5 Mpc. E is the photon energy. The strongest line features are labeled; the lower curves, where present, show the bound-free emission.

in a number of cases the low-energy x-ray lines are stronger than would be expected based on these hydrostatic models. This indicates that gas is cooling at the cluster center (Sec. III.C.3).

C. Heating and cooling of the intracluster gas

In this section, processes that heat or cool the intracluster gas are reviewed. Only processes that affect the total energy of the gas are considered here, while processes (such as heat conduction or mixing) that redistribute the gas energy are discussed in Sec. V.D.

1. Cooling

The primary cooling process for intracluster gas is the emission of radiation by the processes discussed in Sec.

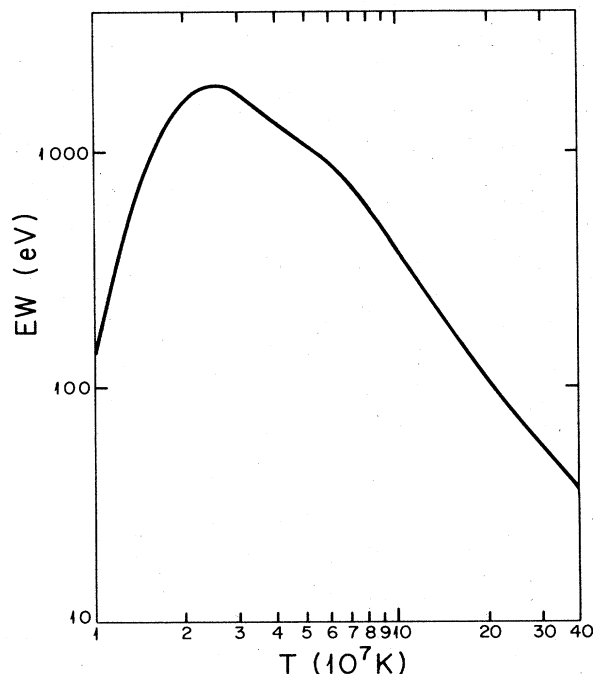


FIG. 34. The equivalent width (in eV) of the Fe K line at 7 keV as a function of gas temperature, from Bahcall and Sarazin (1978). For gas temperatures $\geq 2 \times 10^7$ K, this is the strongest x-ray line feature.

V.B.2 above. At temperatures $T_g \geq 3 \times 10^7$ K, the main emission mechanism is thermal bremsstrahlung, for which the total emissivity is

$$\begin{aligned} \epsilon_{ff} &= 1.435 \times 10^{-27} \bar{g} T_g^{1/2} n_e \sum_i Z_i^2 n_i \text{ ergs cm}^{-3} \text{ sec}^{-1} \\ &\approx 3.0 \times 10^{-27} T_g^{1/2} n_p^2 \text{ ergs cm}^{-3} \text{ sec}^{-1}, \end{aligned} \quad (5.21)$$

where \bar{g} is the integrated Gaunt factor, and Z_i and n_i are the charge and number density of various ions i . The second equation follows from assuming solar abundances and $\bar{g} = 1.1$ in a fully ionized plasma. For $T_g \leq 3 \times 10^7$ K, line cooling becomes very important. Raymond *et al.* (1976) give the cooling rate at lower temperatures; a very crude approximation is (McKee and Cowie, 1977)

$$\begin{aligned} \epsilon &\approx 6.2 \times 10^{-19} T_g^{-0.6} n_p^2 \text{ ergs cm}^{-3} \text{ sec}^{-1}, \\ &10^5 < T_g < 4 \times 10^7. \end{aligned} \quad (5.22)$$

In assessing the role of cooling in the intracluster gas, it is useful to define a cooling time scale as $t_{\text{cool}} \equiv (d \ln T_g / dt)^{-1}$. For the temperatures that apply for the intracluster gas in most clusters, Eq. (5.21) gives a reasonable approximation to the x-ray emission. If the gas cools isobarically, the cooling time is

$$t_{\text{cool}} = 8.5 \times 10^{10} \text{ yr} \left(\frac{n_p}{10^{-3} \text{ cm}^{-3}} \right)^{-1} \left(\frac{T_g}{10^8 \text{ K}} \right)^{1/2}, \quad (5.23)$$

which is longer in most clusters than the Hubble time (age of the universe). Thus cooling is not very important in these cases. However, at the centers of some clusters the cooling time is shorter than the Hubble time, and these clusters are believed to have cooling flows (Sec. V.G).

2. Infall and compressional heating

The heating of the intracluster gas will now be considered. The major point of this discussion is that, although the gas is quite hot, no major ongoing heating of the gas is generally necessary. This is true because the cooling time in the gas is long [Eq. (5.23)], and the thermal energy in the gas is comparable to or less than its gravitational potential energy. Almost any method of introducing the gas into the cluster, either from outside the cluster or from within galaxies, will heat it to temperatures on the order of those observed.

Heating of the gas due to infall into the cluster and compression will be considered here. First, imagine that the cluster was formed before the intracluster gas fell into the cluster, and that the intracluster gas makes a negligible contribution to the mass of the cluster (Sec. III.D). If the gas was initially cold, and located at a large distance from the cluster, then its initial energy can be ignored. If the cluster potential remains fixed while the gas falls into the cluster and the gas neither loses energy by radiation nor exchanges its energy with other components of the cluster, then the total energy of the gas will remain zero. After falling into the cluster, the gas will collide with other elements of gas, and its kinetic energy will be converted to thermal energy. Thus infall and compression can produce temperatures on the order of

$$\frac{3}{2} \frac{kT_g}{\mu m_p} \approx -\phi, \quad (5.24)$$

where ϕ is the gravitational potential in the cluster. At the center of an isothermal cluster, $\phi \approx -9\sigma_r^2$, where σ_r is the line-of-sight velocity dispersion of the cluster. If this is substituted in Eq. (5.24), the derived temperature is

$$T_g \approx 5 \times 10^8 \text{ K} \left(\frac{\sigma_r}{10^3 \text{ km sec}^{-1}} \right)^2, \quad (5.25)$$

which is a factor of 5–10 times larger than the observed temperatures [Eq. (3.10)]. Of course, the gas that falls into a cluster was presumably bound to the cluster before it fell in, so that Eq. (5.25) overestimates the temperature. A similar calculation for gas bound to the cluster is given in Shibazaki *et al.* (1976).

The temperature may also be lower because of cooling during the infall, or because the gas fell in at the same time that the cluster was forming and thus experienced a

smaller potential on average. If the gas fell in at the same time that the cluster collapsed and was heated by the rapid variation of the potential during violent relaxation (Sec. II.I.2), then it might have the same energy per unit mass as the matter in galaxies,

$$\frac{3}{2} \frac{kT_g}{\mu m_p} \approx \frac{3}{2} \sigma_r^2, \quad (5.26)$$

which gives Eq. (5.14) for the temperature. This is in reasonable agreement with the intracluster gas temperatures determined from x-ray spectra [Eq. (3.10)].

These crude estimates are meant only to illustrate the point that the observed gas temperatures are consistent with heating due to infall into the cluster. More detailed models for infall are discussed in Sec. V.J.1.

3. Heating by ejection from galaxies

The presence of a nearly solar abundance of iron in the intracluster gas (Secs. III.C.2 and V.B.3) suggests that a reasonable fraction of the gas may have come from stars in galaxies within the clusters. The gas ejected from galaxies is heated in two ways. First, the gas may have some energy when it is ejected. Let ϵ_{ej} be the total energy per unit mass of gas ejected from a galaxy in the rest frame of that galaxy, but not including the cluster gravitational potential, and define $3kT_{ej}/2 \equiv \mu m_p \epsilon_{ej}$. Second, the gas will initially be moving relative to the cluster center of mass at the galaxy's velocity. The ejected gas will collide with intracluster gas and thermalize its kinetic energy. On average this will give a temperature

$$kT_g \approx \mu m_p \sigma_r^2 + kT_{ej}. \quad (5.27)$$

If the ejection energy can be ignored, the temperature is given by Eq. (5.14), in reasonable agreement with the observations [Eq. (3.10)].

In a steady-state wind outflow from a galaxy, one expects $kT_{ej} \gtrsim \mu m_p \sigma_*^2$, where $\sigma_* \sim 200$ km/sec is the velocity dispersion of stars within the galaxy. If the ejection temperature is near the lower limit given by this expression, then this form of heating will not be very important because $\sigma_*^2 \ll \sigma_r^2$. However, the ejection temperature could be considerably higher. For example, supernovas within galaxies could both produce the heavy elements seen in cluster x-ray spectra and heat the gas in galaxies until it was ejected. Supernovas eject highly enriched gas at velocities of $v_{SN} \sim 10^4$ km/sec. The highly enriched, rapidly moving supernova ejecta would collide with the interstellar medium in a galaxy and heat the gas. If M_{SN} is the mass of ejecta from a supernova and M_{ej} is the resulting total gas mass ejected from the galaxy, then $T_{ej} \approx 2 \times 10^9$ K $(v_{SN}/10^4 \text{ km/sec})^2 (M_{SN}/M_{ej})$, which will be significant if the supernova ejecta are diluted by less than a factor of about 100.

4. Heating by galaxy motions

Although ongoing heating of the intracluster gas may not be necessary to account for the observed gas temperatures, the estimates given above and the history of the gas are sufficiently uncertain that one cannot rule out ongoing heating as an important process. One way in which intracluster gas could be heated would be through friction between the gas and the galaxies that are constantly moving throughout the cluster (Ruderman and Spiegel, 1971; Hunt, 1971; Yahil and Ostriker, 1973; Schipper, 1974; Livio *et al.*, 1978; Rephaeli and Salpeter, 1980). The calculation of the magnitude of this drag force and of the consequent heating of the intracluster gas is complicated by the following problems. First, the motion of an average cluster galaxy through the intracluster medium is likely to be just transonic $M \approx 1$, where $M \equiv v/c_s$ is the Mach number, v is the galaxy velocity, and $c_s = 1480 (T_g/10^8 \text{ K})^{1/2}$ km/sec is the sound speed in the gas. If Eq. (3.10) for the observed gas temperatures is assumed, and the average galaxy velocity is taken to be $\sqrt{3}\sigma_r$, then the average Mach number is $\langle M \rangle \approx 1.5$. Thus the galaxy motion cannot be treated as being either highly supersonic (strong shocks, etc.) or very subsonic (incompressible, etc.). In some cases shocks will be formed by the motion, and in some cases no shocks form. Second, the mean free path λ_i of ions in the intracluster medium due to Coulomb collisions [Eq. (5.34)] is similar to the radius of a galaxy $R_{gal} \sim 20$ kpc (Nulsen, 1982). Thus it is unclear whether the intracluster gas should be treated as a collisionless gas or as a fluid, and the role of transport processes such as viscosity (Sec. V.D.4) is uncertain. For example, the Reynolds number of the flow about an object of radius R is $Re \approx 3(R/\lambda_i)M$ [Eq. (5.46) below], and thus is somewhat larger than unity if $R = R_{gal}$. It is therefore uncertain whether the flow will be laminar or turbulent. The magnetic field can affect transport processes (Sec. V.D.3), but the coherence length of the field l_b estimated from Faraday rotation observations is also comparable to the size of a galaxy (Sec. IV.F). Finally, the nature of the drag force depends on whether the galaxy contains interstellar gas or not. If the galaxy contains no gas, it affects the intracluster medium only through its gravitational field. If the galaxy contains high-density gas, it can give the galaxy an effective surface. For example, a gasless galaxy in supersonic motion probably will not produce a bow shock, while a gas-filled galaxy may (Ruderman and Spiegel, 1971; Hunt, 1971; Gisler, 1976).

It is convenient to write the rate of energy loss by the galaxy and the heating rate of the intracluster medium as

$$\frac{dE}{dt} = \pi R_D^2 \rho_g v^3, \quad (5.28)$$

where ρ_g is the intracluster gas density and R_D is the effective radius of the galaxy for producing the drag force. First, assume that the intracluster gas is collisionless. Then the drag is given by the dynamical friction force of Eq. (2.34) and

$$R_D^2 = R_A^2 \ln(\Lambda) [\operatorname{erf}(x) - x \operatorname{erf}'(x)], \quad (5.29)$$

where $R_A \equiv 2Gm/v^2$ is the accretion radius (Ruderman and Spiegel, 1971), m is the galaxy mass, Λ is given by Eq. (2.29), and $x \equiv \sqrt{5/6}M$. By the virial theorem applied to the galaxy, $R_A \approx R_{\text{gal}}(\sigma_*/\sigma_r)^2$, and the accretion radius is typically much smaller than the galaxy radius, since the galaxy velocity dispersion is smaller than that of a cluster. In the limit of hypersonic motion $M \gg 1$, the term in brackets reduces to unity. In this limit, Rephaeli and Salpeter (1980) have shown that Eq. (5.29) gives the drag force for any value of the mean free path or viscosity if no gas is present in the galaxy. The definition of Λ must be slightly modified (Ruderman and Spiegel, 1971).

For a $10^{11}M_\odot$ galaxy moving at 1000 km/sec through intracluster gas with a proton number density of 10^{-3} cm^{-3} , the rate of heating of the gas is $\sim 10^{41}$ ergs/sec. If the cluster contained 1000 such galaxies, the total heating rate would be $\sim 10^{44}$ ergs/sec. While not trivial, this heating rate is too small to heat the intracluster gas in a Hubble time (Schipper, 1974; Rephaeli and Salpeter, 1980). If the total mass of intracluster gas is $\geq 10^{14}M_\odot$ and the gas temperature is $\sim 6 \times 10^7$ K, then the time required to heat the gas at this rate would be $\geq 7 \times 10^{11}$ yr.

The drag force can be considerably increased if the galaxy contains gas or magnetic fields that prevent the penetration of the galaxy by the intracluster gas (Ruderman and Spiegel, 1971; Yahil and Ostriker, 1973; Livio *et al.*, 1978; Shaviv and Salpeter, 1982; Gaetz *et al.*, 1985). However, the main effect of the drag force may be to remove the gas from the galaxy and heat it to the temperature determined by the galaxy kinetic energy per mass (Sec. V.C.3). The stripping of gas from a galaxy is shown in Sec. V.I to be very efficient, and as discussed in Secs. II.J.2 and III.F, galaxies in x-ray clusters are known to be very deficient in gas. It is possible that galaxies may retain a core of gas produced by stellar mass loss within the galaxy. Gaetz *et al.* (1985) give useful analytic fitting formulas for drag coefficients for galaxies with stellar mass loss, based on two-dimensional hydrodynamic simulations. Yahil and Ostriker (1973) and Livio *et al.* (1978) have suggested very large heating rates produced by having high rates of gas output in galaxies. Livio *et al.* assume a rather large cross section for galaxies and a rather low intracluster gas density. Both of these papers argue that the heating rate due to galaxy motions is so large that the intracluster gas is heated beyond the escape temperature from the cluster, and a cluster wind results (see Sec. V.F).

There is a simple argument against the great importance of heating due to drag forces from the motions of galaxies. The mass associated with intracluster gas in a typical x-ray cluster is comparable to or greater than the mass associated with galaxies (Sec. III.D.1). The average thermal velocities in the gas are comparable to or greater than the typical galaxy velocities (Secs. III.F, V.C.2, and V.E). Thus the total thermal energy in the gas is greater

than or comparable to the total kinetic energy in the galaxies. It is difficult to believe that the galaxies heated the gas under these circumstances. If they did, then the massive galaxies would have lost most of their initial kinetic energy in the process; this should have produced quite extreme mass segregation, which is not observed (Sec. II.G).

5. Heating by relativistic electrons

Clusters of galaxies often contain radio sources having steep spectral indices (Sec. IV.A); the radio emission from these sources is believed to arise from synchrotron emission by relativistic electrons. These electrons (particularly the lower-energy ones) can interact with the intracluster gas and may heat this gas (Sofia, 1973; Lea and Holman, 1978; Rephaeli, 1979; Scott *et al.*, 1980). A relativistic electron passing through a plasma loses energy through Coulomb interactions with electrons within a Debye length of the particle, and through interactions with plasma waves on larger scales. The rate of loss by an electron with total energy $\gamma m_e c^2$ is

$$-\frac{d\gamma}{dt} = \frac{\omega_p^2 r_e}{c} \left[\ln \left[\frac{m_e c^2 \gamma^{1/2}}{\hbar \omega_p} \right] + 0.2 \right], \quad (5.30)$$

where ω_p is the plasma frequency ($\omega_p^2 \equiv 4\pi n_e e^2/m_e$), $r_e \equiv e^2/(m_e c^2)$ is the classical electron radius, and n_e is the electron density in the plasma. The term in square brackets is ≈ 40 for most values of γ and n_e of interest, and does not vary significantly with either parameter. Numerically, the heating rate is $\approx 10^{-18} n_e$ ergs/sec, ignoring the variation of the term in square brackets. The total heating rate is determined by multiplying this rate per electron by the total number of relativistic electrons in the intracluster gas. If the relativistic electrons have a power-law spectrum [Eq. (5.2)], then the heating rate can be determined from the synchrotron radio emission rate given by Eq. (5.7). The heating rate is

$$\begin{aligned} \frac{dE}{dt} &= \frac{1.2 \times 10^9 n_e}{a(p) \alpha_r} \left[\frac{dL_r}{d\nu_r} \nu_r^{\alpha_r} \right] \left[\frac{2.4 \times 10^{-7}}{B} \right]^{\alpha_r+1} \\ &\times \gamma_l^{-2\alpha_r} \text{ ergs/sec}. \end{aligned} \quad (5.31)$$

Here L_r is the radio luminosity at a frequency ν_r , α_r is the radio spectral index, B is the intracluster magnetic field, $a(p)$ is the function given by Eqs. (5.4) and (5.8), and γ_l is the lower limit to the electron spectrum [Eq. (5.2)]. cgs units are to be used for L_r and B . The first quantity in parentheses is independent of the frequency ν_r at which the radio source is observed. Equation (5.31) includes only electrons and should be increased to include the heating by ions, which do not produce observable radio emission. While the radio flux and spectrum can be measured directly, the magnetic field strength must be es-

timated from the radio observations (Sec. IV.F), and the lower limit to the electron spectrum is generally unknown.

This heating rate is significant only for radio sources with steep spectra which extend to very, very low frequencies. Lea and Holman (1978) used low-frequency radio observations of clusters to determine the radio flux and spectral index, and found that the electron spectrum must extend down to $\gamma_l \sim 10(B/\mu\text{G})^{-1}$ if the heating rate is to be comparable to the x-ray luminosity of the cluster. These low-energy electrons would produce radio emission at a frequency of about 400 Hz, which is about 10^5 times too low to be observed. Extrapolating the radio spectrum from the lowest observed frequencies (~ 26 MHz) down to these low frequencies increases the total number of relativistic electrons and the corresponding heating rate by about 10^5 . Thus the hypothesis that relativistic electrons provide significant heating to the intracluster gas according to Eq. (5.31) requires an enormous and untestable extrapolation of cluster radio properties.

Several authors have argued that the heating rate of Eq. (5.31) should be increased by collective plasma interactions between the relativistic electrons and the intracluster gas (Lea and Holman, 1978; Rephaeli, 1979; Scott *et al.*, 1980). In these models, it is assumed that the relativistic electrons are streaming away from a powerful radio source at the center of the cluster. Rephaeli (1979) assumed that the streaming speed is limited by the Alfvén velocity, as has generally been argued (Jaffe, 1977; Sec. IV.D). Then he finds that the relativistic electrons excite Alfvén waves and lose energy at a rate of $-d\gamma/dt \approx v_A \gamma / L_e$, where L_e is the scale length of the relativistic electron distribution. For $B \sim 1 \mu\text{G}$, $L_e \sim 1$ Mpc, and $n_e \sim 10^{-3} \text{ cm}^{-3}$, this gives a heating rate about $10^{-2} \gamma_l$ of that in Eq. (5.31), which is never very significant.

Alternatively, Scott *et al.* (1980) have assumed that the relativistic electrons stream at nearly the speed of light (Holman *et al.*, 1979). As discussed in Sec. IV.D, this hypothesis is controversial. They discuss a number of plasma instabilities that greatly increase the heating rate under these circumstances. The increase could be as much as a factor of 10^5 , which would allow the electrons that produce the observed radio emission in clusters to heat the intracluster gas.

Models in which relativistic electrons heat the intracluster gas suffer from two general problems. First, the total energy requirements of 10^{63-64} ergs are extreme for a single radio source, although it is possible that many cluster sources contribute to the heating over the lifetime of the cluster. Second, the radio sources generally occupy only a small fraction of the cluster; cluster-wide radio halos are rare (Sec. IV.D). It is difficult to see how several discrete radio sources would heat the intracluster gas without producing very strong, observable variations in the x-ray surface brightness, which are not seen.

Vestrand (1982) has suggested that heating of the intracluster gas by relativistic electrons is important only in clusters having radio halos. He noted that Coma, which

has a prominent halo, also has an unusually high gas temperature for its velocity dispersion (Sec. III.E.1).

D. Transport processes

Processes that redistribute energy, momentum, or heavy elements within the intracluster gas will now be reviewed.

1. Mean free paths and equilibration time scales

The mean free paths of electrons and ions in a plasma without a magnetic field are determined by Coulomb collisions. As in the stellar dynamical case, it is important to include distant as well as nearby collisions. The mean free path λ_e for an electron to suffer an energy-exchanging collision with another electron is given by (Spitzer, 1956)

$$\lambda_e = \frac{3^{3/2}(kT_e)^2}{4\pi^{1/2}n_e e^4 \ln \Lambda}, \quad (5.32)$$

where T_e is the electron temperature, n_e is the electron number density, and Λ is the ratio of largest to smallest impact parameters for the collisions. For $T_e \geq 4 \times 10^5$ K, this Coulomb logarithm is

$$\ln \Lambda = 37.8 + \ln \left[\left[\frac{T_e}{10^8 \text{ K}} \right] \left[\frac{n_e}{10^{-3} \text{ cm}^{-3}} \right]^{-1/2} \right], \quad (5.33)$$

which is nearly independent of density or temperature. Equation (5.32) assumes that the electrons have a Maxwellian velocity distribution at the electron temperature. The equivalent mean free path of ions λ_i is given by the same formula, replacing the electron temperature and density with the ion temperature T_i and density, dividing by the ion charge to the fourth power, and slightly increasing $\ln \Lambda$. In the discussion that follows the ions will generally be assumed to be protons, and the diffusion of heavy elements will be discussed in Sec. V.D.5 below. Numerically,

$$\lambda_e = \lambda_i \approx 23 \text{ kpc} \left[\frac{T_g}{10^8 \text{ K}} \right]^2 \left[\frac{n_e}{10^{-3} \text{ cm}^{-3}} \right]^{-1} \quad (5.34)$$

assuming that $T_e = T_i = T_g$.

In general, these mean free paths are shorter than the length scales of interest in clusters (~ 1 Mpc), and the intracluster medium can be treated as a collisional fluid, satisfying the hydrodynamic equations. Note that the mean free paths are comparable to the size of a galaxy, however, and in the interaction between intracluster gas and individual galaxies the gas may be nearly collisionless, as mentioned previously (Sec. V.C.4).

If a homogeneous plasma is created in a state in which the particle distribution is non-Maxwellian, elastic collisions will cause it to relax to a Maxwellian distribution

on a time scale determined by the mean free paths (Spitzer, 1956, 1978). Electrons will achieve this equilibration (isotropic Maxwellian velocity distribution characterized by the electron temperature) on a time scale set roughly by $t_{\text{eq}}(e,e) \equiv \lambda_e / \langle v_e \rangle_{\text{rms}}$, where the denominator is the rms electron velocity,

$$t_{\text{eq}}(e,e) = \frac{3m_e^{1/2}(kT_e)^{3/2}}{4\pi^{1/2}n_e e^4 \ln \Lambda} \approx 3.3 \times 10^5 \text{ yr} \left[\frac{T_e}{10^8 \text{ K}} \right]^{3/2} \left[\frac{n_e}{10^{-3} \text{ cm}^{-3}} \right]^{-1}. \quad (5.35)$$

The time scale for protons to equilibrate among themselves is $t_{\text{eq}}(p,p) \approx (m_p/m_e)^{1/2} t_{\text{eq}}(e,e)$, or roughly 43 times longer than the value in Eq. (5.35). Following this time, the protons and ions would each have Maxwellian distributions, but generally at different temperatures. The time scale for the electrons and ions to reach equipartition $T_e = T_i$ is $t_{\text{eq}}(p,e) \approx (m_p/m_e) t_{\text{eq}}(e,e)$, or roughly 1870 times the value in Eq. (5.35). For heavier ions, the time scales for equilibration are generally at least this short if the ions are nearly fully stripped, because the increased charge more than makes up for the increased mass. For $T_g \sim 10^8 \text{ K}$ and $n_e \sim 10^{-3} \text{ cm}^{-3}$, the longest equilibration time scale is only $t_{\text{eq}}(p,e) \sim 6 \times 10^8 \text{ yr}$. Since this is shorter than the age of the cluster or the cooling time, the intracluster plasma can generally be characterized by a single kinetic temperature T_g . Under some circumstances, plasma instabilities may bring about a more rapid equilibration than collisions (McKee and Cowie, 1977).

2. Thermal conduction

In a plasma with a gradient in the electron temperature, heat is conducted down the temperature gradient. If the scale length of the temperature gradient $l_T \equiv T_e / |\nabla T_e|$ is much longer than the mean free path of electrons λ_e , then the heat flux is given by

$$\mathbf{Q} = -\kappa \nabla T_e, \quad (5.36)$$

where the thermal conductivity for a hydrogen plasma is (Spitzer, 1956)

$$\begin{aligned} \kappa &= 1.31 n_e \lambda_e k \left[\frac{kT_e}{m_e} \right]^{1/2} \\ &\approx 4.6 \times 10^{13} \left[\frac{T_e}{10^8 \text{ K}} \right]^{5/2} \\ &\quad \times \left[\frac{\ln \Lambda}{40} \right]^{-1} \text{ ergs sec}^{-1} \text{ cm}^{-1} \text{ K}^{-1}. \end{aligned} \quad (5.37)$$

Because of the inverse dependence on the particle mass, thermal conduction is primarily due to electrons. This equation includes a correction for the self-consistent electric field set up by the diffusing electrons. If the very

weak dependence of $\ln \Lambda$ on density is ignored, then κ is independent of density but depends very strongly on temperature.

If the scale length of the thermal gradient l_T is comparable to or less than the mean free path of electrons, then Eq. (5.36) overestimates the heat flux, since it would imply that the electrons are diffusing at a speed greater than their average thermal speed. Under these circumstances the conduction is said to "saturate," and the heat flux approaches a limiting value Q_{sat} . Cowie and McKee (1977) calculate this saturated heat flux by assuming that the electrons have a Maxwellian distribution and an infinitely steep temperature gradient, and that the correction for a self-consistent electric field is the same as in the unsaturated case. They find

$$Q_{\text{sat}} = 0.4 n_e k T_e \left[\frac{2kT_e}{\pi m_e} \right]^{1/2}. \quad (5.38)$$

A general expression for the heat flux, which interpolates between the two limits of Eqs. (5.36) and (5.38), is then

$$\mathbf{Q} = -\frac{\kappa T_e}{l_T + 4.2 \lambda_e} \frac{\nabla T_e}{|\nabla T_e|}. \quad (5.39)$$

The mean free path of electrons in the intracluster gas [Eq. (5.34)] is typically small compared to the cluster dimensions, and heat conduction within the intracluster gas itself is probably unsaturated. However, the mean free path is comparable to the size of a galaxy, and saturated heat conduction may be important in evaporation from or accretion to galaxies (Secs. V.G and V.I).

Within the intracluster medium, thermal conduction will act to transport heat from hot to cold regions and, in the absence of any competing effect, to make the temperature spatially constant (isothermal). Assuming equal ion and electron temperatures, the temperature in a Lagrangian element of the intracluster gas will vary as

$$\frac{3}{2} \frac{\rho_g k}{\mu m_p} \frac{dT_g}{dt} - \frac{kT_g}{\mu m_p} \frac{d\rho_g}{dt} = -\nabla \cdot \mathbf{Q}, \quad (5.40)$$

where ρ_g is the gas density. It is useful to define a conduction time scale as $t_{\text{cond}} \equiv -(d \ln T_e / dt)^{-1}$, which is on the order of $|t_{\text{cond}}| \sim n_e l_T^2 k / \kappa$. As a specific example, consider a cluster in which the gas is hydrostatic, adiabatic (isentropic), and extends to very large distances but is not in contact with any intercluster gas; such models are discussed in some detail in Sec. V.E.2 below. If the cluster potential is given by the analytic King form [Eq. (5.59) below], the gas is assumed to cool isobarically (at constant pressure), and the variation of $\ln \Lambda$ is ignored, then the conduction time at a radius r is given by

$$\frac{1}{t_{\text{cond}}} = \frac{2\mu m_p \kappa_0}{5\rho_g r_c^2 k} g(r/r_c), \quad (5.41)$$

where κ_0 and ρ_{g0} are the conductivity and gas density at the cluster center, and r_c is the cluster core radius. The function $g(x)$ is

$$g(x) \equiv (x^2 + 1)^{-3/2} - \frac{5}{2x^2 f(x)} [f(x) - (x^2 + 1)^{-1/2}]^2, \quad (5.42)$$

where $f(x) \equiv \phi(r)/\phi_0$ is the ratio of the cluster potential to its central value and is given by Eq. (5.59) below. The function $g(x)$ is plotted in Fig. 35. Because conduction only transports heat, the average temperature of the gas is not changed; in the inner parts the gas is cooled and in the outer parts the gas is heated. However, because the x-ray emission is proportional to the square of the density, temperatures determined from x-ray spectra are mainly affected by the innermost gas and are lowered by conduction. As is clear from Fig. 35, heat conduction is most effective in the cluster core, and $|t_{\text{cond}}|$ increases very rapidly with radius. Since $g(0) = 1$, the central value to the conduction time scale $t_{\text{cond}}(0)$ is given by the first term in Eq. (5.41), or

$$t_{\text{cond}}(0) = 3.3 \times 10^8 \text{ yr} \left[\frac{n_0}{10^{-3} \text{ cm}^{-3}} \right] \left[\frac{T_e}{10^8 \text{ K}} \right]^{-5/2} \times \left[\frac{r_c}{0.25 \text{ Mpc}} \right]^2 \left[\frac{\ln \Lambda}{40} \right], \quad (5.43)$$

where n_0 is the central proton density, and solar abundances have been assumed. Thus heat conduction may be relatively effective in the core of a cluster. At radii $r \gtrsim 2r_c$, the conduction time is typically a factor of ~ 100 longer, and conduction is only marginally effective in the outer parts of the cluster. The conduction time may be increased further by the presence of a magnetic field in the cluster.

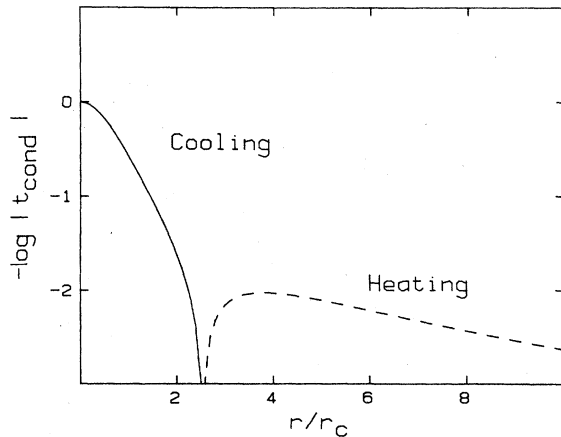


FIG. 35. The conduction time as a function of position in an adiabatic model for the intracluster gas. The conduction time is relative to its central value, and the radius is in units of the cluster core radius r_c . The solid (dashed) curve indicates the portion of the cluster where the gas is cooled (heated) by conduction.

3. Effects of the magnetic field

Charged particles gyrate around magnetic field lines on orbits with a radius (the gyroradius) of $r_g = (mv_{\perp}c/ZeB)$, where m is the particle mass, v_{\perp} is the component of its velocity perpendicular to the magnetic field, Z is the particle charge, and B is the magnetic field strength. If $v_{\perp} = (2kT_g/m)^{1/2}$, which is the rms value in a thermal plasma, then

$$r_g = \frac{3.1 \times 10^8 \text{ cm}}{Z} \left[\frac{T_g}{10^8 \text{ K}} \right]^{1/2} \left[\frac{m}{m_e} \right]^{1/2} \left[\frac{B}{1 \mu\text{G}} \right]^{-1}, \quad (5.44)$$

which is much smaller than any length scale of interest in clusters, and is also much smaller than the mean free path of particles due to collisions $r_g \ll \lambda_e$. Then, the effective mean free path for diffusion perpendicular to the magnetic field is only on the order of r_g^2/λ_e (Spitzer, 1956). Because they have larger gyroradii, the ions are most effective in transport processes perpendicular to the magnetic field. In practice, the gyroradii are so small that diffusion perpendicular to the magnetic field can be ignored in the intracluster gas.

Consider the effect of the magnetic field on thermal conduction, when the temperature gradient lies at an angle θ to the local magnetic field direction. Only the component of the gradient parallel to the field is effective in driving a heat flux, and only the component of the resulting heat flux in the direction of the temperature gradient transports any net energy. If the conduction is unsaturated, the heat flux parallel to the thermal gradient is thus reduced by a factor of $\cos^2 \theta$. If the conduction is saturated, the heat flux is independent of the temperature gradient; the appropriate factor is just $\cos \theta$ (Cowie and McKee, 1977).

Observations suggest that the magnetic field in clusters may be tangled, so that the direction θ varies throughout the intracluster gas (Sec. IV.F). Let l_B be the coherence length of the magnetic field, so that the field will typically have changed direction by $\sim 90^\circ$ over this distance. Let l_T be the temperature scale height (Sec. V.D.2 above) and let λ_e be the mean free path of electrons. Consider first the case where $\lambda_e \ll l_T$, so that the conduction is unsaturated. Then, if $l_B \gtrsim l_T$, the magnetic field is ordered over the scales of interest in the cluster, and the value of $\cos^2 \theta$ depends on the geometry of the magnetic field. For example, for a cluster with a radial temperature gradient and a circumferential magnetic field, thermal conduction would be suppressed. Alternatively, if $l_T \gg l_B \gg \lambda_e$, then the field direction can be treated as a random variable, and the heat flux is reduced by $\sim \langle \cos^2 \theta \rangle = \frac{1}{3}$. If the coherence length of the magnetic field is less than the mean free path $l_B \ll \lambda_e$, the conductivity depends on the topology of the magnetic field (i.e., whether it is connected over distances greater than l_B). In general, the effective mean free path for diffusion will always be at least as

small as l_B , and could be as small as l_B^2/λ_e if the magnetic field is disconnected on the scale of l_B . In this limit, the thermal conduction would be very significantly reduced.

The Faraday rotation observations (Sec. IV.F) suggest that $l_B \sim \lambda_e \sim 20$ kpc. Thus thermal conduction will probably be reduced by a factor of at least $\frac{1}{3}$, and the conductivity time scale [Eqs. (5.41) and (5.43)] should be increased by at least this factor.

4. Viscosity

If there are shears in the velocity in a fluid, then viscosity will produce forces that act against these shears. A unit volume of the fluid will be subjected to a force given by

$$\mathbf{F}_{\text{vis}} = \eta (\nabla^2 \mathbf{v} + \frac{1}{3} \nabla \nabla \cdot \mathbf{v}), \quad (5.45)$$

where η is the dynamic viscosity, and the bulk viscosity has been assumed to be zero. For an ionized plasma without a magnetic field, η is given by

$$\eta \approx \frac{1}{3} m_i n_i \langle v_i \rangle_{\text{rms}} \lambda_i \approx 5500 \text{ g cm}^{-1} \text{ sec}^{-1} \left[\frac{T_e}{10^8 \text{ K}} \right]^{5/2} \left[\frac{\ln \Lambda}{40} \right]^{-1}, \quad (5.46)$$

where m_i , n_i , $\langle v_i \rangle_{\text{rms}}$, and λ_i are the mass, number density, rms velocity, and mean free path of ions, respectively. Like the thermal conductivity, the dynamic viscosity is independent of density and depends strongly on the temperature. However, because of the dependence on the particle mass, the viscosity is primarily due to ions, not electrons. The Reynolds number for flow at a speed v past an object of size l is defined as $\text{Re} \equiv \rho_g v l / \eta$, which can be written as

$$\text{Re} \approx 3M \left[\frac{l}{\lambda_i} \right], \quad (5.47)$$

where $M \equiv v/c_s$ is the Mach number and c_s is the sound speed. As noted in Sec. V.C.4, this indicates that the flow around moving galaxies in a cluster is probably laminar, but not certainly so. The viscosity affects the rate of heating of the intracluster gas by galaxy motions (Sec. V.C.4), and the rate of stripping by interstellar gas in cluster galaxies (Sec. V.I).

As with thermal conduction, one can define a velocity scale length l_v so that the absolute value of the term in parentheses in Eq. (5.45) is $\langle v_i \rangle_{\text{rms}}/l_v^2$. Then, if the ion mean free path λ_i is shorter than l_v , Eq. (5.45) applies. However, if $l_v < \lambda_i$, then Eq. (5.45) requires that the viscous stresses exceed the ion pressure and that momentum be transported faster than the thermal speed of the ions. This is not possible, and the viscous stresses must saturate at a value comparable to the ion pressure. To my knowledge, this effect has not been included in calculations of astrophysical fluid flows. It should be particularly important in flows around galaxies, where previous cal-

culations, particularly those involving Kelvin-Helmholtz instabilities, have applied Eq. (5.45) to flows with very large shears.

5. Diffusion and settling of heavy ions

At the same temperature, heavy ions will move more slowly than light ions, and all ions will move more slowly than electrons. As a result, the heavy ions will tend to settle towards the center of the cluster. This settling is generally halted when it results in an electric field large enough to balance the extra gravitational force on the heavier ions. Models for the distribution of heavy elements in clusters, assuming that settling has occurred rapidly enough to reach this equilibrium, are discussed in Sec. V.E.5 below. Here, the rate of settling will be considered.

Heavy ions that diffuse toward the cluster center rapidly reach a drift velocity at which gravitational acceleration is balanced by the slowing effect of collisions (Fabian and Pringle, 1977; Rephaeli, 1978). Using the expression for the mean free path of a slow-moving heavy ion in a plasma (Spitzer, 1956), we obtain the drift velocity \mathbf{v}_D ,

$$A m_p \mathbf{g} = \mathbf{v}_D \frac{16\sqrt{\pi} Z^2 e^4 m_p^{1/2}}{3(2kT_g)^{3/2}} \sum_i Z_i^2 A_i^{1/2} n_i \ln \Lambda_i, \quad (5.48)$$

where A and Z are the heavy-ion atomic number and charge, \mathbf{g} is the gravitational acceleration, T_g is the gas temperature, and the sum is over the various ions in the plasma. Assuming cosmic abundances, one finds

$$\begin{aligned} v_D = 2.9 & \left[\frac{A}{56} \right] \left[\frac{Z}{26} \right]^{-2} \left[\frac{|g|}{3 \times 10^{-8} \text{ cm sec}^{-2}} \right] \\ & \times \left[\frac{T_g}{10^8 \text{ K}} \right]^{3/2} \left[\frac{n_p}{10^{-3} \text{ cm}^{-3}} \right]^{-1} \\ & \times \left[\frac{\ln \Lambda}{40} \right]^{-1} \text{ km/sec.} \end{aligned} \quad (5.49)$$

The values of A and Z in Eq. (5.49) are those for fully ionized iron. The x-ray lines of iron are the strongest lines observed from clusters, and have been detected in a large number of clusters (Sec. III.C.2). These lines play an important role in considerations of the origin and energetics of the intracluster gas (Sec. V.J), and thus the distribution of iron is particularly important. As noted by Rephaeli (1978), the value of the drift velocity in Eq. (5.49) is considerably smaller than the value given by Fabian and Pringle (1977) because they failed to include helium and heavier elements in the slowing time.

According to Eq. (5.49), the drift velocity depends on the cluster gravitational potential and the density and temperature of the intracluster gas. If the cluster potential is given by the King analytic approximation to the isothermal distribution [Eqs. (2.13) and (5.59)], then the

largest value of g occurs at roughly the core radius r_c (actually $r = 1.027 r_c$), and

$$g \leq 2.0 \times 10^{-8} \left(\frac{\sigma_r}{10^3 \text{ km/sec}} \right)^2 \times \left(\frac{r_c}{0.25 \text{ Mpc}} \right)^{-1} \text{ cm sec}^{-2}, \quad (5.50)$$

where σ_r is the radial velocity dispersion of the cluster. The time to drift in a small distance dr is then $dt = dr/v_D$. If one sets $dr \approx r_c$, then the drift time is

$$t_D \approx 1.2 \times 10^{11} \text{ yr} \left(\frac{A}{56} \right)^{-1} \left(\frac{Z}{26} \right)^2 \left(\frac{T_g}{10^8 \text{ K}} \right)^{-3/2} \times \left(\frac{n_0}{10^{-3} \text{ cm}^{-3}} \right) \left(\frac{\ln \Lambda}{40} \right) \times \left(\frac{\sigma_r}{10^3 \text{ km/sec}} \right)^{-2} \left(\frac{r_c}{0.25 \text{ Mpc}} \right)^2 \text{ yr}. \quad (5.51)$$

If the intracluster gas is adiabatic (constant entropy per particle; Sec. V.E), then $n_p \propto T_g^{3/2}$, and the variation of these two quantities does not affect the drift time. If the gas is isothermal, then the reduction of density with distance from the cluster center shortens the drift time, although the increase in the distance to be traversed and the decrease in the gravitational acceleration more than make up for this. Rephaeli (1978) has integrated the drift time for a variety of equations of state for the gas, and finds that the drift times from radii greater than four core radii into one core radius is always greater than 10^{11} yr times the cluster parameters in Eq. (5.51), with the gas density and temperature evaluated at the cluster center. Since this means the drift time is generally at least ten times the probable age of the cluster, the settling of iron into the cluster center is unlikely to occur.

As noted by Rephaeli (1978), the presence of a magnetic field in the intracluster gas would inhibit the sedimentation of iron even further. The situation is similar to that for thermal conduction (Sec. V.D.3); iron ions could only drift along the direction of magnetic field lines. Unless the magnetic field were predominantly radial, settling of iron would be very strongly inhibited. The effect is even larger than that on thermal conduction, because the sedimentation of iron ions requires that the individual ions drift over large distances, while heat can be conducted from the inner to the outer portions of a cluster without having an individual electron traverse these distances. For example, loop structures in the magnetic field would tend to prevent any sedimentation beyond the bottom of the loop.

Although it appears unlikely that heavy elements like iron would have settled to the cluster center, this does not mean that the abundance of heavy elements is necessarily uniform. Heavy elements might be concentrated in the cluster core if they were injected into the intracluster gas in the core. If the heavy elements were produced in stars within galaxies, as is usually assumed (Secs. III.C.2 and

V.J), then this gas might have been predominantly deposited in the cluster core because either ram pressure or collisional stripping will occur more easily there. Of course, if all the intracluster gas were produced by this mechanism, then no abundance gradients would be produced if all galaxies in the cluster contained gas with the same average abundances. If, however, the intracluster medium were partly due to heavy-element-containing gas stripped from galaxies, and partly due to heavy-element-lacking intergalactic gas that fell into the cluster, and if the stripping were concentrated at the cluster core, then a gradient in the abundance of heavy elements could result (Nepveu, 1981b). Subsequent mixing of the intracluster gas (Sec. V.D.6 below) might still destroy such abundance variations.

Such an abundance gradient could greatly reduce the amount of iron needed to produce the observed iron lines. If the iron were concentrated at the cluster core, it would all be located in regions of high electron density, so that the iron line emissivity per iron ion would be higher than the average emissivity per hydrogen ion (Sec. V.B). The amount of iron needed to produce the observed iron lines could be reduced by as much as a factor of 20 (Abramopoulos *et al.*, 1981). Since the production of a nearly solar abundance of iron is one of the major problems with galaxy formation in clusters and the origin of the intracluster gas, the possibility that the real abundance might be much lower is very important. Unfortunately, all of the available spectra of the 7-keV iron line in clusters have been made with low-spatial-resolution detectors, which do not provide sufficient information on the location of the iron. The observation of spatially resolved spectra of clusters including the 7-keV iron line are critically important to our understanding of clusters, and will be possible if the *AXAF* satellite is launched (Sec. VI).

6. Convection and mixing

The diffusive transport processes discussed so far tend to cause the gas in a cluster to be isothermal, tend to damp out fluid motions, and tend to cause heavy elements to settle to the cluster center. On the other hand, mixing processes due to turbulent motions of the intracluster gas tend to make the specific entropy (the entropy per atom) equal within the cluster, tend to make the composition of the gas homogeneous, and drive fluid motions. It is conventional to describe a gas in which the entropy per atom is constant as an "adiabatic" gas. If mixing occurs on a time scale that is rapid compared to the age of the cluster or the time scale for diffusive transport, the resulting intracluster gas distribution will tend to be adiabatic and to have constant heavy-element abundances.

One possible source of mixing motions in the gas is convection. If the intracluster gas were hydrostatic but had a steep temperature gradient

$$-\frac{d \ln T_g}{dr} > -\frac{2}{3} \frac{d \ln n_p}{dr}, \quad (5.52)$$

it would be unstable to convective mixing. If the temperature gradient in Eq. (5.52) were exceeded by a significant amount, mixing would occur within several sound crossing times in the cluster. Since this is a rather short time [Eq. (5.54) below], it is reasonable to assume that the temperature gradient is smaller than that in Eq. (5.52).

Motions of galaxies through the intracluster gas may mix the gas. This process has not been treated in any great detail in the literature. It might be reasonable to assume that each galaxy mixes the gas within a wake of radius R_W . Very roughly, the gas within the whole cluster would be mixed on a time scale given by

$$t_{\text{mix}} \sim \frac{1}{n_{\text{gal}} \sigma_r \pi R_W^2} \left[\frac{r_c}{R_W} \right]^2, \quad (5.53)$$

where n_{gal} is the number density of galaxies, σ_r is their velocity dispersion, and r_c is the cluster core radius. Depending on whether the galaxy contained any interstellar medium or not, the wake radius might be ~ 10 kpc, or only as large as the accretion radius (Sec. V.C.4). The resulting value of t_{mix} is generally much longer than 10^{11} yr for any reasonable values of the cluster parameters, and mixing due to galaxy motions is probably not very important. Nepveu (1981b) discussed the mixing of gas ejected from cluster galaxies and showed that the mixing was not effective unless the galaxy motions were highly subsonic, which is not the case. His calculations indicated that the gas remained inhomogeneous on both small and large scales.

Large-scale hydrodynamic motions during the formation of the cluster may be effective in mixing the intracluster gas. Similarly, mixing may occur when subclusters merge within the cluster.

E. Distribution of the intracluster gas—hydrostatic models

In general, the elastic collision times for ions and electrons [Eqs. (5.32) and (5.33)] in the intracluster gas are much shorter than the time scales for heating or cooling (Sec. V.C) or any dynamical process, and the gas can be treated as a fluid. The time required for a sound wave in the intracluster gas to cross a cluster is given by

$$t_s = 6.6 \times 10^8 \text{ yr} \left[\frac{T_g}{10^8 \text{ K}} \right]^{-1/2} \left[\frac{D}{\text{Mpc}} \right], \quad (5.54)$$

where T_g is the gas temperature and D is the cluster diameter. Since this time is short compared to the probable age of a cluster of 10^{10} yr, the gas will be hydrostatic unless the cluster gravitational potential varies on a shorter time scale or the gas is heated or cooled more rapidly than this. The cooling time due to thermal bremsstrahlung [Eq. (5.23)] is much longer than the sound crossing time, and the same is true for the time scales for heating by any of the processes that have been suggested (Sec. V.C). Thus the gas distribution is usually assumed to be hydrostatic:

$$\nabla P = -\rho_g \nabla \phi(r), \quad (5.55)$$

where $P = \rho_g k T_g / \mu m_p$ is the gas pressure, ρ_g is the gas density, and $\phi(r)$ is the gravitational potential of the cluster. If the cluster is assumed to be spherically symmetric, Eq. (5.55) reduces to

$$\frac{1}{\rho_g} \frac{dP}{dr} = -\frac{d\phi}{dr} = -\frac{GM(r)}{r^2}, \quad (5.56)$$

where r is the radius from the cluster center and $M(r)$ is the total cluster mass within r . If the contribution of the intracluster gas to the gravitational potential is ignored, then the distribution of the intracluster gas is determined by the cluster potential $\phi(r)$ and the temperature distribution of the gas $T_g(r)$. Further, then Eq. (5.56) is a linear equation for the logarithm of the gas density; the central density (or any other value) can be specified in order to determine the full run of densities. If self-gravity is included, then the density scale, temperature variation, and cluster potential cannot be given independently.

In most models, the cluster potential is assumed to be that of a self-gravitating isothermal sphere (Sec. II.G.1). For convenience, the analytic King approximation to the isothermal sphere is often assumed [Eq. (2.13)], so that the cluster total density, mass, and potential are given by

$$\rho(r) = \rho_0 (1 + x^2)^{-3/2}, \quad (5.57)$$

$$M(r) = 4\pi\rho_0 r_c^3 \left\{ \ln [x + (1 + x^2)^{1/2}] - x (1 + x^2)^{-1/2} \right\}, \quad (5.58)$$

$$\phi(r) = -4\pi G\rho_0 r_c^2 \frac{\ln [x + (1 + x^2)^{1/2}]}{x}, \quad (5.59)$$

$$x \equiv \frac{r}{r_c}.$$

Here, ρ_0 is the central density and r_c is the core radius of the cluster (Sec. II.G). The central density and core radius are related to the line-of-sight velocity dispersion σ_r (Sec. II.F) of an isothermal cluster by

$$\sigma_r^2 = \frac{4\pi G\rho_0 r_c^2}{9}, \quad (5.60)$$

which follows from Eq. (2.9). Thus the central value of the cluster gravitational potential is

$$\phi_0 = -9\sigma_r^2. \quad (5.61)$$

It is perhaps worth noting that although the analytic King model is a good fit to the inner portions of an isothermal sphere, the analytic King potential has a finite depth [given by Eq. (5.61)], while the isothermal sphere potential is infinitely deep. The total mass associated with the analytic King distribution diverges as the radius increases, and it is usual to cut the distribution off in some way [Eqs. (2.11) and (2.12)]. The effect of these cut-offs on the cluster potential and on the resulting hydrostatic gas models is discussed in Sarazin and Bahcall (1977) and Bahcall and Sarazin (1978).

In calculating the cluster potential, we have ignored the effect of individual galaxies. The potential wells associat-

ed with individual galaxies are considerably shallower than those associated with clusters. This is shown by the fact that the velocity dispersions of stars in galaxies ($\sigma_* \sim 300$ km/sec; Faber and Gallagher, 1979) are much smaller than the velocity dispersions of galaxies in clusters ($\sigma_r \sim 1000$ km/sec); the gravitational potentials increase with the square of the velocity dispersions. Thus an individual galaxy will not significantly perturb the distribution of intracluster gas (Gull and Northover, 1975).

1. Isothermal distributions

The simplest distribution of gas temperatures would be an isothermal distribution, with T_g being constant. The intracluster gas would become isothermal if thermal conduction were sufficiently rapid [see Eq. (5.41) for the relevant time scale]. Alternatively, the gas may have been introduced into the cluster with an approximately constant temperature, and its thermal distribution be unchanged since that time. Lea *et al.* (1973) fit the gas distributions in the Coma, Perseus, and M87/Virgo clusters, assuming that the gas distribution was self-gravitating and isothermal. If $\phi(r)$ is due only to ρ_g , then Eq. (5.56) and Poisson's equation for the gravitational potential are equivalent to Eq. (2.9), the equation of an isothermal sphere. Note, however, that this is not trivially true, since Eq. (2.9) was derived from the stellar dynamical equation for a collisionless gas, while Eq. (5.56) is the hydrostatic equation for a collisionally dominated fluid. Lea *et al.* therefore used Eq. (5.57) to fit the gas density ρ_g . This is not consistent, since the gas masses derived from these fits were generally less than 20% of the virial mass of the cluster, and the core radii derived were larger than those of the galaxies (Sec. III.D).

More consistent isothermal models can be derived if the gravitational potential of the cluster is not assumed to come only from the gas (Cavaliere and Fusco-Femiano,

1976,1978; Sarazin and Bahcall, 1977). Equation (5.56) can be written

$$\frac{d \ln \rho_g}{dr} = -\frac{\mu m_p}{k T_g} \frac{d\phi(r)}{dr}. \quad (5.62)$$

If the potential is given by Eqs. (5.59) and (5.61), then the gas distribution is given by

$$\rho_g(r) = \rho_{g0} \left[1 + \left(\frac{r}{r_c} \right)^2 \right]^{-3\beta/2}. \quad (5.63)$$

Here

$$\begin{aligned} \beta &\equiv \frac{\mu m_p \sigma_r^2}{k T_g} \\ &= 0.76 \left[\frac{\sigma_r}{10^3 \text{ km sec}^{-1}} \right]^2 \left[\frac{10^8 \text{ K}}{T_g} \right]^{-1}, \end{aligned} \quad (5.64)$$

where the numerical value follows if solar abundances are assumed so that $\mu = 0.63$. Another way to derive Eq. (5.63) is to note that if the galaxy velocity dispersion is isotropic, the galaxy density ρ_{gal} in a cluster will be given by Eq. (5.62), replacing $kT_g/\mu m_p$ with σ_r^2 . Then eliminating the potential between the equations for ρ_g and ρ_{gal} yields $\rho_g \propto \rho_{\text{gal}}^\beta$, and Eq. (5.63) follows if the galaxy distribution is given by Eq. (5.57) (Cavaliere and Fusco-Femiano, 1976).

This self-consistent isothermal model [Eq. (5.63)] assumes that the gas and galaxy distributions are both static and isothermal and that the galaxy and total mass distributions are identical. While none of these assumptions is fully justified, and the gas is probably not generally isothermal, this model has the advantage that the resulting gas distribution is analytic and that basically all the integrals needed to compare the model to the observations of clusters are also analytic. For example, the total gas mass and emission integral [Eq. (5.20)] are

$$M_g = \begin{cases} \pi^{3/2} \rho_{g0} r_c^3 \frac{\Gamma[3(\beta-1)/2]}{\Gamma(3\beta/2)} & (\beta > 1) \\ 3.15 \times 10^{12} M_\odot \left[\frac{n_0}{10^{-3} \text{ cm}^{-3}} \right] \left[\frac{r_c}{0.25 \text{ Mpc}} \right]^3 \frac{\Gamma[3(\beta-1)/2]}{\Gamma(3\beta/2)}, & \end{cases} \quad (5.65)$$

$$\text{EI} = \begin{cases} \pi^{3/2} \left[\frac{n_e}{n_p} \right] n_0^2 r_c^3 \frac{\Gamma(3\beta - \frac{3}{2})}{\Gamma(3\beta)} & (\beta > \frac{1}{2}) \\ 3.09 \times 10^{66} \text{ cm}^{-3} \left[\frac{n_0}{10^{-3} \text{ cm}^{-3}} \right]^2 \left[\frac{r_c}{0.25 \text{ Mpc}} \right]^3 \frac{\Gamma(3\beta - \frac{3}{2})}{\Gamma(3\beta)}, & \end{cases} \quad (5.66)$$

where n_0 is the central proton density, Γ is the gamma function, and solar abundances have been assumed in deriving the numerical values. The values of β in the parentheses give the limits such that the appropriate integrals converge at large radii. Similarly, the x-ray sur-

face brightness at a projected radius b is proportional to the emission measure EM, defined as

$$\text{EM} \equiv \int n_p n_e dl, \quad (5.67)$$

where l is the distance along the line-of-sight through the

cluster at a projected radius b . Then, for the self-consistent isothermal model, the emission measure is

$$\text{EM} = \sqrt{\pi} \left[\frac{n_e}{n_p} \right] n_0^2 r_c \frac{\Gamma(3\beta - \frac{1}{2})}{\Gamma(3\beta)} (1 + x^2)^{-3\beta + 1/2} \quad (\beta > \frac{1}{6}), \quad (5.68)$$

where $x \equiv b/r_c$. The microwave diminution (Sec. IV.E) at low frequencies is given by

$$\frac{\Delta T_r}{T_r} = - \frac{2\sqrt{\pi}\sigma_T k T_g}{m_e c^2} \left[\frac{n_e}{n_p} \right] n_0 r_c \frac{\Gamma(3\beta/2 - \frac{1}{2})}{\Gamma(3\beta/2)} \times (1 + x^2)^{-(3\beta-1)/2} \quad (\beta > \frac{1}{3}), \quad (5.69)$$

where σ_T is the Thomson cross section, and T_r is the cosmic background radiation temperature. Numerically,

$$\begin{aligned} \Delta T_r &= 0.10 \text{ mK} \left[\frac{n_0}{10^{-3} \text{ cm}^{-3}} \right] \left[\frac{T_g}{10^8 \text{ K}} \right] \\ &\times \left[\frac{r_c}{0.25 \text{ Mpc}} \right] \left[\frac{T_r}{2.7 \text{ K}} \right] \\ &\times \frac{\Gamma(3\beta/2 - \frac{1}{2})}{\Gamma(3\beta/2)} (1 + x^2)^{-3\beta/2 + 1/2}. \quad (5.70) \end{aligned}$$

Equation (5.68) has been used extensively to model the surface brightness $I(b)$ of the x-ray emission from clusters (Gorenstein *et al.*, 1978; Branduardi-Raymont *et al.*, 1981; Abramopoulos and Ku, 1983; Jones and Forman, 1984; Sec. III.D.1). The most accurate data have come from the *Einstein* x-ray satellite, which was sensitive only to low-energy x rays ($h\nu < 4$ keV). For high-temperature gas ($T_g \geq 3 \times 10^7$ K), the low-energy x-ray emissivity is nearly independent of temperature, and thus $I(b) \propto \text{EM}$ even if the gas temperature varies. Large surveys of x-ray distributions fit by Eq. (5.68) have been made by Abramopoulos and Ku (1983), who set $\beta = 1$ (equal gas and galaxy distributions), and Jones and Forman (1984), who allowed β to vary. Figure 11 shows the data on the x-ray surface brightness of three clusters from Jones and Forman (1984) and their best fit models using Eq. (5.68). Equation (5.68) is a good fit to the majority of clusters, but fails in the central regions of some clusters, possibly because these clusters contain cooling accretion flows (Secs. III.C.3, III.D.1, and V.G). The average value of β determined by fits to the x-ray surface brightness of a large number of clusters was found to be (Jones and Forman, 1984)

$$\langle \beta_{\text{fit}} \rangle = 0.65. \quad (5.71)$$

Thus the x-ray surface brightness and implied gas density vary on average as

$$I_x(b) \propto \left[1 + \left[\frac{b}{r_c} \right]^2 \right]^{-3/2}, \quad (5.72)$$

$$\rho_g(r) \propto \left[1 + \left[\frac{r}{r_c} \right]^2 \right]^{-1}. \quad (5.73)$$

This indicates that the gas density should fall off less rapidly with radius than the galaxy density (in agreement with many other observations, such as Abramopoulos and Ku, 1983), and that the energy per unit mass is higher in the gas than in the galaxies (Jones and Forman, 1984). For this average value of β , the total x-ray luminosity converges, but the total gas mass given by Eq. (5.65) does not.

Unfortunately, this does not agree with the determinations of the x-ray spectral temperatures and the galaxy velocity dispersions of clusters (Mushotzky, 1984). For example, the observed correlation between σ_r and T_g in Eq. (3.10) implies that the average value β determined by gas temperatures and galaxy velocity dispersions is $\langle \beta_{\text{spect}} \rangle \approx 1.3$. From a sample of clusters with well-determined spectra, Mushotzky (1984) finds $\langle \beta_{\text{spect}} \rangle \approx 1.2$, which he notes is about twice the value determined from observations of the x-ray surface brightness. While Jones and Forman (1984) argue that their values of β_{fit} are in excellent agreement with the determinations from spectral observations, in fact their data show that the two values do not agree to within the errors in the majority of cases. For the clusters they studied $\langle \beta_{\text{spect}} \rangle \approx 1.1$. Thus the general result seems to be that

$$\langle \beta_{\text{spect}} \rangle \approx 1.2 \approx 2 \langle \beta_{\text{fit}} \rangle. \quad (5.74)$$

A number of suggestions have been made as to the origin of this discrepancy. First, the gas may very well not be isothermal. However, Mushotzky (1984) has argued that the same problem occurs for other thermal distributions in the gas. Second, it may be that the line-of-sight velocity dispersion does not represent accurately the energy per unit mass of the galaxies. Equation (5.63) assumes that the galaxy velocity distribution is isotropic. The distribution could be anisotropic, either if the cluster is highly flattened (Sec. II.I.3) or if the cluster is spherical but galaxy orbits are largely radial (rather than having a uniform distribution of eccentricities; see Sec. II.H). A detailed study (Kent and Sargent, 1983) of the positions and velocities of galaxies in the Perseus cluster has produced a more accurate description of the cluster potential and significantly reduced the discrepancy, although it still is significant. Third, it may be that many of the galaxy velocity dispersions measured for clusters are contaminated by foreground or background groups (Geller and Beers, 1982). The velocity dispersions may also be affected by subclustering or nonvirialization of the cluster. All of these effects will cause the data to overestimate the actual velocity dispersion (the cluster potential), and thus to overestimate β_{spect} . Perhaps one indication that such systematic errors in the velocity dispersion might be occurring is that Coma, the best studied regular cluster, does not show a β discrepancy.

The discrepancy between the globally determined x-ray temperatures of clusters and their surface brightness will

probably only be resolved when spatially resolved x-ray spectra are available, allowing a simultaneous determination of the spatial variation of the gas density and temperature (Sec. VI).

One of the derivations of the self-consistent isothermal model involves noting that the galaxy distribution also solves the hydrostatic equation if the galaxy velocity dispersion is isotropic [see discussion following Eq. (5.64)]. If the galaxy distribution is spherical, but the galaxy velocity dispersions in the directions parallel to the cluster radius (σ_r) and transverse to that direction (σ_t) are different, this derivation fails. However, for a constant (isothermal) galaxy velocity dispersion and a constant anisotropy of the velocity dispersion $\eta \equiv 1 - \sigma_t^2/\sigma_r^2$, the gas density is given by $\rho_g \propto (\rho_{gal} r^{2\eta})^\beta$ (White, 1985).

Finally, Henry and Tucker (1979) have pointed out the existence of a simple relationship $(L_x r_c)^{2/5} \propto T_g$ between x-ray temperatures, luminosities, and core radii in clusters based on the isothermal model.

2. Adiabatic and polytropic distributions

The intracluster gas will be isothermal if thermal conduction is sufficiently rapid (Sec. V.D.2). On the other hand, if thermal conduction is slow, but the intracluster gas is well mixed, then the entropy per atom in the gas will be constant (Sec. V.D.6). In an adiabatic gas, the pressure and density are simply related,

$$P \propto \rho^\gamma, \quad (5.75)$$

where γ is the usual ratio of specific heats and is $\gamma = \frac{5}{3}$ for a monatomic ideal gas. While the value of $\frac{5}{3}$ would be expected to apply if the intracluster gas were strictly adiabatic, Eq. (5.75) is often used to parametrize the thermal distribution of the intracluster gas, with γ taken to be a fitting parameter. For example, $\gamma = 1$ implies that the gas distribution is isothermal. Intracluster gas models with an arbitrary value of γ are often referred to as "polytropic" models, and γ is called the polytropic index. Intracluster gas models with the polytropic index $\gamma > \frac{5}{3}$ are convectively unstable [Eq. (5.52)], and thus hydrostatic polytropic models must have $1 \leq \gamma \leq \frac{5}{3}$.

Adiabatic and polytropic intracluster gas distributions were introduced by Lea (1975), Gull and Northover (1975), and Cavaliere and Fusco-Femiano (1976). Given Eq. (5.75), the hydrostatic equation (5.55) can be rewritten by noting that

$$\frac{1}{\rho_g} \nabla P = \frac{\gamma}{\gamma - 1} \frac{k}{\mu m_p} \nabla T_g, \quad (5.76)$$

so that

$$\begin{aligned} \frac{T_g}{T_{g0}} &= 1 + (\alpha - 1) \left[1 - \frac{\phi(r)}{\phi_0} \right], \\ \frac{\rho_g}{\rho_{g0}} &= \left[\frac{T_g}{T_{g0}} \right]^{1/(\gamma-1)}. \end{aligned} \quad (5.77)$$

Here, ϕ_0 , T_{g0} , and ρ_{g0} are the central values of the cluster gravitational potential, the intracluster gas temperature, and the density, respectively. In nonspherical clusters, "central" means the lowest point in the cluster gravitational potential.

From Eq. (5.77), it is clear that the intracluster gas temperature will always decrease with increasing distance from the cluster center in adiabatic or polytropic models.

The integration constant α is defined as

$$\alpha \equiv \frac{T_{g0}}{T_{g\infty}}, \quad (5.78)$$

where $T_{g\infty}$ is the gas temperature at infinity. If $\alpha > 0$, the gas distribution extends to infinity, and the gas is not gravitationally bound to the cluster. If $\alpha < 0$, the gas extends only to a finite distance at which $\phi(r)/\phi_0 = \alpha/(\alpha-1)$, and the gas is gravitationally bound to the cluster. In the $\alpha > 0$ models, the intracluster gas connects with and is confined by intercluster gas, whose temperature is given by $T_{g\infty}$. In general, the central gas temperature is given by

$$T_{g0} = -\frac{\gamma - 1}{\gamma} \frac{\mu m_p \phi_0}{k(1 - \alpha)}. \quad (5.79)$$

The enthalpy per particle in these models is a constant, both spatially and temporally, and is given by $h = \alpha(\gamma/\gamma-1)kT_{g0}$. Thus models with $\alpha \approx 0$ cool very rapidly (Bahcall and Sarazin, 1978). Reasonably bound, intracluster gas models therefore usually assume $\alpha \leq 0.1$.

If Eq. (5.59) is used for the cluster potential, then the gas density and temperature are analytic functions of radius in the cluster, but are sufficiently complex that the integrals for emission measures, masses, and so on are not analytic. Moreover, since the gas is not isothermal, the x-ray surface brightness and the emission measure are not simply related. Spectra, x-ray surface brightness profiles, masses, microwave diminutions, and a number of other quantities for these models are given in Sarazin and Bahcall (1977) and Bahcall and Sarazin (1978). Fits of these models to the surface brightness and spectra of a number of clusters are given in Bahcall and Sarazin (1977) and Mushotzky *et al.* (1978).

3. More complicated distributions

The models discussed above assume that clusters are spherical, that the gas is hydrostatic, that the cluster potential is known in advance, and that the entropy distribution in the gas is given by a very simple polytropic distribution. Intracluster gas models have been calculated which attempt to generalize each of these assumptions. Here, some more complicated hydrostatic models are reviewed.

Stimpel and Binney (1979; see also Binney and Stimpel, 1978) showed how spheroidal models for the intracluster gas distribution could be derived, using the observed galaxy distribution to determine the shape of the cluster potential. These models were fit to the galaxy counts in

the Coma cluster, and models for the distribution of x-ray emission and microwave diminution (Sec. IV.E) were derived. There is an uncertainty in the shape of the cluster potential because the galaxy counts themselves cannot determine whether the cluster shape is more nearly prolate or oblate. However, Stimpel and Binney show that the resulting x-ray distributions in the two cases are considerably different, and thus x-ray observations can be used to determine the true shapes of elongated clusters.

In general, the entropy distribution in a cluster will depend on the origin of the intracluster gas and the history of cluster. A number of authors have solved the hydrodynamic equations for simple models for the origin of the intracluster gas and of the subsequent history of the cluster; these calculations will be reviewed in Sec. V.J. It is perhaps not surprising that these calculations do not generally lead to entropy distributions of the very simple sort (isothermal, adiabatic, or polytropic) considered above.

A number of authors have attempted to model these more detailed entropy distributions by allowing the polytropic index or the isothermal parameter β to vary with radius. One example is to allow the gas to be isothermal in the cluster core, where conduction is effective (Sec. V.D.2), but adiabatic in the outer parts (Cavaliere and Fusco-Femiano, 1978; Cavaliere, 1980). Cavaliere and Fusco-Femiano (1978) also included the effect of the gas density on the cluster potential.

4. Empirical gas distributions derived by surface brightness deconvolution

The gas distributions in clusters can be derived directly from observations of the x-ray surface brightness of the cluster, if the shape of the cluster is known and if the x-ray observations are sufficiently detailed and accurate. The x-ray surface brightness at a photon frequency ν and at a projected distance b from the center of a spherical cluster is

$$I_\nu(b) = \int_b^\infty \frac{\epsilon_\nu(r) dr^2}{(r^2 - b^2)^{1/2}}, \quad (5.80)$$

where ϵ_ν is the x-ray emissivity. This Abel integral can be inverted to give the emissivity as a function of radius,

$$\epsilon_\nu = \frac{-1}{2\pi r} \frac{d}{dr} \int_r^\infty \frac{I_\nu(b) db^2}{(b^2 - r^2)^{1/2}}. \quad (5.81)$$

Because of the quantized nature of the observations of the x-ray surface brightness (photon counts per solid angle) and the sensitivity of integral deconvolutions to noise in the data, the x-ray surface brightness data are often smoothed, either by fitting a smooth function to the observations or by applying these equations to the surface brightness averaged in rings about the cluster center.

Now, the emissivity is given by Eq. (5.19) and depends on the elemental abundances, the density of the gas, and the gas temperature. Thus the distribution of these three properties in the cluster could be determined from observations of the x-ray surface brightness $I_\nu(b)$. Basically,

the continuum emission is due mainly to free-free emission [Eq. (5.11)] and is relatively insensitive to the heavy-element abundances, while the line emission measures these abundances. For a given set of abundances, the emissivity can be written as

$$\epsilon_\nu = n_e^2 \Lambda_\nu(T_g), \quad (5.82)$$

where $\Lambda_\nu(T_g)$ is n_p/n_e times the sum on the right side of Eq. (5.19). Thus $\epsilon_\nu(r)$ can be found from observations of the x-ray surface brightness as a function of photon frequency, and the frequency dependence and magnitude of ϵ_ν give the local gas temperature and density.

If the density and temperature of the intracluster gas are known, and the gas is assumed to be hydrostatic, the hydrostatic equation (5.56) gives the total cluster mass as a function of radius. This method of determining the mass has a number of advantages over the use of the virial theorem (Sec. II.H). First, the orbits of gas particles (isotropic velocities) are known because the gas is collisional. Second, this method gives the mass as a function of radius, rather than the total mass alone. Third, the statistical accuracy of this method is not limited by the number of galaxies in the cluster; the statistical accuracy can be improved by lengthening the observation time.

Unfortunately, observations of $I_\nu(b)$ are really not available for clusters. These observations require an instrument with good spatial and spectral resolution. Most of the x-ray spectra of clusters have been taken with instruments having very poor spatial resolution (comparable to the size of the cluster; Sec. III.C.1). High-spatial-resolution observations of clusters have primarily come from the *Einstein* x-ray observatory (Sec. III.D). The imaging instruments on *Einstein* had only limited spectral resolution. Moreover, the optics in *Einstein* could only focus soft x-rays ($h\nu \lesssim 4$ keV). At typical gas temperatures in clusters ($kT_g \sim 6$ keV), most of the x-ray emissivity is due to thermal bremsstrahlung, and the emissivity is nearly independent of frequency for $h\nu \lesssim kT_g$. Thus the *Einstein* surface brightness distributions cannot be used directly to determine the local temperature. If the limited spectral resolution of the *Einstein* imagers is ignored, their observations provide $\langle I_x(b) \rangle$, the surface brightness averaged over the sensitivity of the detector as a function of photon frequency. From $\langle I_x(b) \rangle$, the sensitivity-averaged emissivity

$$\langle \epsilon_x(r) \rangle = n_e^2 \langle \Lambda_x(T_g) \rangle \quad (5.83)$$

can be found from Eq. (5.81). Unfortunately, even if the elemental abundances are assumed to be known, this equation provides only one quantity at each radius, and it is impossible to determine both n_e and T_g .

In many analyses of x-ray cluster observations, a second equation for the density and temperature has been provided by assuming that the intracluster gas is hydrostatic and that the cluster potential is known. The hydrostatic equation in a spherical cluster (5.56) can be rewritten as

$$\frac{d \ln (n_e T_g)}{d \ln r} = - \frac{GM(r)\mu m_p}{rkT_g}, \quad (5.84)$$

where $M(r)$ is the total cluster mass and the mean atomic weight $\mu \sim 0.63$ is assumed to be independent of radius. Combining this with Eq. (5.83) gives

$$\left[1 - \frac{1}{2} \frac{d \ln \langle \Lambda_x \rangle}{d \ln T_g} \right] \frac{d \ln T_g}{d \ln r} = - \frac{GM(r)\mu m_p}{rkT_g} - \frac{1}{2} \frac{d \ln \langle \epsilon_x \rangle}{d \ln r}. \quad (5.85)$$

This is an ordinary differential equation for $T_g(r)$, which can be integrated given a boundary condition. This has been taken to be the central temperature (White and Silk, 1980) or the intergalactic pressure (Fabian, Hu, Cowie, and Grindlay, 1981). Given $T_g(r)$, Eq. (5.83) gives the density profile.

Various versions of this method have been used to determine gas distributions in a large number of clusters using data from *Einstein* (White and Silk, 1980; Fabricant *et al.*, 1980; Fabian, Ku *et al.*, 1981; Nulsen *et al.*, 1982; Fabricant and Gorenstein, 1983; Canizares *et al.*, 1983; Stewart, Canizares, Fabian, and Nulsen, 1984; Stewart, Fabian, Jones, and Forman, 1984). In some cases, spectral information from *Einstein* or low-spatial-resolution spectra have been used to further constrain the temperature profiles or to determine the form of the cluster potential necessary for a consistent fit. These analyses have provided information on the mass distribution in clusters and central galaxies (M87, in particular), the gas distributions in clusters, and the prevalence of cooling accretion flows in clusters. These topics will be discussed in more detail later in this review.

Gas temperature and density profiles could be derived more directly if high-spatial-and-spectral-resolution data at photon energies up to 10 keV were available. The proposed *AXAF* satellite will have these capabilities (Sec. VI).

5. Chemically inhomogeneous equilibrium models

The heavier an ion is, the slower its thermal motion in the intracluster gas will be. As a result, heavy ions will tend to drift toward the center of the cluster. In Sec. V.D.5 the drift rate was calculated and shown to be rather slow, although the precise value depends on cluster parameters. Further, the intracluster magnetic field may be very effective in retarding any sedimentation of heavy elements. Nonetheless, it is possible that heavier elements may have drifted to the cluster center in some cases, or been introduced into the intracluster gas quite near the center. Eventually, the motion of heavy ions towards the cluster center will stop when the resulting charge separation produces an electric field that cancels the effect of the gravitational field.

Abramopoulos *et al.* (1981) have calculated chemically inhomogeneous models for the intracluster gas in thermodynamic equilibrium. The temperature of the gas is therefore constant, both spatially and among the various ions and electrons. These models satisfy the hydrostatic equation (5.55) for the total pressure, but this does not uniquely define the chemically inhomogeneous model, since any value of the total pressure can be attributed to an infinite number of different combinations of partial pressures of different ions. In thermodynamic equilibrium, the number density of any ion is given by the Boltzmann equation

$$n_i(r) = n_{i0} \exp \left[- \frac{A_i m_p \phi(r) + Z_i e \phi_E(r)}{kT_g} \right], \quad (5.86)$$

where A_i , Z_i , and n_{i0} are the mass, charge, and central density of the ion i . The cluster gravitational potential ϕ and electrical potential ϕ_E are defined in this equation to be zero at the cluster center. The gravitational potential is assumed to be fixed and known, as in most of the hydrostatic models discussed in the previous sections. The electrical potential is given as a solution of Poisson's equation

$$\nabla^2 \phi_E(r) = -4\pi \sum_i n_i(r) Z_i e, \quad (5.87)$$

where the sum includes electrons as one of the ionic species. Because the coupling constant for electrical forces exceeds that of gravitational forces by $\sim 10^{40}$, while the fraction of the cluster mass due to intracluster gas is much greater than the inverse of this, the electrical potential will generally be quite small $\phi_E \sim -\phi m_p/e$, and a sufficient approximation to the solution of Eq. (5.87) is to assume that the gas is very nearly electrically neutral:

$$\sum_i n_i Z_i = 0. \quad (5.88)$$

The electric potential is then given by requiring a simultaneous solution of Eqs. (5.86) and (5.88), and requiring that the total abundance $\int n_i dV$ of each of the ions be fixed.

In the case where the plasma can be assumed to consist only of protons and electrons, with the abundances of all heavy elements being so low that they do not contribute to the potential, the solution for the ion and electron densities is the same as the isothermal hydrostatic solution given above [Eq. (5.63)], the electric potential is $\phi_E = -m_p \phi/2e$, and the densities of any trace heavy elements will be

$$n_i = n_{i0} \left(\frac{n_p}{n_{p0}} \right)^{2A_i - Z_i}. \quad (5.89)$$

Unfortunately, the abundance of helium certainly cannot be treated as insignificant, and other heavier elements may contribute to the electric potential near the cluster core. Equations (5.86) and (5.88) have been solved numerically by Abramopoulos *et al.* (1981), assuming an analytic King potential for the cluster, taking the gas tempera-

ture to be $\beta = \frac{2}{3}$ [Eq. (5.64)], and assuming a range of heavy-element abundances from pure hydrogen and helium to solar. They find that the heavy elements are strongly concentrated at the cluster core. To balance the resulting increase in the charge density, the electrons also must be centrally condensed.

The concentration of heavy elements at the cluster core, where the electron density is high, results in an increase in the x-ray line intensity for a given set of heavy-element abundances. As a result, Abramopoulos *et al.* (1981) argue that the observed line strengths could be produced by gas with iron abundances of only $\frac{1}{20}$ of solar.

F. Wind models for the intracluster gas

If the rate of heating of the intracluster medium is sufficiently large, the gas will be heated to the escape temperature from the cluster, and will form a wind leaving the cluster. Since the sound crossing time across a cluster is relatively short [Eq. (5.54)], the cluster would be emptied of gas rapidly unless gas were constantly being added to the cluster. Yahil and Ostriker (1973) suggested that gas is being injected into the intracluster medium at rates of $10^3 - 10^4 M_\odot/\text{yr}$, and is sufficiently heated to produce a steady-state outflow of gas.

Let $\dot{\rho}$ be the rate of mass input per unit volume into the intracluster gas, and let $h(r)$ be the heating rate per unit volume. If the cluster is assumed to be spherically symmetric, with a gravitational potential $\phi(r)$, and the gas is injected into the cluster with no net velocity, but with the velocity dispersion of the galaxies, then the hydrodynamic equations for a steady-state wind are

$$\begin{aligned} \frac{1}{r^2} \frac{d}{dr} (r^2 \rho_g v) &= \dot{\rho}, \\ \dot{\rho} v + \rho_g v \frac{dv}{dr} + \frac{dP}{dr} + \rho_g \frac{d\phi(r)}{dr} &= 0, \\ \frac{1}{r^2} \frac{d}{dr} \left[r^2 \rho_g v \left(\frac{v^2}{2} + \frac{5}{2} \frac{P}{\rho_g} + \phi(r) \right) \right] &= h(r) + \dot{\rho} \left[\frac{3}{2} \sigma_r^2(r) + \phi(r) \right], \end{aligned} \quad (5.90)$$

where ρ_g , P , and v are, respectively, the gas density, pressure, and velocity, and σ_r is the one-dimensional velocity dispersion of the galaxies in the cluster.

Yahil and Ostriker argued that the source of mass input into the cluster was mass loss by stars in cluster galaxies, and that

$$\dot{\rho}(r) = \alpha_* \rho(r), \quad (5.91)$$

where ρ is the total mass density of the cluster and α_*^{-1} is the characteristic time scale for gas ejection from galaxies. They argued that $\alpha_*^{-1} \sim 10^{12}$ yr.

Yahil and Ostriker considered two mechanisms that might heat the gas. First, if the gas were ejected by supernovas it could be heated within galaxies before being ejected into the cluster [Sec. V.C.3; Eq. (5.27)]; they referred to this as the HIG (heating in galaxies) model. De-

fining $\lambda \equiv 3kT_{\text{ej}}/(2\mu m_p \sigma_r^2)$, the heating rate due to ejection from galaxies becomes

$$h(r) = \lambda \sigma_r^2 \dot{\rho}. \quad (5.92)$$

Alternatively, Yahil and Ostriker suggested that the heating might be due to the motion of galaxies through the cluster (Sec. V.C.4); they referred to this as the HBF (heating by friction) model. Then, the heating rate is

$$h(r) = \pi \langle R_D^2 \Delta v^3 \rangle \rho_g \left[\frac{\rho(r)}{m_{\text{gal}}} \right], \quad (5.93)$$

where R_D is the drag radius [Eq. (5.28)], $m_{\text{gal}} \equiv \rho/n_{\text{gal}}$ is the total cluster mass per galaxy, Δv is the velocity of the galaxy relative to the gas (which is moving at v), and the average is over the Gaussian distribution of galaxy velocities. It is useful to define $\lambda(r)$ such that $h(r) \equiv \lambda(r) \sigma_r^2 \dot{\rho}$, so that λ is constant in the HIG model, and $\lambda(r) \sim \pi R_D^2 \rho_g \sigma_r / \alpha_* m_{\text{gal}}$ in the HBF model.

Let the cluster density be given by $\rho = \rho_0 g(x)$, where ρ_0 is the central density, $x \equiv r/r_c$, r_c is the cluster core radius, and $g(x)$ is a dimensionless function. Similarly, let the cluster potential be written as $\phi(r) = \phi_0 \bar{\phi}(x)$, where ϕ_0 is the central potential. If the mass distribution is assumed to be isothermal, so that σ_r is constant and is related to the cluster central potential ϕ_0 and the central density ρ_0 by Eqs. (5.60) and (5.61), then the equation of continuity becomes

$$\begin{aligned} x^2 \rho_g v &= \alpha_* \rho_0 r_c G(x), \\ G(x) &\equiv \int_0^x g(x') (x')^2 dx'. \end{aligned} \quad (5.94)$$

If the King analytic form of the cluster density is assumed, then g , G , and $\bar{\phi}$ are given by the functions on the right sides of Eqs. (5.57), (5.58), and (5.59), respectively. The energy equation can also be integrated to give

$$\frac{1}{2} v^2 + \frac{5}{2} \frac{P}{\rho_g} = \sigma_r^2 \left[\Lambda(x) + \frac{3}{2} + 9\bar{\phi} - 9\Phi \right], \quad (5.95)$$

where Λ and Φ are the integrated heating rate and potential energy

$$\begin{aligned} \Lambda(x) &\equiv \frac{\int_0^x g(x') \lambda(x') (x')^2 dx'}{G(x)}, \\ \Phi(x) &\equiv \frac{\int_0^x g(x') \bar{\phi}(x') (x')^2 dx'}{G(x)}. \end{aligned} \quad (5.96)$$

The left-hand side of Eq. (5.95) is positive definite, which implies that there is a minimum heating rate at any radius

$$\Lambda(x) > 9\Phi - 9\bar{\phi} - \frac{3}{2}. \quad (5.97)$$

If the King analytic model for the potential is assumed, then the maximum value for the right-hand side of Eq. (5.97) is 1.35, and this is the minimum value of λ in the HIG model [Eq. (5.92)]. Similarly, the central temperature is given by

$$kT_0 = \frac{2}{3} \sigma_r^2 \mu m_p \left[\Lambda(0) + \frac{3}{2} \right], \quad (5.98)$$

so that the minimum central temperature in the HIG model is

$$T_0(\text{HIG}) > 8.7 \times 10^7 \text{ K} \left[\frac{\sigma_r}{1000 \text{ km/sec}} \right]^2. \quad (5.99)$$

Similar arguments for the HBF model indicate that $\pi R_D^2 \rho_g \sigma_r / \alpha_* m_{\text{gal}} \gtrsim \frac{3}{2}$, and that the central temperature is

$$T_0(\text{HBF}) \gtrsim 3.4 \times 10^8 \text{ K} \left[\frac{\sigma_r}{1000 \text{ km/sec}} \right]^2. \quad (5.100)$$

These analytic results were given in Bahcall and Sarazin (1978). The temperatures are lower than those in Yahil and Ostriker (1973) because they assumed $\mu = 1$, which is not valid for an ionized plasma.

The observed cluster temperatures (Sec. III.C.1) are generally below those required by Eqs. (5.99) or (5.100), so it does not seem that the gas is heated sufficiently to produce a wind. The energy required to support such a wind also seems to be prohibitively large, since it would require that considerably more than the whole thermal content of the gas (more because of the kinetic energy of the flow) be produced in a flow time, which for a transonic wind is comparable to a sound crossing time. In the HIG model, this would require a very large supernova rate or other energy source; in the HBF model, it would require that the galaxies have delivered to the gas much more kinetic energy than they currently possess (Sec. V.C.4). As a result, it seems unlikely that wind models fit the distribution of the intracluster gas at all radii, but it remains possible that gas is flowing out from the outer portions of clusters.

Livio *et al.* (1978) argue that viscous drag between intracluster and interstellar gas can produce a very large heating rate due to galaxy motions if the intracluster gas is sufficiently hot, so that the Reynolds number is small [Eqs. (5.46) and (5.47)]. As discussed in Sec. V.C.4, this requires that galaxies maintain large amounts of intracluster gas; it seems more likely that the drag forces will strip the gas from the galaxies. Unless the galaxies have a large rate of mass outflow, Rephaeli and Salpeter (1980) have shown that the drag does not increase for small Reynolds number (Sec. V.D.4). Again, there is the problem that the heating required to support a strong wind is greater than the total kinetic energy content of the galaxies.

Lea and Holman (1978) discussed winds driven by heating by relativistic electrons (Sec. V.C.5). They derived analytic heating limits like those of Eq. (5.59). To produce a steady-state wind, the heating rate must be much greater than that necessary to heat the gas in a Hubble time, and as a result the required values of γ_l are very low. They find that even in the Perseus cluster, which is one of the strongest radio clusters known, $\gamma_l \ll (B/\mu\text{G})^{-(\alpha_r+1)/2\alpha_r}$ is required for a steady-state wind. Moreover, this mechanism suffers the problem that extended halo radio sources, of the sort necessary to heat the intracluster gas, are relatively rare.

In summary, it seems unlikely that the intracluster gas in most clusters is involved in steady-state outflow, although gas may be flowing out of the outer portions of clusters.

G. Cooling flows and accretion by cd's

1. Cooling flows

If the rate of cooling in the intracluster gas is sufficiently rapid, gas may cool and flow into the center of the cluster. Lea *et al.* (1973), Silk (1976), Cowie and Binney (1977), and Fabian and Nulsen (1977) noted that the cooling times t_{cool} [Eq. (5.23)] in the more luminous x-ray clusters are comparable to the Hubble time t_H (the age of the universe and approximate age of clusters). This might be a coincidence, but it would also be a natural consequence of the cooling of the intracluster gas. Imagine that a certain amount of gas was introduced into the cluster when it formed. Initially, the cooling time in this gas might be much longer than the age of the cluster, and cooling would be unimportant. However, as long as cooling was more rapid than heating, and the gas was not removed from the cluster, the cooling time would not increase, and eventually the age of the cluster would exceed the cooling time. Once this occurs, the gas will cool in the cluster core, and the pressure of the surrounding gas will cause the cool gas to flow into the cluster center. The surrounding hot intracluster gas will always have $t_{\text{cool}} \approx t_H$. Silk (1976) and Cowie and Binney (1977) showed that this cooling condition could explain a number of the observed correlations between the optical and x-ray properties of clusters, particularly the $L_x - \sigma_r$ relation [Eq. (3.8)]. The subject of these cooling flows has been reviewed recently by Fabian *et al.* (1984).

Silk (1976) suggested that the intracluster gas was introduced into the cluster when it formed, and that cooling has reduced the amount of intracluster gas so as to maintain $t_c \approx t_H$. Cowie and Binney (1977), on the other hand, argued that the intracluster gas is constantly being replenished by ejection from cluster galaxies. Then, the density of gas in the cluster center would increase until the age exceeded the cooling time. After this point, a stable steady state would be achieved, in which the rate of ejection of gas by galaxies into the cluster was balanced by the rate of removal of gas through cooling in the cluster core (Cowie and Binney, 1977; Cowie and Perrenod, 1978). As long as the mass ejection rate is not too low, cooling would regulate the inflow, and the densest hot gas at the cluster center would always have $t_{\text{cool}} \sim t_H$.

The equations for a steady-state cooling flow in a spherically symmetric cluster are identical to those for a wind [Eq. (5.90)], except that the heating rate $h(r)$ is replaced by the cooling rate ϵ [Eqs. (5.21) and (5.22)]. Because the cooling rate is proportional to the square of the density, it is useful to define $\epsilon \equiv \rho_g^2 \Lambda(T_g)$. Then,

$$\frac{1}{r^2} \frac{d}{dr} (r^2 \rho_g v) = \dot{\rho},$$

$$\dot{\rho} v + \rho_g v \frac{dv}{dr} + \frac{dP}{dr} + \rho_g \frac{d\phi(r)}{dr} = 0, \quad (5.101)$$

$$\frac{1}{r^2} \frac{d}{dr} \left[r^2 \rho_g v \left(\frac{v^2}{2} + \frac{5}{2} \frac{P}{\rho_g} + \phi(r) \right) \right]$$

$$= -\rho_g^2 \Lambda(T_g) + \dot{\rho} \left[\frac{3}{2} \sigma_r(r)^2 + \phi(r) \right],$$

and the other symbols are defined following Eq. (5.90). If the gas is injected continuously into the cluster ($\dot{\rho} \neq 0$), then the boundary conditions are set by requiring no inflow from outside the cluster. If the gas is not constantly being added to the cluster ($\dot{\rho} = 0$), then no cluster-wide steady-state flow will be possible. However, these equations will still apply approximately within the radius defined by setting the cooling time equal to the age of the cluster (the "cooling surface"). In order to match the hydrostatic intracluster gas distribution beyond this radius, the proper density and temperature is specified on this surface. Because the inflow is generally extremely subsonic except in the innermost parts, the outer parts of these cooling flows are very nearly hydrostatic [the middle equation in (5.101) reduces to (5.55)]. The velocity is determined by the inflow rate $\dot{M} \equiv 4\pi\rho_g v r^2$, which must be constant in a steady-state inflow without sources or sinks for mass.

Thermal conduction (Sec. V.D.2) has not been included in the cooling flow equations. Generally, the existence of cooling flows requires that conduction not be very important, since otherwise cooling in the cluster core will be balanced by heat transported inwards by conduction, rather than heat convected inwards by the cooling flow (Mathews and Bregman, 1978; Takahara and Takahara, 1979; Binney and Cowie, 1981; Nulsen *et al.*, 1982). In most cases, conduction must be much slower than the Spitzer rate [Eq. (5.37)] for a nonmagnetic plasma; the suppression of conduction might be due to a very tangled or circumferential magnetic field (Sec. V.D.3).

These equations have been solved for cooling in clusters by Cowie and Binney (1977), assuming a King model for the cluster density [Eq. (2.13)], mass ejection by galaxies as given by Yahil and Ostriker [1973; Eq. (5.91)], pure bremsstrahlung cooling [Eq. (5.21)], and subsonic flow [dropping the quadratic velocity terms in Eqs. (5.101)]. Figure 36 shows the density and temperature variations in a typical model. The density rises continuously into the center; this contrasts with hydrostatic models, in which it levels off (Sec. V.E). The temperature has a maximum at about two core radii and declines into the cluster center. The behavior of these solutions in the inner regions can be understood approximately. Assuming that the mass flux is fixed ($\dot{M} = \text{const}$), that the flow is subsonic, that the gravitational potential is not important (so that the pressure is nearly constant and the flow is driven by pressure and cooling and not by gravity), and that the cooling function is a power law in the temperature $\Lambda \propto T_g^\alpha$, the temperature and density are found to vary as

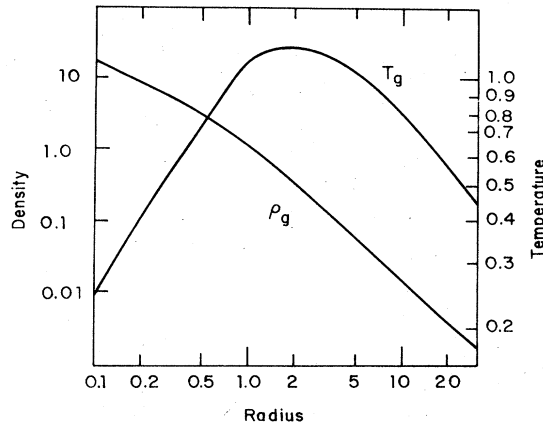


FIG. 36. The gas temperature and density in a cluster with a steady-state cooling flow, from the models in Cowie and Binney (1977). The gas density is normalized to its value at the cluster core radius, and the gas temperature is normalized to $\mu m_p \sigma_r^2 / k$, where σ_r is the cluster velocity dispersion and μ is the mean atomic mass. The radius from the cluster center is in units of the cluster core radius.

$\rho_g \propto 1/T_g \propto r^{-3/(3-\alpha)}$ (Nulsen *et al.*, 1982). For $T_g \gtrsim 4 \times 10^7$, cooling is due to thermal bremsstrahlung [Eq. (5.21)], $\alpha = \frac{1}{2}$, and $\rho_g \propto r^{-6/5}$. At lower temperatures, $\alpha \approx -0.6$ [Eq. (5.22)] and $\rho_g \propto r^{-5/6}$. When the gas has cooled sufficiently for the gravitational potential to be important (or if the potential gradient is increased by a central galaxy), then the temperature tends to vary as $kT_g / \mu m_p \sim GM(r)/r$, where $M(r)$ is the total mass within r (Fabian and Nulsen, 1977).

Evidence for the existence of such cooling flows in x-ray clusters includes the detection of peaks in the soft x-ray surface brightness at the cluster center (Branduardi-Raymont *et al.*, 1981; Fabian, Hu, Cowie, and Grindlay, 1981; Canizares *et al.*, 1983; Fabricant and Gorenstein, 1983; Jones and Forman, 1984; Stewart, Canizares, Fabian, and Nulsen, 1984; Stewart, Fabian, Jones, and Forman, 1984), the measurement of inverted temperature gradients $dT_g/dr > 0$ (Gorenstein *et al.*, 1977; Ulmer and Jernigan, 1978; White and Silk, 1980), and the observation of central x-ray surface brightnesses and temperatures that imply cooling times much less than the Hubble time (Canizares *et al.*, 1983; Stewart, Fabian, Jones, and Forman, 1984). The strongest evidence comes from the detection of soft x-ray line emission from low-ionization stages produced at temperatures of $T_g \approx 10^6 - 10^7$ K, coming from the cluster center (Canizares *et al.*, 1979, 1982; Canizares, 1981; Mushotzky *et al.*, 1981; Lea *et al.*, 1982; Nulsen *et al.*, 1982; Mushotzky, 1984; Sec. III.C.3).

Theoretical models for cooling flows can be used to estimate the rates of cooling in clusters from these x-ray observations. A simple estimate may also be derived by noting that for steady-state, isobaric cooling, the luminosity emitted in any temperature range dT_g is

TABLE V. Clusters that show evidence for cooling flows. Accretion rates scale as h_{50}^{-2} . First, Abell clusters are listed, then non-Abell clusters. The references for the x-ray or optical emission line observations are listed below.

Cluster	\dot{M} M_{\odot}/yr	X ray	References	Optical
A85	120	t		k,d
A262	28	t		
A400	2	t		
A426 Perseus	300	e,p,a,o		l,d
A496	200	q,o		k,f,d
A576	40	u,r		
A978	500			k
A1060	6	t		
A1126	500			k
A1795	400	t,o		k,d
A1983	7	t		
A1991	115	t		
A2029	250	t,o		d
A2052	120			k
A2063	26	t		
A2107	18	t		
A2142	28	m		d
A2199	110	t,o		d
A2319	75	t,u		d
A2415	15	t		
A2626	10	t		
A2657	36	t		
A2670	78	t		
SC0107-46	4	t		
AWM7	40	c		
3A0335 + 096	280	s,o		
MKW4	20	c		
M87/Virgo	3-20	h,i,b,n,o		j
Centaurus	22			g
MKW3s	100	c		
AWM4	25	c		
SC1842-63	3	t		
SC2059-247	500	v		

^aCanizares (1981).

^bCanizares *et al.* (1979,1982).

^cCanizares *et al.* (1983).

^dCowie *et al.* (1983).

^eFabian, Hu, Cowie, and Grindlay (1981).

^fFabian, Ku, Malin, Mushotsky, Nulsen, and Stewart (1981).

^gFabian, Atherton, Taylor, and Nulsen (1982).

^hFabricant *et al.* (1980).

ⁱFabricant and Gorenstein (1983).

^jFord and Butcher (1979).

^kHeckman (1981).

^lKent and Sargent (1979).

^mLea *et al.* (1981).

ⁿLea *et al.* (1982).

^oMushotzky (1984).

^pMushotzky *et al.* (1981).

^qNulsen *et al.* (1982).

^rRothenflug *et al.* (1984).

^sSchwartz, Schwarz, and Tucker (1980).

^tStewart, Canizares, Fabian, and Nulsen (1984).

^uWhite and Silk (1980).

^vWhite, Sarazin, Quintana, and Jaffe (1981).

$$dL(T_g) = \frac{5}{2} \frac{\dot{M}}{\mu m_p} k dT_g \quad (5.102)$$

if the gravitational potential does not change significantly during the cooling (Cowie, 1981). Here, μ is the mean atomic mass. This equation can be used to estimate the luminosity in any spectral feature produced in the cooling flow by integrating $dL(T_g)$ over the fraction of the total emission in that feature as a function of temperature.

Table V gives a list of clusters showing evidence for cooling flows, with estimates for the cooling rate \dot{M} . The values for \dot{M} range from 3 to 500 M_\odot/yr . The Perseus cluster has one of the largest observed cooling rates (see also Sec. III.E.2). A very small cooling rate of 3 – 20 M_\odot/yr is found in M87 in the Virgo cluster; such a small cooling flow would be difficult to observe in more distant clusters. It is particularly interesting that cooling flows have now been detected in poor clusters (Canizares *et al.*, 1983), as well as in a large number of rich clusters (Stewart, Fabian, Jones, and Forman, 1984).

It should perhaps be pointed out that all of the above evidence shows that there is *cool* gas in the cores of these clusters, but it does not directly show that there is *cooling* gas flowing into the cluster core. That is, the motion of the gas has not been detected directly, as x-ray spectral observations have insufficient resolution to detect Doppler shifts produced by the slow inflow. It has occasionally been argued that the gas might actually be in hydrostatic and thermal equilibrium, with the extra emission at the cluster center being due to some central heat source (see, for example, Tucker and Rosner, 1983). Since the cooling rate of a gas at constant pressure decreases with temperature at all temperatures of interest for x-ray emission ($10^5 \lesssim T_g \lesssim 10^9$ K), the higher the heating rate (or the nearer the cluster center), the cooler the gas would be in thermal equilibrium. However, such hydrostatic, thermal equilibrium models (in which one heats the gas in order to cool it) can generally be shown to be thermally unstable on the cooling time scale (Stewart, Canizares, Fabian, and Nulsen, 1984; Fabian *et al.*, 1984). The gas must either heat up and expand out of the core, or cool down and form a cooling flow on this time scale. Moreover, such a thermal equilibrium model for the x-ray emission would not explain the observed association of cooling flows with optical-line-emitting filaments, as discussed below.

2. Accretion by central galaxies

Many clusters of galaxies have luminous galaxies located at their centers (Sec. II.J.1), and these galaxies appear to be moving relatively slowly compared to the average cluster galaxy (Quintana and Lawrie, 1982). In fact, such a luminous galaxy is found at the center of nearly every cooling flow that has been observed (Jones and Forman, 1984). The cooling intracluster gas may, then, be accreted by the central galaxy in the cluster when its temperature has fallen to the point where it can be bound to the

galaxy, and the gas can cool further and flow into the galaxy center (Silk, 1976; Cowie and Binney, 1977; Fabian and Nulsen, 1977; Mathews and Bregman, 1978).

It is unlikely that the presence of the central galaxy causes the cooling flow (that is, increases the cooling rate significantly) because the gravitational potential associated with a galaxy is much smaller than that associated with a cluster (cluster velocity dispersions are much larger than those of galaxies). Thus the presence of a central galaxy will not cause a large perturbation in the density of hydrostatic intracluster gas (Sec. V.E) and will not affect the cooling rate significantly. Initially, the inflow of cooling gas is driven by the pressure of the surrounding hot medium; only when the gas has cooled significantly does the gravitational potential of the galaxy influence the flow. If the mass of the central galaxy is small, the flow may be pressure-driven over most of its extent (Fabian and Nulsen, 1977; Binney and Cowie, 1981).

In order to accrete cooling gas, a galaxy must be moving slowly through the intracluster medium. The gas must be able to cool before the galaxy has moved away. Thus the velocity is limited to

$$v_{\text{gal}} \lesssim \frac{R_{\text{gal}}}{t_{\text{cool}}} \approx 100 \text{ km sec}^{-1} \left[\frac{R_{\text{gal}}}{100 \text{ kpc}} \right] \left[\frac{t_{\text{cool}}}{10^9 \text{ yr}} \right]^{-1} \quad (5.103)$$

Thus a typical cluster galaxy with $v_{\text{gal}} \sim \sigma_r \sim 10^3$ km/sec will have great difficulty accreting. Central dominant galaxies are expected to have velocities of at least ~ 100 km/sec on average, due to gravitational encounters with other galaxies (Sec. II.I.1). Based on the asymmetry in the nonthermal radio emission and optical line filaments around the galaxy M87 in the Virgo cluster, De Young *et al.* (1980) argued that this accreting galaxy was moving about 200 km/sec to the north. Dones and White (1985) showed that this was inconsistent with the observed temperature structure in the cooling flow; that is, it would strongly violate this cooling limit.

Models for the accretion of cooling gas onto central galaxies have been given by Fabian and Nulsen (1977), Mathews and Bregman (1978), and Binney and Cowie (1981). All of these calculations assume the $\dot{\rho} = 0$ in Eqs. (5.101); the sources of the gas are external to the central galaxy, so that \dot{M} is constant within the galaxy. Mathews and Bregman integrate Eqs. (5.101) inward through a sonic radius r_s at which the inflow becomes supersonic. The structure of the flow is determined by \dot{M} and the gas temperature at the sonic radius T_s . The sonic radius is a solution of the following equation (Mathews and Bregman, 1978):

$$r_s = \frac{3\mu m_p}{10kT_s} \left[GM(r_s) + \frac{\dot{M} \Lambda(T_s) \mu m_p}{10\pi k T_s} \right], \quad (5.104)$$

where $M(r)$ is the total galactic and cluster mass within the radius r . This equation can have multiple solutions,

although usually only one of these at most corresponds to an astrophysically interesting density. For reasonable values of \dot{M} and T_s , one finds $r_s \sim 0.1\text{--}2$ kpc (Mathews and Bregman, 1978). A simple estimate of the sonic radius can be derived in a number of ways. First, if the inflow is driven by cooling rather than gravity, then the second term in Eq. (5.104) will be more important. This is essentially equivalent to arguing that the inflow time and cooling time must be roughly equal. Second, even if gravity is important to the inflow, $kT_g/\mu m_p \sim GM(r)/r$ [see discussion after Eqs. (5.101)], and the first term in Eq. (5.104) only increases r_s by several times. Thus an estimate for r_s is

$$r_s \sim 0.1 \text{ kpc} \left[\frac{\dot{M}}{100 M_\odot/\text{yr}} \right] \left[\frac{T_s}{10^7 \text{ K}} \right]^{-2.6}, \quad (5.105)$$

where the cooling function in Eq. (5.22) has been used. Note that r_s is proportional to \dot{M} .

On the other hand, Fabian and Nulsen (1977) and Cowie *et al.* (1980) argued that the gas cannot flow in as far as r_s because the inflowing gas must have at least a small amount of angular momentum. Let $l \equiv \mathbf{r} \times \mathbf{v}$ be the angular momentum per unit mass of the incoming gas, and assume that this is conserved. Then the inflow will stop and the gas will form a rotating disk at a stagnation radius r_{st} given by

$$\begin{aligned} r_{st} &= \frac{l^2}{GM(r_{st})} \\ &= 2.3 \text{ kpc} \left[\frac{l}{10^3 \text{ kpc km/sec}} \right]^2 \left[\frac{M(r_{st})}{10^{11} M_\odot} \right]^{-1}. \end{aligned} \quad (5.106)$$

Ideally, the angular momentum of inflowing gas in a spherical cluster would be zero, but realistically the gas must have some nonradial velocity. Cowie *et al.* argued that the gas was ejected by cluster galaxies, and that the angular momentum of the central cooling gas would be determined by the rms residual velocity of galaxies in the cluster core,

$$l \sim \frac{\sigma_r}{(N_{gal})^{1/2}} r_c \sim 2 \times 10^4 \text{ kpc km/sec}, \quad (5.107)$$

where σ_r is the cluster velocity dispersion, $N_{gal} \sim 100$ is the number of galaxies in the cluster core, and r_c is the cluster core radius. Alternatively, if the gas had no nonradial motion relative to the cluster, l might be due to the central galaxy orbital velocity, which for $v_{gal} \sim 100$ km/sec and a galaxy orbital radius of ~ 30 kpc gives $l \sim 3 \times 10^3$ kpc km/sec. However, both of these estimates imply gas velocities relative to the central galaxy that exceed the cooling time scale limit [Eq. (5.103)]. Taking this limit at a cooling radius of 200 kpc gives $l \lesssim 4 \times 10^3$ kpc km/sec. Thus, unless the inflow is much more radial than these estimates suggest, it is likely that the flow will stagnate before becoming supersonic ($r_{st} \geq r_s$).

Viscosity (Sec. V.D.4) might transport angular momentum out of the flow and reduce l . If ionic viscosity is effective, thermal conduction will probably also be important and may suppress the cooling flow (Cowie *et al.*, 1980). However, the magnetic field may couple the inner and outer parts of the flow and provide an effective viscosity; a circumferential field could both transport angular momentum out of the inflow, and suppress thermal conduction. Alternatively, if the magnetic field were too weak to be dynamically important and the ionic viscosity were small, the Reynolds number for the flow would be large and the flow would become turbulent. Turbulent viscosity would transport angular momentum out of the flow (Nulsen *et al.*, 1984), and, at the same time, the turbulence would tangle the magnetic field and inhibit thermal conduction.

Cowie *et al.* (1980) treated the inflow as radial (which is reasonable for $r \gg r_{st}$), and included the effect of angular momentum by adding a repulsive centrifugal potential $\phi_{cent} = l^2/2r^2$ to the gravitational potential ϕ in Eqs. (5.101). Moreover, they assumed that $r_{st} \gg r_s$, and therefore they dropped all quadratic or higher-order terms in the flow velocity v .

If the accretion rate in the flow decreases inward ($d\dot{M}/dr > 0$), the radial flow can continue into the center of the galaxy without passing through a sonic radius (Nulsen *et al.*, 1984). There is some evidence that \dot{M} does decrease inwards in M87/Virgo and NGC1275/Perseus (Fabian *et al.*, 1984; Stewart, Canizares, Fabian, and Nulsen, 1984). It may be that some of the cooling gas is being converted into stars (Sec. V.G.4 below).

Many central galaxies in clusters with cooling flows have nuclear nonthermal radio sources, which may be powered by the further accretion of a small portion of the cooling gas onto the central "engines" (black holes?) of these sources (Burns, White, and Hough, 1981; Valentijn and Bijleveld, 1983; Jones and Forman, 1984; Nulsen *et al.*, 1984). There is evidence for a correlation between the radio luminosity and accretion rate in these galaxies (Valentijn and Bijleveld, 1983; Jones and Forman, 1984).

3. Optical filamentation

As the gas cools, any inhomogeneities in the gas density will tend to be amplified (Fabian and Nulsen, 1977). In a region of higher than average density, the temperature will tend to be lower, to preserve pressure equilibrium. Both higher density and lower temperature will speed up the cooling rate, and lowering the temperature will increase the density contrast. Mathews and Bregman (1978) analyzed the growth of density inhomogeneities and the thermal instability of the cooling gas. They considered only comoving, isobaric perturbations (no change in the velocity or pressure as compared to the unperturbed flow at the same position). They found that the gas is thermally unstable if

$$\Upsilon(T_g) \equiv \frac{2\Lambda(T_g)}{kT_g} - \frac{d\Lambda(T_g)}{dk T_g} > 0. \quad (5.108)$$

This is true for any interesting gas temperature ($T_g \geq 10^4$ K). Assuming that there is an initial perturbation of relative amplitude $(\Delta\rho/\rho)_i$ at some large radius r_i , the amplified perturbation at an inner radius $r < r_i$ is

$$\left[\frac{\Delta\rho}{\rho} \right] = \left[\frac{\Delta\rho}{\rho} \right]_i \exp \left[\frac{2}{5} \frac{\dot{M} \mu m_p}{4\pi} \int_{r_i}^r \Upsilon(T_g) \frac{dr}{(vr)^2} \right] \quad (5.109)$$

in the linear regime [$(\Delta\rho/\rho) \ll 1$] and assuming \dot{M} is constant. Mathews and Bregman found that amplification factors of 10^3 – 10^4 were likely for flows into the sonic radius.

Cowie *et al.* (1980) generalized this analysis by considering the motion of finite sized “blobs” with a finite density perturbation, without assuming that the blobs comove with the flow. They argue that the motion of blobs relative to the unperturbed gas will stabilize some perturbations, but that the gas will still be unstable for some blob sizes and densities. Because they assume the flow stagnates, the inflow must become very unstable for $r \sim r_{st}$.

Optical emission line filaments are often seen near the centers of clusters having cooling flows, often within the central galaxies that are accreting the cooling gas (Ford and Butcher, 1979; Kent and Sargent, 1979; Stauffer and Spinrad, 1979; Heckman, 1981; Fabian, Ku, Malin, Mushotzky, Nulsen, and Stewart, 1981; Fabian, Atherton, Taylor, and Nulsen, 1982; Cowie *et al.*, 1983; Hu *et al.*, 1983; van Breugel *et al.*, 1984). The size of these extended filament systems ranges roughly from 1 to 100 kpc. These filaments emit the Balmer lines of hydrogen, as well as forbidden lines from heavier elements. Their spectra are similar to those seen in astrophysical shocks. The emission from these filaments is generally believed to be the result of the same cooling flows; the gas is visible in optical line emission as it cools through the temperature range $T_g \sim 10^4$ K. The clumpy nature of these filaments is due, at least in part, to thermal instability in the cooling gas, as discussed above. Figure 15 shows the optical filaments around NGC1275 in the Perseus cluster, which is one of the best studied examples of this optical filamentation (Lynds, 1970). Clusters with cooling flows having optical filamentation are listed in Table V.

Cowie *et al.* (1980,1983) have derived the total luminosity in the $H\alpha$ line expected in a cooling flow; they find

$$L(H\alpha) \approx 5 \times 10^{40} \text{ ergs sec}^{-1} \left[\frac{\dot{M}}{100 M_\odot/\text{yr}} \right]. \quad (5.110)$$

This is somewhat larger than would be derived from Eq. (5.102), which assumes isobaric cooling. Thermally unstable blobs of gas probably cool nearly isobarically until $T_g \sim 10^6$ K; at lower temperatures the cooling time is shorter than the sound crossing time for the filaments, and the gas initially cools isochorically (at constant density). The cool clumps reach pressure equilibrium with the

surrounding hot gas by the passage of repressurizing shocks (Mathews and Bregman, 1978; Cowie *et al.*, 1980). The $H\alpha$ flux may also be increased by photoionization by x rays and ultraviolet radiation from the surrounding hot gas or from the nuclear source in the accreting galaxy.

Cowie *et al.* (1983) have suggested, based on extensive observations of optical line emission, that these filament systems consist of two components: a cluster core component, which is 20–100 kpc in size, and a galaxy component, which is smaller. In some clusters both components are present; in some, only one or the other is observed. The larger cluster components tend to consist of highly elongated filaments, which may be stretched by tidal effects in the cluster or along the magnetic field lines. The galaxy components are more homogeneous, and are also somewhat elongated. Cowie *et al.* suggest that they are gas disks at the stagnation radius. However, velocity measurements in NGC1275 indicate that the gas is not rotating fast enough to be a centrifugally supported disk (Hu *et al.*, 1983).

The filament system around NGC1275 in the Perseus cluster is the most luminous such system known, and is considerably brighter than would be expected given the accretion rate determined from the x-ray measurements. Hu *et al.* (1983) argue that it is also too luminous to be due to photoionization by the nuclear source in NGC1275. They show that the optical filaments at the velocity of NGC1275 are elongated at the same position and in the same direction as the filaments due to the spiral galaxy that is moving towards NGC1275 at 3000 km/sec (see Sec. III.E.2). They suggest that this galaxy is actually colliding with the base of the accretion flow onto NGC1275, and that the kinetic energy in this collision powers the emission line filaments. Two problems with this model, which are discussed by Hu *et al.*, are the lack of intermediate-velocity gas and the difficulty of a gas-rich galaxy penetrating into the core of the Perseus cluster without having its gas stripped (Secs. II.J.2 and V.I).

4. Accretion-driven star formation on cD's

What is the duration of these cooling flows in clusters? Both optical and x-ray clusters have been observed at moderately high redshifts, and the gas distributions in clusters are relaxed and smooth; both suggest that the intracluster medium has been present in clusters for a significant fraction of the Hubble time. As described above, the cooling times at the centers of these flows are less than the Hubble time, which suggests that the flows have persisted for a significant fraction of the cluster lifetime. Thus the total mass of gas that has cooled and been accreted by the central galaxy in the cluster should be

$$M_{acc} \sim 10^{12} M_\odot \left[\frac{\dot{M}}{100 M_\odot/\text{yr}} \right]. \quad (5.111)$$

This assumes that the accreted mass is not ejected from the cluster center.

Although this is a small fraction of the total gas mass in a cluster ($\sim 10^{14} M_\odot$), it is comparable to the mass in

luminous material in a very large (cD) galaxy. It is important to understand where this gas goes after it cools. Many possibilities can be ruled out. First, the gas could remain gaseous. However, the observations of the x-ray and optical line emission give upper limits on the total amount of ionized gas well below the total accreted mass. Observations of the 21-cm hydrogen line from central galaxies in clusters with cooling flows (Sec. III.G) give upper limits on the total amount of neutral atomic hydrogen, typically $M_{\text{HI}} \leq 10^9 M_{\odot}$ (Burns, White, and Haynes, 1981; Valentijn and Giovanelli, 1982). Because of the instrumental sensitivity, current observations do not rule out the possibility that the accreted gas could be molecular hydrogen, although it seems likely that the large amounts of molecular gas required would lead to an efficient conversion into stars. As mentioned above, many of the accreting galaxies are radio sources (Burns, White, and Hough, 1981), and this may indicate that some of the accreted gas flows into the galactic nucleus and is used to power the central engine of the radio source. However, these sources require only $\lesssim 10^{-2} M_{\odot}/\text{yr}$ of gas to provide their observed radio power (Burns, White, and Hough, 1981), so it is likely that the fraction of the gas accreted by the central engine is small. Moreover, there could not be as much as $10^{12} M_{\odot}$ in the nucleus of these galaxies, given their observed stellar velocity dispersions (Sarazin and O'Connell, 1983).

Generally, conversion of gas into stars is quite efficient within galaxies, and this conversion could provide both a stable reservoir for the accreted gas and a partial explanation for the existence of central dominant galaxies. Burns, White, and Haynes (1981) argued that star formation cannot be occurring at a high rate in these galaxies, because they would then contain more neutral hydrogen than is observed (see above). However, Fabian, Nulsen, and Canizares (1982) and Sarazin and O'Connell (1983) showed that the cooling times for neutral hydrogen were short enough that all the accreted gas could be cooling through this temperature range and forming stars. Within the disk of our own galaxy, stars are formed with a very wide range of masses extending up to $\sim 100 M_{\odot}$ (Salpeter, 1955). Stars more massive than $\sim 10 M_{\odot}$ produce Type-II supernovas when they die, and the rate of these supernovas would probably heat the accreted gas sufficiently to prevent the formation of cooling flows (Wirth *et al.*, 1983). Moreover, if the spectrum of stellar masses formed from the cooling gas (the "initial mass function") were similar to that in our own galaxy, the central galaxies in the accretion flows would be considerably bluer and brighter than they are observed to be (Fabian, Nulsen, and Canizares, 1982; Sarazin and O'Connell, 1983). Burns, White, and Haynes (1981) gave similar arguments and concluded that star formation cannot be the ultimate reservoir for the cooling gas.

However, there is really no reason why the initial mass function for star formation in these cooling flows should be the same as that in the disk of our galaxy. If the forming stars had low masses $\lesssim 1 M_{\odot}$, these stars would not be very different from the stars found in typical elliptical

galaxies (Cowie and Binney, 1977). Since star formation is very poorly understood and there is no successful quantitative theory for this process, one cannot calculate the initial mass function directly. However, Fabian, Nulsen, and Canizares (1982) and Sarazin and O'Connell (1983) have given a simple plausibility argument as to why the initial mass function for star formation in cooling flows might be limited to low-mass stars; a similar argument for elliptical galaxies in general was given by Jura (1977). It is assumed that stars form eventually from the thermally unstable clouds of gas that are seen as optical filaments. Star formation is assumed to start when these clouds become gravitationally unstable and can no longer support themselves against their own gravity and the pressure of the surrounding medium. Clouds become gravitationally unstable when their mass exceeds the Jeans's mass, which for a spherical, static, nonmagnetic isothermal cloud of temperature T immersed in a low-density medium of pressure P is given by (Spitzer, 1978)

$$\begin{aligned} M_J &= 1.2 \left[\left[\frac{kT}{\mu m_p} \right]^4 \frac{1}{G^3 P} \right]^{1/2} \\ &= 0.64 M_{\odot} \left[\frac{T}{10 \text{ K}} \right]^2 \left[\frac{\mu}{\text{amu}} \right]^{-2} \\ &\quad \times \left[\frac{P}{10^7 k \text{ cm}^{-3} \text{ K}} \right]^{-1/2}. \end{aligned} \quad (5.112)$$

Once a cloud starts to collapse, the pressure within the cloud will increase and the Jeans's mass may be reduced; this can cause the cloud to fragment and result in lower-mass stars' being formed. It is difficult to produce stars more massive than M_J , however, because before a suitably massive cloud could be assembled, it would become unstable and collapse. Thus it is possible that the Jeans's mass may provide an upper limit on the mass of the largest stars that form. In the disk of our galaxy, the interstellar medium typically has a pressure of $P \sim 2 \times 10^3 k \text{ cm}^{-3} \text{ K}$, and Eq. (5.112) gives $M_J \sim 50 M_{\odot}$. In the cooling flows in clusters, the pressures derived from models for the x-ray emission or determined directly from the optical-line-emitting filaments are 10^3 – 10^4 times larger ($P \sim 10^{6-7} k \text{ cm}^{-3} \text{ K}$), and thus the Jeans's mass is $M_J \sim 1 M_{\odot}$. Thus it is possible that only low-mass stars are formed from the cooling gas in clusters. [A similar argument was given earlier for low-mass star formation in normal elliptical galaxies by Jura (1977).] In Fabian *et al.* (1982) and Sarazin and O'Connell (1983), this conclusion is shown to be unaffected by the temperature dependence in Eq. (5.112).

Fabian, Nulsen, and Canizares (1982) also point out that star formation in cooling flows may be different than in the disk of our galaxy because the star-forming regions in these flows are unlikely to contain dust grains. In star-forming regions in our galaxy, most of the refractory heavy elements are in the form of solid dust grains, and these grains absorb starlight, emit infrared radiation, and act as a heat source for the gas. Dust grains are destroyed

in high-temperature gas. Since the gas in cooling flows is initially very hot, any grains would have evaporated (Cowie and Binney, 1977; Fabian, Nulsen, and Canizares, 1982), and it is very difficult for grains to form in low-density gas, even if it is cool. Thus it is unlikely that grains will be present in the cooling flows, even in the coolest, star-forming clouds. The lack of grains probably lowers the gas temperature, which also tends to reduce \dot{M}_J . Further, any attempt to estimate the star-forming rate in these galaxies from the infrared emission of dust (Wirth *et al.*, 1983) is likely to greatly underestimate the real rate.

Sarazin and O'Connell (1983) have calculated the expected colors and optical spectra of central galaxies assuming that their stellar populations are a mixture of a normal giant elliptical population with a continuously forming population due to accretion-driven star formation. A variety of values for the upper mass limit and the shape of the initial mass function were used. They found that the accreting galaxies should have spectra and colors measurably different from those of nonaccreting giant ellipticals [color differences of typically $\Delta(U - V) \approx -0.3$ mag]. They also found that with accretion rates of typically $\dot{M} \gtrsim 100M_\odot/\text{yr}$, the entire stellar population of the central galaxies in many clusters could be due to accretion-driven star formation.

Valentijn (1983) has attempted to measure the colors of the stellar populations in seven cD galaxies and their spatial variations by surface photometry in two colors (B and V). He finds very large color gradients within these galaxies of typically $\Delta(B - V) \approx 0.4$ mag, with the galaxy centers being extremely red. Valentijn argues that these gradients are the result of accretion-driven star formation, and that as the pressure increases inward in the cooling flow, the Jeans's mass is lowered [Eq. (5.112)] and the stellar population becomes redder. One problem is that the innermost regions of these galaxies are so red that the required stellar population would have a very small mass-to-light ratio and could not provide enough light (for the observed accretion rates) to account for the observed galaxy luminosity. The color gradients observed by Valentijn are very large (larger than Sarazin and O'Connell predicted), and it is very important that they be confirmed by further observations. Valentijn's photometry appears to disagree, in some cases, with that of other observers (Hoessel, 1980; Malumuth and Kirshner, 1985).

Color gradients might also result from dust extinction, abundance gradients in an old stellar population, or mergers of galaxies having differing colors. A more direct way to detect a stellar population due to accretion is to observe absorption features due to that population in the spectrum of the cD galaxy. The galaxy NGC1275 in the Perseus cluster (Fig. 15; Sec. III.E.2) is particularly interesting in this regard. Its stellar surface brightness distribution is similar to that of a typical giant elliptical galaxy (Oemler, 1976). However, the stellar population is very blue, and has an A-star absorption spectrum (Kent and Sargent, 1979), whereas typical giant elliptical galax-

ies are dominated by K stars. Sarazin and O'Connell (1983) show that the colors and spectrum of this galaxy can be understood if the luminous portion of the galaxy is entirely due to accretion-driven star formation at a rate of $\sim 300M_\odot/\text{yr}$ as given by the x-ray observations, and the upper mass cutoff of the stars formed is $2.8M_\odot$. [By contrast, Wirth *et al.* (1983) present a model for NGC1275 in which the initial mass function for star formation is similar to that in our galaxy, and very massive O stars are formed. However, in this model the star formation rate is more than an order of magnitude less than the observed rate of accretion onto NGC1275.]

One concern with NGC1275 is the presence of the foreground spiral galaxy. Hu *et al.* (1983) have suggested that this galaxy is colliding with the cooling flow and that this collision powers the optical line emission. It is also possible that this collision might affect the rate and initial mass function of star formation in the galaxy. It is thus very important to observe the spectra of other accreting central dominant galaxies, and see if a younger stellar population can be detected in them. Recently, O'Connell *et al.* (1985) obtained spectra for the inner regions of a number of accreting galaxies. The cD in A1795, which has a very large accretion rate $\dot{M} \sim 400M_\odot/\text{yr}$ (Table V), has an F-star stellar spectrum, consistent with the entire galaxy's being the result of accretion-driven star formation with an upper mass cutoff of about $1.5M_\odot$.

If cooling gas is being converted into stars in cooling flows, then terms representing the loss of gas should be added to the equations for the flow [Eqs. (5.101)]. The mass flow rate \dot{M} will no longer be constant, and this should result in an observable reduction in the amount of emission from cooler gas near the center of the flow. The observations of the cooling flows in M87/Virgo and in NGC1275/Perseus may already show such an effect (Fabian *et al.*, 1984; Stewart, Canizares, Fabian, and Nulsen, 1984). For example, the range of the derived mass flow rates of $3\text{--}20M_\odot/\text{yr}$ (Table V) may actually be a radial gradient.

Work so far has concentrated on detecting the presence of a younger stellar population due to accretion in central galaxies in cooling flows. It is also very important to study the spatial distribution of this population. Models that predict the distribution of stars formed in cooling flows are needed to compare to the observations of the central galaxies. As discussed in Sec. II.J.1, central dominant galaxies in clusters appear to be composed of an extended giant elliptical interior, surrounded in the case of rich cluster cD's by a very extended halo. Which of these components could be the result of accretion-driven star formation? If accretion produces the giant elliptical interiors, why do these resemble the stellar distributions in other nonaccreting giant ellipticals? Giant ellipticals have light distributions that are reasonably fit by de Vaucouleurs or Hubble profiles (Sec. II.J.1), and recent numerical studies have suggested that these form naturally in violent relaxation (Sec. II.I.2). Accretion-driven star formation is a slow process; why should it give a similar distribution?

Accretion-driven star formation may result in different stellar orbits in cD galaxies than in nonaccreting giant ellipticals. If the flows have little angular momentum (see above) and are radial, the resulting stellar orbits may be radial. If the gas stagnates and forms a disk, stellar disks may be found within cD galaxies.

Central dominant cluster galaxies appear, in many cases, to have a very large number of globular star clusters (spherical clusters of $\sim 10^{5-6}$ stars) associated with them (Harris, Smith, and Myra, 1983). Fabian *et al.* (1984) have suggested that these globular clusters might be produced by accretion-driven star formation. They note that the mass of a globular cluster is similar to the Jeans's mass of gas in the cooling flows at a temperature of 10^4 K, the temperature at which thermally unstable clouds are repressurized.

One important question is what effect the evolution of clusters has on these cooling flows. An important type of evolution is the merging of subclusters; the observed double clusters (Sec. III.D.2) may be systems undergoing this process. Such a merger will probably heat up the gas and disrupt any existing cooling flows (McGlynn and Fabian, 1984). Along these lines, Stewart, Fabian, Jones, and Forman (1984) speculate on the possibility that the Coma cluster, with its pair of D galaxies, is the result of such a merger of two subclusters. Perhaps each of the subclusters had a cooling flow, and accretion-driven star formation produced the two D galaxies. The merger would disrupt the flow, which would explain why Coma apparently lacks a cooling flow despite its high x-ray luminosity. The heating of the gas during the merger might explain the unusually high temperature of the intracluster medium in Coma (Sec. III.E.1). In this way, accretion could have formed the central galaxies in clusters that do not currently have accretion flows.

As was noted above, accreting central galaxies are often strong radio sources, indicating that some small portion of the cooling gas is accreted by the nucleus of the galaxy. Quasars appear to be galaxies with extremely luminous nonthermal nuclei. Perhaps they are also powered by accretion through cooling flows (Sarazin and O'Connell, 1983).

Although this review is concerned with clusters, elliptical galaxies outside of clusters might also have cooling flows that could produce observable x-ray emission (Bierman and Kronberg, 1983; Nulsen *et al.*, 1984). Nulsen *et al.* suggest that these cooling flows might be powered by stellar mass loss within the galaxy, rather than accretion of intracluster gas. For giant ellipticals, stellar mass loss rates of $\sim 1M_{\odot}/\text{yr}$ are expected.

In summary, it appears possible that most of the accreted gas in cooling flows is converted into low-mass stars, and that this accretion-driven star formation may provide most of the luminous mass of central galaxies in clusters with cooling flows. This process obviously competes with mergers and tidal effects as a mechanism for the formation of cD galaxies (Sec. II.J.1). It is important to determine the frequency of these cooling flows in order to determine the relative importance of these processes.

H. X-ray emission from individual galaxies

A number of topics concerning the x-ray emission from hot gas associated with individual galaxies in clusters will now be discussed. Material on the accretion of gas by central galaxies in clusters with cooling flows was reviewed in the previous section.

1. Massive halos around M87 and other central galaxies

The x-ray emission from the M87/Virgo cluster is considerably different from the emission from richer and more regular clusters (Sec. III.E.3). The gas is much cooler and less extended, and the x-ray luminosity is rather small. Initially, this was explained by noting that the x-ray luminosity and temperature of clusters appeared to correlate with the cluster velocity dispersion [Eqs. (3.8) and (3.10)], although this argument was somewhat circular, since M87/Virgo was one of the strongest pieces of evidence in favor of these correlations.

Bahcall and Sarazin (1977) and Mathews (1978b) suggested an alternative; the gas in M87/Virgo might be hydrostatic and bound to the galaxy M87, rather than to the cluster as a whole. To bind the gas, the galaxy would have to have a much deeper gravitational potential well than it would appear to have from its optical emission. Based on the best observations at that time, Bahcall and Sarazin showed that M87 must have a massive halo, with a total mass of $\approx 3 \times 10^{13} M_{\odot}$ extending out to ≈ 100 kpc from the galaxy center. Bahcall and Sarazin assumed a number of reasonable equations of state for the gas (adiabatic, polytropic, etc.; see Sec. V.E). Mathews (1978b) reached a similar conclusion, although he assumed that the gas was exactly isothermal and that the mass distribution was the King analytic form for an isothermal distribution (5.57). Because such isothermal gas models diverge unless the gas is cool compared to the potential [Eqs. (5.65) and (5.66)], Mathews required much more mass, $\geq 10^{14} M_{\odot}$. This high mass limit is very sensitive to the assumption that the gas is exactly isothermal (Bahcall and Sarazin, 1978; Fabricant *et al.*, 1980).

There is considerable evidence that M87/Virgo has a cooling flow (Sec. V.G). However, at large distances from the galaxy center the flow is highly subsonic, and the hydrostatic equation applies. Thus the cooling flow does not alter the requirement that the mass be large.

Binney and Cowie (1981) suggested that the mass of M87 might be much lower ($\approx 3 \times 10^{11} M_{\odot}$). They argued that the gas around M87 is bound by the *pressure* of surrounding, hotter gas, rather than by the *gravity* of M87. This hotter gas was in turn assumed to be extended and bound by the cluster gravitation potential of Virgo. The hot, diffuse, confining, intracluster gas is required to have a density and temperature of $n_p \approx 10^{-3} \text{ cm}^{-3}$ and $T_g \approx 10^8$ K. The cool gas is produced by a cooling flow, which is drawn from the hot gas.

A key point in the Binney and Cowie model is that there must be enough hot, diffuse gas to provide a pressure that confines the cool gas around M87. Because this gas would be less dense than the cooler gas, it would have a lower surface brightness, but it should be detectable in hard x-rays. Davison (1978) and Lawrence (1978) found a hard x-ray component from M87/Virgo, which they suggested was extended. However, more recent observations indicate that this hard component is not extended, has a power-law spectrum, and is centered on M87 (Lea *et al.*, 1981,1982). This hard source is probably nonthermal emission from the nucleus of M87. The present limits on the amount of extended hard x-ray emission are, at best, marginally consistent with the Binney and Cowie model (Fabricant and Gorenstein, 1983).

The *Einstein* satellite observations of the x-ray emission from M87 have been analyzed in detail by Fabricant *et al.* (1980), Fabricant and Gorenstein (1983), and Stewart, Canizares, Fabian, and Nulsen (1984). All of these papers used basically the method of analysis outlined in Sec. V.E.4; that is, the observed surface brightness was deconvolved to give the variation of emissivity with radius from the galaxy center. At the time of the first paper, the spectral response of the IPC on *Einstein* was poorly calibrated, and the density was derived from the emissivity assuming that the gas was isothermal. From the hydrostatic equation, the total mass $M(r)$ interior to a radius r is

$$M(r) = -\frac{kT_g r}{G\mu m_p} \left[\frac{d \ln \rho_g}{d \ln r} + \frac{d \ln T_g}{d \ln r} \right]. \quad (5.113)$$

Beyond 3 arcmin from the center of M87, the surface brightness is well represented as a power law $\sim r^{-1.62}$ (Fabricant and Gorenstein, 1983). Thus, as long as the temperature gradient is not significant, the density derivative in this equation is a constant, and the mass increases with the radius. Fabricant *et al.* (1980) found a total mass of $2-4 \times 10^{13} M_\odot$ within a radius of 230 kpc.

Binney and Cowie (1981) analyzed the same *Einstein* data and found consistency with their low-mass model for M87. They argued that the disparity between their conclusion and that of Fabricant *et al.* (1980) was due to two differences. First, Fabricant *et al.* assumed that the surface brightness approached zero far from M87, whereas Binney and Cowie invoke extended intracluster gas. More importantly, in the Binney and Cowie cooling flow model the gas temperature decreases rapidly towards the center, $d \ln T_g / d \ln r \approx 0.8$. This large temperature gradient nearly cancels the density gradient (i.e., the pressure is nearly constant), and the resulting mass is significantly reduced.

The *Einstein* data were reanalyzed by Fabricant and Gorenstein (1983) and Stewart, Canizares, Fabian, and Nulsen (1984), who found that the mass of M87 is $3-6 \times 10^{13} M_\odot$ within a radius of 260 kpc. By this time, the spectral response of the IPC had been calibrated and the temperature gradient could be derived directly from the data, albeit with large errors. (Note that this is possi-

ble for M87/Virgo and not for most cluster sources because the temperature in M87/Virgo is low enough to be measured with the soft x-ray sensitivity of *Einstein*.) In addition, the temperature gradient was constrained by the wide field proportional counter observations from previous satellites, and by data from the SSS and FPCS x-ray spectrometers on *Einstein*. The observed temperature gradient appears to be inconsistent with that required by Binney and Cowie. These data appear to rule out the Binney and Cowie model.

Thus M87 appears to have a very massive halo, which extends well beyond the region where the galaxy is luminous. Like the massive halos around spiral galaxies (Sec. II.H), the mass appears to increase roughly in proportion to the radius in the outer portions of M87. However, spiral galaxies have rotation velocities nearly independent of radius, on the order of 300 km/sec (Faber and Gallagher, 1979). The inferred circular orbital velocity in the halo of M87 is much higher, about 750 km/sec. This is also much higher than the orbital velocities of stars in the visible portion of M87, and thus the orbital velocities in M87 are not independent of radius over the span from the luminous portions of the galaxy to the outer halo.

One important question is whether other elliptical galaxies have massive dark halos. Dark halos have been deduced for spiral galaxies from the rotational velocities of the neutral hydrogen in the disks of the galaxies far outside of their optically luminous regions. Elliptical galaxies do not possess much neutral hydrogen, and thus this technique cannot be applied to them. The masses of elliptical galaxies can be determined from the orbital velocities of their stars (actually the line-of-sight component of the stellar velocity dispersion; see Dressler, 1979,1981). Unfortunately, these observations are very difficult and cannot be done in the outermost portions of the galaxies. Moreover, the masses are uncertain because the shapes of the orbits of the stars are not known (they may be radial or isotropic, for example; see Sec. II.H). The orbital velocities of globular star clusters can also be used to determine the masses of elliptical galaxies (Hesser *et al.*, 1984). Masses can be derived from studies of binary galaxies, but here the orbital characteristics are even more uncertain (Faber and Gallagher, 1979).

The use of x-ray-emitting gas to measure the masses of elliptical galaxies out to large distances has a number of important advantages. First, this gas can be traced out beyond the luminous region of the galaxy. Second, the orbits of gas particles are known to be isotropic because the gas is a collisional fluid. Thus x-ray measurements can give important information on the possible existence of massive halos around elliptical galaxies, provided such galaxies contain extended hot gas (Sec. V.H.3).

2. Other models for M87 and other central galaxies

In Secs. V.G and V.H.1, a standard model for M87 (and other x-ray-emitting central galaxies) has been given,

in which there is a cooling flow leading to accretion by M87. The outer parts of the flow are very subsonic, and the gas is nearly hydrostatic and bound either by the massive halo of M87 or by the pressure of surrounding gas. One feature of this standard model is that thermal conduction must be suppressed in order to ensure that the losses due to cooling in the center of the galaxy are balanced by the enthalpy flux of inflowing gas rather than by heat conducted inwards. Two alternative models are now discussed in which conduction is not suppressed.

Takahara and Takahara (1979,1981) suggested that gas was actually being thermally evaporated and flowing out from M87, rather than flowing inward. They argued that the gas in the evaporative flow was supplied by mass loss from stars in M87, at a rate of about $1M_{\odot}/\text{yr}$. This gas is heated by thermal conduction from surrounding, extended hot intracluster gas, in which the galaxy is assumed to be immersed.

One problem with this model is that the range of temperatures in the gas is rather small, and the gas is generally hotter than 2×10^7 K. This model cannot produce the very strong soft x-ray line emission seen in M87 (Canizares *et al.*, 1979,1982; Lea *et al.*, 1982; Stewart, Canizares, Fabian, and Nulsen, 1984). It does not provide a very good fit to the x-ray surface brightness in the inner regions of the galaxy, and does not explain the origin of the line-emitting filaments in M87 (Sec. V.G.3).

Tucker and Rosner (1983) suggested that the gas in M87 (and other central dominant galaxies) is actually hydrostatic (not moving). In their model, the cooling of the gas is balanced by heating from thermal conduction in the outer regions and by heating by the relativistic electrons associated with the radio source in the inner parts. As discussed in Sec. V.G.1, the extra heating by relativistic electrons actually results in thermal equilibrium being attained at a lower temperature, since cooling increases rapidly as the temperature is reduced. Such a model is necessarily thermally unstable (Stewart, Canizares, Fabian, and Nulsen, 1984), and might form a cooling flow due to the growth of thermal fluctuations. This model requires a fairly large rate of heating from relativistic electrons (Scott *et al.*, 1980; Sec. V.C.5), and there is considerable uncertainty about such large heating rates. The model does have the advantage that the similarity in the morphology of the x-ray and diffuse radio emission in M87 is explained.

In Sec. V.G.2 the suggestion was made that the radio emission of central cluster galaxies was powered by having a small portion of the accreting gas reach the nucleus. In the Tucker and Rosner model, the gas is static. Thus there is no inflow to power the radio source. Tucker and Rosner suggest that these sources might be episodic. Initially, gas cooling in the core of the cluster might produce an accretion flow on the central galaxy, and start the radio source. The radio source would produce large numbers of relativistic electrons, which would heat the gas and turn off the accretion flow. This would stop the radio source, and the heating would decline as the relativistic electrons lost their energy. This would allow the ac-

cretion flow to restart, and the process might oscillate in this fashion indefinitely.

3. X-ray emission from noncentral cluster galaxies

X-ray emission from noncentral galaxies, both ellipticals and spirals, has been detected in both the Virgo cluster (Forman *et al.*, 1979; Forman and Jones, 1982) and in A1367 (Bechtold *et al.*, 1983). These are the nearest irregular clusters with weak x-ray emission, and thus this may be a common property of such clusters. X-ray emission has also been detected from relatively isolated elliptical galaxies (Nulsen *et al.*, 1984). In Virgo, about a dozen galaxies have been detected with luminosities $L_x \sim 10^{39} - 2 \times 10^{41}$ ergs/sec (Sec. III.E.3). The most luminous are M86 and M84, which are shown in Fig. 21. The x-ray emission from M86 is more extended than the emission from M84, and forms a plume extending to the north of the galaxy. In A1367, 11 galaxies were detected in x rays by Bechtold *et al.* [Sec. III.E.4; Fig. 22(b)], of which 8 were found to be spatially extended. The luminosities of these galaxies range from $L_x \sim 1 - 7 \times 10^{41}$ ergs/sec. Because these galaxies are not generally radio sources, it seems unlikely that the emission is nonthermal. Their luminosities are larger than would be expected from a stellar sources, given their optical luminosities. Thus Bechtold *et al.* (1983) and Nulsen *et al.* (1984) argued that they contain hot gas, which emits thermal x rays. It should be noted, however, that the direct spectral evidence in favor of thermal emission is weak (Forman *et al.*, 1979; Nulsen *et al.*, 1984). If the emission is thermal, typically $\sim 10^9 M_{\odot}$ of gas is required at a temperature of $\sim 10^7$ K.

A model for the x-ray emission from these galaxies, and particularly M86, was suggested by Forman *et al.* (1979) and developed further by Fabian *et al.* (1980), Bechtold *et al.* (1983), and Nulsen *et al.* (1984). The source of the gas is assumed to be mass loss from stars in the galaxy, at a rate of $\sim 10^{-12} M_{\odot}$ per year per solar mass of stars in the galaxy. This gas may be heated by supernovas or simply by adiabatic compression (Nulsen *et al.*, 1984; Secs. V.C.2 and V.C.3). The cooling time of the gas will be rather short unless the gas is reasonably hot and also not very centrally condensed. Fabian *et al.* argue that the gas temperature must be greater than 2.5×10^7 in M86, which requires a supernova rate of about 1 per 100 yr. Now, this gas must be bound to the galaxy, or a strong wind would be produced and the gas would leave the galaxy. The gas could be bound by a massive halo around the galaxy, although Fabian *et al.* and Bechtold *et al.* argue against this possibility, because the required masses do not appear to correlate with the optical luminosities of the galaxies and because confinement by the gravitational potential of a galaxy would tend to make the gas centrally condensed and decrease its cooling time. Instead, they propose that the gas is confined by the pressure of intracluster gas. The required pressures

are roughly consistent with those deduced from the x-ray surface brightnesses of these clusters.

A galaxy that is moving slowly might thus be able to retain some of the gas produced by stellar mass loss (Forman *et al.*, 1979; Fabian *et al.*, 1980; Takeda *et al.*, 1984). A more rapidly moving galaxy would tend to lose its gas due to stripping (Sec. V.I). Based on their radial velocities, M84 appears to be moving fairly slowly, while M86 is moving rapidly. Because its velocity is considerably larger than the average in the Virgo cluster, Forman *et al.* and Fabian *et al.* suggest that the orbit of M86 will carry it far outside the cluster core, where the intracluster gas density is low. In these outer regions of the cluster, stripping of gas may be ineffective, and the galaxy will accumulate gas (Takeda *et al.*, 1984). Forman *et al.* and Fabian *et al.* estimate an orbital period for M86 of roughly 5×10^9 yr. Thus the galaxy could amass roughly $5 \times 10^9 M_{\odot}$ of gas during each orbit. This gas would be stripped during each passage through the cluster core. In this interpretation, the plume to the north of M86 is the trail of gas being stripped from M86 as it enters the core of the Virgo cluster (Forman *et al.*, 1979; Fabian *et al.*, 1982).

As discussed in Sec. V.G.4, gas in these galaxies can also form a cooling flow if the rate of supernova heating is not too high.

I. Stripping of gas from galaxies in clusters

The galaxies found in rich clusters generally have considerably less gas than galaxies in the field (Sec. II.J.2). Their 21-cm radio line luminosities indicate that they have less neutral gas than more isolated galaxies (see Sec. IV.G and the many references therein), and they also appear to have weaker optical line fluxes from ionized gas (Gisler, 1978). The galaxies in rich, regular, x-ray luminous clusters are predominantly ellipticals and SO's (Secs. II.E and II.J.1, Table II), and the spirals that are seen in clusters often have weak ("anemic") spiral arms (van den Bergh, 1976) and tend to be found at large projected distances from the cluster center (Gregory, 1975; Melnick and Sargent, 1977). The fraction of spiral galaxies is anticorrelated with the x-ray luminosity of the cluster [Bahcall, 1977c; Melnick and Sargent, 1977; Tytler and Vidal, 1979; Sec. III.; Fig. 25; Eq. (3.9)] and with the local galaxy density (Dressler, 1980b). A primary difference between spiral galaxies and ellipticals or SO's is that spirals contain large amounts of gas.

These observations suggest that gas in galaxies in clusters may be removed by some process. In Sec. II.J.2 the possibility that the differences in the galaxian populations of clusters and the field might result from the stripping of gas from spiral galaxies was discussed. This hypothesis is very controversial, and it appears unlikely that spiral stripping alone accounts for all the differences between different types of galaxies. Nonetheless, even within individual galaxy classes (Hubble types), galaxies in clusters

appear to have less gas (Sullivan *et al.*, 1981; Giovanardi *et al.*, 1983; Sec. IV.G). This suggests that some process must remove gas from galaxies in clusters, even if this stripping does not solely determine the morphology of galaxies.

In addition to this indirect evidence for gas removal, the x-ray observations of M86 suggest that it is currently being stripped of gas (Forman *et al.*, 1979; Fabian *et al.*, 1980; Secs. III.E.3 and V.H.3). There are also a number of cases where optical or 21-cm radio observations may show gas currently being stripped from galaxies (see, for example, Gallagher, 1978).

Mathews and Baker (1971) showed that, once an isolated elliptical or SO galaxy had been stripped of its gas, supernova-driven winds would keep it gas free. If the interstellar gas density is low, then the energy input from supernovas cannot be radiated away, and heats the gas until it flows out of the galaxy (Secs. V.C.3 and V.F). If the galaxy is immersed in intracluster gas, this mechanism is less effective, since the wind must overcome the confining pressure of the intracluster gas.

Spitzer and Baade (1951) suggested that collisions between spiral galaxies in the cores of compact clusters remove the interstellar medium from the disks of these galaxies. Their basic argument was that the stellar components of galaxies could pass through one another, because two-body gravitational interaction between galaxies or their component stars is very ineffective (Sec. II.I.1). However, the mean free paths of gas atoms or ions (Sec. V.D.1) are relatively short, and in the center-of-mass frame for the collision, the kinetic energy of the gas will be thermalized. If the gas cannot cool rapidly, it will be heated to a temperature at which it is no longer bound to either galaxy, since galaxies within a cluster move much more rapidly than stars move within galaxies. If the gas cools rapidly, it will still be left at rest in the center-of-mass frame, while the galaxies move away from it. In either case, the gas is no longer bound to either galaxy, since it has more kinetic energy (either thermal or bulk) than the maximum galaxy binding energy.

Spitzer and Baade estimated the rate of gas removal in the Coma cluster assuming all the galaxies were equivalent, and that the galaxies all had radial orbits, and found that a galaxy should be stripped in less than 10^8 yr. This is probably an underestimate of the time scale, since galaxy orbits are probably not radial, and a typical off-center collision between two galaxies of dissimilar mass and density may not remove all of the gas from both galaxies. Moreover, subsequent increases in the extragalactic distance scale have had the effect of increasing the time scale for this process. Sarazin (1979) estimated the mean time scale for collisional stripping of galaxies in a cluster, averaging over the cluster velocity dispersion, the spatial distribution of galaxies, and the diameters and masses of galaxies, and found a rate about 100 times smaller.

Gunn and Gott (1972) suggested that galaxies lose their interstellar gas by ram pressure ablation because of the rapid motion of the galaxies through the intracluster gas.

They were primarily concerned with stripping gaseous disks from spiral galaxies to make SO's. Based on a static force balance argument, they suggested that a gaseous disk would be removed when the ram pressure $P_r = \rho_g v^2$ exceeded the restoring gravitational force per unit area in the disk $2\pi G \sigma_D \sigma_{\text{ISM}}$ (where ρ_g is the intracluster gas density, v is the galaxy velocity, σ_D the surface density of the spiral disk, and σ_{ISM} the surface density of interstellar gas in the disk). Taking $v^2 = 3 \sigma_r^2$ for a typical galaxy in a cluster with a line-of-sight velocity dispersion σ_r , and assuming the disk has a uniform surface density, with a radius r_D and mass M_D , this condition becomes

$$\left[\frac{n_g}{10^{-3} \text{ cm}^{-3}} \right] \left[\frac{\sigma_r}{10^3 \text{ km/sec}} \right]^2 \gtrsim 3 \left[\frac{M_D}{10^{11} M_\odot} \right]^2 \left[\frac{r_D}{10 \text{ kpc}} \right]^{-4} \left[\frac{M_{\text{ISM}}}{0.1 M_D} \right], \quad (5.114)$$

where n_g is the number density of atoms in the intracluster medium and M_{ISM} is the mass of interstellar medium in the disk.

Tarter (1975) and Kritsuk (1983) have given simple semianalytical treatments of the stripping of gas disks in spiral galaxies in clusters by integrating the net force due to ram pressure and gravity, assuming one-dimensional motion. For a given intracluster gas distribution, they found the smallest distance from the cluster center at which a galaxy could retain its gas. The calculations by Tarter indicated that most spirals should be stripped fairly easily in x-ray clusters, and that remaining spirals would only be found in the outer parts. On the other hand, Kritsuk suggested that molecular clouds might be very difficult to strip from spirals.

It is interesting to calculate the expected dependence of the spiral fraction and the typical distance of spirals from the cluster center on the cluster x-ray luminosity, if one assumes that all clusters originally had the same spiral-rich galactic populations at all positions. If one also assumes that the reduction in the fraction of spirals is due to ram pressure ablation, that a spiral is stripped whenever the ram pressure exceeds a critical amount [given by Eq. (5.114) or something similar], that the galaxies in clusters have an analytic King isothermal distribution [Eq. (5.57)], and that the gas is isothermal and hydrostatic [Eq. (5.63)], then the spiral fraction varies as $f_{\text{sp}} \approx A - B \ln L_x$, where L_x is the x-ray luminosity and A and B are constants. This is just the empirical relationship found by Bahcall (1977c) [Eq. (3.9); Fig. 25]. The radius of a typical spiral varies as $r_{\text{sp}}/r_c \propto (L_x)^{1/6\beta}$, where r_c is the core radius and β is the ratio of gas and galaxy temperatures [Eq. (5.64)].

The majority of galaxies presently in x-ray clusters are ellipticals and SO's that have a more spherical stellar distribution. Sarazin (1979) gave a semianalytic treatment of the stripping of gas from spherical galaxies, using basically the same formulation as Tarter (1975). He found that galaxies would be stripped if the ram pressure were

greater than about $2GM_{\text{gal}}\sigma_{\text{ISM}}/R^2$, where M_{gal} and R are the galaxy mass and radius, respectively. Takeda *et al.* (1984) performed numerical hydrodynamic simulations and derived a critical ram pressure of $2\rho_{\text{ISM}}\sigma_*^2$. Assuming that the ram pressure is much greater than this limit, the time scale for ram pressure stripping of a galaxy, defined as $t_{\text{rp}} \equiv (d \ln M_{\text{ISM}}/dt)^{-1}$, is

$$t_{\text{rp}} \sim \frac{R}{v} \left[\frac{2\rho_{\text{ISM}}}{\rho_g} \right]^{1/2} \approx 3 \times 10^7 \text{ yr} \left[\frac{\rho_{\text{ISM}}}{\rho_g} \right]^{1/2} \left[\frac{v}{10^3 \text{ km/sec}} \right]^{-1} \times \left[\frac{R}{20 \text{ kpc}} \right], \quad (5.115)$$

where ρ_{ISM} is the average interstellar gas density, ρ_g is the intracluster gas density, v and M_{gal} are the galaxy velocity and mass, respectively. The calculations of Tarter and Sarazin assume that there are no sources of gas in the galaxy.

Gisler (1976,1979) pointed out that it would be more difficult to strip a galaxy if the stars in the galaxy were constantly resupplying it with gas. Then, the ram pressure must overcome the momentum flux due to this mass input, as well as the gravitational attraction of the galaxy. He derived an approximate analytical relationship for the ram pressure needed to strip gas out of a galaxy out to a projected radius b , ignoring pressure forces in the gas and assuming one-dimensional motion. If the rate of gas loss by stars in the galaxy is $\dot{\rho}_{\text{ISM}} = \alpha_* \rho_*$ where ρ_* is the mass density of stars in the galaxy, then he found that gas would be stripped at any projected radius b such that the ram pressure exceeded $\sim 8\alpha_* \Sigma_*(b) \sigma_*$. Here, $\Sigma_*(b)$ is the projected stellar mass density at b , and σ_* is the line-of-sight velocity dispersion of stars in the galaxy. For a typical giant elliptical galaxy in a typical x-ray cluster, Gisler found that all the gas is lost if the rate of input is less than $0.1 M_\odot/\text{yr}$, and that all the gas is retained if it is greater than about $3 M_\odot/\text{yr}$. For intermediate values, a core of interstellar gas is retained by the galaxy.

Gisler's treatment ignored pressure forces, which must be important in elliptical galaxies (Jones and Owen, 1979; Takeda *et al.*, 1984). Jones and Owen argued that extended gas in elliptical galaxies must be hot (the sound speed in the gas must be comparable to the velocity dispersion of stars), and that pressure forces in the gas cannot be ignored. A pressure gradient may be set up in the interstellar gas that opposes the ram pressure; they argued that this increases the region of a galaxy that is shielded from stripping by about a factor of 10 over Gisler's result. Then elliptical galaxies will typically retain cores of interstellar gas with radii of about 10 kpc, and Jones and Owen argue that this gas can explain the existence of well-defined radio jets in the inner parts of head-tail radio sources (Sec. IV.C; Fig. 31).

Takeda *et al.* (1984) recently rederived Gisler's condition for continuous stripping of gas from galaxies with stellar gas loss, including pressure forces. They find that

the correct condition for stripping is that the ram pressure exceed

$$\rho_g v^2 \gtrsim \frac{2}{v} \int \alpha_* \rho_* |\phi_*| dl \approx \frac{16 \alpha_* \Sigma_*(b) \sigma_*^2}{v}, \quad (5.116)$$

where ϕ_* is the galaxy gravitational potential. Equation (5.116) differs from Gisler's result by a factor of $\sim 2\sigma_*/v$.

Most of these calculations of stripping have been based on semianalytic estimates, which assume the motion to be one-dimensional, generally ignore the finite temperature and compressibility of the gases, and ignore any viscous forces. To avoid these assumptions and test the efficiency of ram pressure ablation, a large number of numerical hydrodynamic simulations have been made by Gisler (1976), Lea and De Young (1976), Toyama and Ikeuchi (1980), and Nepveu (1981a). These studies have all taken the galaxy to be spherical, and the simulations have been two dimensional, with the flows assumed to be axially symmetric. Lea and De Young started with a galaxy with a significant amount of interstellar gas, moving in the midst of intracluster gas. On the other hand, Gisler was mainly interested in the effects of stellar mass loss on ram pressure ablation, and he started with an empty galaxy. The numerical calculations indicate that stripping occurs even more easily than the simple analytic force balance arguments suggest. Unless the rate of mass input due to stars is high, a typical galaxy will be stripped almost completely during a single passage through the core of a cluster if the intracluster gas density exceeds roughly 10^{-4} atoms cm^{-3} .

Recently, Shaviv and Salpeter (1982) and Gaetz *et al.* (1985) made two-dimensional hydrodynamic calculations of ram pressure ablation for galaxies with stellar mass loss, including the cooling of the gas. Gaetz *et al.* also included star formation. They found that gas was ablated from the outer portions of the galaxy, but was retained in the inner portions and formed a cooling flow. One very useful feature of Gaetz *et al.* is that the hydro simulations were used to derive analytic fitting formulas for many physical quantities associated with the gas flows.

All of these numerical calculations start with the galaxy in the middle of a uniform cluster. Recently, Takeda *et al.* (1984) calculated the stripping of gas from a galaxy moving on a radial orbit from the outer parts of the cluster into the core. Stellar mass loss was assumed to add to the interstellar gas in the galaxy. The stripping was determined from two-dimensional hydrodynamic simulations. After the first passage through the cluster core, the behavior was periodic, with the galaxy accumulating interstellar gas when far from the core and losing nearly all of it when it passed through the core on each orbit. A large fraction of the accumulated interstellar gas was pushed out in a single "blob" on each passage through the cluster core. These calculations may provide a model for the galaxy M86, other gas-containing galaxies, and the galaxyless extended x-ray sources in A1367 (Secs. III.E.3, III.E.4, and V.H.3). The latter might be

"blobs" released from stripped galaxies (Takeda *et al.*, 1984).

Under many circumstances, transport processes such as viscosity and turbulent mixing can be more important than ram pressure in removing gas from a galaxy in a cluster (Livio *et al.*, 1980; Nepveu, 1981b; Nulsen, 1982). Nulsen has calculated the rate of laminar viscous stripping and stripping due to turbulence, and finds a viscous stripping time scale

$$t_{\text{vs}} \approx \frac{4R}{3v} \left[\frac{\rho_{\text{ISM}}}{\rho_g} \right] \left[\frac{12}{\text{Re}} + 1 \right]^{-1}, \quad (5.117)$$

where Re is the Reynolds number [Eq. (5.47)]. In many cases, this is faster than the rate of ram pressure ablation given by Eq. (5.115). However, one caution is that the viscous stresses may saturate, since the mean free paths of ions are similar to the sizes of galaxies (Sec. V.D.4).

Livio *et al.* (1980) suggest that the Kelvin-Helmholtz instability at the boundary between interstellar and intracluster gas can produce "spikes" of interstellar gas protruding into the intracluster gas, which are sheared off, increasing the stripping rate. They estimate a mass loss rate roughly $\dot{M}_{\text{KH}} \sim \rho_{\text{ISM}} \pi R^2 \lambda_{\text{KH}} / t_{\text{KH}}$, where $\lambda_{\text{KH}} \sim 10^{21}$ cm and $t_{\text{KH}} \sim 10^6$ yr are the wavelength and growth time of the fastest growing modes. This stripping rate is considerably smaller than that given by Eq. (5.117). Moreover, Nulsen (1982) has argued that Livio *et al.* overestimated this rate because they ignored the effect of compressibility on the instability, and because they did not include the effect of the mass loss on the instability. Another problem is that the wavelength of the fastest growing mode is shorter than the ion mean free path $\lambda_{\text{KH}} \ll \lambda_i$, and the viscosity expression used is therefore not valid (Sec. V.D.4). Nulsen showed that the instability was suppressed when viscosity is significant, and that the mass loss is not controlled by the fastest growing modes but by the induced velocities on the largest scales.

Another mechanism for removing gas from galaxies, which can operate even when the galaxies are moving slowly through the intracluster gas, is evaporation (Gunn and Gott, 1972; Cowie and McKee, 1977; Cowie and Songaila, 1977). Heat is conducted into the cooler galactic gas from the hotter intracluster gas, and if the rate of heat conduction exceeds the cooling rate, the galactic gas will heat up and evaporate. If cooling is assumed to be small, the evaporation rate with unsaturated conduction for a spherical galaxy immersed in intracluster gas of temperature T_g is (Cowie and Songaila, 1977)

$$\begin{aligned} \dot{M}_{\text{ev}} &\approx \frac{16\pi\mu t_p \kappa R}{25k} \\ &\approx 700 M_{\odot} / \text{yr} \left[\frac{T_g}{10^8 \text{ K}} \right]^{5/2} \\ &\quad \times \left[\frac{R}{20 \text{ kpc}} \right] \left[\frac{\ln \Lambda}{40} \right]^{-1}, \end{aligned} \quad (5.118)$$

where κ is the thermal conductivity [Sec. V.D.2; Eq.

(5.37)] and Λ is the Coulomb logarithm [Eq. (5.33)]. The stripping rate is a factor of $(2/\pi)$ smaller for a disk galaxy with the same radius. The evaporation rate will be significantly reduced if the conductivity saturates (Sec. V.D.2), as is probably the case at least for disk galaxies. Unfortunately, thermal conductivity also depends critically on the magnetic field geometry (Sec. V.D.3). If the conductivity is not suppressed by the magnetic field, this mechanism can play an important role in stripping gas from galaxies.

As pointed out by Nulsen (1982), there is a simple connection between mass loss by evaporation and mass loss by laminar viscosity [the Re term in Eq. (5.117)]. At low velocities, this term dominates, and the viscous stripping rate is nearly independent of velocity, because the Reynolds number is proportional to velocity. Since both thermal conduction and ionic viscosity are transport processes and the ion and electron mean free paths are essentially equal, the rates of stripping from these two processes are simply related:

$$\dot{M}_{ev} \approx 3.5\dot{M}_{vs} . \quad (5.119)$$

While this expression was derived for unsaturated conduction and viscosity and no magnetic suppression of either, it probably will remain approximately true even when these effects are included, since both thermal conduction and viscosity are affected similarly.

J. The origin and evolution of the intracluster medium

Where does all of this x-ray-emitting intracluster gas come from? Did it fall into clusters from intergalactic space, or was it ejected from galaxies? When did it first fill the great volumes of space between galaxies in clusters? What can we learn about the origin of galaxies and clusters from the intracluster gas? Theories of the origin of the intracluster medium attempt to explain the current properties of x-ray clusters, to make predictions about their past history that can be tested with observations of clusters at high redshift, and to relate the history of the intracluster gas to theories of the origin of structure in the universe.

There are two basic constraints on such theories from the observations of present-day x-ray clusters. First, these clusters typically contain $\sim 10^{14}M_{\odot}$ of intracluster gas, an amount comparable to the mass of luminous material in galaxies and about one-tenth of the total mass of the cluster. Second, this gas produces x-ray lines from iron that require that the abundance of that element be about one-half of its solar value if the gas is homogeneous.

At present, there are very few observations of high-redshift x-ray clusters, and thus the constraints that can be imposed on theories of the evolution of x-ray clusters by these observations are fairly weak. The only safe statement one can make at the present time is that x-ray clusters do not show any evidence of very dramatic evolution out to redshifts of $z \sim 0.5$ (Sec. III.H). Another con-

straint on the evolution of x-ray clusters comes from the diffuse x-ray background (Fabian and Nulsen, 1979); the total emission from high-redshift clusters cannot exceed the background brightness.

The question of the origin of the intracluster gas is strongly tied to the question of the origin of clusters and galaxies. This is a major area of astronomical research, and I shall not even attempt to summarize the theories in this area. Instead, I shall deal very narrowly with theories of the intracluster medium and shall largely ignore their dependence on models for galaxy formation, except when the x-ray cluster models provide information that affects these theories. Discussions of the effects that x-ray cluster observations have on theories of galaxy formation include Silk (1978), Binney and Silk (1978), White and Rees (1978), Fabian and Nulsen (1979), Binney (1980), and Field (1980).

There is an increasingly large amount of observational information on the evolution of galaxies; here only a few points will be noted. First, galaxies contain stars with a range of ages and heavy-element abundances. Elliptical and SO galaxies contain mainly older stars, with ages of around 10^{10} yr (Fall, 1981). Although galaxies do contain some stars with very low heavy-elements abundances, there is no significant population of stars with *no* heavy elements, and the number of low-abundance stars is less than might be expected if all the heavy elements were formed in stars like the present stellar population (Carr *et al.*, 1984). No mechanism is known to produce heavy elements in any quantity outside of stars. This has led to the suggestion that there was an early (before 10^{10} yr ago) generation of stars, which produced the minimum level of heavy elements seen in stars today (Carr *et al.*, 1984). Second, there is some evidence that the population of galaxies has evolved in some clusters since redshifts of $z \sim 0.5$; this is the "Butcher-Oemler effect" (Sec. II.J.2). These clusters have an excess of blue galaxies, which suggests that they were undergoing fairly rapid star formation at that time. Finally, violent activity in the nuclei of galaxies appears to have been much more common in the past (Schmidt, 1978); this activity produces Seyfert galaxies, radio galaxies, and quasars. There were many more very luminous quasars at a time corresponding to a redshift of two than are seen around us today. On the other hand, since few quasars are known with redshifts greater than 3.5 (Osmer, 1978), something must have occurred then to start the violent nuclear activity in galaxies. Also, if quasars are all located in the nuclei of galaxies, then galaxies must have formed by a redshift of three. Although this nuclear activity in galaxies is very poorly understood, most current theories require that gas be supplied to the nucleus (Rees, 1978); thus its variation may be related to the supply of intracluster gas and the stripping of gas from galaxies.

1. Infall models

Gunn and Gott (1972) suggested that the intracluster medium was primordial intergalactic gas that had fallen

into clusters. This intergalactic gas was never associated with stars or galaxies, and thus could be expected to have no heavy elements. They also noted that some of the intracluster medium could come from ram pressure stripping of interstellar gas out of galaxies. Assuming that clusters were immersed in uniform intergalactic medium, they estimated the amount that would fall into clusters. By comparing this to the amount of intracluster gas deduced from the early x-ray observations of clusters, they could give an upper limit on the density of the intergalactic gas. (This is an upper limit because some of the intracluster gas could have come out of galaxies.) These limits are usually given in terms of ρ_c , the density of matter necessary to close the universe,

$$\rho_c \equiv \frac{3H_0^2}{8\pi G} = 4.7 \times 10^{-30} h_{50}^2 \text{ g cm}^{-3}, \quad (5.120)$$

where H_0 is the Hubble constant (see footnote 4). If ρ_{IG} is the density of intergalactic gas, then Gunn and Gott found $\rho_{IG}/\rho_c \lesssim 0.01$. They used a rather low value for the gas mass in clusters, and more recent calculations (for example, Cowie and Perrenod, 1978) give $\rho_{IG}/\rho_c \lesssim 0.2$. Gunn and Gott also noted that infall would heat the intracluster gas to about the observed temperatures (Sec. V.C.2).

To determine the final configuration and evolution of the intracluster gas in the infall model, hydrodynamic simulations of the infall have been done by a number of authors (Gull and Northover, 1975; Lea, 1976; Takahara *et al.*, 1976; Cowie and Perrenod, 1978). These calculations all assumed that the cluster potential was fixed; the gas was assumed to fall into the cluster after the cluster itself had collapsed. All of these calculations were one-dimensional simulations of spherical clusters, although a number of different techniques were used to solve the hydrodynamic equations. With the exception of Lea's calculations, these simulations have given similar results.

As the gas first collapses into the core, its density increases and a shock propagates outward from the cluster center and heats the gas. This shock passes through the cluster in $\sim 10^9$ yr, essentially the sound crossing time for the cluster [Eq. (5.54)]. After the passage of the shock, the hot intracluster gas is nearly hydrostatic, and its further evolution is quasistatic. As the shock moves into the outer parts of the cluster, it weakens; less gas is added to the cluster, and the cluster luminosity is nearly constant. On the other hand, Lea found that the shock heating caused the gas pressure to increase until the inflow was reversed and the intracluster gas expanded. This cooled the gas adiabatically, lowered its pressure, and it collapsed again. This process repeated itself, producing a large number of pulsations with a period of about 5×10^9 yr. During these pulsations, the x-ray luminosity oscillated wildly between roughly 10^{41} and 10^{48} ergs/sec. The other calculations of the infall of intracluster gas have failed to find these oscillations (Gull and Northover, 1975; Takahara *et al.*, 1976; Cowie and Perrenod, 1978; Perrenod, 1978b), and they are probably an artifact of Lea's numerical method. Such oscillations are in violent

disagreement with the observed x-ray luminosity function of clusters (Schwartz, 1978).

Gull and Northover (1975) found that the shock strength was nearly constant as it propagated outward; they argued that this occurred because the shock speed was always about the free-fall speed in the cluster. They found that the resulting intracluster gas distribution was nearly adiabatic (Sec. V.E.2). On the other hand, more detailed calculations by Cowie and Perrenod (1978) and Perrenod (1978b) found that the cluster gas distributions were not well represented by any polytropic distribution, unless thermal conduction was so effective that the gas was isothermal.

In the absence of significant cooling or thermal conduction, Cowie and Perrenod (1978) showed that the infall models with a fixed cluster potential are characterized by a single parameter, which gives the depth of the cluster potential well, $K \equiv (\sigma_r/H_0 r_c)^2$ where σ_r and r_c are the cluster velocity dispersion and core radius, respectively. Models with significant cooling are also characterized by $B \equiv t_{\text{cool}} H_0$, where the cooling time is evaluated at the cluster center. If thermal conduction is important, the cluster evolution is also determined by the value of $C \equiv \kappa T_g / r_c \rho_g c_s^3$, where κ is the thermal conductivity, and T_g , ρ_g , and c_s are the gas temperature, density, and sound speed. When conduction saturates, the models are independent of C . In general, the gas temperatures in these models scale with σ_r^2 .

Cowie and Perrenod found that models without significant cooling or conduction showed a very small decrease in the x-ray luminosity with time, less than a 40% reduction from $z=1$ to the present. This decrease in luminosity resulted from the slow reexpansion of the intracluster gas as the shock weakened. In models with significant cooling, the cluster evolved to a nearly steady-state cooling flow (Sec. V.G). In models with conduction, the x-ray luminosity increased slowly with time, by about 40% from a redshift $z=1$ to the present. This occurred because conduction lowered the temperature in the cluster core (Sec. V.D.2). The core then contracted so that the increasing density could maintain the pressure in the core. Since the x-ray luminosity increases more rapidly with density than does the pressure [Eq. (5.21)], the luminosity went up.

These models all assumed that the cluster potential was static; the cluster was assumed to collapse before any gas fell into it. Of course, there is no reason why intergalactic gas should wait until the cluster has formed before gaseous infall can occur. Perrenod (1978a, 1978b) calculated the evolution of the intracluster gas in infall models in which the cluster potential varied in time. The cluster potential was taken from White's (1976c) N -body calculations of the collapse of a Coma-like cluster (Sec. II.I; Fig. 4). In White's models, the cluster first collapses with violent relaxation, then contracts slowly due to two-body interactions between galaxies. This contraction causes the cluster potential well to become deeper, and as a result the intracluster gas temperature and density increase with time. In contrast to the static potential models, Perrenod

finds that the x-ray luminosity of his model clusters increases by about an order of magnitude from $z=1$ to the present. The sizes of the gas distributions also shrink considerably. If thermal conduction is important, the further contraction in the gas distributions it produces makes them smaller than the observed sizes of x-ray clusters.

One interesting aspect of Perrenod's models is that many of the infall models have a temperature inversion ($dT_g/dr > 0$) in the cluster core, even if there is no significant cooling. This occurs because gas in the core has fallen through a shallower gravitational potential than gas further out. If such a temperature inversion were observed, it might be confused with a cooling flow (Sec. V.G).

In White's N -body models, the cluster shows very strong subclustering at the beginning of its collapse, and forms two roughly equal subclusters, which merge as the cluster undergoes violent relaxation. Several double x-ray clusters are known (Sec. III.D.2; Fig. 13) that appear to be in just this stage of evolution (Forman *et al.*, 1981). Obviously, such subclustering cannot be treated in one-dimensional, spherical, hydrodynamic simulations. Gingold and Perrenod (1979) have made simplified three-dimensional hydro simulations of the evolution of clusters. When applied to the cluster potential from White's N -body models, these verified the previous one-dimensional calculations of Perrenod (1978b). They found that there was no significant enhancement of the x-ray emission from merging subclusters, beyond that predicted by single-cluster models. Similar calculations were made by Ikeuchi and Hirayama (1979).

One major concern about all the Perrenod varying-potential models is the use of White's (1976c) N -body calculations for the cluster potential. In this particular set of models by White, the total virial mass of the cluster was assumed to reside in the individual galaxies. This gave the galaxies large masses, which increased their two-body interactions (Sec. II.I.1), and caused the cluster core to contract rapidly. However, associating the "missing mass" in clusters with individual galaxies appears to produce more two-body relaxation in clusters than is observed (Secs. II.H and II.I.4); in fact, this was one of White's conclusions from his models. Thus it seems likely that Perrenod's calculations may significantly overestimate the increase with time of the x-ray luminosity and gas temperature and the decrease in the gas core size.

Clusters of galaxies are the largest organized structures in the universe, and x-ray emission from them should be recognizable to large redshifts (Sec. VI). They might therefore be useful as probes of the cosmological structure of the universe. Several cosmological tests have been proposed using x-ray clusters (Schwartz, 1976; Silk and White, 1978); although some of these tests are relatively insensitive to x-ray cluster evolution, most are strongly affected. These models suggest that it will be difficult to apply any tests that require that x-ray clusters have remained unchanged since $z=1$ (Perrenod, 1978b; Falle and Meszaros, 1980). On the other hand, in Perrenod's models the luminosity and size of x-ray clusters depend

strongly on the density of material in the universe, since this determines the speed with which clusters contract. In principle, this dependence of cluster evolution on density might provide useful cosmological information; in practice, the evolution models are too uncertain to be used reliably for this purpose.

The models described so far have dealt with the evolution of single clusters. Perrenod (1980) has attempted to predict the evolution of the luminosity function of x-ray clusters (Sec. III.B). He assumed that galaxies formed before clusters, and that clusters were formed by the gravitational attraction of galaxies. He argued that the merging of clusters tends to produce larger clusters with deeper potential wells, and as a result the average x-ray luminosity increases. Recently, White (1982) showed that this argument is incorrect; the increase in the depth of cluster potential wells is more than offset by the decrease in their characteristic densities. Perrenod found a very rapid evolution of the luminosity function to higher luminosities; he predicted that there should be few luminous x-ray clusters at redshifts $z \gtrsim \frac{1}{2}$. This evolution depends strongly on the average density of matter in the universe, and Perrenod proposed using it as a cosmological test. However, his basic model for clustering is apparently incorrect (White, 1982).

2. Ejection from galaxies

The observation that the intracluster medium contains a significant abundance of heavy elements shows that it cannot be *entirely* due to the infall of primordial gas (Secs. III.C.2 and V.B). The only way known for producing reasonable quantities of heavy elements is through nuclear reactions in stars. Since there is no significant luminous stellar population outside of galaxies at present, there are two possibilities. First, there may have been an early generation of pregalactic stars (Carr *et al.*, 1984), or second, it may be that some portion of the intracluster gas was ejected from galaxies. This section considers the second possibility.

Are the present rates of mass loss from stars in galaxies sufficient to produce the required amount of gas if all the stellar mass loss is added to the intracluster gas? Let us assume that the intracluster gas is chemically homogeneous (Sec. V.D.5), so that the inferred heavy-element abundance is about half of the solar value. Then, since this is comparable to the present abundances in the stars in elliptical galaxies in clusters, ejection from galaxies would have to supply a significant portion of the observed intracluster gas. The total mass of intracluster gas is comparable to the total mass of stars in galaxies in a luminous x-ray cluster, and both are only about 10% of the virial mass. Now the current rate of mass loss expected from the stellar populations seen in elliptical or SO galaxies is $\alpha_* \leq 10^{-11} M_\odot/\text{year}/M_\odot$. Thus, only one-tenth of the intracluster gas could be supplied in a Hubble time $\sim 10^{10}$ yr at the current rate.

In doing estimates of this sort, it is very important to

remember that mass loss from stars is due to their evolution as they exhaust their nuclear fuel, and thus the mass loss from a stellar population is primarily due to the most luminous stars. In estimating the rate of mass loss, the rate per luminous star should be multiplied by the mass of luminous matter, and not the total (virial) mass. Another way of stating this is that the rate of mass loss is proportional to the luminosity of a stellar population and not to its mass; thus the rate of mass loss per unit mass varies inversely with the mass-to-light ratio (Sec. II.H); Yahil and Ostriker (1973) give

$$\alpha_* \approx 10^{-10} \text{ yr}^{-1} \left[\frac{M}{L} \right]_{\odot}^{-1}, \quad (5.121)$$

where $(M/L)_{\odot}$ is the mass-to-light ratio in solar units. Then, if the total cluster mass is used, the total cluster mass-to-light ratio $(M/L)_{\odot} \approx 300$ must be used as well. The result is the same as treating only the mass in the luminous portions of galaxies and using the mass-to-light ratio there, $(M/L)_{\odot} \approx 10-30$.

The rate of mass loss from stars in galaxies must have been higher in the past, if stellar mass loss has contributed significantly to the intracluster medium. One simple way this can have occurred is for elliptical and SO galaxies to have contained more massive stars in the past, since massive stars have higher rates of mass loss. At present, these galaxies have only relatively low-mass stars $M_* \lesssim 0.8 M_{\odot}$ (Fall, 1981). Since stellar lifetimes decrease with mass, and the presently observed stars have lifetimes comparable to the Hubble time, any higher-mass stars produced at the time of galaxy formation would no longer exist. High-mass stars tend to die as supernovas, which are very effective in producing and dispersing heavy elements, so these stars might provide the heavy elements in the intracluster gas and in the stars seen in the galaxies today without leaving any very low-abundance stars (Carr *et al.*, 1984). Moreover, the supernovas could aid in the removal of gas from the galaxies into the intracluster medium.

It is often suggested that all the stars in an elliptical or SO galaxy formed at one time during the formation of the galaxy itself. Stars with a wide range of masses are usually assumed to have been made in protogalaxies, and the present stellar population is only those lower-mass stars whose lifetimes exceed the age of the galaxy. Usually, the distribution of the masses of stars that form (the initial mass function or IMF) is taken to be a power law, and the star formation rate is assumed to decline exponentially with the age of the galaxy:

$$\frac{\partial^2 N_*}{\partial M_* \partial t} \propto M_*^{-a} \exp(-t/t_*), \quad M_L \leq M_* \leq M_U, \quad (5.122)$$

where N_* is the number of stars formed of mass M_* , the lower and upper limits to the IMF are M_L and M_U , and t_* is the time scale for star formation. A power law with $a = 2.35$ is called the "Salpeter IMF" (Salpeter, 1955) and

fits the current star formation in the disk of our galaxy. The time scale for star formation is often taken to be comparable to the dynamical time in a galaxy, $t_* \sim 3 \times 10^8$ yr. The resulting model for the gas loss from a galaxy depends on the IMF assumed and on the values of t_* and t_{st} , the time scale for the removal of gas from the galaxy.

Larson and Dinerstein (1975) calculated the properties of the intracluster gas based on this model. They assumed a Salpeter IMF. The only gas-loss process they considered was supernova heating from the same stellar population; this may underestimate the ejected mass if collisions or ram pressure ablation also contribute. Based on this model, they found that the majority of the gas was not removed in galaxies more massive than about $10^{10} M_{\odot}$. The total gas mass ejected from galaxies in a cluster was about 30% of the mass in stars in galaxies, and the ejected mass had roughly solar abundances. Because these calculations preceded the detection of the iron x-ray lines in clusters, they successfully predicted that nearly solar abundances would be found.

Fairly similar results were found by Ikeuchi (1977), Biermann (1978), De Young (1978), and Sarazin (1979). Biermann assumed most of the galaxies were spirals that were stripped by collisions and ram pressure; this resulted in a more complete removal of interstellar gas, but over a longer time ($t_{st} \geq t_*$). Biermann found somewhat lower heavy-element abundances of 0.1–0.5 of solar, with the gas mass ranging from 1 to 0.1 of that of the stars. De Young noted that the supernova energy was sufficient to unbind the gas produced by stellar mass loss in galaxies, and thus assumed that nearly all the gas was ejected quite rapidly ($t_s < t_*$). He also considered a wider range of IMF's, and generally found heavy-element abundances that were larger, 1–3 times solar. This was primarily sensitive to the exponent a in the IMF. The ejected gas masses were 0.15–0.5 of the stellar mass. One exception to the agreement among these authors was Vigroux (1977), who claimed that galaxies could not make enough iron during the course of their normal evolution. The account he gave of his calculations was rather sketchy, so it is difficult to compare them to the others. With this exception, the general conclusion was that galaxies could eject an amount of gas about half the stellar mass with roughly solar abundances during their normal stellar evolution. If this gas were diluted with roughly an equal amount of unprocessed primordial gas, either within the forming galaxies or in the cluster, the observed mass and heavy-element abundances in the intracluster gas would be reproduced.

In most of these models, the time scale of star formation is assumed to be short, $t_* \lesssim 10^9$ yr. During this time, most of the stars in the galaxy are formed, and the more massive and luminous stars live and die explosively in supernovas. As a result, it is expected that the newly formed galaxies would be very bright during this era (De Young, 1978; Bookbinder *et al.*, 1980).

The evolution of the intracluster gas in models with ejection from galaxies depends on the length of time it takes the newly enriched gas to be stripped, t_{st} . De

Young (1978) noted that the energy input from the supernovas produced by a stellar population which would give the needed iron abundance would be sufficient to unbind the interstellar gas. This assumes that the supernova energy is efficiently converted to kinetic energy in the gas.

On the other hand, if the supernova energy is radiated away, the gas may remain bound to the galaxy. Norman and Silk (1979) and Sarazin (1979) showed that this was likely to be the case, because the large quantity of intracluster gas in clusters implies that there was a large density of gas in protogalaxies. At high densities the gas cools rapidly, and individual supernova remnants radiate away their energy before they overlap. Under these circumstances, the galaxies may retain their gas. Norman, Silk, and Sarazin suggested that galaxies retain much of their initial gas content as extended hot coronas. If this gas cannot be removed by supernovas, then collisions or ram pressure remain as stripping mechanisms (Sec. V.I). They further assumed that galaxy formation is very efficient, in the sense that nearly all the gas in a cluster was initially contained in galaxies. Then, there would be very little intracluster gas at first, and ram pressure ablation would not be effective. The galaxies would first lose gas slowly through collisions, and when the intracluster density was high enough, ram pressure stripping would start. Because ram pressure ablation both increases the gas density and increases with increasing gas density, this leads to a runaway stripping of cluster galaxies. The evolution of the gas in a cluster would then occur in two extended stages, with a rapid transition between them. First, all the gas would be bound to galaxies. Then, it would be rapidly stripped and remain distributed in the intracluster medium after that time. This was proposed as an explanation of the Butcher-Oemler effect (Sec. II.J.2); the Butcher-Oemler clusters were still in this first stage. Unfortunately, this model predicts that these clusters have very little intracluster gas, when in fact they were subsequently observed to be luminous x-ray sources (Sec. III.H). Larson *et al.* (1980) argued that the disks of spiral and SO galaxies are produced by infall from coronas of gas bound to galaxies, and that a spiral galaxy becomes an SO when the corona is stripped and the gas supply to the disk stops. In this way, there would be a longer interval between the stripping of the corona and the cessation of star formation in the disk. Perhaps Butcher-Oemler clusters are within this interval. One problem with these models for gaseous coronas is that they require a rather delicate and unstable balance between supernova heating and cooling.

Biermann (1978) proposed a similar model in which gas produced by disk galaxies is stored in their disks, and is eventually stripped by collisions and ram pressure. Himmes and Biermann (1980) gave a somewhat more detailed model, in which elliptical galaxies in a cluster lose their interstellar gas rapidly by supernova heating and provide an initial amount of intracluster gas, which begins the process of ram pressure stripping of spiral galaxies. They argued that this model can reproduce the present intracluster gas masses, iron abundances, and dependence of the galactic population on x-ray luminosity

(Sec. III.F). In this model, the spiral fraction in cluster decreases continuously with time, and the variation from a redshift of $z \sim 0.4$ to the present is consistent with the Butcher-Oemler effect.

One general feature of these models in which gas is ejected from galaxies over a long period of time is that the luminosities of x-ray clusters are expected to increase with time. Unfortunately, this is the same prediction made by Perrenod's infall models with deepening cluster potentials, as discussed in the previous section.

A number of one-dimensional, spherically symmetric, hydrodynamic simulations have been made of the evolution of intracluster gas, including ejection from galaxies. Cowie and Perrenod (1978) calculated models with a fixed cluster potential and assumed that the rate of gas ejection from galaxies varied inversely with time $\dot{m} \propto 1/t$. There was no primordial intracluster gas in these models. The gas was ejected at zero temperature (Sec. V.C.3) and assumed to mix immediately with the intracluster gas. When the gas ejection rate is large, the models evolve to steady-state cooling flows (Cowie and Binney, 1977; Sec. V.G.1). In models with lower ejection rates, the x-ray luminosity either is roughly constant (no thermal conduction) or increases by about a factor of 2 (thermal conduction) from a redshift $z=1$ to the present. Perrenod (1978b) calculated ejection models in a varying cluster potential; the results were very similar to those described above for infall models. He found a better fit to the present gas distributions with these models than with infall models, and the ejection models were less sensitive to the assumed initial conditions and model parameters. These models showed a rapid increase in x-ray luminosity with time, as did the infall models.

Ikeuchi and Hirayama (1980) ran hydro models with no primordial gas, in which gas is ejected from all the galaxies simultaneously and very rapidly ($t_{st} \leq 10^7$ yr). This seems rather unlikely, since this time scale is less than the sound crossing time for a single galaxy. Because of this assumption of rapid ejection, they chose the following initial conditions: at the start of their calculation, the ejected gas was placed in the cluster in a nonhydrostatic distribution determined by their ejection model, and then "let go." The gas then adjusted to the cluster potential on a sound crossing time (Sec. V.E). These models have very large x-ray luminosities $\sim 10^{48}$ ergs/sec during this initial relaxation time $t \sim 3 \times 10^8$ yr. It seems very unlikely that such high luminosities would be realized, since the actual gas ejection must take considerably longer than was assumed.

It has generally been assumed that the ejected gas mixes rapidly (both chemically and thermally) with the intracluster gas (De Young, 1978). However, Nepveu (1981b) argues that this will not occur (although the only mechanism he considers is turbulent mixing), and that the ejected and intracluster gases must be treated as two separate fluids.

Hirayama (1978) and Nepveu (1981b) have given hydrodynamic models for the evolution of the intracluster medium including both gas ejected from galaxies and pri-

mordial gas. In both cases, the primordial gas is initially relaxed, and galaxy gas is injected at a constant rate. In both of these calculations, the ejected gas is concentrated at the cluster center ($R \lesssim 2$ Mpc), and there is a large gradient in the heavy-element abundance across the cluster. As noted previously (Secs. V.D.5 and V.E.5), such a concentration of heavy elements at the cluster center will increase the strengths of the x-ray lines from these elements. Thus the abundances derived from the x-ray spectra of clusters could overestimate the real abundances. However, because most of the x-ray emission in these models comes from radii of less than 2 Mpc, this effect is not very serious. Spatially resolved x-ray spectra across a cluster might detect such a gradient, and this would allow one to deduce the proportions of ejected and intracluster gas.

VI. PROSPECTS FOR THE FUTURE AND AXAF

What advances can be expected in the near future in the study of x-ray clusters? In this brief look at future prospects, I shall concentrate on new observational opportunities. At present, observational x-ray astronomy is in a rather quiet period. The *Einstein* x-ray satellite, which revolutionized the study of x-ray astronomy, is no longer operational. As this review was being written, the European Space Agency x-ray satellite *EXOSAT* was launched, although few scientific results from it have appeared as yet. It is a somewhat less powerful imaging instrument than *Einstein*, and may be very useful for followup studies of the results from *Einstein*, but it will not dramatically increase the state of the art in x-ray observations. What advances in the technology of x-ray astronomy are needed to answer the major questions we have about x-ray clusters, and what plans are there for the realization of these advances?

The basic data in the x-ray study of clusters consist of the surface brightness of x rays I_ν , as a function of the photon frequency ν and the position on the sky. Given these data and a suitable assumption of symmetry for the cluster, the x-ray emissivity $\epsilon_\nu(r)$ as a function of position in the cluster can be derived by deconvolution of the surface brightness (Sec. V.E.4). The emissivity varies as the square of the density ρ_g , and its frequency dependence is determined by the gas temperature T_g and by the abundances of heavy elements [Eq. (5.19)]. At the temperatures usually found in the intracluster gas, the heavy element abundances mainly affect the emission in several narrow line features, and the temperature produces an exponential falloff in the intensity for frequencies $h\nu > kT_g$. Thus, given suitable observations of the x-ray surface brightness I_ν , one can derive the gas density, temperature, and several heavy-element abundances, all as a function of position in the cluster.

In relatively nearby clusters, the required instrument for these observations must measure the x-ray surface brightness with at least moderate spatial resolution (< 1 arcmin), and modest spectral resolution (better than about

15%), and must be sensitive to x rays with photon energies $h\nu$ of at least 7 keV. Obviously, it must also have a sufficient sensitivity to detect the clusters. Unfortunately, no past or currently existing satellite has had all these capabilities. Proportional counter systems, such as the *Uhuru* satellite, have modest spectral resolution out to high x-ray energies, but have very poor spatial resolution. The *Einstein* satellite had excellent spatial resolution, fairly poor spectral resolution in the imaging detectors, and no sensitivity for photon energies $h\nu \gtrsim 4$ keV.

The Advanced X-ray Astronomy Facility (*AXAF*) would provide the new observational capabilities needed for the further study of x-ray clusters (Giacconi *et al.*, 1980). *AXAF* is a 1.2-m-diam x-ray telescope, which would be carried into orbit by the Space Shuttle. As currently planned, *AXAF* would have roughly 100 times the sensitivity of the *Einstein* telescope for point sources and a considerably increased sensitivity for extended sources as well. Its mirrors would produce images with a spatial resolution of better than one second of arc, and would be sensitive to x rays with photon energies of at least 8 keV. At least some of the imaging detectors being considered would have moderate spectral resolution (10–20% or better), and the satellite would have a number of higher-resolution spectrometers. With its high spatial resolution, moderate spectral resolution, and sensitivity to harder x rays, it would provide exactly the data on cluster x-ray surface brightnesses needed to derive their densities, temperatures, and abundances.

Given the run of density and temperature of the gas in a cluster or in an individual galaxy, the hydrostatic equation [Eq. (5.56)] allows one to determine the total mass in the galaxy or cluster as a function of position (Secs. V.E.4 and V.H.1). These mass determinations are less uncertain than those based on the radial velocities of galaxies in clusters or stars in galaxies because the gas atoms are known to be moving isotropically. These mass distributions would provide very important information on the distribution and nature of the missing mass component in clusters and galaxies.

If measurements of the microwave diminutions of clusters can be made reliably, they can be combined with the determinations of the variation of the gas temperature and density to give distances to clusters that are independent of the Hubble constant (Sec. IV.E). This will provide a direct determination of the Hubble constant, independent of the usual extragalactic distance scale. If this method could be applied to high-redshift clusters, it might allow the determination of the overall structure of the universe.

From the variation of the gas temperature with density and with position in a cluster, the influence of the various heating, cooling, and energy transport processes (Secs. V.C and V.D) can be deduced. As discussed in Sec. V.E.1, the surface brightness distributions in nearby clusters from the *Einstein* satellite are consistent with isothermal gas distributions, although temperatures could not be determined directly. Unfortunately, the temperatures required by the surface brightness fits are generally

not consistent with temperatures derived from the integrated spectra of the clusters. Given this discrepancy, we cannot claim to have any real understanding of the thermal processes in intracluster gas. Direct measurements of the temperature profiles of clusters are needed to resolve this problem.

The moderate spectral resolution of *AXAF*'s imaging detectors and sensitivity to 7-keV x rays will allow this instrument to map out the abundance of iron and possibly other heavy elements in clusters. The distribution of heavy elements in clusters must be known if accurate abundances are to be derived for them. As noted in Secs. V.D.5 and V.E.5, if the iron in clusters is concentrated in the core, the iron abundances may have been significantly overestimated. These abundances are used to determine the amount of gas that must have been ejected from stars in galaxies, and affect models for the origin and early evolution of galaxies (Sec. V.J.2). Moreover, the distributions of heavy elements provide information on the relative proportions of ejected galactic gas and primordial intergalactic gas in clusters.

The higher-resolution spectrometers on *AXAF* can be used to determine the abundances of additional elements and give more precise information on the temperature structure. It is particularly useful that the 7-keV iron lines will be observable, as these are the strongest lines in the intracluster gas and have many fine-structure components whose intensities are sensitive to temperature. High-resolution line studies will be particularly useful in studying the physical conditions in cooling flows (Sec. V.G). They may also permit the determination of redshifts for x-ray clusters for which optical data are not available, and will certainly resolve any ambiguities when several clusters at different redshifts are seen along the same line of sight. At the highest spectral resolution, it may be possible to determine directly the flow velocities in clusters, particularly those with cooling flows.

The high spatial resolution of *AXAF* will be very important to the study of cooling flows and of other gas associated with individual galaxies (Secs. V.G and V.H). The increased sensitivity and enhanced spectral response of *AXAF* should make it possible to get spectra of the gas in these individual galaxy sources, in order to test the hypothesis that the emission is from hot gas. Gas in individual galaxies in clusters has so far been studied only in relatively nearby clusters. Of particular interest is the interaction of this gas with the intracluster medium.

AXAF should detect x-ray clusters out to very high redshifts, $z \sim 1-4$. From the study of these clusters, we shall learn directly about the origin of the intracluster gas and its evolution in clusters. We may actually see the gas being ejected from galaxies. If galaxy morphologies are altered by the galaxy's environment, and the main mechanism is gas stripping by intracluster gas, the buildup of the intracluster gas should be related to the evolution of galaxy morphologies. With the Hubble Space Telescope (Hall, 1982), it should be possible to classify galaxies out to at least moderate redshifts. The variation in the heavy-element abundances in clusters as a function of red-

shift should constrain models for the chemical evolution of galaxies. The variations in the temperature of the gas will allow us to assess the effects of heating and cooling.

It will also be interesting to see if there is any relationship between the evolution of x-ray clusters and that of quasars and other active galactic nuclei.

One problem with these studies of high-redshift clusters is that few are currently known. Because *AXAF* is not a survey instrument, it will probably not detect many previously unknown clusters, but will instead study in detail those that are previously known. It is possible that deeper ground-based optical surveys or studies with the Hubble Space Telescope will provide longer lists of cosmological clusters. It is also possible they may be found by studying high-redshift radio galaxies and quasars with the morphological distortions normally associated with sources in clusters (Sec. III.C). Another exciting possibility involves the *ROSAT* x-ray satellite. This instrument will perform an all-sky soft x-ray survey, with a spatial resolution of about one minute of arc and a sensitivity limit similar to that of the *Einstein* satellite. A luminous x-ray cluster at a redshift of one might possibly be detected in this survey. Because an x-ray cluster at a redshift of one would have an angular size of about one minute of arc, it might appear as a resolved source. The most common extragalactic x-ray sources found in deep surveys are quasars, which are point sources. Thus most of the resolved high-galactic-latitude sources in the *ROSAT* survey should be clusters, and some of those should be at high redshifts. This survey may provide a valuable list of x-ray clusters for further study.

ACKNOWLEDGMENTS

I should like to thank Edwin Salpeter for suggesting this review, and for his patience with my very slow completion of it. Andrew Fabian, Richard Mushotzky, Paul Nulsen, and Simon White very kindly provided detailed comments on the draft of this paper, and caught many significant errors. I really would like to thank them for all their help. I am also indebted to John Bahcall, James Binney, Patrick Henry, Hernan Quintana, Yoel Rephaeli, Herbert Rood, Hyron Spinrad, Melville Ulmer, and Raymond White for helpful comments, suggestions, and unpublished results. I should particularly like to thank John Bahcall for his encouragement. Figures for this review and the permission to publish them were very kindly provided by Neta Bahcall, Jack Burns, Claude Canizares, Christine Jones, Andrew Fabian, William Forman, Paul Gorenstein, Mark Henriksen, Roger Lynds, George Miley, Richard Mushotzky, Chris O'Dea, Herb Rood, Steve Strom, and Simon White. I should like particularly to thank Christine Jones and William Forman for producing special figures from the *Einstein* x-ray data for this review. Much of this review was written while I was a visitor at the Institute for Advanced Study in Princeton, N.J., and I should like to thank the Institute and particularly John Bahcall for their hospitality. Part of the review was written during visits to the Aspen Center for Physics and

the National Radio Astronomy Observatory, and I should also like to thank them. The Department of Applied Mathematics and Computer Science at the University of Virginia kindly provided some computer time for this work, which was very helpful. This work was supported in part by NSF Grant No. AST 81-20260.

REFERENCES

- Aarseth, S. J., and J. Binney, 1978, *Mon. Not. R. Astron. Soc.* **185**, 227.
- Abell, G. O., 1958, *Astrophys. J. Suppl.* **3**, 211.
- Abell, G. O., 1961, *Astron. J.* **66**, 607.
- Abell, G. O., 1962, in *Problems of Extra-Galactic Research*, edited by G. C. McVittie (University of Chicago, Chicago), p. 213.
- Abell, G. O., 1965, *Annu. Rev. Astron. Astrophys.* **3**, 1.
- Abell, G. O., 1975, in *Stars and Stellar Systems IX: Galaxies and the Universe*, edited by A. Sandage, M. Sandage, and J. Kristian (University of Chicago, Chicago), p. 601.
- Abell, G. O., 1977, *Astrophys. J.* **213**, 327.
- Abell, G. O., 1982, private communication.
- Abell, G. O., J. Neyman, and E. L. Scott, 1964, *Astron. J.* **69**, 529.
- Abramopoulos, F., G. Chanan, and W. Ku, 1981, *Astrophys. J.* **248**, 429.
- Abramopoulos, F., and W. Ku, 1983, *Astrophys. J.* **271**, 446.
- Adams, M. T., K. M. Strom, and S. E. Strom, 1980, *Astrophys. J.* **238**, 445.
- Adams, T. F., 1977, *Publ. Astron. Soc. Pac.* **89**, 488.
- Albert, C. E., R. A. White, and W. W. Morgan, 1977, *Astrophys. J.* **211**, 309.
- Allen, C. W., 1973, *Astrophysical Quantities* (Athlone, London), p. 197.
- Andernach, H., J. R. Baker, A. von Kap-herr, and R. Wielebinski, 1979, *Astron. Astrophys.* **74**, 93.
- Andernach, H., D. Schallwisch, C. Haslam, and R. Wielebinski, 1981, *Astron. Astrophys. Suppl.* **43**, 155.
- Andernach, H., H. Waldthausen, and R. Wielebinski, 1980, *Astron. Astrophys. Suppl.* **41**, 339.
- Arp, H., and J. Lorre, 1976, *Astrophys. J.* **210**, 58.
- Auriemma, C., G. Perola, R. Ekers, R. Fanti, C. Lari, W. Jaffe, and M. Ulrich, 1977, *Astron. Astrophys. Suppl.* **57**, 41.
- Austin, T. B., J. G. Godwin, and J. V. Peach, 1975, *Mon. Not. R. Astron. Soc.* **171**, 135.
- Austin, T. B., and J. V. Peach, 1974a, *Mon. Not. R. Astron. Soc.* **167**, 437.
- Austin, T. B., and J. V. Peach, 1974b, *Mon. Not. R. Astron. Soc.* **168**, 591.
- Avni, Y., 1976, *Astrophys. J.* **210**, 642.
- Avni, Y., and N. Bahcall, 1976, *Astrophys. J.* **209**, 16.
- Baan, W. A., A. D. Haschick, and B. F. Burke, 1978, *Astrophys. J.* **225**, 339.
- Bahcall, J. N., and N. A. Bahcall, 1975, *Astrophys. J. Lett.* **199**, L89.
- Bahcall, J. N., and C. L. Sarazin, 1977, *Astrophys. J. Lett.* **213**, L99.
- Bahcall, J. N., and C. L. Sarazin, 1978, *Astrophys. J.* **219**, 781.
- Bahcall, N. A., 1971, *Astron. J.* **76**, 995.
- Bahcall, N. A., 1972, *Astron. J.* **77**, 550.
- Bahcall, N. A., 1973a, *Astrophys. J.* **180**, 699.
- Bahcall, N. A., 1973b, *Astrophys. J.* **183**, 783.
- Bahcall, N. A., 1974a, *Astrophys. J.* **187**, 439.
- Bahcall, N. A., 1974b, *Astrophys. J.* **193**, 529.
- Bahcall, N. A., 1974c, *Nature* **252**, 661.
- Bahcall, N. A., 1975, *Astrophys. J.* **198**, 249.
- Bahcall, N. A., 1977a, *Annu. Rev. Astron. Astrophys.* **15**, 505.
- Bahcall, N. A., 1977b, *Astrophys. J. Lett.* **217**, L77.
- Bahcall, N. A., 1977c, *Astrophys. J. Lett.* **218**, L93.
- Bahcall, N. A., 1979a, *Astrophys. J.* **232**, 689.
- Bahcall, N. A., 1979b, *Astrophys. J. Lett.* **232**, L83.
- Bahcall, N. A., 1980, *Astrophys. J. Lett.* **238**, L117.
- Bahcall, N. A., 1981, *Astrophys. J.* **247**, 787.
- Bahcall, N. A., D. E. Harris, and R. G. Strom, 1976, *Astrophys. J. Lett.* **209**, L17.
- Bahcall, N. A., and W. L. W. Sargent, 1977, *Astrophys. J. Lett.* **217**, L19.
- Bahcall, N. A., and R. M. Soneira, 1982, *Astrophys. J.* **262**, 419.
- Baldwin, J. E., and P. F. Scott, 1973, *Mon. Not. R. Astron. Soc.* **165**, 259.
- Barnes, J., 1983, *Mon. Not. R. Astron. Soc.* **203**, 223.
- Basko, M. M., B. V. Komberg, and E. I. Moskalenko, 1981, *Astron. Zh.* **58**, 701 [*Sov. Astron.* **25**, 402 (1981)].
- Bautz, L. P., and G. O. Abell, 1973, *Astrophys. J.* **184**, 709.
- Bautz, L. P., and W. W. Morgan, 1970, *Astrophys. J. Lett.* **162**, L149.
- Bechtold, J., W. Forman, R. Giacconi, C. Jones, J. Schwarz, W. Tucker, and L. Van Speybroeck, 1983, *Astrophys. J.* **265**, 26.
- Beers, T. C., M. J. Geller, and J. P. Huchra, 1982, *Astrophys. J.* **257**, 23.
- Beers, T. C., J. P. Huchra, and M. J. Geller, 1983, *Astrophys. J.* **264**, 356.
- Begelman, M. C., M. J. Rees, and R. D. Blandford, 1979, *Nature* **279**, 770.
- Berthelsdorf, R. F., and J. L. Culhane, 1979, *Mon. Not. R. Astron. Soc.* **187**, 17p.
- Bieging, J. H., and P. Biermann, 1977, *Astron. Astrophys.* **60**, 361.
- Biermann, P., 1978, *Astron. Astrophys.* **62**, 255.
- Biermann, P., and P. Kronberg, 1983, *Astrophys. J.* **268**, L69.
- Biermann, P., P. P. Kronberg, and B. F. Madore, 1982, *Astrophys. J. Lett.* **256**, L37.
- Biermann, P., and S. L. Shapiro, 1979, *Astrophys. J. Lett.* **230**, L33.
- Bijleveld, W., and E. A. Valentijn, 1982, *Astron. Astrophys.* **111**, 50.
- Binggeli, B., 1982, *Astron. Astrophys.* **107**, 338.
- Binney, J., 1977, *Mon. Not. R. Astron. Soc.* **181**, 735.
- Binney, J., 1980, in *X-ray Astronomy*, edited by R. Giacconi and G. Setti (Reidel, Dordrecht), p. 245.
- Binney, J., and L. L. Cowie, 1981, *Astrophys. J.* **247**, 464.
- Binney, J., and J. Silk, 1978, *Comments Astrophys.* **7**, 139.
- Binney, J., and O. Strimpel, 1978, *Mon. Not. R. Astron. Soc.* **185**, 473.
- Birkinshaw, M., 1978, *Mon. Not. R. Astron. Soc.* **184**, 387.
- Birkinshaw, M., 1979, *Mon. Not. R. Astron. Soc.* **187**, 847.
- Birkinshaw, M., 1980, *Mon. Not. R. Astron. Soc.* **190**, 793.
- Birkinshaw, M., and S. F. Gull, 1984, *Mon. Not. R. Astron. Soc.* **206**, 359.
- Birkinshaw, M., S. F. Gull, and H. Hardebeck, 1984, *Nature* **309**, 34.
- Birkinshaw, M., S. F. Gull, and A. T. Moffet, 1981, *Astrophys. J. Lett.* **251**, L69.
- Birkinshaw, M., S. F. Gull, and K. J. Northover, 1978, *Mon.*

- Not. R. Astron. Soc. **185**, 245.
- Birkinshaw, M., S. F. Gull, and K. J. Northover, 1981, Mon. Not. R. Astron. Soc. **197**, 571.
- Blumenthal, G. R., S. M. Faber, J. R. Primack, and M. J. Rees, 1984, Nature **311**, 517.
- Bohlin, R. C., R. C. Henry, and J. R. Swandic, 1973, Astrophys. J. **182**, 1.
- Boldt, E., 1976, Astrophys. J. Lett. **208**, L15.
- Bookbinder, J., L. L. Cowie, J. H. Krolik, J. P. Ostriker, and M. Rees, 1980, Astrophys. J. **237**, 647.
- Bothun, G. D., M. J. Geller, T. C. Beers, and J. P. Huchra, 1983, Astrophys. J. **268**, 47.
- Boydton, P. E., S. J. Radford, R. A. Schommer, and S. S. Murray, 1982, Astrophys. J. **257**, 473.
- Bradt, H., W. Mayer, S. Narayan, S. Rappaport, and G. Spuda, 1967, Astrophys. J. Lett. **161**, L1.
- Braid, M. K., and H. T. MacGillivray, 1978, Mon. Not. R. Astron. Soc. **182**, 241.
- Branduardi-Raymont, G., D. Fabricant, E. Feigelson, P. Gorenstein, J. Grindlay, A. Soltan, and G. Zamorani, 1981, Astrophys. J. **248**, 55.
- Brecher, K., and G. R. Burbidge, 1972, Astrophys. J. **174**, 253.
- Bridle, A. H., and P. A. Feldman, 1972, Nature (London) Phys. Sci. **235**, 168.
- Bridle, A. H., and E. B. Fomalont, 1976, Astron. Astrophys. **52**, 107.
- Bridle, A. H., E. B. Fomalont, G. K. Miley, and E. A. Valentijn, 1979, Astron. Astrophys. **80**, 201.
- Bridle, A. H., and J. P. Vallee, 1981, Astron. J. **86**, 1165.
- Brown, R. L., and R. J. Gould, 1970, Phys. Rev. D **1**, 2252.
- Bruzual A., G., and H. Spinrad, 1978, Astrophys. J. **220**, 1; **222**, 1119(E) (1978).
- Bucknell, M. J., J. G. Godwin, and J. V. Peach, 1979, Mon. Not. R. Astron. Soc. **188**, 579.
- Burns, J. O., 1981, Mon. Not. R. Astron. Soc. **195**, 523.
- Burns, J. O., J. A. Eilek, and F. N. Owen, 1982, in *IAU Symposium 97: Extragalactic Radio Sources*, edited by D. Heeschen and C. Wade (Reidel, Dordrecht), p. 45.
- Burns, J. O., S. A. Gregory, and G. D. Holman, 1981, Astrophys. J. **250**, 450.
- Burns, J. O., C. P. O'Dea, S. A. Gregory, and T. J. Balonek, 1985, "Observational Constraints on Bending the Wide Angle Tail Radio Galaxy 1919 + 479," University of New Mexico report.
- Burns, J. O., and F. N. Owen, 1977, Astrophys. J. **217**, 34.
- Burns, J. O., and F. N. Owen, 1979, Astron. J. **84**, 1478.
- Burns, J. O., and F. N. Owen, 1980, Astron. J. **85**, 204.
- Burns, J. O., F. N. Owen, and L. Rudnick, 1978, Astron. J. **83**, 312.
- Burns, J. O., and M. P. Ulmer, 1980, Astron. J. **85**, 773.
- Burns, J. O., R. A. White, and R. J. Hanisch, 1980, Astron. J. **85**, 191.
- Burns, J. O., R. A. White, and M. P. Haynes, 1981, Astron. J. **86**, 1120.
- Burns, J. O., R. A. White, and D. H. Hough, 1981, Astron. J. **86**, 1.
- Burstein, D., 1979a, Astrophys. J. **234**, 435.
- Burstein, D., 1979b, Astrophys. J. **234**, 829.
- Butcher, H., and A. Oemler, Jr., 1978a, Astrophys. J. **219**, 18.
- Butcher, H., and A. Oemler, Jr., 1978b, Astrophys. J. **226**, 559.
- Byram, E. T., T. A. Chubb, and H. Friedman, 1966, Science **152**, 66.
- Cane, H. V., W. C. Erickson, R. J. Hanisch, and P. J. Turner, 1981, Mon. Not. R. Astron. Soc. **196**, 409.
- Canizares, C. R., 1981, in *Proceedings of the HEAD Meeting on X-ray Astronomy*, edited by R. Giacconi (Reidel, Dordrecht), p. 215.
- Canizares, C. R., G. W. Clark, J. G. Jernigan, and T. H. Markert, 1982, Astrophys. J. **262**, 33.
- Canizares, C. R., G. W. Clark, T. H. Markert, C. Berg, M. Smedira, D. Bardas, H. Schnopper, and K. Kalata, 1979, Astrophys. J. **234**, L33.
- Canizares, C. R., G. C. Stewart, and A. C. Fabian, 1983, Astrophys. J. **272**, 449.
- Capelato, H. V., D. Gerbal, G. Mathez, A. Mazure, E. Salvador-Sole, and H. Sol, 1980, Astrophys. J. **241**, 521.
- Carnevali, P., A. Cavaliere, and P. Santangelo, 1981, Astrophys. J. **249**, 449.
- Carr, B. J., J. R. Bond, and W. D. Arnett, 1984, Astrophys. J. **277**, 445.
- Carter, D., 1977, Mon. Not. R. Astron. Soc. **178**, 137.
- Carter, D., 1980, Mon. Not. R. Astron. Soc. **190**, 307.
- Carter, D., and J. G. Godwin, 1979, Mon. Not. R. Astron. Soc. **187**, 711.
- Carter, D., and N. Metcalfe, 1980, Mon. Not. R. Astron. Soc. **191**, 325.
- Cash, W., R. F. Malina, and R. S. Wolff, 1976, Astrophys. J. Lett. **209**, L111.
- Catura, R. C., P. G. Fisher, M. M. Johnson, and A. J. Meyerott, 1972, Astrophys. J. Lett. **177**, L1.
- Cavaliere, A., 1980, in *X-ray Astronomy*, edited by R. Giacconi and G. Setti (Reidel, Dordrecht), p. 217.
- Cavaliere, A., L. Danese, and G. deZotti, 1977, Astrophys. J. **217**, 6.
- Cavaliere, A., L. Danese, and G. deZotti, 1979, Astron. Astrophys. **75**, 322.
- Cavaliere, A., G. DeBiase, P. Santangelo, and N. Vittorio, 1983, in *Clustering in the Universe*, edited by D. Gerbal and A. Mazure (Editions Frontières, Paris, France), p. 15.
- Cavaliere, A., and R. Fusco-Femiano, 1976, Astron. Astrophys. **49**, 137.
- Cavaliere, A., and R. Fusco-Femiano, 1978, Astron. Astrophys. **70**, 677.
- Cavaliere, A., and R. Fusco-Femiano, 1981, Astron. Astrophys. **100**, 194.
- Cavaliere, A., H. Gursky, and W. H. Tucker, 1971, Nature **231**, 437.
- Cavallo, G., and N. Mandolesi, 1982, Astrophys. Lett. **22**, 119.
- Chamaraux, P., C. Balkowski, and E. Gerard, 1980, Astron. Astrophys. **83**, 38.
- Chandrasekhar, S., 1939, *An Introduction to the Study of Stellar Structure* (University of Chicago, Chicago), p. 155.
- Chandrasekhar, S., 1942, *Principles of Stellar Dynamics* (University of Chicago, Chicago), p. 231.
- Chandrasekhar, S., 1968, *Ellipsoidal Figures of Equilibrium* (Yale University, New Haven).
- Chincarini, G., 1984, Adv. Space Res. **3**, 393.
- Chincarini, G. L., R. Giovanelli, M. Haynes, and P. Fontanelli, 1983, Astrophys. J. **267**, 511.
- Chincarini, G., and H. J. Rood, 1976, Astrophys. J. **206**, 30.
- Chincarini, G., and H. J. Rood, 1977, Astrophys. J. **214**, 351.
- Chincarini, G., M. Tarenghi, and C. Bettis, 1978, Astrophys. J. **221**, 34.
- Chincarini, G., M. Tarenghi, and C. Bettis, 1981, Astron. Astrophys. **96**, 106.
- Christiansen, W. A., A. G. Pacholczyk, and J. S. Scott, 1981, Astrophys. J. **251**, 518.
- Ciardullo, R., H. Ford, F. Bartko, and R. Harms, 1983, Astro-

- phys. J. 273, 24.
- Coleman, G., P. Hintzen, J. Scott, and M. Tarenghi, 1976, *Nature* 262, 476.
- Cooke, B. A., and D. Maccagni, 1976, *Mon. Not. R. Astron. Soc.* 175, 65p.
- Cooke, J. A., D. Emerson, B. D. Kelly, H. T. MacGillivray, and R. J. Dodd, 1981, *Mon. Not. R. Astron. Soc.* 196, 397.
- Corwin, H. G., 1974, *Astron. J.* 79, 1356.
- Costain, C. H., A. H. Bridle, and P. A. Feldman, 1972, *Astrophys. J. Lett.* 175, L15.
- Cowie, L. L., 1981, in *Proceedings of the HEAD Meeting on X-ray Astronomy*, edited by R. Giacconi (Reidel, Dordrecht), p. 227.
- Cowie, L. L., and J. Binney, 1977, *Astrophys. J.* 215, 723.
- Cowie, L. L., A. C. Fabian, and P. E. Nulsen, 1980, *Mon. Not. R. Astron. Soc.* 191, 399.
- Cowie, L., E. Hu, E. Jenkins, and D. York, 1983, *Astrophys. J.* 272, 29.
- Cowie, L. L., and C. F. McKee, 1975, *Astron. Astrophys.* 43, 337.
- Cowie, L. L., and C. F. McKee, 1977, *Astrophys. J.* 211, 135.
- Cowie, L. L., and S. C. Perrenod, 1978, *Astrophys. J.* 219, 254.
- Cowie, L. L., and A. Songaila, 1977, *Nature* 266, 501.
- Crane, P., and J. A. Tyson, 1975, *Astrophys. J. Lett.* 201, L1.
- Da Costa, L. N., and E. Knobloch, 1979, *Astrophys. J.* 230, 639.
- Dagkesamansky, R. D., A. G. Gubanov, A. D. Kuzmin, and O. B. Slee, 1982, *Mon. Not. R. Astron. Soc.* 200, 971.
- Danese, L., G. deZotti, and G. di Tullio, 1980, *Astron. Astrophys.* 82, 322.
- Davidson, A., S. Bowyer, M. Lampton, and R. Cruddace, 1975, *Astrophys. J.* 198, 1.
- Davidson, A., and W. Welch, 1974, *Astrophys. J. Lett.* 191, L11.
- Davies, R. D., and B. M. Lewis, 1973, *Mon. Not. R. Astron. Soc.* 165, 231.
- Davis, M., J. Huchra, D. Latham, and J. Tonry, 1982, *Astrophys. J.* 253, 423.
- Davison, P. J., 1978, *Mon. Not. R. Astron. Soc.* 183, 39p.
- Dawe, J., R. Dickens, and B. Peterson, 1977, *Mon. Not. R. Astron. Soc.* 178, 675.
- Dennison, B., 1980a, *Astrophys. J.* 236, 761.
- Dennison, B., 1980b, *Astrophys. J. Lett.* 239, L93.
- des Forets, G., R. Dominguez-Tenreiro, D. Gerbal, G. Mathez, Alain Mazure, and E. Salvador-Sole, 1984, *Astrophys. J.* 280, 15.
- de Vaucouleurs, G., 1948a, *Ann. Astrophys.* 11, 247.
- de Vaucouleurs, G., 1948b, *Contrib. Inst. Astrophys. Paris A*, No. 27.
- de Vaucouleurs, G., 1953, *Astron. J.* 58, 30.
- de Vaucouleurs, G., 1956, *Mem. Mt. Stromlo Obs.* 15, No. 13.
- de Vaucouleurs, G., 1961, *Astrophys. J. Suppl.* 6, 213.
- de Vaucouleurs, G., 1975, in *Stars and Stellar Systems IX: Galaxies and the Universe*, edited by A. Sandage, M. Sandage, and J. Kristian (University of Chicago, Chicago), p. 557.
- de Vaucouleurs, G., 1976, *Astrophys. J.* 203, 33.
- de Vaucouleurs, G., and A. de Vaucouleurs, 1970, *Astrophys. Lett.* 5, 219.
- de Vaucouleurs, G., and J.-L. Nieto, 1978, *Astrophys. J.* 220, 449.
- De Young, D. S., 1972, *Astrophys. J.* 173, L7.
- De Young, D. S., 1978, *Astrophys. J.* 223, 47.
- De Young, D. S., J. J. Condon, and H. Butcher, 1980, *Astrophys. J.* 242, 511.
- Dickens, R. J., and C. Moss, 1976, *Mon. Not. R. Astron. Soc.* 174, 47.
- Dickey, J. M., and E. E. Salpeter, 1984, *Astrophys. J.* 284, 461.
- Disney, M. J., 1974, *Astrophys. J. Lett.* 193, L103.
- Dones, L., and S. D. M. White, 1985, *Astrophys. J.* 290, 94.
- Doroshkevich, A. G., S. F. Shandarin, and E. Saar, 1978, *Mon. Not. R. Astron. Soc.* 184, 643.
- Dressler, A., 1978a, *Astrophys. J.* 222, 23.
- Dressler, A., 1978b, *Astrophys. J.* 223, 765.
- Dressler, A., 1978c, *Astrophys. J.* 226, 55.
- Dressler, A., 1979, *Astrophys. J.* 231, 659.
- Dressler, A., 1980a, *Astrophys. J. Suppl.* 42, 565.
- Dressler, A., 1980b, *Astrophys. J.* 236, 351.
- Dressler, A., 1981, *Astrophys. J.* 243, 26.
- Dressler, A., 1984, *Annu. Rev. Astron. Astrophys.* 22, 185.
- Dressler, A., and J. E. Gunn, 1982, *Astrophys. J.* 263, 533.
- Duus, A., and B. Newell, 1977, *Astrophys. J. Suppl.* 35, 209.
- Eggen, O. J., D. Lynden-Bell, and A. Sandage, 1962, *Astrophys. J.* 136, 748.
- Einasto, J., M. Joeveer, and E. Saar, 1980, *Mon. Not. R. Astron. Soc.* 193, 353.
- Einasto, J., A. Kaasik, and E. Saar, 1974, *Nature* 250, 309.
- Elvis, M., 1976, *Mon. Not. R. Astron. Soc.* 177, 7p.
- Elvis, M., B. A. Cooke, K. A. Pounds, and M. J. Turner, 1975, *Nature* 257, 33.
- Elvis, M., E. Schreier, J. Tonry, M. Davis, and J. Huchra, 1981, *Astrophys. J.* 246, 20.
- Erickson, W. C., T. A. Matthews, and M. R. Viner, 1978, *Astrophys. J.* 222, 761.
- Fabbri, R., F. Melchiorri, and V. Natale, 1978, *Astrophys. Space Sci.* 59, 223.
- Faber, S. M., and A. Dressler, 1976, *Astrophys. J. Lett.* 210, L65.
- Faber, S. M., and A. Dressler, 1977, *Astron. J.* 82, 187.
- Faber, S. M., and J. S. Gallagher, 1976, *Astrophys. J.* 204, 365.
- Faber, S. M., and J. S. Gallagher, 1979, *Annu. Rev. Astron. Astrophys.* 17, 135.
- Fabian, A. C., P. D. Atherton, K. Taylor, and P. E. Nulsen, 1982, *Mon. Not. R. Astron. Soc.* 201, L17.
- Fabian, A. C., E. M. Hu, L. L. Cowie, and J. Grindlay, 1981, *Astrophys. J.* 248, 47.
- Fabian, A. C., W. H. Ku, D. F. Malin, R. F. Mushotzky, P. E. Nulsen, and G. C. Stewart, 1981, *Mon. Not. R. Astron. Soc.* 196, 35p.
- Fabian, A. C., and P. E. Nulsen, 1977, *Mon. Not. R. Astron. Soc.* 180, 479.
- Fabian, A. C., and P. E. Nulsen, 1979, *Mon. Not. R. Astron. Soc.* 186, 783.
- Fabian, A. C., P. E. Nulsen, and C. R. Canizares, 1982, *Mon. Not. R. Astron. Soc.* 201, 933.
- Fabian, A. C., P. E. Nulsen, and C. R. Canizares, 1984, *Nature* 310, 733.
- Fabian, A. C., and J. E. Pringle, 1977, *Mon. Not. R. Astron. Soc.* 181, 5p.
- Fabian, A. C., J. E. Pringle, and M. J. Rees, 1976, *Nature* 263, 301.
- Fabian, A. C., J. Schwarz, and W. Forman, 1980, *Mon. Not. R. Astron. Soc.* 192, 135.
- Fabricant, D., and P. Gorenstein, 1983, *Astrophys. J.* 267, 535.
- Fabricant, D., M. Lecar, and P. Gorenstein, 1980, *Astrophys. J.* 241, 552.
- Fabricant, D., K. Topka, F. R. Harnden, and P. Gorenstein, 1978, *Astrophys. J. Lett.* 226, L107.
- Fall, S. M., 1981, in *The Structure and Evolution of Normal*

- Galaxies*, edited by M. Fall and D. Lynden-Bell (Cambridge University, Cambridge), p.1.
- Falle, S. A., and P. Meszaros, 1980, *Mon. Not. R. Astron. Soc.* **190**, 195.
- Fanti, C., R. Fanti, L. Feretti, I. Gioia, G. Giovannini, L. Gregorini, B. Marano, L. Padrielli, P. Parma, P. Tomasi, and V. Zitelli, 1983, *Astron. Astrophys. Suppl.* **52**, 411.
- Farouki, R., G. L. Hoffman, and E. E. Salpeter, 1983, *Astrophys. J.* **271**, 11.
- Farouki, R., and E. E. Salpeter, 1982, *Astrophys. J.* **253**, 1.
- Farouki, R., and S. L. Shapiro, 1980, *Astrophys. J.* **241**, 928.
- Farouki, R., and S. L. Shapiro, 1981, *Astrophys. J.* **243**, 32.
- Feigelson, E. D., T. Maccacaro, and G. Zamorani, 1982, *Astrophys. J.* **255**, 392.
- Felten, J. E., R. J. Gould, W. A. Stein, and N. J. Woolf, 1966, *Astrophys. J.* **146**, 955.
- Felten, J. E., and P. Morrison, 1966, *Astrophys. J.* **146**, 686.
- Field, G. E., 1980, *Astron. Gesell. Mitt.* **47**, 7.
- Flannery, B. P., and M. Krook, 1978, *Astrophys. J.* **223**, 447.
- Fomalont, E., and A. H. Bridle, 1978, *Astrophys. J. Lett.* **223**, L9.
- Fomalont, E., and D. Rogstad, 1966, *Astrophys. J.* **146**, 52.
- Ford, H. C., and H. Butcher, 1979, *Astrophys. J. Suppl.* **41**, 147.
- Forman, W., J. Bechtold, W. Blair, R. Giacconi, L. Van Speybroeck, and C. Jones, 1981, *Astrophys. J. Lett.* **243**, L133.
- Forman, W., and C. Jones, 1982, *Annu. Rev. Astron. Astrophys.* **20**, 547.
- Forman, W., C. Jones, L. Cominsky, P. Julien, S. Murray, G. Peters, H. Tananbaum, and R. Giacconi, 1978, *Astrophys. J. Suppl.* **38**, 357.
- Forman, W., C. Jones, S. Murray, and R. Giacconi, 1978, *Astrophys. J. Lett.* **225**, L1.
- Forman, W., E. Kellogg, H. Gursky, H. Tananbaum, and R. Giacconi, 1972, *Astrophys. J.* **178**, 309.
- Forman, W., J. Schwarz, C. Jones, W. Liller, and A. C. Fabian, 1979, *Astrophys. J. Lett.* **234**, L27.
- Forster, J. R., 1980, *Astrophys. J.* **238**, 54.
- Fritz, G., A. Davidsen, J. F. Meekins, and H. Friedman, 1971, *Astrophys. J. Lett.* **164**, L81.
- Gaetz, T. J., and E. E. Salpeter, 1983, *Astrophys. J. Suppl.* **223**, 386.
- Gaetz, T. J., E. E. Salpeter, and G. Shaviv, 1985, "Gas Dynamics of Flows Past Galaxies: Flows with Radiative Cooling," Cornell University report.
- Gallagher, J. S., 1978, *Astrophys. J.* **223**, 386.
- Gallagher, J. S., and J. P. Ostriker, 1972, *Astrophys. J.* **77**, 288.
- Gavazzi, G., 1978, *Astron. Astrophys.* **69**, 355.
- Gavazzi, G., G. C. Perola, and W. Jaffe, 1981, *Astron. Astrophys.* **103**, 35.
- Geller, M. J., and T. C. Beers, 1982, *Publ. Astron. Soc. Pac.* **94**, 421.
- Geller, M. J., and P. J. Peebles, 1976, *Astrophys. J.* **206**, 939.
- Giacconi, R., *et al.*, 1979, *Astrophys. J.* **230**, 540.
- Giacconi, R., *et al.*, 1980, "Advanced X-ray Astrophysics Facility—Science Working Group Report," NASA Report No. TM-78285.
- Giacconi, R., S. Murray, H. Gursky, E. Kellogg, E. Schreier, T. Matilsky, D. Koch, and H. Tananbaum, 1974, *Astrophys. J. Suppl.* **27**, 37.
- Giacconi, R., S. Murray, H. Gursky, E. Kellogg, E. Schreier, and H. Tananbaum, 1972, *Astrophys. J.* **178**, 281.
- Gingold, R. A., and S. C. Perrenod, 1979, *Mon. Not. R. Astron. Soc.* **187**, 371.
- Gioia, I. M., M. J. Geller, J. P. Huchra, T. Maccacaro, J. E. Steiner, and J. Stocke, 1982, *Astrophys. J. Lett.* **255**, L17.
- Giovanardi, C., G. Helou, E. E. Salpeter, and N. Krumm, 1983, *Astrophys. J.* **267**, 35.
- Giovanelli, R., G. Chincarini, and M. P. Haynes, 1981, *Astrophys. J.* **247**, 383.
- Giovanelli, R., M. P. Haynes, and G. L. Chincarini, 1982, *Astrophys. J.* **262**, 422.
- Gisler, G. R., 1976, *Astron. Astrophys.* **51**, 137.
- Gisler, G. R., 1978, *Mon. Not. R. Astron. Soc.* **183**, 633.
- Gisler, G. R., 1979, *Astrophys. J.* **228**, 385.
- Gisler, G. R., and G. K. Miley, 1979, *Astron. Astrophys.* **76**, 109.
- Godwin, J. C., and J. V. Peach, 1977, *Mon. Not. R. Astron. Soc.* **181**, 323.
- Goldstein, S. J., 1966, *Science* **151**, 3706.
- Gorenstein, P., P. Bjorkholm, B. Harris, and F. R. Harnden, Jr., 1973, *Astrophys. J. Lett.* **183**, L57.
- Gorenstein, P., D. Fabricant, K. Topka, and F. Harnden, 1979, *Astrophys. J.* **230**, 26.
- Gorenstein, P., D. Fabricant, K. Topka, F. R. Harnden, and W. H. Tucker, 1978, *Astrophys. J.* **224**, 718.
- Gorenstein, P., D. Fabricant, K. Topka, W. Tucker, and F. R. Harnden, 1977, *Astrophys. J. Lett.* **216**, L95.
- Gott, J. R., 1977, *Annu. Rev. Astron. Astrophys.* **15**, 235.
- Gott, J. R., and T. X. Thuan, 1976, *Astrophys. J.* **204**, 649.
- Gould, R. J., and Y. Rephaeli, 1978, *Astrophys. J.* **219**, 12.
- Gregory, S. A., 1975, *Astrophys. J.* **199**, 1.
- Gregory, S. A., and L. A. Thompson, 1978, *Astrophys. J.* **222**, 784.
- Gregory, S. A., L. A. Thompson, and W. G. Tifft, 1981, *Astrophys. J.* **243**, 411.
- Gregory, S. A., and W. G. Tifft, 1976, *Astrophys. J.* **205**, 716.
- Grindlay, J. A., D. R. Parsignault, H. Gursky, A. C. Brinkman, J. Heise, and D. E. Harris, 1977, *Astrophys. J. Lett.* **214**, L57.
- Gudehus, D. H., 1973, *Astron. J.* **78**, 583.
- Gudehus, D. H., 1976, *Astrophys. J.* **208**, 267.
- Guindon, B., 1979, *Mon. Not. R. Astron. Soc.* **186**, 117.
- Guindon, B., and A. H. Bridle, 1978, *Mon. Not. R. Astron. Soc.* **184**, 221.
- Gull, S. F., and K. J. Northover, 1975, *Mon. Not. R. Astron. Soc.* **173**, 585.
- Gull, S. F., and K. J. Northover, 1976, *Nature* **263**, 572.
- Gunn, J. E., 1977, *Astrophys. J.* **218**, 592.
- Gunn, J. E., 1978, in *Observational Cosmology*, edited by A. Maeder, L. Martinet, and G. Tammann (Geneva Observatory, Geneva).
- Gunn, J. E., and J. R. Gott, 1972, *Astrophys. J.* **176**, 1.
- Gunn, J. E., and J. B. Oke, 1975, *Astrophys. J.* **195**, 255.
- Gunn, J. E., and B. M. Tinsley, 1976, *Astrophys. J.* **210**, 1.
- Gursky, H., E. Kellogg, C. Leong, H. Tananbaum, and R. Giacconi, 1971a, *Astrophys. J. Lett.* **165**, L43.
- Gursky, H., E. M. Kellogg, S. Murray, C. Leong, H. Tananbaum, and R. Giacconi, 1971b, *Astrophys. J. Lett.* **167**, L81.
- Gursky, H., and D. Schwartz, 1977, *Annu. Rev. Astron. Astrophys.* **15**, 541.
- Gursky, H., A. Solinger, E. Kellogg, S. Murray, H. Tananbaum, R. Giacconi, and A. Cavaliere, 1972, *Astrophys. J. Lett.* **173**, L99.
- Guthrie, B. N., 1974, *Mon. Not. R. Astron. Soc.* **168**, 15.
- Hall, D. N., 1982, "The Space Telescope Observatory," NASA Report No. CP-2244.
- Hall, A., and D. Sciama, 1979, *Astrophys. J. Lett.* **228**, L15.
- Hamilton, A. J., C. L. Sarazin, and R. A. Chevalier, 1983, *As-*

- trophys. J. Suppl. 51, 115.
- Hanisch, R. J., 1980, *Astron. J.* 85, 1565.
- Hanisch, R. J., 1982a, *Astron. Astrophys.* 111, 97.
- Hanisch, R. J., 1982b, *Astron. Astrophys.* 116, 137.
- Hanisch, R. J., and W. C. Erickson, 1980, *Astron. J.* 85, 183.
- Hanisch, R. J., T. A. Matthews, and M. M. Davis, 1979, *Astron. J.* 84, 946.
- Hanisch, R. J., and R. A. White, 1981, *Astron. J.* 86, 806.
- Harris, D. E., P. Dewdney, C. Costain, H. Butcher, and A. Willis, 1983, *Astrophys. J.* 270, 39.
- Harris, D. E., V. K. Kapahi, and R. D. Ekers, 1980, *Astron. Astrophys. Suppl.* 39, 215.
- Harris, D. E., and G. K. Miley, 1978, *Astron. Astrophys. Suppl.* 34, 117.
- Harris, D. E., J. G. Robertson, P. E. Dewdney, and C. H. Costain, 1982, *Astron. Astrophys.* 111, 299.
- Harris, D. E., and W. Romanishin, 1974, *Astrophys. J.* 188, 209.
- Harris, E. W., M. G. Smith, and E. S. Myra, 1983, *Astrophys. J.* 272, 456.
- Hartwick, F. D., 1973, *Astrophys. J.* 219, 345.
- Hartwick, F. D., 1976, *Astrophys. J. Lett.* 208, L13.
- Haslam, C., P. Kronberg, H. Waldthausen, R. Wielebinski, and D. Schallwisch, 1978, *Astron. Astrophys. Suppl.* 31, 99.
- Hausman, M. A., and J. P. Ostriker, 1978, *Astrophys. J.* 224, 320.
- Havlen, R. J., and H. Quintana, 1978, *Astrophys. J.* 220, 14.
- Haynes, M. P., R. L. Brown, and M. S. Roberts, 1978, *Astrophys. J.* 221, 414.
- Heckman, T. M., 1981, *Astrophys. J. Lett.* 250, L59.
- Helfand, D., W. Ku, and F. Abramopoulos, 1980, *Highlights Astron.* 5, 747.
- Helmken, H., J. P. Delvaille, A. Epstein, M. J. Geller, H. W. Schnopper, and J. G. Jernigan, 1978, *Astrophys. J. Lett.* 221, L43.
- Helou, G., and E. E. Salpeter, 1982, *Astrophys. J.* 252, 75.
- Helou, G., E. E. Salpeter, and N. Krumm, 1979, *Astrophys. J. Lett.* 228, L1.
- Henriksen, M. J., 1985, Ph.D. thesis (University of Maryland).
- Henriksen, M. J., and R. F. Mushotzky, 1985, "The X-ray Spectrum of the Coma Cluster," Nasa Goddard Space Flight Center report.
- Henry, J. P., G. Branduardi, U. Briel, D. Fabricant, E. Feigelson, S. Murray, A. Soltan, and H. Tananbaum, 1979, *Astrophys. J. Lett.* 239, L15.
- Henry, J. P., M. J. Henriksen, P. A. Charles, and J. R. Thorstensen, 1981, *Astrophys. J. Lett.* 243, L137.
- Henry, J. P., A. Soltan, U. Briel, and J. E. Gunn, 1982, *Astrophys. J.* 262, 1.
- Henry, J. P., and W. Tucker, 1979, *Astrophys. J.* 229, 78.
- Hesser, J. E., H. C. Harris, S. van den Bergh, and G. L. Harris, 1984, *Astrophys. J.* 276, 491.
- Hickson, P., 1977, *Astrophys. J.* 217, 16.
- Hickson, P., 1982, *Astrophys. J.* 255, 382.
- Hickson, P., and P. J. Adams, 1979a, *Astrophys. J. Lett.* 234, L87.
- Hickson, P., and P. J. Adams, 1979b, *Astrophys. J. Lett.* 234, L91.
- Hill, J. M., J. R. Angel, J. S. Scott, D. Lindley, and P. Hintzen, 1980, *Astrophys. J. Lett.* 242, L69.
- Hill, J. M., and M. S. Longair, 1971, *Mon. Not. R. Astron. Soc.* 154, 125.
- Himmes, A., and P. Biermann, 1980, *Astron. Astrophys.* 86, 11.
- Hintzen, P., G. O. Boeshaar, and J. S. Scott, 1981, *Astrophys. J. Lett.* 246, L1.
- Hintzen, P., J. M. Hill, D. Lindley, J. S. Scott, and J. R. Angel, 1982, *Astron. J.* 87, 1656.
- Hintzen, P., and J. S. Scott, 1978, *Astrophys. J. Lett.* 224, L47.
- Hintzen, P., and J. S. Scott, 1979, *Astrophys. J. Lett.* 232, L145.
- Hintzen, P., and J. S. Scott, 1980, *Astrophys. J.* 239, 765.
- Hintzen, P., J. S. Scott, and J. D. McKee, 1980, *Astrophys. J.* 242, 857.
- Hintzen, P., J. S. Scott, and M. Tarenghi, 1977, *Astrophys. J.* 212, 8.
- Hintzen, P., J. Ulvestad, and F. Owen, 1983, *Astron. J.* 88, 709.
- Hirayama, Y., 1978, *Prog. Theor. Phys.* 60, 724.
- Hirayama, Y., Y. Tanaka, and T. Kogure, 1978, *Prog. Theor. Phys.* 59, 751.
- Hoessel, J. G., 1980, *Astrophys. J.* 241, 493.
- Hoessel, J. G., J. E. Gunn, and T.X. Thuan, 1980, *Astrophys. J.* 241, 486.
- Hoffman, A. A., and P. Crane, 1977, *Astrophys. J.* 215, 379.
- Hoffman, G. L., and E. E. Salpeter, 1982, *Astrophys. J.* 263, 485.
- Holman, G. D., J. A. Ionson, and J. S. Scott, 1979, *Astrophys. J.* 228, 576.
- Holman, G. D., and J. D. McKee, 1981, *Astrophys. J.* 249, 35.
- Holmberg, E. B., A. Lauberts, H. E. Schuster, and R. M. West, 1974, *Astron. Astrophys. Suppl.* 18, 463.
- Holt, S., and R. McCray, 1982, *Annu. Rev. Astron. Astrophys.* 20, 323.
- Hooley, T., 1974, *Mon. Not. R. Astron. Soc.* 166, 259.
- Hu, E. M., L. L. Cowie, P. Kaaret, E. B. Jenkins, D. G. York, and F. L. Roesler, 1983, *Astrophys. J. Lett.* 275, L27.
- Hubble, E. P., 1930, *Astrophys. J.* 71, 231.
- Huchra, J. P., and M. F. Geller, 1982, *Astrophys. J.* 257, 423.
- Huchtmeier, W. K., G. A. Tammann, and H. J. Wendker, 1976, *Astron. Astrophys.* 46, 381.
- Humason, M. L., N. U. Mayall, and A. R. Sandage, 1956, *Astron. J.* 61, 97.
- Humason, M. L., and A. Sandage, 1957, *Carnegie Inst. Washington Yearb.* 56, 62.
- Hunt, R., 1971, *Mon. Not. R. Astron. Soc.* 154, 141.
- Ikeuchi, S., 1977, *Prog. Theor. Phys.* 58, 1742.
- Ikeuchi, S., and Y. Hirayama, 1979, *Prog. Theor. Phys.* 61, 881.
- Ikeuchi, S., and Y. Hirayama, 1980, *Prog. Theor. Phys.* 64, 81.
- Ives, J. C., and P. W. Sanford, 1976, *Mon. Not. R. Astron. Soc.* 176, 13p.
- Jaffe, W. J., 1977, *Astrophys. J.* 212, 1.
- Jaffe, W. J., 1980, *Astrophys. J.* 241, 924.
- Jaffe, W. J., 1982, *Astrophys. J.* 262, 15.
- Jaffe, W. J., and G. C. Perola, 1973, *Astron. Astrophys.* 26, 423.
- Jaffe, W. J., and G. Perola, 1975, *Astron. Astrophys. Suppl.* 21, 137.
- Jaffe, W. J., and G. Perola, 1976, *Astron. Astrophys.* 46, 273.
- Jaffe, W. J., G. C. Perola, and E. A. Valentijn, 1976, *Astron. Astrophys.* 49, 179.
- Jaffe, W. J., and L. Rudnick, 1979, *Astrophys. J.* 233, 453.
- Jenner, D. C., 1974, *Astrophys. J.* 191, 55.
- Joeveer, M., J. Einasto, and E. Tago, 1978, *Mon. Not. R. Astron. Soc.* 185, 357.
- Johnson, H. M., 1981, *Astrophys. J. Suppl.* 47, 235.
- Johnson, H. M., H. W. Schnopper, and J. P. Delvaille, 1980, *Astrophys. J.* 236, 738.

- Johnson, M. W., R. G. Cruddace, G. Fritz, S. Shulman, and H. Friedman, 1979, *Astrophys. J. Lett.* **231**, L45.
- Johnson, M. W., R. G. Cruddace, M. P. Ulmer, M. P. Kowalski, and K. S. Wood, 1983, *Astrophys. J.* **266**, 425.
- Johnston, M. D., H. V. Bradt, R. E. Doxsey, B. Margon, F. E. Marshall, and D. A. Schwartz, 1981, *Astrophys. J.* **245**, 799.
- Jones, C., and W. Forman, 1978, *Astrophys. J.* **224**, 1.
- Jones, C., and W. Forman, 1984, *Astrophys. J.* **276**, 38.
- Jones, C., E. Mandel, J. Schwarz, W. Forman, S. S. Murray, and F. R. Harnden, 1979, *Astrophys. J. Lett.* **234**, L21.
- Jones, T. W., and F. N. Owen, 1979, *Astrophys. J.* **234**, 818.
- Jura, M., 1977, *Astrophys. J.* **212**, 634.
- Just, K., 1959, *Astrophys. J.* **129**, 268.
- Karzas, W., and R. Latter, 1961, *Astrophys. J. Suppl.* **6**, 167.
- Karachentsev, I. D., and A. I. Kopylov, 1980, *Mon. Not. R. Astron. Soc.* **192**, 109.
- Kato, T., 1976, *Astrophys. J. Suppl.* **30**, 397.
- Katz, J. L., 1976, *Astrophys. J.* **207**, 25.
- Kellogg, E. M., 1973, in *X- and Gamma-Ray Astronomy*, edited by H. Bradt and R. Giacconi (Reidel, Dordrecht), p.171.
- Kellogg, E. M., 1974, in *X-Ray Astronomy*, edited by R. Giacconi and H. Gursky (Reidel, Dordrecht), p. 321.
- Kellogg, E. M., 1975, *Astrophys. J.* **197**, 689.
- Kellogg, E. M., 1977, *Astrophys. J.* **218**, 582.
- Kellogg, E. M., 1978, *Astrophys. J. Lett.* **220**, L63.
- Kellogg, E. M., J. R. Baldwin, and D. Koch, 1975, *Astrophys. J.* **199**, 299.
- Kellogg, E. M., H. Gursky, C. Leong, E. Schreier, H. Tananbaum, and R. Giacconi, 1971, *Astrophys. J. Lett.* **165**, L49.
- Kellogg, E. M., H. Gursky, H. Tananbaum, R. Giacconi, and K. Pounds, 1972, *Astrophys. J. Lett.* **174**, L65.
- Kellogg, E. M., and S. Murray, 1974, *Astrophys. J. Lett.* **193**, L57.
- Kellogg, E. M., S. Murray, R. Giacconi, H. Tananbaum, and H. Gursky, 1973, *Astrophys. J. Lett.* **185**, L13.
- Kent, S. M., and J. E. Gunn, 1982, *Astron. J.* **87**, 945.
- Kent, S. M., and W. L. Sargent, 1979, *Astrophys. J.* **230**, 667.
- Kent, S. M., and W. L. Sargent, 1983, *Astron. J.* **88**, 697.
- Kiang, T., 1961, *Mon. Not. R. Astron. Soc.* **122**, 263.
- King, I. R., 1962, *Astron. J.* **67**, 471.
- King, I. R., 1966, *Astron. J.* **71**, 64.
- Kirshner, R. P., A. Oemler, and P. L. Schechter, 1978, *Astron. J.* **83**, 1549.
- Kirshner, R. P., A. Oemler, P. L. Schechter, and S. A. Schectman, 1981, *Astrophys. J. Lett.* **248**, L57.
- Klemola, A. R., 1969, *Astron. J.* **74**, 804.
- Knobloch, Edgar, 1978a, *Astrophys. J.* **222**, 779.
- Knobloch, Edgar, 1978b, *Astrophys. J. Suppl.* **38**, 253.
- Koo, D. C., 1981, *Astrophys. J. Lett.* **251**, L75.
- Kotanyi, C., J. H. van Gorkom, and R. D. Ekers, 1983, *Astrophys. J. Lett.* **273**, L7.
- Kowalski, M., M. P. Ulmer, and R. Cruddace, 1983, *Astrophys. J.* **268**, 540.
- Kraan-Korteweg, R. C., 1981, *Astron. Astrophys.* **104**, 280.
- Kriss, G. A., C. E. Canizares, J. E. McClintock, and E. D. Feigelson, 1980, *Astrophys. J. Lett.* **235**, L61; **245**, L51(E) (1981).
- Kriss, G. A., D. F. Cioffi, and C. R. Canizares, 1983, *Astrophys. J.* **272**, 439.
- Kristian, J., A. Sandage, and J. A. Westphal, 1978, *Astrophys. J.* **221**, 383.
- Kritsuk, A. G., 1983, *Astrophys.* **19**, 263.
- Kron, R. G., H. Spinrad, and I. R. King, 1977, *Astrophys. J.* **217**, 951.
- Krumm, N., and E. E. Salpeter, 1976, *Astrophys. J. Lett.* **208**, L7.
- Krumm, N., and E. E. Salpeter, 1979, *Astrophys. J.* **227**, 776.
- Krupp, E. C., 1974, *Publ. Astron. Soc. Pac.* **86**, 385.
- Ku, W., F. Abramopoulos, P. Nulsen, A. Fabian, G. Stewart, G. Chincarini, and M. Tarengi, 1983, *Mon. Not. R. Astron. Soc.* **203**, 253.
- Lake, G., and R. B. Partridge, 1977, *Nature* **270**, 502.
- Lake, G., and R. B. Partridge, 1980, *Astrophys. J.* **237**, 378.
- Larson, R. B., and H. L. Dinerstein, 1975, *Publ. Astron. Soc. Pac.* **87**, 911.
- Larson, R. B., B. M. Tinsley, and C. N. Caldwell, 1980, *Astrophys. J.* **237**, 692.
- Lasenby, A. N., and R. D. Davies, 1983, *Mon. Not. R. Astron. Soc.* **203**, 1137.
- Lawler, J. M., and B. Dennison, 1982, *Astrophys. J.* **252**, 81.
- Lawrence, A., 1978, *Mon. Not. R. Astron. Soc.* **185**, 423.
- Lea, S. M., 1975, *Astrophys. Lett.* **16**, 141.
- Lea, S. M., 1976, *Astrophys. J.* **203**, 569.
- Lea, S. M., and D. S. De Young, 1976, *Astrophys. J.* **210**, 647.
- Lea, S. M., and G. D. Holman, 1978, *Astrophys. J.* **222**, 29.
- Lea, S. M., K. Mason, G. Reichert, P. Charles, and G. Reigler, 1979, *Astrophys. J. Lett.* **227**, L67.
- Lea, S. M., R. Mushotzky, and S. Holt, 1982, *Astrophys. J.* **262**, 24.
- Lea, S. M., G. Reichert, R. Mushotzky, W. A. Baity, D. E. Gruber, R. Rothschild, and F. A. Primini, 1981, *Astrophys. J.* **246**, 369.
- Lea, S. M., J. Silk, E. Kellogg, and S. Murray, 1973, *Astrophys. J. Lett.* **184**, L105.
- Lecar, M., 1975, in *Dynamics of Stellar Systems*, edited by A. Hayli (Reidel, Dordrecht), p. 161.
- Leir, A. A., and S. van den Bergh, 1977, *Astrophys. J. Suppl.* **34**, 381.
- Limber, D. N., and W. G. Mathews, 1960, *Astrophys. J.* **132**, 286.
- Livio, M., O. Regev, and G. Shaviv, 1978, *Astron. Astrophys.* **70**, L7.
- Livio, M., O. Regev, and G. Shaviv, 1980, *Astrophys. J. Lett.* **240**, L83.
- Lugger, P. M., 1978, *Astrophys. J.* **221**, 745.
- Lynden-Bell, D., 1967, *Mon. Not. R. Astron. Soc.* **136**, 101.
- Lynds, R., 1970, *Astrophys. J. Lett.* **159**, L151.
- Maccacaro, T., B. A. Cooke, M. J. Ward, M. V. Penston, and R. F. Haynes, 1977, *Mon. Not. R. Astron. Soc.* **180**, 465.
- Maccagni, D., and M. Tarengi, 1981, *Astrophys. J.* **243**, 42.
- MacDonald, R., S. Kenderdine, and A. Neville, 1968, *Mon. Not. R. Astron. Soc.* **138**, 259.
- MacGillivray, H. T., and R. J. Dodd, 1979, *Mon. Not. R. Astron. Soc.* **186**, 743.
- MacGillivray, H. T., R. Martin, N. M. Pratt, V. C. Reddish, H. Seddon, L. W. Alexander, G. S. Walker, and P. R. Williams, 1976, *Mon. Not. R. Astron. Soc.* **176**, 649.
- Malina, R., M. Lampton, and S. Bowyer, 1976, *Astrophys. J.* **209**, 678.
- Malina, R. F., S. M. Lea, M. Lampton, and C. S. Bowyer, 1978, *Astrophys. J.* **219**, 795.
- Malumuth, E. M., and R. P. Kirshner, 1981, *Astrophys. J.* **251**, 508.
- Malumuth, E. M., and R. P. Kirshner, 1985, *Astrophys. J.* **291**, 8.
- Malumuth, E. M., and D. O. Richstone, 1984, *Astrophys. J.* **276**, 413.
- Marchant, A. B., and S. L. Shapiro, 1977, *Astrophys. J.* **215**, 1.

- Margon, B., M. Lampton, S. Bowyer, and R. Cruddace, 1975, *Astrophys. J.* **197**, 25.
- Markert, T. H., C. R. Canizares, G. W. Clark, F. K. Li, P. L. Northridge, G. F. Sprott, and G. F. Wargo, 1976, *Astrophys. J.* **206**, 265.
- Markert, T., P. Winkler, F. Laird, G. Clark, D. Hearn, G. Sprott, F. Li, V. Bradt, W. Lewin, and H. Schnopper, 1979, *Astrophys. J. Suppl.* **39**, 573.
- Marshall, F. E., E. A. Boldt, S. S. Holt, R. F. Mushotzky, S. H. Pravdo, R. E. Rothschild, and P. J. Serlemitsos, 1979, *Astrophys. J. Suppl.* **40**, 657.
- Mason, K. O., H. Spinrad, S. Bowyer, G. Reichert, and J. Stauffer, 1981, *Astron. J.* **86**, 803.
- Materne, J., G. Chincarini, M. Tarengi, and U. Hopp, 1982, *Astron. Astrophys.* **109**, 238.
- Mathews, T. A., W. W. Morgan, and M. Schmidt, 1964, *Astrophys. J.* **140**, 35.
- Mathews, W. G., 1978a, *Astrophys. J.* **219**, 408.
- Mathews, W. G., 1978b, *Astrophys. J.* **219**, 413.
- Mathews, W. G., and J. C. Baker, 1971, *Astrophys. J.* **170**, 241.
- Mathews, W. G., and J. N. Bregman, 1978, *Astrophys. J.* **224**, 308.
- Mathieu, R. D., and H. Spinrad, 1981, *Astrophys. J.* **251**, 485.
- McGlynn, T. A., and A. C. Fabian, 1984, *Mon. Not. R. Astron. Soc.* **208**, 709.
- McGlynn, T. A., and J. P. Ostriker, 1980, *Astrophys. J.* **241**, 915.
- McHardy, I. M., 1974, *Mon. Not. R. Astron. Soc.* **169**, 527.
- McHardy, I. M., 1978a, *Mon. Not. R. Astron. Soc.* **184**, 783.
- McHardy, I. M., 1978b, *Mon. Not. R. Astron. Soc.* **185**, 927.
- McHardy, I. M., 1979, *Mon. Not. R. Astron. Soc.* **188**, 495.
- McHardy, I. M., A. Lawrence, J. P. Pye, and K. A. Pounds, 1981, *Mon. Not. R. Astron. Soc.* **197**, 893.
- McKee, C. F., and L. L. Cowie, 1977, *Astrophys. J.* **215**, 213.
- McKee, J. D., R. F. Mushotzky, E. A. Boldt, S. S. Holt, F. E. Marshall, S. H. Pravdo, and P. J. Serlemitsos, 1980, *Astrophys. J.* **242**, 843.
- Meekins, J. F., F. Gilbert, T. A. Chubb, H. Friedman, and R. C. Henry, 1971, *Nature* **231**, 107.
- Melnick, J., and H. Quintana, 1975, *Astrophys. J. Lett.* **198**, L97.
- Melnick, J., and H. Quintana, 1981a, *Astron. Astrophys. Suppl.* **44**, 87.
- Melnick, J., and H. Quintana, 1981b, *Astron. J.* **86**, 1567.
- Melnick, J., and W. L. Sargent, 1977, *Astrophys. J.* **215**, 401.
- Melnick, J., S. D. M. White, and J. Hoessel, 1977, *Mon. Not. R. Astron. Soc.* **180**, 207.
- Merritt, D., 1983, *Astrophys. J.* **264**, 24.
- Merritt, D., 1984, *Astrophys. J.* **276**, 26.
- Merritt, D., 1985, *Astrophys. J.* **289**, 18.
- Mewe, R., and E. H. Gronenschild, 1981, *Astron. Astrophys. Suppl.* **45**, 11.
- Meyer, S. S., A. D. Jeffries, and R. Weiss, 1983, *Astrophys. J.* **271**, L1.
- Miley, G., 1973, *Astron. Astrophys.* **26**, 413.
- Miley, G., 1980, *Annu. Rev. Astron. Astrophys.* **18**, 165.
- Miley, G., and D. E. Harris, 1977, *Astron. Astrophys.* **61**, L23.
- Miley, G., G. Perola, P. van der Kruit, and H. van der Laan, 1972, *Nature* **237**, 269.
- Miller, G. E., 1983, *Astrophys. J.* **274**, 840.
- Mills, B. Y., 1960, *Aust. J. Phys.* **13**, 550.
- Minkowski, R., 1960, *Astrophys. J.* **132**, 908.
- Minkowski, R., 1961, *Astron. J.* **66**, 558.
- Minkowski, R., and G. O. Abell, 1963, in *Basic Astronomical Data*, edited by K. A. Strand (University of Chicago, Chicago), p. 481.
- Mitchell, R. J., P. A. Charles, J. L. Culhane, P. J. Davison, and A. C. Fabian, 1975, *Astrophys. J. Lett.* **200**, L5.
- Mitchell, R. J., and J. L. Culhane, 1977, *Mon. Not. R. Astron. Soc.* **178**, 75p.
- Mitchell, R. J., J. L. Culhane, P. J. Davison, and J. C. Ives, 1976, *Mon. Not. R. Astron. Soc.* **176**, 29p.
- Mitchell, R. J., R. J. Dickens, S. J. Bell Burnell, and J. L. Culhane, 1979, *Mon. Not. R. Astron. Soc.* **189**, 329.
- Mitchell, R. J., J. C. Ives, and J. L. Culhane, 1977, *Mon. Not. R. Astron. Soc.* **131**, 25p.
- Mitchell, R. J., and R. Mushotzky, 1980, *Astrophys. J.* **236**, 730.
- Morgan, W. W., 1961, *Proc. Natl. Acad. Sci. U. S. A.* **47**, 905.
- Morgan, W. W., S. Kayser, and R. A. White, 1975, *Astrophys. J.* **199**, 545.
- Morgan, W. W., and J. Lesh, 1965, *Astrophys. J.* **142**, 1364.
- Moss, C., and R. J. Dickens, 1977, *Mon. Not. R. Astron. Soc.* **178**, 701.
- Mottmann, J., and G. O. Abell, 1977, *Astrophys. J.* **218**, 53.
- Murray, S. S., W. Forman, C. Jones, and R. Giacconi, 1978, *Astrophys. J. Lett.* **219**, L89.
- Mushotzky, R. F., 1980, in *X-ray Astronomy*, edited by R. Giacconi and G. Setti (Reidel, Dordrecht), p. 171.
- Mushotzky, R. F., 1984, *Phys. Scr.* **T7**, 157.
- Mushotzky, R. F., W. A. Baity, and L. E. Peterson, 1977, *Astrophys. J.* **212**, 22.
- Mushotzky, R. F., S. S. Holt, B. W. Smith, E. A. Boldt, and P. J. Serlemitsos, 1981, *Astrophys. J. Lett.* **244**, L47.
- Mushotzky, R. F., P. J. Serlemitsos, B. W. Smith, E. A. Boldt, and S. S. Holt, 1978, *Astrophys. J.* **225**, 21.
- Nepveu, M., 1981a, *Astron. Astrophys.* **98**, 65.
- Nepveu, M., 1981b, *Astron. Astrophys.* **101**, 362.
- Noonan, T. W., 1973, *Astron. J.* **78**, 26.
- Noonan, T. W., 1974, *Astron. J.* **79**, 775.
- Noonan, T. W., 1975, *Astrophys. J.* **202**, 551.
- Noonan, T. W., 1976, *Astrophys. J.* **196**, 683.
- Noonan, T. W., 1980, *Astrophys. J.* **238**, 793.
- Noonan, T. W., 1981, *Astrophys. J. Suppl.* **45**, 613.
- Noordam, J. E., and A. G. de Bruyn, 1982, *Nature* **299**, 597.
- Norman, C., and J. Silk, 1979, *Astrophys. J. Lett.* **233**, L1.
- Nugent, J., K. Jensen, J. Nousek, G. Garmire, K. Mason, F. Walter, C. Bowyer, R. Stern, and G. Riegler, 1983, *Astrophys. J. Suppl.* **51**, 1.
- Nulsen, P. E., 1982, *Mon. Not. R. Astron. Soc.* **198**, 1007.
- Nulsen, P. E., and A. C. Fabian, 1980, *Mon. Not. R. Astron. Soc.* **191**, 887.
- Nulsen, P. E., A. C. Fabian, R. F. Mushotzky, E. A. Boldt, S. S. Holt, F. J. Marshall, and P. J. Serlemitsos, 1979, *Mon. Not. R. Astron. Soc.* **189**, 183.
- Nulsen, P. E., G. C. Stewart, and A. C. Fabian, 1984, *Mon. Not. R. Astron. Soc.* **208**, 185.
- Nulsen, P. E., G. C. Stewart, A. C. Fabian, R. F. Mushotzky, S. S. Holt, W. Ku, and D. Malin, 1982, *Mon. Not. R. Astron. Soc.* **199**, 1089.
- O'Connell, R. W., C. L. Sarazin, and B. McNamara, 1985, "Stellar Populations in Central Cluster Galaxies with Cooling Flows," University of Virginia report.
- O'Dea, C. P., and F. N. Owen, 1985, "Multifrequency VLA Observations of the Prototypical Narrow-Angle Tail Radio Source, NGC1265," Natl. Radio Astron. Obs. report.
- Oemler, A., Jr., 1973, *Astrophys. J.* **180**, 11.
- Oemler, A., Jr., 1974, *Astrophys. J.* **194**, 1.

- Oemler, A., Jr., 1976, *Astrophys. J.* **209**, 693.
- Omer, G. C., T. L. Page, and A. G. Wilson, 1965, *Astron. J.* **70**, 440.
- Oort, J. H., 1983, *Annu. Rev. Astron. Astrophys.* **21**, 373.
- Osmer, P. S., 1978, *Phys. Scr.* **17**, 357.
- Osterbrock, D. E., 1974, *Astrophysics of Gaseous Nebulae* (Freeman, San Francisco).
- Ostriker, J. P., 1980, *Comments Astrophys.* **8**, 177.
- Ostriker, J. P., and M. A. Hausman, 1977, *Astrophys. J. Lett.* **217**, L125.
- Ostriker, J. P., P. J. Peebles, and A. Yahil, 1974, *Astrophys. J. Lett.* **193**, L1.
- Ostriker, J. P., and S. D. Tremaine, 1975, *Astrophys. J. Lett.* **202**, L113.
- Owen, F. N., 1974, *Astrophys. J. Lett.* **189**, 155.
- Owen, F. N., 1975, *Astrophys. J.* **195**, 593.
- Owen, F. N., J. O. Burns, and L. Rudnick, 1978, *Astrophys. J. Lett.* **226**, L119.
- Owen, F. N., J. O. Burns, L. Rudnick, and E. W. Greison, 1979, *Astrophys. J. Lett.* **229**, L59.
- Owen, F. N., and L. Rudnick, 1976a, *Astrophys. J.* **203**, 307.
- Owen, F. N., and L. Rudnick, 1976b, *Astrophys. J. Lett.* **205**, L1.
- Owen, F. N., R. A. White, K. C. Hilldrup, and R. J. Hanisch, 1982, *Astron. J.* **87**, 1083.
- Paal, G., 1964, *Mitt. Sternwarted. Ungarischen Akad. Wissenschaften*, No. 54.
- Pacholczyk, A. G., and J. S. Scott, 1976, *Astrophys. J.* **203**, 313.
- Pariiskii, Y. N., 1973, *Sov. Astron. AJ* **16**, 1048.
- Peach, J. V., 1969, *Nature* **223**, 1140.
- Peebles, P. J., 1974, *Astron. Astrophys.* **32**, 197.
- Perola, G. C., and M. Reinhardt, 1972, *Astron. Astrophys.* **17**, 432.
- Perrenod, S. C., 1978a, *Astrophys. J.* **224**, 285.
- Perrenod, S. C., 1978b, *Astrophys. J.* **226**, 566.
- Perrenod, S. C., 1980, *Astrophys. J.* **236**, 373.
- Perrenod, S. C., and J. P. Henry, 1981, *Astrophys. J. Lett.* **247**, L1.
- Perrenod, S. C., and C. J. Lada, 1979, *Astrophys. J. Lett.* **234**, L173.
- Perrenod, S. C., and M. P. Lesser, 1980, *Publ. Astron. Soc. Pac.* **92**, 764.
- Peterson, B. M., 1978, *Astrophys. J.* **223**, 740.
- Peterson, B. M., S. E. Strom, and K. M. Strom, 1979, *Astron. J.* **84**, 735.
- Piccinotti, G., R. F. Mushotzky, E. A. Boldt, S. S. Holt, F. E. Marshall, P. J. Serlemitsos, and R. A. Shafer, 1982, *Astrophys. J.* **253**, 485.
- Pravdo, S., E. Boldt, F. Marshall, J. McKee, R. Mushotzky, and B. Smith, 1979, *Astrophys. J.* **234**, 1.
- Press, W. H., 1976, *Astrophys. J.* **203**, 14.
- Press, W. H., and P. Schechter, 1974, *Astrophys. J.* **187**, 425.
- Primini, F., E. Basinska, S. Howe, F. Lang, A. Levine, W. Lewin, R. Rothschild, W. Baity, D. Gruber, F. Knight, J. Matteson, S. Lea, and G. Reichert, 1981, *Astrophys. J. Lett.* **243**, L13.
- Pye, J. P., and B. A. Cooke, 1976, *Mon. Not. R. Astron. Soc.* **177**, 21p.
- Quintana, H., 1979, *Astron. J.* **84**, 15.
- Quintana, H., and D. G. Lawrie, 1982, *Astron. J.* **87**, 1.
- Quintana, H., and J. Melnick, 1982, *Astron. J.* **87**, 972.
- Raymond, J. C., D. P. Cox, and B. W. Smith, 1976, *Astrophys. J.* **204**, 290.
- Raymond, J. C., and B. W. Smith, 1977, *Astrophys. J. Suppl.* **35**, 419.
- Rees, M. J., 1978, *Phys. Scr.* **17**, 193.
- Reichert, G., K. Mason, S. Lea, P. Charles, S. Bowyer, and S. Pravdo, 1981, *Astrophys. J.* **247**, 803.
- Rephaeli, Y., 1977a, *Astrophys. J.* **212**, 608.
- Rephaeli, Y., 1977b, *Astrophys. J.* **218**, 323.
- Rephaeli, Y., 1978, *Astrophys. J.* **225**, 335.
- Rephaeli, Y., 1979, *Astrophys. J.* **227**, 364.
- Rephaeli, Y., 1980, *Astrophys. J.* **241**, 858.
- Rephaeli, Y., 1981, *Astrophys. J.* **245**, 351.
- Rephaeli, Y., and E. E. Salpeter, 1980, *Astrophys. J.* **240**, 20.
- Richstone, D. O., 1975, *Astrophys. J.* **200**, 535.
- Richstone, D. O., 1976, *Astrophys. J.* **204**, 642.
- Richstone, D. O., and E. M. Malumuth, 1983, *Astrophys. J.* **268**, 30.
- Richter, O. E., J. Materne, and W. K. Huchtmeier, 1982, *Astron. Astrophys.* **111**, 193.
- Ricketts, M. J., 1978, *Mon. Not. R. Astron. Soc.* **183**, 51p.
- Riley, J. M., 1975, *Mon. Not. R. Astron. Soc.* **170**, 53.
- Robertson, J. G., 1985, "Radio Emission from Clusters of Galaxies," Anglo-Australian Observatory report.
- Roland, J., H. Sol, I. Pauliny-Toth, and A. Witzel, 1981, *Astron. Astrophys.* **100**, 7.
- Roland, J., P. Veron, I. Pauliny-Toth, E. Preuss, and A. Witzel, 1976, *Astron. Astrophys.* **50**, 165.
- Rood, H. J., 1965, Ph.D. thesis (University of Michigan).
- Rood, H. J., 1969, *Astrophys. J.* **158**, 657.
- Rood, H. J., 1975, *Astrophys. J.* **201**, 551.
- Rood, H. J., 1976, *Astrophys. J.* **207**, 16.
- Rood, H. J., 1981, *Rep. Prog. Phys.* **44**, 1077.
- Rood, H. J., and G. O. Abell, 1973, *Astrophys. Lett.* **13**, 69.
- Rood, H. J., and A. A. Leir, 1979, *Astrophys. J. Lett.* **231**, L3.
- Rood, H. J., T. L. Page, E. C. Kintner, and I. R. King, 1972, *Astrophys. J.* **175**, 627.
- Rood, H. J., V. C. Rothman, and B.E. Turnrose, 1970, *Astrophys. J.* **162**, 411.
- Rood, H. J., and G. N. Sastry, 1971, *Publ. Astron. Soc. Pac.* **83**, 313.
- Rood, H. J., and G. N. Sastry, 1972, *Astron. J.* **77**, 451.
- Roos, N., and C. A. Norman, 1979, *Astron. Astrophys.* **95**, 349.
- Rose, J. A., 1976, *Astron. Astrophys. Suppl.* **23**, 109.
- Rothflug, R., L. Vigroux, R. Mushotzky, and S. Holt, 1984, *Astrophys. J.* **279**, 53.
- Rothschild, R. E., W. A. Baity, A. P. Marscher, and W. A. Wheaton, 1981, *Astrophys. J. Lett.* **243**, L9.
- Rowan-Robinson, M., and A. C. Fabian, 1975, *Mon. Not. R. Astron. Soc.* **170**, 199.
- Rubin, V. C., W. K. Ford, C. J. Peterson, and C. R. Lynds, 1978, *Astrophys. J. Suppl.* **37**, 235.
- Rubin, V. C., W. K. Ford, C. J. Peterson, and J. H. Oort, 1977, *Astrophys. J.* **211**, 693.
- Ruderman, M. A., and E. A. Spiegel, 1971, *Astrophys. J.* **165**, 1.
- Rudnick, L., 1978, *Astrophys. J.* **223**, 37.
- Rudnick, L., and F. N. Owen, 1976a, *Astron. J.* **82**, 1.
- Rudnick, L., and F. N. Owen, 1976b, *Astrophys. J. Lett.* **203**, L107.
- Ryle, M., and M. D. Windram, 1968, *Mon. Not. R. Astron. Soc.* **138**, 1.
- Salpeter, E. E., 1955, *Astrophys. J.* **121**, 161.
- Salpeter, E. E., and J. M. Dickey, 1985, *Astrophys. J.* **292**, 426.
- Sandage, A., 1972, *Astrophys. J.* **178**, 1.
- Sandage, A., 1976, *Astrophys. J.* **205**, 6.

- Sandage, A., K. C. Freeman, and N. R. Stokes, 1970, *Astrophys. J.* **160**, 831.
- Sandage, A., J. Kristian, and J. A. Westphal, 1976, *Astrophys. J.* **205**, 688.
- Sandage, A., and G. A. Tammann, 1975, *Astrophys. J.* **197**, 265.
- Sandage, A., and N. Visvanathan, 1978, *Astrophys. J.* **225**, 742.
- Sarazin, C. L., 1979, *Astrophys. Lett.* **20**, 93.
- Sarazin, C. L., 1980, *Astrophys. J.* **236**, 75.
- Sarazin, C. L., and J. N. Bahcall, 1977, *Astrophys. J. Suppl.* **34**, 451.
- Sarazin, C. L., and R. W. O'Connell, 1983, *Astrophys. J.* **268**, 552.
- Sarazin, C. L., and H. Quintana, 1985, "Galaxy Distributions in Abell Clusters," University of Virginia report.
- Sarazin, C. L., H. J. Rood, and M. F. Struble, 1982, *Astron. Astrophys.* **108**, L7.
- Sargent, W. L., 1973, *Publ. Astron. Soc. Pac.* **85**, 281.
- Sastry, G. N., 1968, *Publ. Astron. Soc. Pac.* **80**, 252.
- Sastry, G. N., and H. J. Rood, 1971, *Astrophys. J. Suppl.* **23**, 371.
- Schallwich, D., and R. Wielebinski, 1978, *Astron. Astrophys.* **71**, L15.
- Schechter, P. L., 1976, *Astrophys. J.* **203**, 297.
- Schechter, P. L., and P. J. E. Peebles, 1976, *Astrophys. J.* **209**, 670.
- Schechter, P. L., and W. H. Press, 1976, *Astrophys. J.* **203**, 557.
- Scheepmaker, A., G. Ricker, K. Brecher, S. Ryckman, J. Ballintine, J. Doty, P. Downey, and W. Lewin, 1976, *Astrophys. J. Lett.* **205**, L65.
- Schild, R., and M. Davis, 1979, *Astron. J.* **84**, 311.
- Schipper, L., 1974, *Mon. Not. R. Astron. Soc.* **168**, 21.
- Schipper, L., and I. R. King, 1978, *Astrophys. J.* **220**, 798.
- Schmidt, M., 1978, *Phys. Scr.* **17**, 329.
- Schneider, D. P., and J. E. Gunn, 1982, *Astrophys. J.* **263**, 14.
- Schneider, D. P., J. E. Gunn, and J. G. Hoessel, 1983, *Astrophys. J.* **264**, 337.
- Schnopper, H. W., J. P. Delvaile, A. Epstein, H. Helmken, D. E. Harris, R. G. Strom, G. W. Clark, and J. G. Jernigan, 1977, *Astrophys. J. Lett.* **217**, L15.
- Schreier, E., P. Gorenstein, and E. Feigelson, 1982, *Astrophys. J.* **261**, 42.
- Schwartz, D. A., 1976, *Astrophys. J. Lett.* **206**, L95.
- Schwartz, D. A., 1978, *Astrophys. J.* **220**, 8.
- Schwartz, D. A., M. Davis, R. E. Doxsey, R. E. Griffiths, J. Huchra, M. D. Johnston, R. F. Mushotzky, J. Swank, and J. Tonry, 1980, *Astrophys. J. Lett.* **238**, L53.
- Schwartz, D. A., J. Schwarz, and W. Tucker, 1980, *Astrophys. J. Lett.* **238**, L59.
- Schwarz, J., U. Briel, R. E. Doxsey, G. Fabbiano, R. Griffiths, M. D. Johnston, D. A. Schwartz, J. D. McKee, and R. F. Mushotzky, 1979, *Astrophys. J. Lett.* **231**, L105.
- Schwarzschild, M., 1954, *Astron. J.* **59**, 273.
- Schwarzschild, M., 1979, *Astrophys. J.* **232**, 236.
- Scott, E. L., 1962, in *Problems in Extra-Galactic Research*, edited by G. C. McVittie (University of Chicago, Chicago), p. 269.
- Scott, J. S., G. D. Holman, J. A. Ionson, and K. Papadopoulos, 1980, *Astrophys. J.* **239**, 769.
- Serlemitsos, P. J., B. W. Smith, E. A. Boldt, S. S. Holt, and J. H. Swank, 1977, *Astrophys. J. Lett.* **211**, L63.
- Sersic, J. L., 1974, *Astrophys. Space Sci.* **28**, 365.
- Shapiro, P. R., and J. N. Bahcall, 1980, *Astrophys. J.* **241**, 1.
- Shaviv, G., and E. E. Salpeter, 1982, *Astron. Astrophys.* **110**, 300.
- Shectman, S. A., 1982, *Astrophys. J.* **262**, 9.
- Shibazaki, N., R. Hoshi, F. Takahara, and S. Ikeuchi, 1976, *Prog. Theor. Phys.* **56**, 1475.
- Shostak, G., D. Gilra, J. Noordam, H. Nieuwenhuijzen, T. deGrauw, and J. Vermne, 1980, *Astron. Astrophys.* **81**, 223.
- Shu, F. H., 1978, *Astrophys. J.* **225**, 83.
- Shull, J. M., 1981, *Astrophys. J. Suppl.* **46**, 27.
- Shull, J. M., and M. Van Steenberg, 1982, *Astrophys. J. Suppl.* **48**, 95.
- Silk, J., 1976, *Astrophys. J.* **208**, 646.
- Silk, J., 1978, *Astrophys. J.* **220**, 390.
- Silk, J., and S. D. M. White, 1978, *Astrophys. J. Lett.* **226**, L103.
- Simon, A. J., 1978, *Mon. Not. R. Astron. Soc.* **184**, 537.
- Simon, A. J., 1979, *Mon. Not. R. Astron. Soc.* **188**, 637.
- Slingo, A., 1974a, *Mon. Not. R. Astron. Soc.* **166**, 101.
- Slingo, A., 1974b, *Mon. Not. R. Astron. Soc.* **168**, 307.
- Smith, B., R. Mushotzky, and P. Serlemitsos, 1979, *Astrophys. J.* **227**, 37.
- Smith, H., Jr., 1980, *Astrophys. J.* **241**, 63.
- Smith, H., Jr., P. Hintzen, G. Holman, W. Oegerle, J. Scott, and S. Sofia, 1979, *Astrophys. J. Lett.* **234**, L97.
- Smith, S., 1936, *Astrophys. J.* **83**, 23.
- Smyth, R. J., and R. S. Stobie, 1980, *Mon. Not. R. Astron. Soc.* **190**, 631.
- Snow, T. P., 1970, *Astron. J.* **75**, 237.
- Sofia, S., 1973, *Astrophys. J. Lett.* **179**, L35.
- Solinger, A. B., and W. H. Tucker, 1972, *Astrophys. J. Lett.* **175**, L107.
- Soltan, A., and J. P. Henry, 1983, *Astrophys. J.* **271**, 442.
- Sparke, L. S., 1983, *Astrophys. Lett.* **23**, 113.
- Spinrad, H., 1985, private communication.
- Spinrad, H., J. Stauffer, and H. Butcher, 1985, *Astrophys. J.* **296**, 784.
- Spitzer, L., Jr., 1956, *Physics of Fully Ionized Gases* (Interscience, New York).
- Spitzer, L., Jr., 1978, *Physical Processes in the Interstellar Medium* (Wiley, New York).
- Spitzer, L., Jr., and W. Baade, 1951, *Astrophys. J.* **113**, 413.
- Spitzer, L., Jr., and J. Greenstein, 1951, *Astrophys. J.* **168**, 283.
- Spitzer, L., Jr., and R. Harm, 1958, *Astrophys. J.* **127**, 544.
- Stauffer, J., 1983, *Astrophys. J.* **264**, 14.
- Stauffer, J., and H. Spinrad, 1978, *Publ. Astron. Soc. Pac.* **90**, 20.
- Stauffer, J., and H. Spinrad, 1979, *Astrophys. J. Lett.* **231**, L51.
- Stauffer, J., and H. Spinrad, 1980, *Astrophys. J.* **235**, 347.
- Stauffer, J., H. Spinrad, and W. Sargent, 1979, *Astrophys. J.* **228**, 379.
- Steiner, J. E., F. E. Grindlay, and T. Maccacaro, 1982, *Astrophys. J.* **259**, 482.
- Stewart, G. C., C. R. Canizares, A. C. Fabian, and P. E. Nulsen, 1984, *Astrophys. J.* **278**, 536.
- Stewart, G. C., A. C. Fabian, C. Jones, and W. Forman, 1984, *Astrophys. J.* **285**, 1.
- Stimpel, O., and J. Binney, 1979, *Mon. Not. R. Astron. Soc.* **188**, 883.
- Strom, K. M., and S. E. Strom, 1978a, *Astron. J.* **83**, 73.
- Strom, K. M., and S. E. Strom, 1978b, *Astron. J.* **83**, 1293.
- Strom, S. E., and K. M. Strom, 1978c, *Astron. J.* **83**, 732.
- Strom, S. E., and K. M. Strom, 1978d, *Astrophys. J. Lett.* **225**, L93.
- Strom, S. E., and K. M. Strom, 1979, *Astron. J.* **84**, 1091.

- Struble, M. F., and H. J. Rood, 1981, *Astrophys. J.* **251**, 471.
- Struble, M. F., and H. J. Rood, 1982, *Astron. J.* **87**, 7.
- Struble, M. F., and H. J. Rood, 1984, *Astron. J.* **89**, 1487.
- Sulentic, J. W., 1980, *Astrophys. J.* **241**, 67.
- Sullivan, W. T., G. D. Bothun, B. Bates, and R. A. Schommer, 1981, *Astron. J.* **86**, 919.
- Sullivan, W. T., and P. E. Johnson, 1978, *Astrophys. J.* **225**, 751.
- Sunyaev, R. A., 1981, *Sov. Astron. Lett.* **6**, 213.
- Sunyaev, R. A., and Y. B. Zel'dovich, 1972, *Comments Astrophys. Space Phys.* **4**, 173.
- Sunyaev, R. A., and Y. B. Zel'dovich, 1980a, *Annu. Rev. Astron. Astrophys.* **18**, 537.
- Sunyaev, R. A., and Y. B. Zel'dovich, 1980b, *Mon. Not. R. Astron. Soc.* **190**, 413.
- Sunyaev, R. A., and Y. B. Zel'dovich, 1981, *Astrophys. Space Sci. Rev.* **1**, 1.
- Takahara, F., and S. Ikeuchi, 1977, *Prog. Theor. Phys.* **58**, 1728.
- Takahara, F., S. Ikeuchi, N. Shibazaki, and R. Hoshi, 1976, *Prog. Theor. Phys.* **56**, 1093.
- Takahara, M., and F. Takahara, 1979, *Prog. Theor. Phys.* **62**, 1253.
- Takahara, M., and F. Takahara, 1981, *Prog. Theor. Phys.* **65**, 1.
- Takeda, H., P. Nulsen, and A. Fabian, 1984, *Mon. Not. R. Astron. Soc.* **208**, 461.
- Tarengi, M., G. Chincarini, H. Rood, and L. Thompson, 1980, *Astrophys. J.* **235**, 724.
- Tarengi, M., and J. S. Scott, 1976, *Astrophys. J. Lett.* **207**, L9.
- Tarter, J. C., 1975, Ph. D. thesis (University of California, Berkeley).
- Tarter, J. C., 1978, *Astrophys. J.* **220**, 749.
- Thomas, J. C., and D. Batchelor, 1978, *Astron. J.* **83**, 1160.
- Thompson, L. A., 1976, *Astrophys. J.* **209**, 22.
- Thompson, L. A., and S. A. Gregory, 1978, *Astrophys. J.* **220**, 809.
- Thompson, L. A., and S. A. Gregory, 1980, *Astrophys. J.* **242**, 1.
- Thuan, T. X., 1980, in *Physical Cosmology: Proceedings of the Les Houches Summer School XXXII*, edited by R. Balian, J. Audouze, and D. N. Schramm (North-Holland, Amsterdam), p. 278.
- Thuan, T. X., and J. Kormendy, 1977, *Publ. Astron. Soc. Pac.* **89**, 466.
- Thuan, T. X., and W. Romanishin, 1981, *Astrophys. J.* **248**, 439.
- Tifft, W. G., 1978, *Astrophys. J.* **222**, 54.
- Tifft, W. G., and S. A. Gregory, 1976, *Astrophys. J.* **205**, 696.
- Tifft, W. G., and M. Tarengi, 1975, *Astrophys. J. Lett.* **198**, L7.
- Tifft, W. G., and M. Tarengi, 1977, *Astrophys. J.* **217**, 944.
- Tinsley, B. M., and A. G. Cameron, 1974, *Astrophys. Space Sci.* **31**, 31.
- Toomre, A., and J. Toomre, 1972, *Astrophys. J.* **178**, 623.
- Toyama, K., and S. Ikeuchi, 1980, *Prog. Theor. Phys.* **64**, 831.
- Tremaine, S., 1981, in *The Structure and Evolution of Normal Galaxies*, edited by M. Fall and D. Lynden-Bell (Cambridge University, Cambridge), p. 67.
- Tremaine, S. D., and D. O. Richstone, 1977, *Astrophys. J.* **212**, 311.
- Tucker, W. H., and R. Rosner, 1983, *Astrophys. J.* **267**, 547.
- Turner, E. L., and J. R. Gott, 1976a, *Astrophys. J.* **209**, 6.
- Turner, E. L., and J. R. Gott, 1976b, *Astrophys. J. Suppl.* **32**, 409.
- Turner, E. L., and W. L. Sargent, 1974, *Astrophys. J.* **194**, 587.
- Tytler, D., and N. V. Vidal, 1979, *Mon. Not. R. Astron. Soc.* **182**, 33p.
- Ulmer, M. P., and R. G. Cruddace, 1981, *Astrophys. J. Lett.* **246**, L99.
- Ulmer, M. P., and R. G. Cruddace, 1982, *Astrophys. J.* **258**, 434.
- Ulmer, M. P., R. G. Cruddace, K. Wood, J. Meekins, D. Yentis, W. D. Evans, H. Smathers, E. Byram, T. Chubb, and H. Friedman, 1980, *Astrophys. J.* **236**, 58.
- Ulmer, M. P., and J. G. Jernigan, 1978, *Astrophys. J. Lett.* **222**, L85.
- Ulmer, M. P., R. Kinzer, R. G. Cruddace, K. Wood, W. Evans, E. Byram, T. Chubb, and H. Friedman, 1979, *Astrophys. J. Lett.* **227**, L73.
- Ulmer, M. P., M. Kowalski, R. Cruddace, M. Johnson, J. Meekins, H. Smathers, D. Yentis, K. Wood, D. McNutt, T. Chubb, E. Byram, and H. Friedman, 1981, *Astrophys. J.* **243**, 681.
- Ulmer, M. P., S. Shulman, W. D. Evans, W. N. Johnson, D. McNutt, J. Meekins, G. H. Share, D. Yentis, K. Wood, E. T. Byram, T. A. Chubb, and H. Friedman, 1980, *Astrophys. J.* **235**, 351.
- Ulrich, M., 1978, *Astrophys. J.* **221**, 422.
- Uson, J. M., and D. T. Wilkinson, 1985, private communication.
- Valentijn, E. A., 1978, *Astron. Astrophys.* **68**, 449.
- Valentijn, E. A., 1979a, *Astron. Astrophys. Suppl.* **38**, 319.
- Valentijn, E. A., 1979b, *Astron. Astrophys.* **78**, 362.
- Valentijn, E. A., 1979c, *Astron. Astrophys.* **78**, 367.
- Valentijn, E. A., 1983, *Astron. Astrophys.* **118**, 123.
- Valentijn, E. A., and W. Bijleveld, 1983, *Astron. Astrophys.* **125**, 223.
- Valentijn, E. A., and R. Giovanelli, 1982, *Astron. Astrophys.* **114**, 208.
- Valentijn, E. A., and G. C. Perola, 1978, *Astron. Astrophys.* **63**, 29.
- Vallee, J. P., 1981, *Astrophys. Lett.* **22**, 193.
- Vallee, J. P., A. H. Bridle, and A. S. Wilson, 1981, *Astrophys. J.* **250**, 66.
- Vallee, J. P., and A. S. Wilson, 1976, *Nature* **259**, 451.
- Vallee, J. P., A. S. Wilson, and H. van der Laan, 1979, *Astron. Astrophys.* **77**, 183.
- Valtonen, M., and G. Byrd, 1979, *Astrophys. J.* **230**, 655.
- van Albada, T. S., 1982, *Mon. Not. R. Astron. Soc.* **201**, 939.
- van Breugel, W. J., 1980, *Astron. Astrophys.* **88**, 248.
- van Breugel, W. J., T. Heckman, and G. Miley, 1984, *Astrophys. J.* **276**, 79.
- van den Bergh, S., 1961a, *Z. Astrophys.* **53**, 219.
- van den Bergh, S., 1961b, *Astrophys. J.* **134**, 970.
- van den Bergh, S., 1976, *Astrophys. J.* **206**, 883.
- van den Bergh, S., 1977a, *Publ. Astron. Soc. Pac.* **89**, 746.
- van den Bergh, S., 1977b, *Vistas Astron.* **21**, 71.
- van den Bergh, S., 1983a, *Publ. Astron. Soc. Pac.* **95**, 275.
- van den Bergh, S., 1983b, *Astrophys. J.* **265**, 606.
- van den Bergh, S., and J. de Roux, 1978, *Astrophys. J.* **219**, 352.
- van Gorkom, J. H., and R. D. Ekers, 1983, *Astrophys. J.* **267**, 528.
- Vestrand, W. T., 1982, *Astron. J.* **87**, 1266.
- Vidal, N. V., 1975a, *Astron. Astrophys.* **42**, 145.
- Vidal, N. V., 1975b, *Publ. Astron. Soc. Pac.* **87**, 625.
- Vidal, N. V., 1980, in *IAU Symposium No. 92: Objects of High*

- Redshift*, edited by G. O. Abell and P. J. E. Peebles (Dordrecht, Holland), p. 69.
- Vidal, N. V., and B. A. Peterson, 1975, *Astrophys. J. Lett.* **196**, L95.
- Vidal, N. V., and D. T. Wickramasinghe, 1977, *Mon. Not. R. Astron. Soc.* **180**, 305.
- Vigroux, L., 1977, *Astron. Astrophys.* **56**, 473.
- Villumsen, J. V., 1982, *Mon. Not. R. Astron. Soc.* **199**, 493.
- Waldthausen, H., C. Haslam, R. Wielebinsky, and P. Kronberg, 1979, *Astron. Astrophys. Suppl.* **36**, 237.
- Weinberg, S., 1972, *Gravitation and Cosmology: Principles and Applications of the General Theory of Relativity* (Wiley, New York).
- Wellington, K., G. Miley, and H. van der Laan, 1973, *Nature* **244**, 502.
- West, R. M., 1974, *Euro. South. Obs. Bull.* **10**, 25.
- West, R. M., and S. Frandsen, 1981, *Astron. Astrophys. Suppl.* **44**, 329.
- Westphal, J. A., J. Kristian, and A. R. Sandage, 1975, *Astrophys. J. Lett.* **197**, L95.
- White, R. A., 1978, *Astrophys. J.* **226**, 591.
- White, R. A., and J. O. Burns, 1980, *Astron. J.* **85**, 117.
- White, R. A., and Hernan Quintana, 1985, private communication.
- White, R. A., C. L. Sarazin, and H. Quintana, 1985, "X-ray Emission from an Optically Selected Sample of High-Redshift Southern Clusters," University of Virginia report.
- White, R. A., C. L. Sarazin, H. Quintana, and W. J. Jaffe, 1981, *Astrophys. J. Lett.* **245**, L1.
- White, S. D. M., 1976a, *Mon. Not. R. Astron. Soc.* **174**, 19.
- White, S. D. M., 1976b, *Mon. Not. R. Astron. Soc.* **174**, 467.
- White, S. D. M., 1976c, *Mon. Not. R. Astron. Soc.* **177**, 717.
- White, S. D. M., 1977a, *Comments Astrophys.* **7**, 95.
- White, S. D. M., 1977b, *Mon. Not. R. Astron. Soc.* **179**, 33.
- White, S. D. M., 1978, *Mon. Not. R. Astron. Soc.* **184**, 185.
- White, S. D. M., 1979, *Mon. Not. R. Astron. Soc.* **189**, 831.
- White, S. D. M., 1982, in *Morphology and Dynamics of Galaxies*, edited by L. Martinet and M. Mayor (Geneva Observatory, Geneva), p. 289.
- White, S. D. M., 1985, private communication.
- White, S. D. M., and M. J. Rees, 1978, *Mon. Not. R. Astron. Soc.* **183**, 341.
- White, S. D. M., and J. Silk, 1980, *Astrophys. J.* **241**, 864.
- White, S. D. M., J. Silk, and J. P. Henry, 1981, *Astrophys. J. Lett.* **251**, L65.
- Wilkinson, A., and J. B. Oke, 1978, *Astrophys. J.* **220**, 376.
- Willson, M., 1970, *Mon. Not. R. Astron. Soc.* **151**, 1.
- Wilson, A. S., and J. P. Vallee, 1977, *Astron. Astrophys.* **58**, 79.
- Wirth, A., S. J. Kenyon, and D. A. Hunter, 1983, *Astrophys. J.* **269**, 102.
- Wolf, M., 1906, *Astron. Nachr.* **170**, 211.
- Wolf, R. A., and J. N. Bahcall, 1972, *Astrophys. J.* **176**, 559.
- Wolff, R. S., H. Helava, T. Kifune, and M. C. Weisskopf, 1974, *Astrophys. J. Lett.* **193**, L53.
- Wolff, R. S., H. Helava, and M. C. Weisskopf, 1975, *Astrophys. J. Lett.* **197**, L99.
- Wolff, R. S., R. J. Mitchell, P. A. Charles, and J. L. Culhane, 1976, *Astrophys. J.* **208**, 1.
- Yahil, A., and J. P. Ostriker, 1973, *Astrophys. J.* **185**, 787.
- Yahil, A., and N. V. Vidal, 1977, *Astrophys. J.* **214**, 347.
- Young, P. J., 1976, *Astron. J.* **81**, 807.
- Zel'dovich, Y. B., and R. A. Sunyaev, 1969, *Astrophys. Space Sci.* **4**, 301.
- Zel'dovich, Y. B., and R. A. Sunyaev, 1981, *Sov. Astron. Lett.* **6**, 285.
- Zwicky, F., 1933, *Helv. Phys. Acta* **6**, 110.
- Zwicky, F., 1957, *Morphological Astronomy* (Springer, Berlin).
- Zwicky, F., E. Herzog, P. Wild, M. Karpowicz, and C. T. Kowal, 1961–1968, *Catalogue of Galaxies and Clusters of Galaxies* (Caltech, Pasadena), Vols. 1–6.

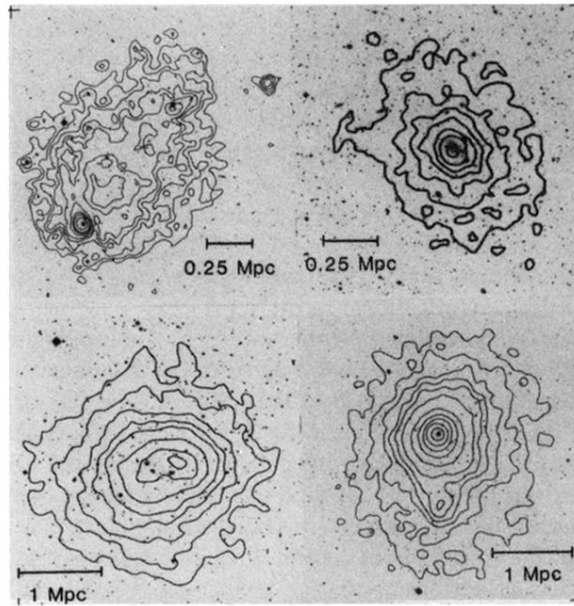


FIG. 12. The x-ray morphology of several clusters of galaxies from Jones and Forman (1984). Contours of constant x-ray surface brightness are shown superimposed on optical images of the clusters. (Top left), the prototypical irregular nXD cluster A1367. (Top right), the irregular XD cluster A262. (Bottom left), the regular nXD cluster A2256. (Bottom right), the regular XD cluster A85, showing the x-ray emission centered on the cD galaxy.

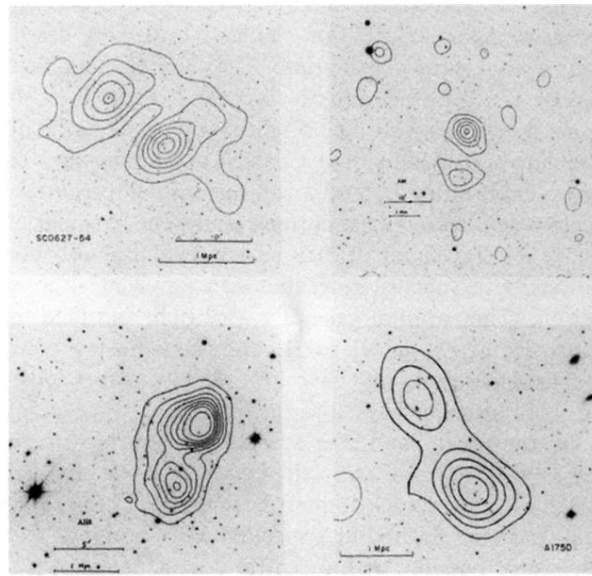


FIG. 13. The x-ray surface brightness in four double clusters, from Forman *et al.* (1981). Contours of constant x-ray surface brightness are shown superimposed on optical images of the clusters.

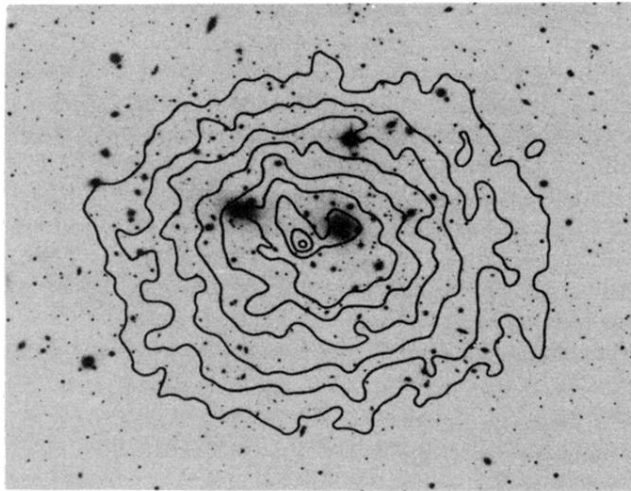


FIG. 14. The x-ray surface brightness of the Coma cluster of galaxies from the IPC on *Einstein*, kindly provided by Christine Jones and Bill Forman. Contours of constant x-ray surface brightness are shown superimposed on the optical image of the cluster.

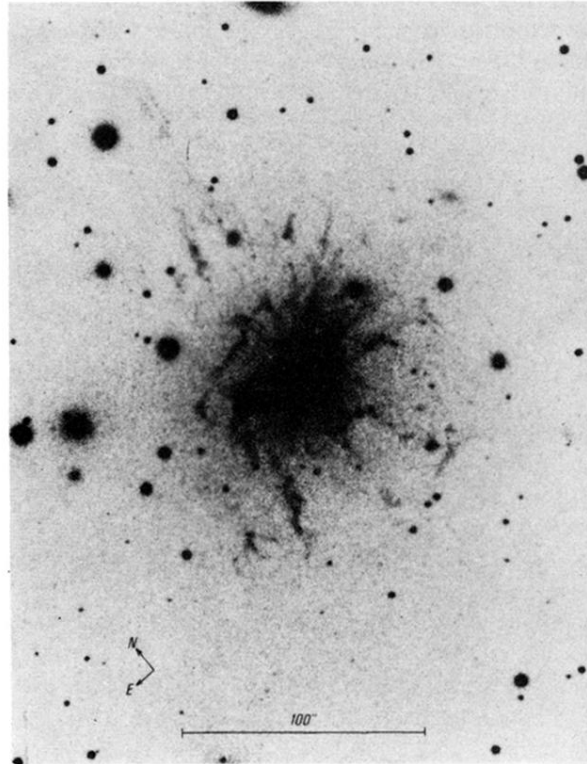


FIG. 15. An optical photograph of the spectacular galaxy NGC1275 in the Perseus cluster from Lynds (1970), copyright 1970 AURA, Inc., National Optical Astronomy Observatories, Kitt Peak. The photograph was taken with a filter sensitive to the $H\alpha$ emission line, and shows the prominent optical emission line filaments around this galaxy.

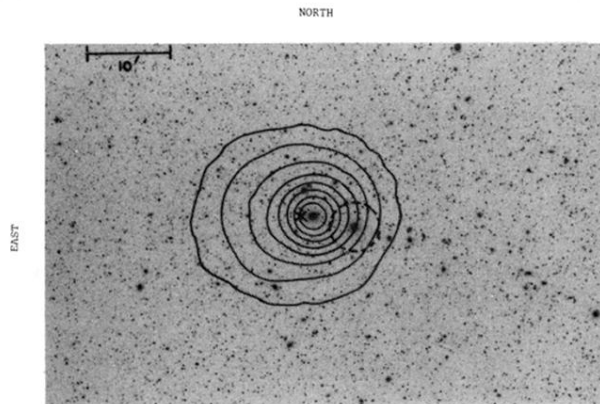


FIG. 16. The x-ray surface brightness of the Perseus cluster of galaxies, observed by Branduardi-Raymont *et al.* (1981) with the IPC on the *Einstein* satellite. Contours of constant x-ray surface brightness are shown superimposed on the optical image of the cluster. The center of the galaxy distribution in the cluster is shown as a dashed circle, while the centroid of the extended x-ray emission is the \times . The peak in the x-ray surface brightness is centered on the galaxy NGC1275.

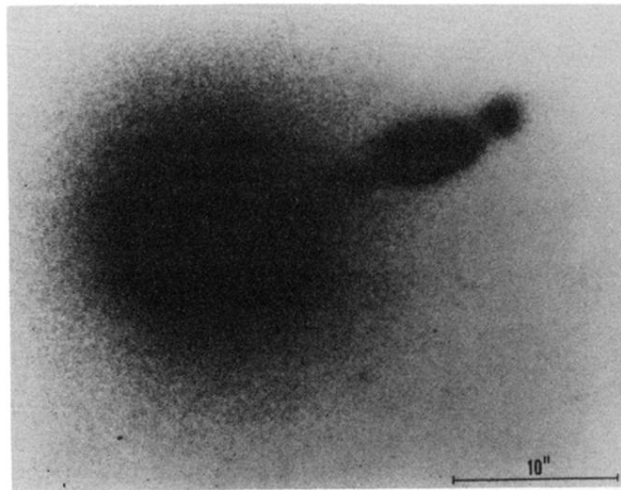
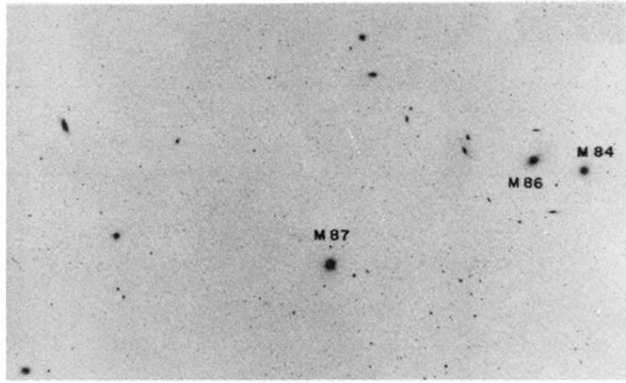


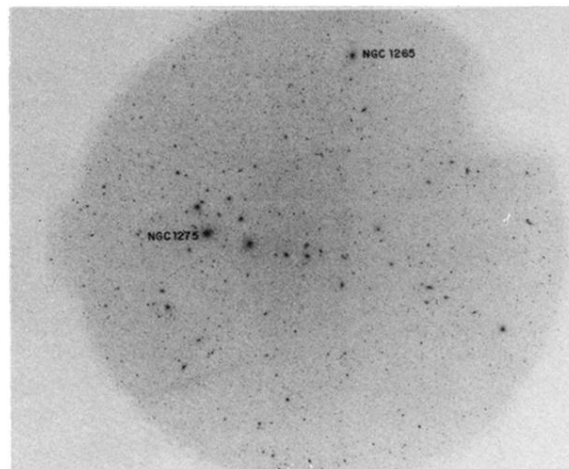
FIG. 18. An optical photograph of the elliptical galaxy M87 in the Virgo cluster, showing the jet in the interior of the galaxy (Arp and Lorre, 1976).



(a)

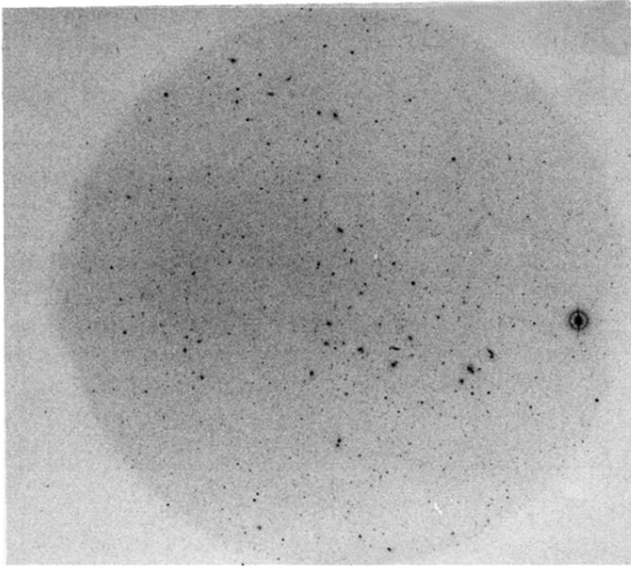


(b)

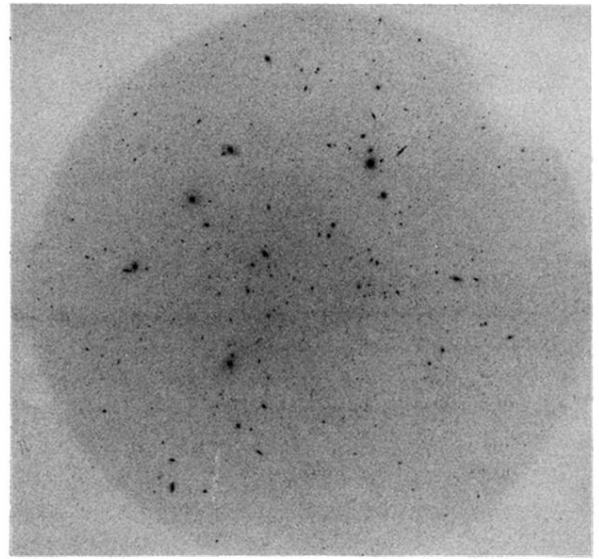


(c)

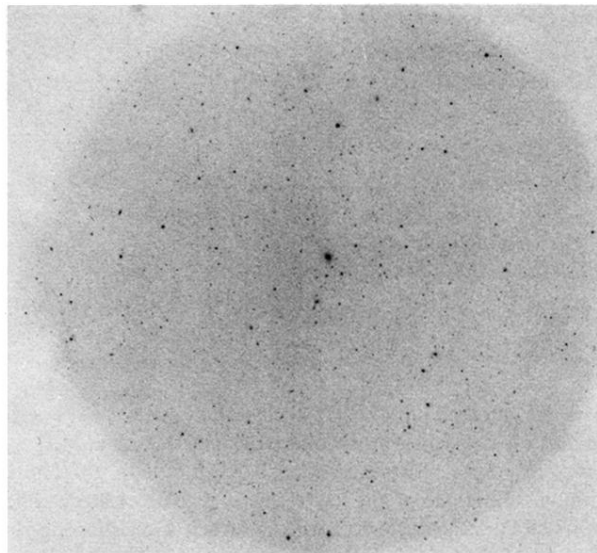
FIG. 1. Optical photographs of clusters of galaxies. (a) The Virgo cluster of galaxies, an irregular cluster that is the nearest cluster to our galaxy. The galaxy M87, on which the x-ray emission is centered, is marked, as are the two bright galaxies M84 and M86. Photograph from the Palomar Observatory Sky Survey (Minkowski and Abell, 1963). (b) The Coma cluster of galaxies (Abell 1656), showing the two dominant D galaxies. Coma is one of the nearest rich, regular clusters. Photograph copyright 1973 The National Optical Astronomy Observatories. (c) The Perseus cluster of galaxies (Abell 476), showing the line of bright galaxies. NGC1275 is the brightest galaxy, on the east (left) end of the chain. NGC1265 is a head-tail radio galaxy. Photograph from Strom and Strom (1978c). (d) The irregular Hercules cluster (Abell 2151), which contains a large number of spiral galaxies. Photograph from Strom and Strom (1978b). (e) The irregular cluster Abell 1367. Photograph from Strom and Strom (1978c). (f) The regular cluster Abell 2199, showing the dominant cD galaxy NGC6166 at its center. Photograph from Strom and Strom (1978b).



(d)



(e)



(f)

FIG. 1. (Continued).

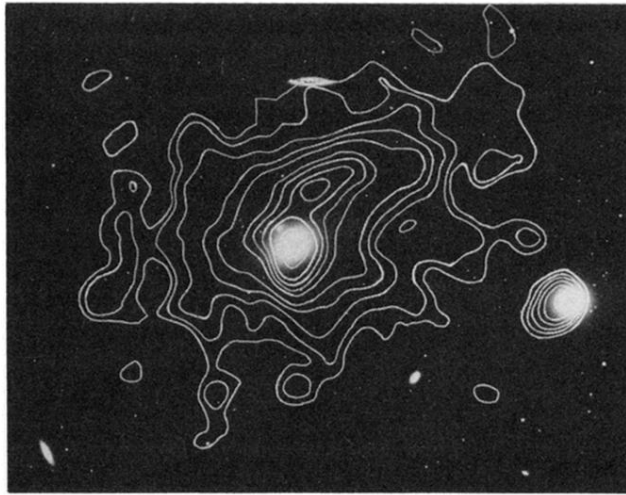
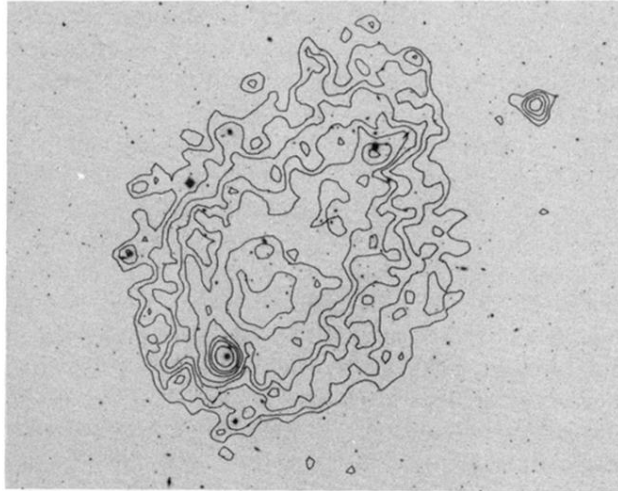


FIG. 21. The x-ray emission from the Virgo cluster galaxies M86 (east or left) and M84 (west or right) from Forman and Jones (1982). Contours of constant x-ray surface brightness are shown superimposed on an optical image of the galaxies. Note the plume of x-ray emission extending to the north of M86, which may indicate that this galaxy is currently being stripped of its gas.

(a)



(b)

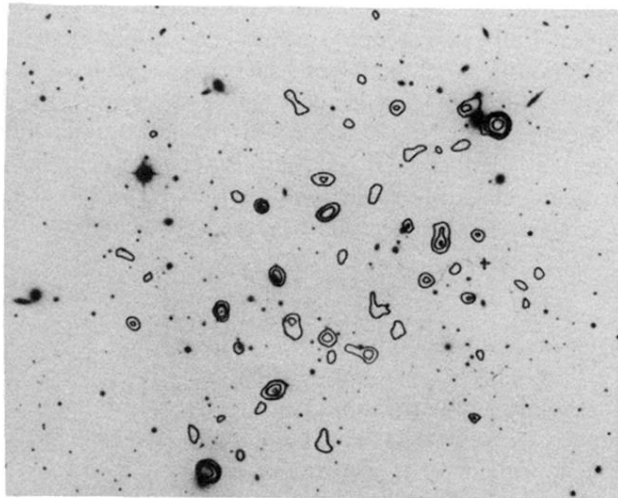


FIG. 22. The x-ray surface brightness of the A1367 cluster of galaxies, observed by Bechtold *et al.* (1983) with the *Einstein* satellite. Contours of constant x-ray surface brightness are shown superimposed on the optical image of the cluster. (a) The lower-resolution IPC image, showing the irregular cluster emission. (b) The higher-resolution HRI image, showing many discrete sources within the cluster, many of which are associated with individual cluster galaxies.

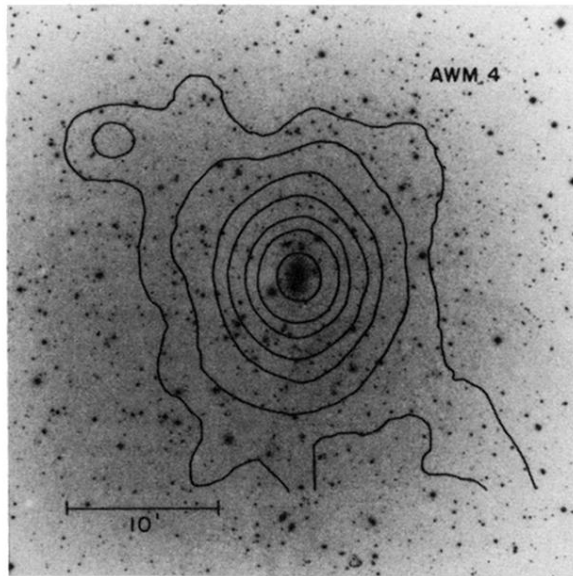


FIG. 28. The x-ray emission from the AWM4 poor cluster of galaxies, from Kriss *et al.* (1983) with the IPC on the *Einstein* satellite. Contours of constant x-ray surface brightness are shown superimposed on the optical image of the cluster. The emission is centered on the cD galaxy.

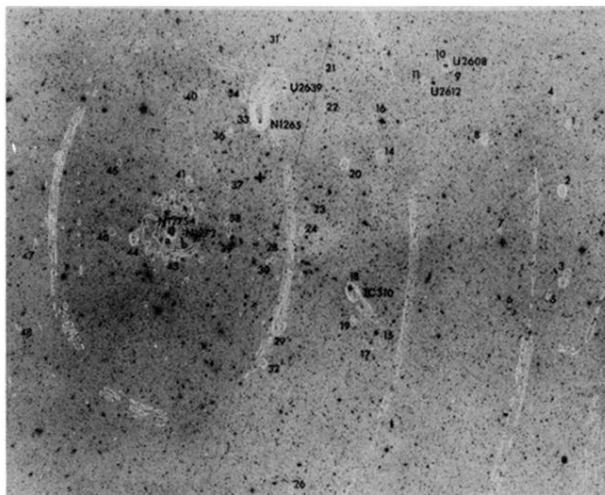


FIG. 29. A radio map of the Perseus cluster of galaxies from Gisler and Miley (1979). Contours of constant radio surface brightness at 610 MHz are shown superimposed on the optical image of the cluster. Note the very strong source associated with the galaxy NGC1275 (the highest contours associated with this source have been removed), and the two head-tail radio sources associated with NGC1265 and IC310. The rings are diffraction features due to NGC1275 and are not real.

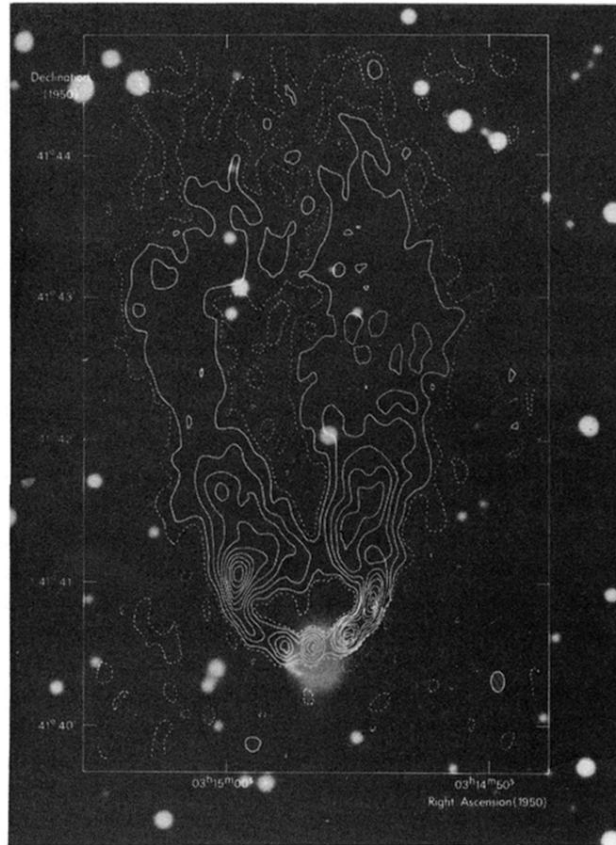


FIG. 30. A low-resolution radio map at a frequency of 5 GHz of the head-tail radio source associated with the galaxy NGC1265 in the Perseus cluster, from Wellington *et al.* (1973). Contours of constant radio surface brightness are shown superimposed on the optical image of the galaxy.



FIG. 32. A Very Large Array radio image at a frequency of 1420 MHz of the wide-angle-tail (WAT) radio galaxy 1919 + 479 associated with a cD galaxy in a Zwicky cluster, from Burns *et al.* (1985).